

Investigating RNA editing in the pathogenesis of Amyotrophic Lateral Sclerosis

By: Khayria Yassin Alsomali



Submitted for the degree of Doctor of Philosophy (PhD)

Sheffield Institute for Translational Neuroscience

University of Sheffield

May 2015



Translation: My lord! Increase me in knowledge (The Holy Quran, Sura Ta-Ha and Verse 114)

Abstract

The susceptibility of MNs to injury in amyotrophic lateral sclerosis (ALS) may result from excitotoxicity and subsequent dysregulation of intracellular calcium homeostasis. Post-transcriptional editing of the AMPA and Kainate glutamate receptor (GLUR) subunit(s) may alter the calcium ion permeability of the receptor pore, leading to neurodegeneration.

The aims of the study are (i) to investigate *GLUR2*, *GLUR5* and *GLUR6* RNA editing at Q/R site and its editing enzyme *ADAR2* and *ADAR3* in ALS/*C9ORF72*-positive and ALS/*C9ORF72*-negative compared to non-neurological controls, and (ii) to determine the aberrant expression of *EAAT2* transcripts in the astrocytes of the spinal cord of ALS cases and controls. (iii) To characterise p-TDP43, p62, *GLUR2*, *ADAR2*, *ADAR3* and GFAP and *EAAT2* proteins in motor neurons of ALS/*C9ORF72*-positive and ALS/*C9ORF72*-negative cases and controls. (iv) To develop new methodology to look at different levels of the mRNA expression in *GLUR2*, *GLUR5*, *GLUR6*, *ADAR2*, *ADAR3* and *EAAT2* that might exist in ALS.

RNA was extracted from MNs and cDNA was prepared followed by amplification of cDNA by PCR that was used to generate amplified *GLUR2*, *GLUR5* and *GLUR6*. These products were digested to produce cuts in the internal site of *GLUR* mRNA and differentiate edited from non-edited *GLUR* by analysis using agarose gel electrophoresis and the Agilent Bioanalyser. Independently the mRNA expression of *ADAR2*, *ADAR3* and *EAAT2* alternative transcripts of normal and aberrant exon 4 and 9 were quantified by qPCR. p-TDP-43, p62, *GLUR2*, *ADAR2*, *ADAR3* and GFAP and *EAAT2* protein levels were assessed by immunohistochemistry. The mRNA expression of *GLUR2*, *GLUR5*, *GLUR6*, *ADAR2*, *ADAR3* and *EAAT2* was assessed by next generation sequencing.

It was demonstrated that *GLUR2* was fully edited in the MNs of ALS/*C9ORF72*-positive, ALS/*C9ORF72*-negative cases and controls. *GLUR5* was 39% edited in MNs of ALS/*C9ORF72*-positive, 57% edited in ALS/*C9ORF72*-negative cases and 30% edited in controls. *GLUR6* editing in MNs was 86% editing in the ALS/*C9ORF72*-positive and 77% editing in ALS/*C9ORF72*-negative cases compared to 72% editing in controls. An elevated mRNA expression in *EAAT2* aberrant and normal transcripts of exon 4 and exon 9 was shown, but did not reach statistical significance.

ADAR2 immunoreactivity was associated with the nuclei of MNs, in contrast to ADAR3 which was exclusively associated with the neuronal cytoplasm. No significant differences in the pattern or distribution of immunoreactivity was detected across all groups. Phosphorylated TDP-43⁺ and p62⁺ skein-like bodies and compact inclusions were significantly elevated in both ALS/*C9ORF72*-positive cases and ALS/*C9ORF72*-negative cases, compared to control subjects which exhibited neither p-TDP-43 nor p62 expression. No significant difference in the pattern of immunoreactivity of *EAAT2* in ALS groups and controls.

In conclusion, full editing of *GLUR2* in dissected motor neurons isolated by LCM was confirmed in ALS/*C9ORF72*-positive and ALS/*C9ORF72*-negative and control individuals. Whereas partial editing has been identified in *GLUR5* and *GLUR6* receptors. The mRNA and protein expression of ADAR2 and ADAR3 on spinal cord have shown similar levels between tested groups. No significant difference in the mRNA and protein expression of *EAAT2*.

MNs in ALS cases, both with and without *C9ORF72* expansion expressed pathogenic inclusions of phosphorylated TDP-43 and p62, which are a hallmark for ALS. ADAR2 and ADAR3 have shown no differences in ALS groups compared to controls.

Acknowledgements

First of all, I would like to thank Allah, the most gracious, the most merciful, for giving me this chance to make a dream come true. Secondly, I would like to express my greatest appreciation to my parents for their unconditional love, encouragement, support and for helping me survive all the stress in the last three years and not letting me give up. I would like to thank my siblings for their support especially my brother Abdulrahman and my sister Afrah who have always been a guiding star for me. I would like to express my profound gratitude to my fiancé Abdulrahman for his encouragement, support, understanding and love. I would also like to thank my dear friends for their support.

I am very grateful to my supervisor Dr. Paul Heath who showed me the path and helped me on my PhD. His enthusiasm, encouragement, patience and faith in me throughout have been extremely helpful. He was always available for my questions and he was positive and gave generously of his time and knowledge. I specially owe a debt of gratitude to Dr. Julie Simpson who helped me in writing this thesis and gave me lots of feedback. She was kind and supportive and without her help this work would have not been possible.

My thanks are also extended to Prof. Paul Ince for his guidance and support and for his lab group. I would also like to thank Mr. Matthew Wyles and Dr. Johnathan Cooper-Knock for his help with the next generation sequencing. Last but not least, I would like to thank the staff in SITraN who gave me and my colleagues a very welcoming environment to work.

List of Contents

Abstract.....	I
Acknowledgements.....	III
List of tables.....	VII
List of figures	VIII
List of abbreviations.....	VIII
Chapter 1: Introduction.....	1
1.1 History of Amyotrophic Lateral Sclerosis	1
1.2 Clinical features.....	2
1.3 Aetiology of ALS	3
1.3.1 Incidence and age at onset.....	3
1.3.2 Genetic risk factors	4
1.3.2.1 <i>SOD1</i>	8
1.3.2.2 <i>TARDBP</i>	9
1.3.2.3 <i>FUS/TLS</i>	9
1.3.2.4 <i>C9ORF72</i>	11
1.3.3 Environmental risk factors	13
1.4 Pathological factors associated with ALS	14
1.4.1 Glutamate excitotoxicity	14
1.4.2 Oxidative stress	20
1.4.3 Mitochondrial dysfunction	20
1.4.4 Dysregulation of RNA processing.....	21
1.4.5 Glial cell dysfunction	22
1.4.6 Protein aggregation.....	23
1.4.7 Impaired axonal transport	24
1.5 Aberrant RNA editing of glutamate receptors in ALS.....	27
1.7 Aims and Hypothesis.....	33
Chapter 2: Materials and Methods.....	36
2.1 Materials and their suppliers	36
2.2 Human CNS tissue.....	39
2.3 RNA applications	44
2.3.1 FFPE and frozen preparations	44
2.3.2 Histological staining of spinal cord for laser capture microdissection	44
2.3.3 RNA extraction from FFPE tissue.....	47
2.3.4 RNA extraction from frozen total spinal cord	48

2.3.5	RNA extraction from LCM-isolated motor neurons and astrocytes	48
2.3.6	RNA integrity and cDNA synthesis.....	48
2.4	Designing primers.....	48
2.5	Reverse transcription-polymerase chain reaction (RT-PCR)	52
2.5.1	Gel purification	52
2.6	Restriction enzyme digest	53
2.6.1	Quantification of editing levels.....	54
2.7	Quantitative PCR (qPCR) experiments	55
2.7.1	Statistical analysis	57
2.8	Immunohistochemistry (IHC).....	58
2.8.1	Statistical analysis	60
2.9	Next generation sequencing.....	60
Chapter 3: RNA editing of glutamate receptors in SALS patients		66
3.1	Introduction	66
3.2	Results.....	71
3.2.1	Optimisation development.....	71
3.2.2	RNA editing of glutamate receptor subunits in different CNS regions.....	81
3.2.3	RNA editing of glutamate receptors in MNs of ALS.....	94
3.2.4	ADAR mRNA expression in ALS.....	103
3.2.5	The potential role of normal and aberrant alternative transcripts of <i>EAAT2</i> in astrocytes.....	106
3.3	Discussion	112
Chapter 3: Neuropathological characterisation of ALS tissue.....		122
4.1	Introduction	122
4.2	Results.....	126
4.2.1	Cases used in this study.....	126
4.2.2	p-TDP43 and p62 pathology in ALS patients	127
4.2.3	The expression of <i>GLUR2</i> in ALS patients	133
4.2.4	ADAR2 and ADAR3 localisation in ALS	139
4.2.5	Expression of glutamate transporter <i>EAAT2</i> in astrocytes of ALS cases	147
4.3	Discussion	155
Chapter 5: Next generation sequencing		161
5.1	Introduction	161
5.2	Results.....	167
5.1	Discussion.....	181
Chapter 6: General Discussion.....		183

6.1	Discussion.....	183
6.2	Future work	188
	References	190
	Appendix I.....	215
	Appendix II.....	216

List of tables.

Table 1.1	Genetic subtypes linked to familial ALS.....	6
Table 1.2	Glutamate receptors and function.....	16
Table 2.1	Equipment, chemicals and enzymes, antibodies and solutions.....	36
Table 2.2	Detailed clinical information for ALS cases and controls.....	41
Table 2.3	Sequence of <i>GLUR2</i>, <i>GLUR5</i> and <i>GLUR6</i> primers used in the study.....	51
Table 2.4	Primers used.....	57
Table 2.5	QPCR condition.....	57
Table 2.6	Antibodies used in the study, their antigen retrieval method and dilution of primary antibody.....	59
Table 3.1	FFPE sections obtained from spinal cord of ALS patients.....	71
Table 3.2	Nanodrop of spinal cord sections of ALS patients.....	72
Table 3.3	Multiple CNS regions of several ALS patients and one PICK patient.....	81
Table 3.4	Frozen thoracic spinal cord from ALS cases and controls.....	94
Table 3.5	<i>GLUR</i> editing at Q/R site of ALS patients.....	102
Table 3.6	Summary of <i>GLUR</i> editing at Q/R site of various diseases.....	113
Table 4.1	FFPE thoracic spinal cord tissue of ALS cases.....	126
Table 5.1	Cases used in the study.....	167
Table 5.2	Quantitation statistics of the sequencing run for less dilute library.....	177
Table 5.3	Quantitation statistics of the sequencing run for more dilute library.....	178
Table 5.4	Mapping reads to the human genome.....	180

List of figures

Figure 1.1	Normal glutamate neurotransmission process.....	19
Figure 1.2	The pathogenic mechanisms that contribute to motor neuron injury in ALS.....	26
Figure 1.3	<i>ADAR2</i> deamination of <i>GLUR2</i> at Q/R site.....	31
Figure 1.4	Permeability of <i>GLUR2</i> at Q/R site.	32
Figure 2.1	<i>GLUR2</i> (NM-000826) sequence showing editing at Q/R site.....	48
Figure 2.2	<i>GLUR5</i> (NM-000830) sequence showing editing at Q/R site.....	49
Figure 2.3	<i>GLUR6</i> (NM-021956) sequence showing editing at Q/R site.....	50
Figure 2.4	Restriction digest enzymes.....	54
Figure 2.5	Primers of <i>EAAT2</i> transcripts (NM-004171); exon 4 and exon 9.....	56
Figure 3.1	DNA chip bioanalyser of PCR of ALS.....	72
Figure 3.2	Microdissection of MNs by LCM.....	75
Figure 3.3	RNA concentration of MNs of ALS patients.....	76
Figure 3.4	PCR optimisation of <i>GLUR2</i> , <i>GLUR5</i> and <i>GLUR6</i> primers.....	77
Figure 3.5	Restriction digest analysis of <i>GLUR2</i> editing.....	78
Figure 3.6	Restriction digest analysis of <i>GLUR5</i> editing.....	79
Figure 3.7	Restriction digest analysis of <i>GLUR6</i> editing.....	80
Figure 3.8	Screening <i>GLUR2</i> RNA in the motor cortex of SALS patients.....	85
Figure 3.9	Screening <i>GLUR2</i> RNA in the motor cortex of SALS patients.....	86
Figure 3.10	Screening <i>GLUR2</i> RNA in the motor cortex of SALS patients.....	87
Figure 3.11	Restriction digest analysis of <i>GLUR2</i> editing.....	88
Figure 3.12	Restriction digest analysis of <i>GLUR5</i> editing.....	89
Figure 3.13	Restriction digest analysis of <i>GLUR6</i> editing.....	90
Figure 3.14	Percentage of <i>GLUR2</i> RNA editing.....	91
Figure 3.15	Percentage of <i>GLUR5</i> RNA editing.....	92
Figure 3.16	Percentage of <i>GLUR6</i> RNA editing.....	93
Figure 3.17	RNA editing of <i>GLUR2</i> in the spinal cord of ALS case.....	96
Figure 3.18	RNA editing of <i>GLUR2</i> in MNs of ALS case.....	97
Figure 3.19	RNA editing of <i>GLUR5</i> in the spinal cord of ALS case.....	98
Figure 3.20	RNA editing of <i>GLUR5</i> in MNs of ALS case.....	99
Figure 3.21	RNA editing of <i>GLUR6</i> in the spinal cord of ALS case.....	100
Figure 3.22	RNA editing of <i>GLUR6</i> in MNs of ALS case.....	101
Figure 3.23	The relative expression of <i>ADAR2</i> in spinal cord of ALS cases.....	104
Figure 3.24	The relative expression of <i>ADAR3</i> in spinal cord of ALS cases.....	105

Figure 3.25	The mRNA expression of EAAT⁴ in the grey matter of the spinal cord of ALS cases.....	108
Figure 3.26	The mRNA expression of EAAT⁴ in the grey matter of the spinal cord of ALS cases.....	109
Figure 3.27	The mRNA expression of EAAT⁹ in the grey matter of the spinal cord of ALS cases.....	110
Figure 3.28	The mRNA expression of EAAT⁹ in the grey matter of the spinal cord of ALS cases.....	111
Figure 4.1	p62 reactivity in MNs of the spinal cord of ALS patients.....	129
Figure 4.2	p-TDP-43 reactivity in MNs of the spinal cord of ALS patients.....	130
Figure 4.3	p62 and p-TDP-43 inclusions in MNs of ALS cases.....	131
Figure 4.4	p62 and p-TDP-43 inclusions in MNs of ALS with and without C9ORF72 expansion.....	132
Figure 4.5	Optimisation of GLUR2 staining in the cingulate gyrus of a non-neurological control case.....	135
Figure 4.6	GLUR2 staining of MNs in the anterior horn of spinal cord of ALS patients.....	136
Figure 4.7	The expression of GLUR2 in MNs of ALS.....	137
Figure 4.8	The expression of GLUR2 in MNs of ALS with and without C9ORF72 expansion.....	138
Figure 4.9	Optimisation of ADAR2 antibody dilution.....	141
Figure 4.10	Optimisation of ADAR3 antibody dilution.....	142
Figure 4.11	Pattern of ADAR2 reactivity associated with MNs of spinal cord.....	143
Figure 4.12	Pattern of ADAR3 reactivity associated with MNs of spinal cord.....	144
Figure 4.13	Expression levels of ADAR2 and ADAR3 in MNs of SALS patients.....	145
Figure 4.14	Expression levels of ADAR2 and ADAR3 in MNs of ALS patients with and without C9ORF72 expansion.	146
Figure 4.15	GFAP reactivity in the grey matter of spinal cord of ALS patients.....	149
Figure 4.16	GFAP reactivity in the white matter of spinal cord of ALS patients.....	150
Figure 4.17	EAAT2 reactivity in the grey matter of spinal cord of ALS patients.....	151
Figure 4.18	EAAT2 reactivity in white matter of spinal cord of ALS patients.....	152
Figure 4.19	GFAP and EAAT2 reactivity in the grey and white matter of ALS patients.....	153

Figure 4.20	GFAP and EAAT2 reactivity in the grey and white matter of ALS patients with and without C9ORF72 expansion.....	154
Figure 5.1	The workflow of Illumina genome analyser.....	164
Figure 5.2	Sequencing of Paired-End libraries.....	165
Figure 5.3	DNA chip bioanalyser for DNA library.....	169
Figure 5.4	Flow cell containing clusters.....	170
Figure 5.5	The base call quality of all libraries.....	171
Figure 5.6	The quality call of library 7 and library 8	172
Figure 5.7	Q score heat map of libraries.....	173
Figure 5.8	The level of cluster density and PF in each lane.....	174
Figure 5.9	The base quality call of library number 7.....	175
Figure 5.10	Q score heat map of library number 7.....	176
Figure 5.11	DNA chip bioanalyser of library samples.....	179

List of abbreviations

ALS	Amyotrophic Lateral Sclerosis
ALS2	Alsin
AD	Autosomal dominant
ADAR2	Adenosine deaminase acting on RNA2
ADAR3	Adenosine deaminase acting on RNA3
AMPA	α -Amino-3-hydroxy-5-methyl-4-isoxazolepropionic acid
AR	Autosomal recessive
ANG	Angiogenin
APOAII	Apolipoprotein AII
C9ORF72	Chromosome 9 open reading frame 72
CHMP2B	Charged multivesicular body protein 2B
CNS	Central nervous system
CSF	Cerebrospinal fluid
CFTR	Cystic fibrosis transmembrane receptor
CHCHD10	coiled-coil-helix-coiled-coil-helix domain containing 10
DAO	D-amino acid oxidase
D90A	Substitution of alanine for aspartate of position 90
DCTN1	Dynactin1
dsRBMs	Double-stranded RNA binding motifs
EAAT2	Excitatory amino acid transporter2
FALS	Familial amyotrophic lateral sclerosis
ER	Endoplasmic reticulum
FIG4	Polyphosphoinositide phosphatase
FTD	Frontotemporal dementia
FUS/TLS	Fused in sarcoma/ translocated in liposarcoma
FFPE	Formalin fixed paraffin embedded
GFAP	Glial fibrillary acidic protein
NRNPA1	Heterogeneous nuclear ribonucleoprotein A1
IPSC	Induced pluripotent stem cell
IPSN	Induced pluripotent neuron
KA	Kainate receptors
LMN	Lower motor neuron
L-BMAA	β -N-methylamino-L-alanine
MND	Motor neuron disease
MN	Motor neuron
MATR3	Matrin 3
NO	Nitric oxide
NMDA	N-methyl-D-aspartate receptor
PBP	Progressive bulbar palsy
PLS	Primary lateral sclerosis
PMA	Progressive muscular atrophy
Pin1	Peptidyl-prolyl cis-trans isomerase NIMA-interacting 1
PF	Passing filter
PFN1	Profilin 1

QGSY	Glutamine-glycine-serine-tyrosine residues
RGG	Arginine- glycine-glycine
ROS	Reactive oxygen species
OPTN	Optineurin
OH[·]	Hydroxyl radicals
O^{2·-}	Superoxide radicals
ONOO⁻	Peroxynitrite
SALS	Sporadic amyotrophic lateral sclerosis
SBMA	Spinal and bulbar muscular atrophy
SETX	Senataxin
SIGMAR1	A σ non-opioid receptor 1
SOD1	Superoxide dismutase 1
SQSTM1/p62	Sequestosome1
SPG11	Spatacsin
TARDBP	TAR DNA binding protein
TDP-43	TAR DNA protein-43
Trp	Transportin
UMN	Upper motor neuron
UHRR	Universal human reference RNA
VAPB	VAMP-associated membrane protein B
VCP	Valosin-containing protein
ERBB4	v-erb-b2 avian erythroblastic leukemia viral oncogene homolog 4
WWP2	WW domain-containing protein 2
Zn/Cu	Zinc/copper

Chapter 1
Introduction

Chapter 1: Introduction

1.1 History of Amyotrophic Lateral Sclerosis

The first clinical description of motor neurons disease was credited to Aran and Duchenne. In 1848, Aran reported a patient with progressive muscle weakness and correctly suspected a neurogenic cause. Two years later, Aran published a paper reporting 12 cases with the syndrome and named it progressive muscular atrophy (PMA) (Mitsumoto, 2006). Aran was influenced by Duchenne's opinion; and both concluded that PMA is a muscular disease. In 1853, Jean Baptiste Cruveilhier demonstrated that his patient died from a disease in the spinal cord with atrophy of anterior nerve roots (Mitsumoto, 2006). Bell independently confirmed previous findings of the description of PMA patients with degeneration in the spinal cord. Later, Charcot demonstrated the involvement of both the anterior roots and lateral columns; in 1874, Charcot successfully defined the clinical and pathological features of amyotrophic lateral sclerosis (ALS) (Mitsumoto, 2006). He defined, and separated ALS from PMA based on differing prognosis and bulbar movement. He referred to PMA as protopathic or primary, and conditions with both amyotrophy and spasticity as deuteropathic. Progressive bulbar Palsy (PBP) was recognized by Duchenne in 1860 and it was Charcot who linked PBP to ALS. The term motor neurone disease (MND) was introduced by Brain to describe PMA, PBP and ALS (Mitsumoto, 2006).

1.2 Clinical features

ALS is the most common adult-onset motor neurodegenerative disease. It is characterised by the loss of upper motor neurons in the motor cortex and/or lower motor neurons in the brain stem and the spinal cord. In this context, ALS refers to degeneration in both upper and lower motor neurons, which is the most common form of MND (Shaw & Wood-Allum, 2010). Deterioration in the upper motor neurons, termed as primary lateral sclerosis (PLS), which is a rare form of MND is characterised by limb-onset. Whereas, the loss of lower motor neurons, termed as progressive muscular atrophy (PMA), describes spinal cord dysfunction. The majority of PMA and PLS patients progress to ALS over the disease course. PMA and PLS are recognised as spectrum, which also includes FTD (Mitsumoto, 2006). The common initial symptom of ALS is weakness in the limbs, in approximately 51% to 81% of the cases, which is more common than bulbar onset of the disorder. Patients with ALS-limb onset exhibit weakness in the arms and /or legs, hemiparesis and difficulty in walking (Gubbay *et al.*, 1985; Haverkamp *et al.*, 1995; Traynor *et al.*, 2000). Weakness of the proximal and distal muscles gradually progress to spasticity and eventually severe physical disability (Leigh & Ray-Chaudhuri, 1994). Moreover, the symptoms of ALS-bulbar onset include fasciculation, stiffness, cramps and salivation accompanied with severe bulbar symptoms due to the loss of automatic swallowing and straight head posture, which in turn can lead to stress and anxiety for patients (Gubbay *et al.*, 1985; Leigh & Ray-Chaudhuri, 1994; Haverkamp *et al.*, 1995; Traynor *et al.*, 2000). Dysphagia is also regarded as a major problem for approximately 50-70% of cases, as well as difficulty with speech, choking, dehydration, weight loss and aspiration pneumonia (Leigh & Ray-Chaudhuri, 1994).

Diagnostic criteria for ALS, as outlined by El Escorial World Federation of Neurology, are based on the clinical history of the patient and appropriate neurological examination(s) to determine clinical features, which may then result in the classification of ALS as: suspected, possible, probable and definite. Definitive diagnosis for ALS occurs when the loss of both UMN and LMN occurs involving four regions of the central nervous system (CNS); bulbar, cervical, thoracic and lumbosacral (Brooks, 1994). However, it is currently difficult to establish a technique or clinical measurement that is able to definitively diagnose ALS at the early stages of disease, and whether it is associated with UMN or LMN pathology (Miller *et al.*, 1999). Currently ALS patients are diagnosed approximately 12 months after the onset of their clinical symptoms, however, it is highly likely they would have had the disease for three years or even longer before their first clinical signs. This likely reflects the loss of motor neurons required to exceed a threshold for clinical symptoms to develop (Mitsumoto, 2006).

1.3 Aetiology of ALS

1.3.1 Incidence and age at onset

The global incidence rate of ALS is 2 per 100,000 individuals, with risk of disease increasing in the older population (over 50 years of age) (Cleveland & Rothstein, 2001; Lewis & Gordon, 2007; Shaw & Wood-Allum, 2010). In the UK, the incidence of ALS ranges from 1.06 to 2.4 per 100,000 individuals (Hoppitt *et al.*, 2011). Based on epidemiological studies, the incidence of ALS among European and US populations is 2.1 per 100,000 people (McGuire *et al.*, 1996; Logroscino *et al.*, 2010). ALS cases are more prevalent in men than women, with an odds ratio of 1.5:1 (Leigh & Ray-

Chaudhuri, 1994). Several studies have reported that the mean age of onset is 40 years with a survival range from 3-5 years (Rowland & Shneider, 2001; Johnston *et al.*, 2006; Chen *et al.*, 2007). Recent reports have suggested that the incidence of ALS in the elderly population (over 75 years of age) decreases, which may either reflect the shorter survival interval associated with disease in the elderly or that ALS is not merely a result of ageing (Dykens, 1994; Logroscino *et al.*, 2010; Turner *et al.*, 2012). Young-onset sporadic ALS occurs in those aged 20 years old or younger which is similar to age of onset in juvenile patients, those expressing ALS symptoms before age 25 years carrying a defined genetic risk factor (Reaume *et al.*, 1996; Sabatelli *et al.*, 2008). To date it is unclear whether ALS disease is an age related disease that specifically occurs as part of the ageing process (Turner *et al.*, 2012).

1.3.2 Genetic risk factors

The majority of ALS patients are sporadic (90-95%) (SALS), the disease occurring with unknown genetic risk factors with no family history of ALS (Cleveland & Rothstein, 2001) and about 5-10% of ALS patients are familial (FALS), the disease resulted from an inherited genetic mutation. Of these familial ALS cases, 20% of the patients have mutation in the gene that encodes zinc superoxide dismutase 1 (*SOD1*). Genetic mutations associated with FALS have been shown to exist in some SALS cases at low frequencies of about 0.61% (Shatunov *et al.*, 2010). Mutations associated with SALS are difficult to study due to a lack of indication of mutations in the family history.

Several further genes have been identified to be linked to FALS (See table 1) that are inherited in an autosomal dominant manner, including mutations in, TAR DNA

binding protein (*TARDBP*), Fused in sarcoma or translocated in liposarcoma (*FUS/TLS*) and Chromosome 9 Open Reading Frame 72 (*C9ORF72*). However, some mutations can also be inherited recessively or as X-linked (See table 1.1) (Ince *et al.*, 2011a). The genes responsible for most ALS cases are known, but a complete understanding is lacking. Further investigation of genetic associated disease may contribute to the understanding of some of the key mechanisms likely to be involved in ALS.

Table 1.1: Genetic subtypes linked to familial ALS.

Genes	Genetic subtypes	Chromosomal locus	Onset/ inheritance	ALS Pathogenesis	References
Cu/Zn superoxide Dismutase (<i>SOD1</i>)	ALS1	21q22.1	Adult/AD	Oxidative stress	(Rosen <i>et al.</i> , 1993)
Alsin (<i>ALS2</i>)	ALS2	2q33	Juvenile/AR	Vesicle trafficking, guanine-nucleotide exchange factor (GEF).	(Yang <i>et al.</i> , 2001)
Unknown	ALS3	18q21	Adult/AD	(Hand <i>et al.</i> , 2002)
Senataxin (<i>SETX</i>)	ALS4	9q34.13	Juvenile/AD	RNA processing	(Chen <i>et al.</i> , 2004)
Spatascin/ spastic paraplegia 11 (<i>SPG11</i>)	ALS5	15q14	Juvenile/AR	(Orlacchio <i>et al.</i> , 2010)
Fused in sarcoma (<i>FUS</i>)	ALS6	16q11.2	Adult/AD	RNA processing	(Vance <i>et al.</i> , 2009)
Unknown	ALS7	20p13	Adult/AD	Unknown	(Sapp <i>et al.</i> , 2003)
VAMP-associated membrane protein B (<i>VAPB</i>)	ALS8	20q13.33	Adult/AD	Intracellular Membrane trafficking, calcium metabolism	(Nishimura <i>et al.</i> , 2004)
Angiogenin (<i>ANG</i>)	ALS9	14q11.1	Adult/AD	RNA processing	(Greenway <i>et al.</i> , 2006)
TAR-DNA binding protein (<i>TARDBP</i>)	ALS10	1p36.22	Adult/AD	RNA processing	(Sreedharan <i>et al.</i> , 2008)
Polyphosphoinositide phosphatase (<i>FIG4</i>)	ALS11	6q21	Adult/AD	Endoplasmic trafficking and cell signalling	(Chow <i>et al.</i> , 2009)
Optineurin (<i>OPTN</i>)	ALS12	10p15-p14	Adult/AD &AR	Endoplasmic Trafficking & cell signalling	(Maruyama <i>et al.</i> , 2010)

Ataxin 2 (<i>ATXN2</i>)	ALS13	12q23-q24.1	Adult/AD	RNA processing	(Elden <i>et al.</i> , 2010)
Valosin-containing protein (<i>VCP</i>)	ALS14	9q13-p12	Adult/AD	Protein degradation	(Johnson <i>et al.</i> , 2010)
Ubiquillin (<i>UBQLN2</i>)	ALS15	Xp11.21	Adult/X-linked	Protein degradation	(Deng <i>et al.</i> , 2011)
A σ Non-opioid receptor 1 (<i>SIGMAR1</i>)	ALS16	9p13.3	Adult/AD Juvenile/AR	Calcium homeostasis	(Luty <i>et al.</i> , 2010) (Al-Saif <i>et al.</i> , 2011)
Charged multivesicular body protein 2B (<i>CHMP2B</i>)	ALS17	3p11.2	Adult/AD	Vesicle trafficking	(Parkinson <i>et al.</i> , 2006)
Profilin 1 (<i>PFN1</i>)	ALS18	17p13.3	Adult/AD	Cytoskeleton arrangement	(Wu <i>et al.</i> , 2012)
v-erb-b2 avian erythroblastic leukemia viral oncogene homolog 4 (<i>ERBB4</i>)	ALS19	2q33.3-q34	Adult/AD	(Takahashi <i>et al.</i> , 2013)
Heterogeneous nuclear ribonucleoprotein A1 (<i>HNRNPA1</i>)	ALS20	12q13.1	Adult/AD	Protein degradation	(Kim <i>et al.</i> , 2013)
Matrin 3 (<i>MATR3</i>)	ALS21	5q31.2	Adult/AD	RNA processing	(Johnson <i>et al.</i> , 2014)
Chromosome 9 open reading frame 72 (<i>C9ORF72</i>)	ALS/FTD	9p21-p22	Adult/AD	RNA processing	(Renton <i>et al.</i> , 2011) (DeJesus-Hernandez <i>et al.</i> , 2011)
coiled-coil-helix-coiled-coil-helix domain containing 10 (<i>CHCHD10</i>)	ALS/FTD	22q11.23	Adult/AD	Mitochondrial dysfunction	(Bannwarth <i>et al.</i> , 2014)
<i>SQSTM1/p62</i>	ALS	5q35	Adult/AD	Protein degradation	(Fecto <i>et al.</i> , 2011)
Dynactin1 (<i>DCTN1</i>)	ALS	2p13	Adult	Vesicle trafficking	(Münch <i>et al.</i> , 2004)
D-amino-acid oxidase (<i>DAO</i>)	ALS	12q24	Adult/AD	Glutamate excitotoxicity	(Mitchell <i>et al.</i> , 2010)

1.3.2.1 SOD1

Mutation(s) in the zinc/copper (Zn/Cu) superoxide dismutase1 encoded gene (*SOD1*) located on chromosome 21 were the first identified causative gene for ALS, accounting for approximately 20% of familial cases (Rosen *et al.*, 1993) and 5% of SALS cases (Rowland & Shneider, 2001; Rothstein, 2009). *SOD1* is a cytosolic protein that act as a homodimer to bind with equal affinity to zinc and copper atoms (Shaw, 2005) and catalyses the superoxide (O_2^-) radicals, produced by errors within mitochondria, to hydrogen peroxide and water. It protects neuronal cells from oxidative stress by regulating levels of reactive oxygen species (ROS) (Yamanaka & Cleveland, 2005). The majority of *SOD1* related ALS cases are inherited in an autosomal dominant pattern. However, the exact mechanism(s) by which mutant *SOD1* cause ALS is, as yet, unknown. More than 114 mutations in *SOD1* have been reported and none of these mutations have a clear impact on decreased *SOD1* activity. The pathogenicity of mutant *SOD1* is independent of its dismutase activity (Yamanaka & Cleveland, 2005; Boillée *et al.*, 2006). This was established when inactivation or total absence of *SOD1* gene by deletion did not cause ALS in mice whereas, transgenic mice with mutant *SOD1* gene developed muscle wasting and progressive paralysis without affecting enzyme activity (Deng *et al.*, 1993; Gurney *et al.*, 1994). Several theories have attempted to explain toxic mutant *SOD1* mediated ALS, including the accumulation of unstable misfolded *SOD1* protein in the cytosol and within mitochondria in the spinal cord of both animal models and familial ALS patients (Liu *et al.*, 2004; Pasinelli *et al.*, 2004; Vijayvergiya *et al.*, 2005). It has also been shown to enhance damage within motor neurons and subsequently, if compounded by impaired non-neuronal neighbouring cells, could accelerate disease progression (Sato *et al.*, 2005).

1.3.2.2 TARDBP

Transactive response DNA binding protein-43 (TDP-43) is an RNA binding protein, that is ubiquitously expressed, highly conserved, and normally acts as a nuclear protein. However, pathogenic TDP-43 is transferred to the cytoplasm under the following conditions: cell stress (granules); over expression; interference with TDP-43 nuclear localisation signal; transporting pathogenic mutations subsequently leading to fragmentation, phosphorylation and/or aggregation (Neumann *et al.*, 2006b). TDP-43 mutations have been found in approximately 7% of FALS cases and 1-5% of SALS cases (Beleza-Meireles & Al-Chalabi, 2009). TDP-43 is involved in multiple steps of RNA processing including, regulation of alternative splicing, transcription, RNA stabilization, microRNA processing (Neumann *et al.*, 2006b). It has been reported that TDP-43 protein binds to UG repeats in large introns, to 3'UTR of mRNA, other mRNA binding sites and RNA processing genes, resulting in the broad dysfunctional mechanisms caused by mutation of TDP-43 in ALS (Sreedharan *et al.*, 2008; Sephton *et al.*, 2011).

1.3.2.3 FUS/TLS

Fused in sarcoma (*FUS*) or translocated in liposarcoma (*TLS*), is a ribonucleoprotein that is expressed in the nucleus of neuronal cells and can be found in limited proportions in the cytoplasm of most cells (Kwiatkowski *et al.*, 2009). It has an important role in the regulation of gene expression, including exon splicing, DNA damage repair and maintaining genomic structure. Like TDP-43, FUS is also involved in alternative splicing, transcription, and microRNA processing (DeJesus-Hernandez *et al.*, 2010), and mutations in FUS have been identified in approximately 4% of FALS cases and 1% of sporadic cases (Kwiatkowski *et al.*, 2009 ; DeJesus-Hernandez *et al.*,

2010). Evidence has shown abnormal cytoplasmic inclusions immunoreactive of FUS but not TDP-43 in neurons and glia of some ALS patients (Kwiatkowski, *et al.* 2009), suggesting that FUS has an independent role in neurodegeneration (Vance, *et al.* 2009). The exact mechanism(s) by which *FUS* and *TARDBP* mutations cause neurodegeneration is, as yet, unknown. Nonetheless, based on functional data, a number of hypotheses have been generated. TDP-43 sequestration into inclusions could cause a loss of function resulting in transcriptional deregulation and aberrant splicing of pre-mRNA. The loss of TDP-43 activity could disrupt the low molecular weight neurofilament mRNA via a direct interaction with the 3'UTR, thus changing the stoichiometry of neurofilament subunits and consequently leading to the formation of neurofilament aggregates as observed in ALS (Strong *et al.*, 2007). Alternatively, the aggregation of C-terminal domain of TDP-43 could cause toxic gain of function by altering TDP-43 splicing regulatory function (Forman *et al.*, 2007).

The persistence of pathogenic cytoplasmic FUS inclusions impairs the proteolytic process by inhibiting protein tagging by ubiquitin and p62 (Baumer *et al.* 2010; Neumann *et al.* 2009). Ubiquitin and p62 covalently tags proteins for degradation by the ubiquitin-proteasome system. Sequestosome 1 (also known as *SQSTM1*) binds ubiquitinated proteins and targets them for degradation by proteasome and autophagy process. Mutations in *SQSTM1* have been identified as a rare cause of ALS (Rubino *et al.* 2012).

In vitro experiments using cultured cells have shown that FUS prion domain mutation causes an increase in its propensity to aggregate and form intranuclear inclusion. However, pathology studies from patients with prion domain mutant FUS are still lacking (Dormann *et al.* 2010; Kino *et al.* 2011; Nomura *et al.* 2014). Interestingly, this is similar to the case for TDP-43, which the majority of ALS-causing mutations

cluster in its prion domain and may not directly affect its nuclear localization, but rather increase its aggregation propensity *in vitro* (Johnson *et al.* 2009).

FUS mutations in ALS families suggest that mutations result in either a novel, toxic gain of function or create a dominant negative effect that interferes with the normal activity of wild type FUS. The FUS-positive cytoplasmic inclusions found in degenerating MNs of patients may play a role in the pathogenesis of the disease; they could be toxic directly to the cell independent of normal FUS activity, or they might sequester, and functionally deplete wild type FUS in abnormal cytoplasmic aggregates (Kwiatkowski, *et al.* 2009; Vance, *et al.* 2009).

1.3.2.4 C9ORF72

A mutational event in the Chromosome 9 Open Reading Frame 72 (*C9ORF72*) gene was recently identified as the most common causative gene of frontotemporal dementia (FTD) and ALS. FTD is a progressive neurodegenerative disease characterised by neuronal loss in the frontal and anterior temporal lobes, which leads to language impairment and personality changes (McKhann *et al.*, 2001). FTD is clinically recognised in 5% of ALS cases although some sort of cognitive impairment is seen in up to 50% of ALS cases (Ferrari *et al.*, 2011). FTD and ALS can clinically co-occur, and share many similarities at both the genetic and the neuropathological level, and are proposed to constitute the same spectrum disorder (Lillo & Hodges, 2009). The mutation change in *C9ORF72* comprises a large intronic hexanucleotide (GGGGCC) repeat expansion between two non-coding exons, and is present in approximately 40 % of FALS and 7% of SALS patients (DeJesus-Hernandez *et al.*, 2011; Renton *et al.*, 2011; Mahoney *et al.*, 2012; van Rheenen *et al.*, 2012). In a healthy

population, less than 30 repeats are found, however, ALS-FTD patients have large expansions carrying potentially hundreds or even thousands of repeats. It is thought that *C9ORF72* mutations in SALS cases arise from an inherited genomic instability in the repeat region, whereas familial *C9ORF72* cases are brought about in an autosomal dominant manner (Fratta *et al.*, 2012). Examination of post-mortem brain and spinal cord tissues from ALS-FTD patients with the *C9ORF72* mutation have demonstrated immunoreactive TDP-43 cytoplasmic inclusions in neurons and glia (Stewart *et al.*, 2012). A recent study has shown that all *C9ORF72* positive patients display similar neuropathology compared to the *C9ORF72* negative patients. However, the same study showed that patients with the *C9ORF72* mutation exhibited a significantly shorter disease duration compared to their counterparts (Cooper-Knock *et al.*, 2012). It has been suggested that the *C9ORF72* expansion could contribute to the pathogenesis of ALS by three possible mechanisms: i) the sequestration of important RNA binding-proteins by sense and/or antisense toxicity of repeat RNA, ii) the toxic function of dipeptide-repeat proteins (DPR) that are generated by repeat-associated non-ATG (RAN) translation, or iii) the reduced expression of *C9ORF72* (Fratta *et al.*, 2012; Harms *et al.*, 2013). The latter possible mechanism is thought to be the least likely, because of the absence of a *C9ORF72* coding mutation (Fratta *et al.*, 2012; Mizielinska *et al.*, 2014) and the lack of severe phenotype in cases with a homozygous mutation (Harms *et al.*, 2013). RNA aggregates (RNA foci) that are formed from sense and antisense repeat transcripts are frequently found in *C9ORF72*-FTD-ALS patient brains (Gendron *et al.*, 2013; Lagier-Tourenne *et al.*, 2013; Lee *et al.*, 2013; Mizielinska *et al.*, 2013; Zu *et al.*, 2013). The GGGGCC expanded repeats can be transcribed bi-directionally in an unpredictable fashion in the absence of an initiating codon (RAN translation) producing detectable expression of sense and

antisense transcripts (Gendron *et al.*, 2013). To date, little is known about the function of the normal C9ORF72 protein and how it might contribute to disease pathogenesis.

1.3.3 Environmental risk factors

The cause of the fatal multifactorial ALS is largely unknown due to its increased complexity and association with one or more environmental risk factors. Sex, age at onset (usually after the age of 40 years) (Rowland & Shneider, 2001), and residence in specific parts of the western pacific region are linked with motor neuron diseases (Leigh & Ray-Chaudhuri, 1994). Several studies have suggested possible environmental cause(s) for ALS, these include smoking (Armon, 2009; Weisskopf *et al.*, 2010), head injury (Chen *et al.*, 2007), exposure to toxins such as pesticides used in farming (Armon *et al.*, 1991) (Muddasir Qureshi *et al.*, 2006), and heavy physical activities (Kurtzke, 1991; Chancellor & Warlow, 1992; Veldink *et al.*, 2005). Previous infection with *Retrovirus* and *Poliovirus* (Jubelt, 1992; Swingler *et al.*, 1992; Cermelli *et al.*, 2003) raise the incidence of ALS when accompanied with other environmental risk factors and the potential accumulation of reactive oxygen species (ROS) leading to critical metabolic alteration (Gros-Louis *et al.*, 2006). Another environmental risk factor associated with ALS patients is physical trauma (Chen *et al.*, 2007), as well as consumption of a dietary excitotoxin, i.e. β -N-methylamino-L-alanine (L-BMAA) found in cycad flour (Nelson *et al.*, 2000).

1.4 Pathological factors associated with ALS

1.4.1 Glutamate excitotoxicity

One of the leading concepts of a cause of ALS is excitotoxicity, a term that was first proposed in 1969 to describe the increased activation of post-synaptic receptors by excessive release of glutamate (Olney, 1969). Glutamate is the major excitatory neurotransmitter in the mammalian central nervous system. During the process of normal glutamatergic neurotransmission, glutamate is released from presynaptic neuronal terminals into the synaptic cleft where it activates glutamate receptors on the post-synaptic terminal (Laake *et al.*, 1995). The excitatory neurotransmitter signal is terminated by active removal of glutamate by the glutamate re-uptake system like the excitatory amino acid transporters (EAAT). EAAT family consist of EAAT1, EAAT2, EAAT3 and EAAT4. EAAT1 and EAAT2 are mainly expressed by astrocytes whereas EAAT3 and EAAT4 are associated with neurons (Lin *et al.*, 1998). EAAT2 is thought to be the predominant glutamate transporter which plays a central role in maintaining neurotransmitter levels in the synapse. EAAT2 is also known as solute carrier family 1 (glial high affinity glutamate transporter, member 2 (*SLC1A2*)). However, for the purpose of this thesis EAAT2 will be used throughout. Within glial cells, glutamate is converted to glutamine then transported back to presynaptic neurons where glutamine is reconverted to glutamate by glutamine synthetase (Shaw & Ince, 1997; Doble, 1999) (See figure 1.1).

Excitotoxic mechanisms may include elevated extracellular glutamate levels resulting in abnormal glutamate receptor activity and/or aberrant glutamate reuptake mechanisms. High concentrations of intracellular Ca^{+2} resulting from increased glutamate receptor activation may alter cellular Ca^{+2} homeostasis and activate Ca^{+2}

dependent pathways to restore Ca^{+2} homeostasis by compartmentalization, transportation, and sequestration into organelles (Heath & Shaw, 2002; Van Den Bosch *et al.*, 2006b; Bezprozvanny, 2009). Studies have shown a significant increase of glutamate levels in the CSF of ALS patients (Rothstein *et al.*, 1990; Shaw *et al.*, 1995a). These glutamate receptors are composed of AMPA, kainate and NMDA receptors (see table 1.2) (Laake *et al.*, 1995).

Table 1.2: Glutamate receptors and function.

Glutamate receptors	AMPA	KA	NMDA	References
Subunits	GLUR1, GLUR2, GLUR3 and GLUR4	GLUR5, GLUR6, GLUR7, KA1 and KA2	NR1, NR2A, NR2B, NR2C and NR2D	(Barbon <i>et al.</i> , 2003) (Van Den Bosch <i>et al.</i> , 2006)
Editing sites	GLUR2-Q/R (Arg607) GLUR2- R/G (764Gly)	GLUR5-Q/R (636Arg) GLUR6-Q/R (621Arg), GLUR6-Y/C (571 Cys) GLUR6- I/V (567 Val)	n/a	(Köhler <i>et al.</i> , 1993), (Lomeli <i>et al.</i> , 1994), (Sommer <i>et al.</i> , 1991), (Kwak & Kawahara, 2005)
Location	Widely distributed on postsynaptic neurons and glia	Limited distribution on pre/post synaptic neurons	Widely distributed on post-synaptic neurons and some presynaptic and glia	(Barbon <i>et al.</i> , 2003) (Van Den Bosch <i>et al.</i> , 2006b)
Permeability	Impermeable to Ca ⁺²	Impermeable to Ca ⁺²	Permeable to Ca ⁺²	
Function	Fast synaptic transmission	Fast synaptic transmission	Slow synaptic transmission	

Summary of AMPA, KA and NMDA receptors subunit. Each receptor named after their unique agonist, their possible editing sites, and distribution on MNs and glia as well as their specific functions.

The AMPA receptor is a heterotetramer composed of a mixture of the four possible subunits; GLUR1, GLUR2, GLUR3 and GLUR4. These subunits have similar protein structure with the major difference being associated with the GLUR2. This glutamate receptor, ionotropic, AMPA 2 is also known as GRIA2. However, the GLUR2 name will be used throughout the thesis. Whereas, GLUR5 is a glutamate receptor, ionotropic, kainate 1 also known as GRIK1 and GLUR6 is another glutamate receptor, ionotropic, kainate 2 also known as GRIK2. However, the GLUR5 and GLUR6 names will be used throughout the thesis. GLUR2 is the only subunit of the AMPA receptor that is edited as well as GLUR5 and GLUR6 of the KA receptor. Abnormal editing of the GLUR2 subunit increases Ca^{+2} permeability of the receptor channel and the reduce expression of calcium buffering proteins in motor neuron contributes to neuronal mediated toxicity in ALS (Carriedo *et al.*, 1996; Van Damme *et al.*, 2007; Kwak *et al.*, 2010) (see figure 1.4).

It has been reported that the abnormal function and expression of astrocytic glutamate re-uptake system EAAT2 in ALS cases contributes to motor neuron vulnerability to excitotoxic neuronal injury (Rothstein *et al.*, 1992; Rothstein *et al.*, 1995; Lin *et al.*, 1998). Because of the apparent decrease in the efficacy of synaptic clearance of glutamate, neuronal cells are exposed to elevated levels of extracellular glutamate. Any defect in the astrocyte mechanism of glutamate clearance may have an impact on motor neurons.

Studies have shown that a loss of EAAT2 protein is associated with 30-95% of SALS patients (Rothstein *et al.*, 1992; Shaw, 1994; Rothstein *et al.*, 1995; Haugeto *et al.*, 1996; Rothstein *et al.*, 1996). Additionally, abnormal Na^{+} -dependent glutamate transporter systems have also been reported in the synaptosomal preparation of post-mortem ALS tissue isolated from spinal cord and motor cortex (Rothstein *et al.*, 1992).

Immunoblotting studies using anti-peptide polyclonal antibodies to measure EAAT2 protein levels in the homogenates of CNS tissue have shown a large decrease in the astrocytic EAAT2 protein in the spinal cord and motor cortex of ALS patients (Rothstein *et al.*, 1995). The loss of EAAT2 may arise as a result of: (i) aberrant transcripts producing truncated proteins, or (ii) inhibition of EAAT2 transcription (Sue *et al.*, 2003).

Aberrant mRNA species might be produced by mechanisms such as intron-retention and exon-skipping (Lin *et al.*, 1998; Meyer *et al.*, 1998; Meyer *et al.*, 1999). Aberrant mRNA transcripts have been detected in the motor cortex and spinal cord of SALS patients, but not in other brain regions including cerebellum and hippocampus (Lin *et al.*, 1998). These transcripts have been shown to be absent in other neurological diseases such as in Spinal muscular atrophy, Huntington's disease and Alzheimer's disease (Lin *et al.*, 1998). One study showed that the intron 7 retention and exon 9 skipping protein was not detected in the motor cortex or spinal cord of ALS cases. The inability to detect these aberrant transcripts could be the result of unstable and/or degraded EAAT2 protein in the post-mortem tissue (Lin *et al.*, 1998).

However, these aberrant mRNA transcripts have also been detected in non-neurological control tissue (Meyer *et al.*, 1999; Honig *et al.*, 2000; Flowers *et al.*, 2001). In one study, the splice variant of EAAT2 involving the skipping of exon 4 was reported to be highly expressed in control rat brains (Lee *et al.*, 2011). Human exon 4 encodes transmembrane 3 (TM3) region of EAAT2 and consists of a motif that plays the role of a hinge that pulls extracellular glutamate into the astrocytes (Reyes *et al.*, 2009), indicating the important role of EAAT2 in the regulation of glutamate in the synaptic terminal. Defect in the astrocytic glutamate re-uptake system of EAAT2 leads to excitotoxicity, impaired RNA processing, mitochondrial dysfunction or oxidative

damage that may contribute to a range of neuronal injury in stroke, neurotrauma, epilepsy and other neurodegenerative disorders, including ALS (Bruijn *et al.*, 1997; Doble, 1999; Trotti *et al.*, 1999; Van Den Bosch *et al.*, 2006b; Ferraiuolo *et al.*, 2011).

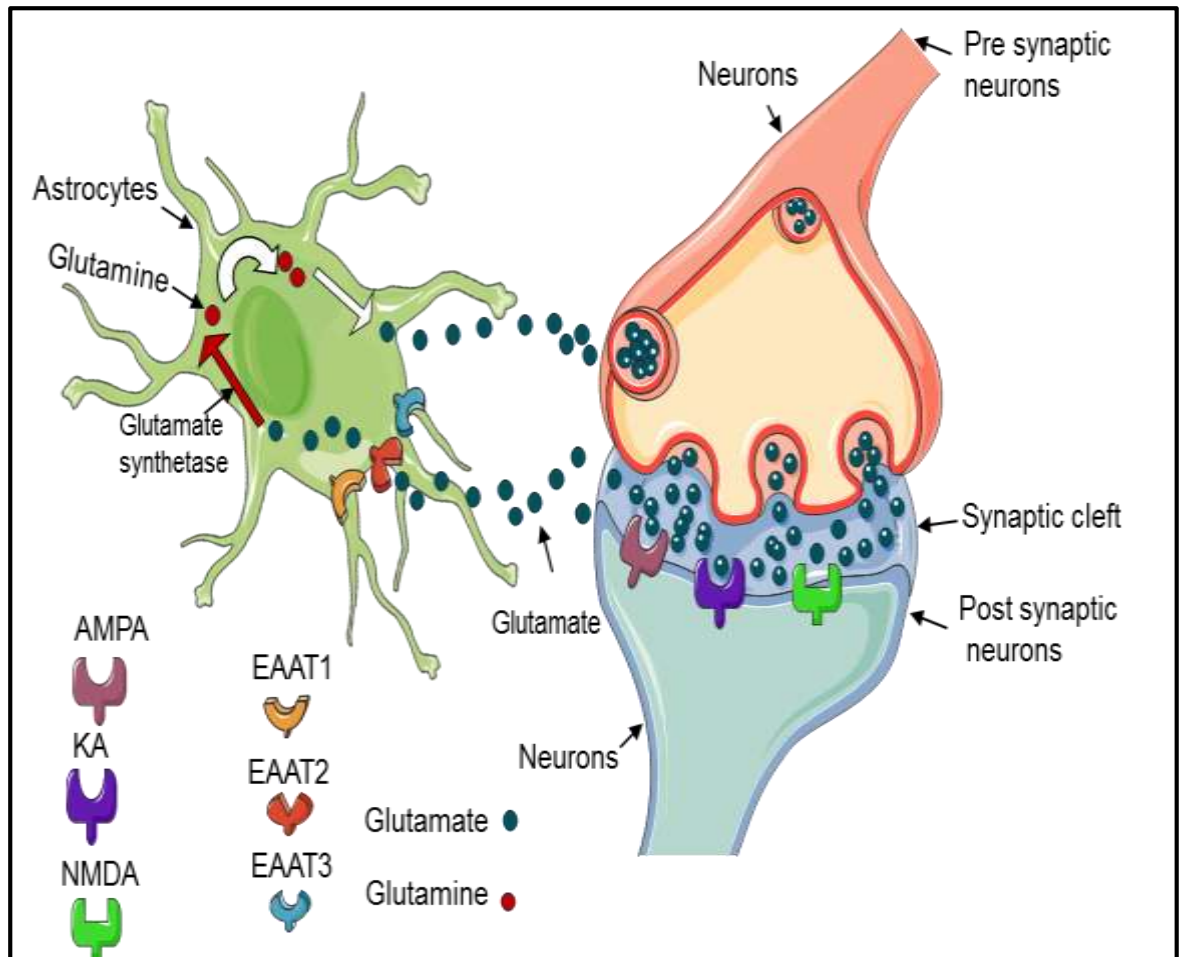


Figure 1.1: Normal glutamate neurotransmission process.

Glutamate is released from the vesicles into the synaptic cleft where it activates glutamate receptors on post synaptic neuronal terminal. Excess glutamate is taken up by EAAT2 located on the astroglia that convert the glutamate to glutamine by glutamate synthetase, thereby removing excess glutamate from the extracellular space, modified from (Heath & Shaw, 2002) with permission 3512500882980.

1.4.2 Oxidative stress

Oxidative stress plays a vital role in the pathogenesis of ALS and in several other neurodegenerative diseases. The correlation between oxidative stress and neuronal death has been extensively investigated. Oxidative stress can damage DNA, RNA, proteins and lipids and may lead to the opening of mitochondrial permeability transition pore which can stimulate the production of further reactive oxygen species (ROS). The imbalance between the creation and depletion of ROS or the failure to repair ROS induced damage leads to oxidative stress (Nicholls, 2004). Increased free radicals can cause excess release of excitotoxic glutamate, inhibition of glutamate removal, and cause an increase in Ca^{+2} influx (Law *et al.*, 2001). *In vitro* studies of the NSC-34 murine motor neuronal cell line transfected with the human Q331K mutation in TDP-43 showed elevated toxicity, which is associated with abnormal phosphorylation of the TDP-43 protein (Duan *et al.*, 2010). Increased levels of toxic free radicals have been identified in the brain and in spinal cord of SALS and FALS patients, providing *in vivo* evidence of oxidative stress in ALS patients (Tohgi *et al.*, 1999a; b; Shaw, 2005). Oxidative damage, an early feature of neurodegeneration, can be associated with other pathophysiological factors underlying neurodegenerative diseases, including mitochondrial dysfunction, excitotoxicity, and protein aggregation (Andersen, 2004; Ferraiuolo *et al.*, 2011).

1.4.3 Mitochondrial dysfunction

The Mitochondria are the centre of energy production and Ca^{+2} buffering in the cell. They act as the site of oxidative phosphorylation, cellular respiration and initiation of apoptosis. Changes in mitochondrial functions have major consequences on signalling pathways and cell survival (Dong *et al.*, 2009). For example, abnormally increased

uptake of Ca^{2+} or ROS production promotes the activation of the mitochondrial permeability transition and results in the release of proapoptotic factors and Ca^{2+} into the cytosol. These factors in turn activate caspase-dependent apoptosis or autophagocytosis by activating DNases and degrading proteins involved in DNA repair and the breakdown of cytoskeletal proteins. Autophagy can also be cytoprotective, in that stress induced mitochondrial depolarization during the permeability transition selectively removes damaged mitochondria. Other processes can also promote mitochondrial permeability transition such as stress ER stress and DNA damage (Dong *et al.*, 2009).

Abnormal mitochondrial shape is reported in SALS patients' anterior horn of spinal cord and proximal axons. Furthermore, muscle biopsies of ALS patients exhibited increased mitochondrial Ca^{2+} and volume. Observations on the function of mitochondria have produced evidence consistent with the morphological observations (Manfredi & Xu, 2005). The modification of the mitochondrial activity was concomitant with a decrease in citrate synthase (CS) activity, a mitochondrial marker in the spinal cord of these patients (Wiedemann *et al.*, 2002; Manfredi & Xu, 2005). Mitochondrial dysfunction and oxidative stress are closely linked and any changes in the bioenergetics capacity of the mitochondria generates damaging ROS leading to neurodegeneration of motor neurons (Menzies *et al.*, 2002; Andersen, 2004; Shaw, 2005).

1.4.4 Dysregulation of RNA processing

Aberrant RNA processes have been shown to contribute to motor neuron injury in ALS affecting several pathways including loss of the normal nuclear functions of TDP-43 and FUS or by toxic gains of function. TDP-43 and FUS may be involved in mRNA

transport and when mutated, could thereby contribute to motor neuron injury through failure of appropriate axonal mRNA transport (Sephton *et al.*, 2011). It has been suggested that Transportin (Trp), which is a nuclear transport receptor, may mediate nuclear import of FUS by binding to the C-terminal of FUS. Knockdown of both Trp1 and Trp2, which are two closely related proteins, results in impaired nuclear import of FUS (Dormann *et al.*, 2010), whilst knockdown of either one of the transportin receptors has no impact on the nuclear import. Mutation in TDP-43 and FUS leads to the formation of cytoplasmic aggregates disturbing cellular function in regulating transcription, alternative splicing and microRNA processing (Mackenzie *et al.*, 2010). Evidence has shown that TDP-43 binds to UG repeats in large introns, to the 3'UTR of mRNA, other mRNA binding sites and RNA processing genes, resulting in the broad dysfunctional states caused by pathogenic TDP-43 protein in ALS (Sephton *et al.*, 2011).

1.4.5 Glial cell dysfunction

Glial cells of the CNS provide the metabolic, structural and trophic support that neurons require to function. As discussed earlier, astrocytes fine-tune synaptic activity by regulating neurotransmitter activity and also play a key role in maintaining the blood-brain barrier, therefore astroglial dysfunction may either directly or indirectly contribute to the development of ALS (Ince *et al.*, 2011b). Microglia, the resident macrophages of the CNS, have crucial role in mediating phagocytosis and secrete pro-inflammatory molecules including ROS, cytokines and nitric oxide (Gonzalez-Scarano & Baltuch, 1999). Activation of microglia is an early event in the pathogenesis of ALS, which has been detected in brain and spinal cords of ALS patients and in mutant SOD₁ mice models (Engelhardt & Appel, 1990; Hall *et al.*, 1998), suggesting

a role in motor neuron degeneration. There is evidence that astrocytes mediate glutamate neurotoxicity by reduction in EAAT2 transporter expression in spinal cord of SOD1-G85R transgenic mice model and in SOD1-G93A transgenic rats (Brujin *et al.*, 1997). The release of ROS from inflammatory mediators may cause damage by increased activation of glial cells and thus reduce the trophic support glial cells provide to neurons. Furthermore, activated glial cells release ROS and activate their neighbouring cells, which may inhibit the ability of glutamate reuptake by astrocytes (Zhao *et al.*, 2004). This process has been proposed to lead to a neurotoxic effect and progressive neuronal damage (Banati *et al.*, 1993).

1.4.6 Protein aggregation

Neuropathological protein aggregates such as ubiquitinated compact and skein-like inclusions are the hallmark of ALS pathology (Ince *et al.*, 1998a; Ince *et al.*, 1998b; Piao *et al.*, 2003). Pathogenic inclusions are exported from the nucleus and accumulate in the cytoplasm (Neumann *et al.*, 2006b). To date, the causes of the protein aggregations are not fully understood, and whether they contribute to disease or are a consequence of pathology is unknown. TDP-43 inclusions may impact the normal physiological nuclear function or promote toxic gain of function due to excessive accumulation in the cytoplasm (Dormann *et al.*, 2010).

There is evidence that misfolded proteins accumulate in ALS due to endoplasmic stress (Yamagishi *et al.*, 2007). Furthermore, the production of misfolded proteins has been shown to occur at the early stages of ALS, along with both ER resident chaperones and the unfolded protein response in the mutated SOD₁ mice model and in samples from human SALS patients (Atkin *et al.*, 2006; Atkin *et al.*, 2008). SOD1 inclusions have been found within motor neurons of FALS patients and transgenic models of

disease (G93A and G85R lines), and small eosinophilic Bunina bodies are observed in MNs in the majority of cases (Shibata *et al.*, 1996; Piao *et al.*, 2003; Okamoto *et al.*, 2008). In ALS patients with FUS mutations, cytoplasmic inclusions of the protein are observed in the spinal cord (Hewitt *et al.*, 2010). The resulting protein aggregates are reported to contain peripherin and neurofilament heavy chain (Ferraiuolo *et al.*, 2011). A greater understanding of the composition of the protein aggregates will provide invaluable information about disease pathogenesis.

1.4.7 Impaired axonal transport

Neurofilaments are the major component of neuronal cytoskeleton which provides structural support for axons and regulate axonal diameter. Neurofilament proteins are synthesized in the motor neuron cell body, and transported through the axon by slow axonal transport. Motor neurons have long axons, which can be in excess of 1m in length; therefore they require transport of RNAs, proteins and organelles to axonal compartments (Shaw, 2005). Microtubule-dependent-kinesins are the axonal molecules that mediate the anterograde transport of axonal products towards the neuromuscular junction (NMJ), whereas cytoplasmic dynein has a retrograde transport activity towards the cell body to provide an effective intracellular transport system (Kieran *et al.*, 2005; De Vos *et al.*, 2007; Bilstrand *et al.*, 2010). The accumulation of abnormal neurofilament rich inclusions, including compact inclusions and Lewy body, is one of the hallmarks of ALS (Shaw, 2005). Mutations in the genes encoding microtubule associated tau protein, neurofilament heavy chain and intermediate filament protein (peripherin) have been identified in ALS patients (Hutton *et al.*, 1998). Transgenic mice with mutant SOD₁ have demonstrated reduced neurofilament protein and a concomitant decline of the axon calibre in the spinal cord, suggesting

correlation between impaired axonal transport and defective neurofilament proteins (Zhang *et al.*, 1997; Beaulieu *et al.*, 1999). As a result, oxidative damage, mitochondrial dysfunction and any other defective cellular mechanisms, may contribute to motor neuronal toxicity in ALS (see figure 1.2).

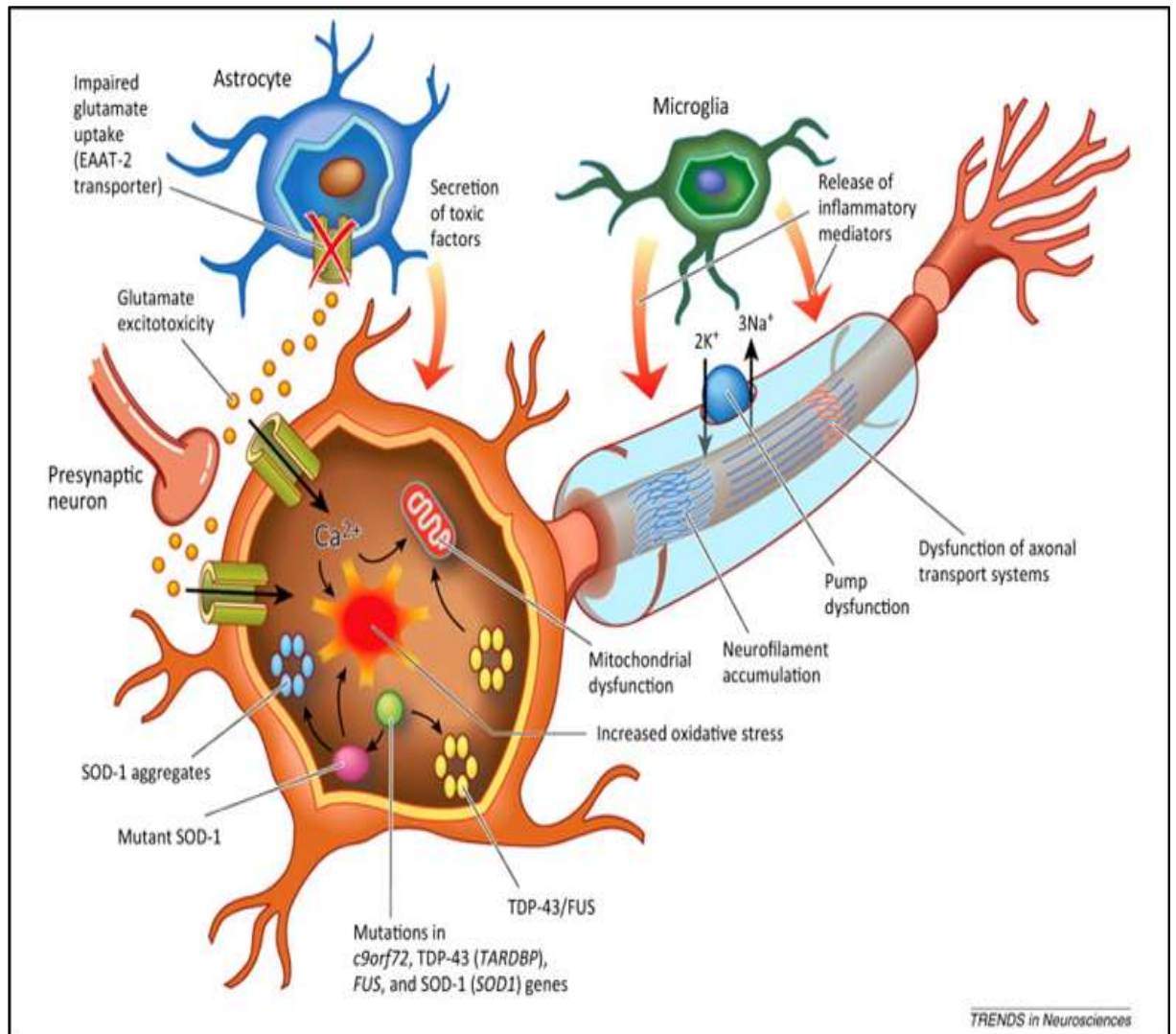


Figure 1.2: The pathogenic mechanisms that contribute to motor neuron injury in ALS

The underlying neurodegenerative pathology of ALS is multifaceted involving molecular and genetic pathways. For instance, the dysfunctional regulation of the excitatory amino acid transporter 2 (EAAT2) leads to glutamate-induced excitotoxicity because of the reduced reuptake of glutamate in the synaptic cleft. Glutamate-induced excitotoxicity promotes the generation of free radicals and the influx of Na⁺ and Ca²⁺ ions, which ultimately leads to neurodegeneration. Additionally, mutations in *TARDBP*, *FUS* and *C9ORF72* can contribute to the formation of harmful intracellular aggregates. Furthermore, the mutation of *SOD1* is known to promote mitochondrial dysfunction, oxidative stress and intracellular aggregates that inhibit neurofilaments and axonal transport process. Increased activation of glial cells promotes the release of ROS from proinflammatory cytokines that may reduce the trophic support of glial cells to neurons, which may inhibit the ability of glutamate reuptake by astrocytes. This process has been proposed to contribute to neurodegeneration, obtained from (Vucic *et al.*, 2014) with permission 3512501326588 (Kiernan *et al.*, 2011).

1.5 Aberrant RNA editing of glutamate receptors in ALS

Adenosine deaminase acting on RNA (*ADAR*) was first discovered in *Xenopus laevis* and calf thymus using a non-specific dsRNA deamination assay (Hough & Bass, 1994; Kim *et al.*, 1994; O'Connell & Keller, 1994). The *ADAR* family of enzymes in mammals consists of three structurally related isoforms; *ADAR1*, *ADAR2* and *ADAR3*, and each of them have two or three double stranded RNA binding domains in the N-terminus and one deaminase domain in the C-terminus (Bass, 2002) (see figure 1.3). *ADAR1* and *ADAR2* are predominantly expressed in the nucleus of most tissues especially in the CNS, in contrast to *ADAR3* that is expressed in the brain, mostly in the cerebellum and thalamus, and can also be found in the cytoplasm (Keegan *et al.*, 2001; Bass, 2002; Keegan *et al.*, 2004). RNA editing is a post-transcriptional modification catalysing the conversion of adenosines into inosines which are then translated to guanosines. The common type of RNA editing is Adenosine-to-Inosine (A-to-I) catalysed by *ADAR2* which, for example, occurs in the pre-mRNA of AMPA receptor subunit *GLUR2* at Q/R site (Bass, 2002; Keegan *et al.*, 2004). Both *ADAR1* and *ADAR2* edits *GLUR2* at the Q/R site as determined in general *ADAR2* knock out mice. *ADAR2* enzymatic activity was inhibited by exchanging exon 4, the enzyme functional adenosine deaminase domain, with PGK-neo cassette (Higuchi *et al.*, 2000). Knockout mice containing the inactive mutant *ADAR2* resulted in reduced *GLUR2* RNA editing compared to wild-type mice. This would suggest that *ADAR2* is the main RNA editing enzyme at the Q/R site, and the residual low level of Q/R site editing in *GLUR2* pre-mRNA is perhaps mediated by *ADAR1*, for which the gene expression was unaltered in *ADAR2* knockout mice (Higuchi *et al.*, 2000).

In the adult it is thought that the AMPA receptor subunit *GLUR2* is fully edited at the Arg607 (Q/R) site, protecting neuronal cells by causing a change from a glutamate to an arginine residue on the receptor channel. Failure to edit at this site could result in increased channel permeability to Ca^{+2} , further anion conductance, as well as alteration of current/voltage kinetics and only allow Na^{+} influxes (Barbon *et al.*, 2003; Kwak & Kawahara, 2005) (see figure 1.4). It has been demonstrated that deficient or absence of *GLUR2* RNA editing occurs specifically in motor neurons of SALS cases, and not in other neuronal cells such as spinocerebellar and Purkinje cells, leading to the hypothesis that altered *GLUR2* editing may be motor neurone specific (Kawahara *et al.*, 2003; Kawahara *et al.*, 2004; Kwak & Kawahara, 2005). It has been suggested that abnormal *GLUR2* is specific to motor neurons of SALS patients and it is not linked to other motor neuron diseases such as spinal and bulbar muscular atrophy and SOD1-associated ALS (Kawahara *et al.*, 2003; Kawahara *et al.*, 2004; Kwak & Kawahara, 2005; Kawahara *et al.*, 2006). However, another study found that abnormal *GLUR2* editing at Q/R site can occur in a wide spectrum of non-motor neurological diseases including the prefrontal cortex of Alzheimer's disease (AD), prefrontal cortex and striatum of schizophrenic patients as well as the striatum of patients with Huntington's disease (HD) (Akbarian *et al.*, 1995). *GLUR2* RNA editing of > 99 % maintains healthy motor neurons (Seeburg *et al.*, 1998). Mice with deficient RNA editing of *GLUR2* are born with epilepsy and die about 3 weeks after birth. The unedited *GLUR2* receptor at Q/R site participates in the slow death of motor neurons, which can be rescued by restoring RNA editing (Brusa *et al.*, 1995; Higuchi *et al.*, 2000).

GLUR5 and *GLUR6* of kainate (KA) receptor subunits also undergo Q/R site editing by *ADAR2* in the channel pore forming the so-called P-loop (at 636Arg and 621Arg, respectively) (Caracciolo *et al.*, 2013). These subunits were found to be partially

permeable to Ca^{+2} and unlike *GLUR2* are not fully edited at the Q/R site (Köhler *et al.*, 1993; Seeburg *et al.*, 1998). *GLUR5* and *GLUR6* editing at the Q/R site is developmentally regulated. The editing of *GLUR5* and *GLUR6* reach values of up to 55% in the rat embryo and 85% in the adult rat brain. The extent of *GLUR5* editing at the Q/R site was differentially modulated in the control human brain of 50% editing in spinal cord and cerebellum reaching to 70% of edited *GLUR5* at the thalamus, amygdala and hippocampus (Barbon *et al.*, 2003). *GLUR6* editing levels in control human brain were differentially regulated and reported to be above 67% editing in thalamus, cerebellum, amygdala and hippocampus, whilst the spinal cord showed 31% editing of *GLUR6* (Barbon *et al.*, 2003). The edited forms of *GLUR5* and *GLUR6* have markedly reduced anion channel permeability and low single channel conductance (Caracciolo *et al.*, 2013).

A-to-I RNA editing of *GLUR2* can also occur at other editing sites including at 764Gly, where an arginine (R) is replaced by glycine (G) changing the desensitisation kinetics of receptors containing edited subunits (Sommer *et al.*, 1991; Lomeli *et al.*, 1994). The R/G editing of *GLUR2* is largely unedited in the embryonic brain and rises after birth.

Other editing sites were found at *GLUR6*; I/V site, where isoleucine can be substituted with valine (at 567Val) and Y/C site, where tyrosine can be replaced by cysteine (at 571Cys) located in the transmembrane 1 domain (TM1) (Bass, 2002) (see table 1.2). Editing at these sites in cooperation with Q/R site modulates finer regulation of Ca^{+2} permeability in the Q/R site. The mechanism of interaction among Q/R, Y/C and I/V sites remains to be elucidated (Köhler *et al.*, 1993; Barbon *et al.*, 2003). A study showed that editing of *GLUR6* at Q/R and Y/C site in the spinal cord of control human

brain had similar levels of 31% editing. Whereas, editing of *GLUR6* at I/V was reduced to 20% of editing (Barbon *et al.*, 2003).

Impaired or absent *ADAR2* may also contribute to the pathogenesis of ALS. Hideyama and colleagues have reported lowered *GLUR2* editing at Q/R site. One method used was the Cre-loxP recombination system to inhibit and restore *ADAR2* activity by exchanging the point mutated allele with wild type allele of *ADAR2* (Hideyama *et al.*, 2010). The other method was a general *ADAR2* knock out mouse, functional null alleles are generated by completely removing the *ADAR2* enzyme and cannot be restored by replacing exon 4 that encodes for functional adenosine deaminase motif with PGK-neo cassette to delete *ADAR2* enzyme and thus stop its function (Higuchi *et al.*, 2000). In both cases either inhibition or absence of *ADAR2* activity has led to the same observation: which is lowered *GLUR2* RNA editing in mice models (Brusa *et al.*, 1995; Higuchi *et al.*, 2000; Hideyama *et al.*, 2010; Hideyama & Kwak, 2011). Reduced *ADAR2*, but not *ADAR1* and *ADAR3*, has been demonstrated in the motor neurons of SALS patients (Hideyama *et al.*, 2012b). Interestingly, deficient *ADAR2* is associated with mislocalisation of TDP-43, similar to the TDP-43 pathology seen in SALS patients (Aizawa *et al.*, 2010; Hideyama *et al.*, 2012a; Hideyama *et al.*, 2012b).

ADAR3 is structurally similar to *ADAR2* containing one deamination domain and two double-stranded RNA binding motifs (dsRBMs) required for RNA editing. However, *ADAR3* is found to be catalytically inactive and unable to bind dsRNA of *GLUR2* at Q/R or R/G site, as determined by studies using purified recombinant *ADAR3* proteins carrying an epitope-tagged peptide FLAG at the N-terminus and produced in Sf9 insect cells *in vitro* (Chen *et al.*, 2000). The function of *ADAR3* is as yet unknown. However, studies have suggested that *ADAR3* might have a role in ALS with *C9ORF72*

expansion repeats. In experiments using induced pluripotent stem cells differentiated into neurons (iPSNs), a group has found ADAR3 within the complex of the *C9ORF72* repeats in the iPSNs tissue of ALS *C9ORF72* without further characterisation of the role of *ADAR3* in ALS with *C9ORF72* nor its relation to RNA editing (Almeida *et al.*, 2013; Donnelly *et al.*, 2013; Todd & Paulson, 2013). Therefore, future studies needed to investigate the impact of ALS cases with the *C9ORF72* expansion on *ADAR3* as a member of the *ADAR* family.

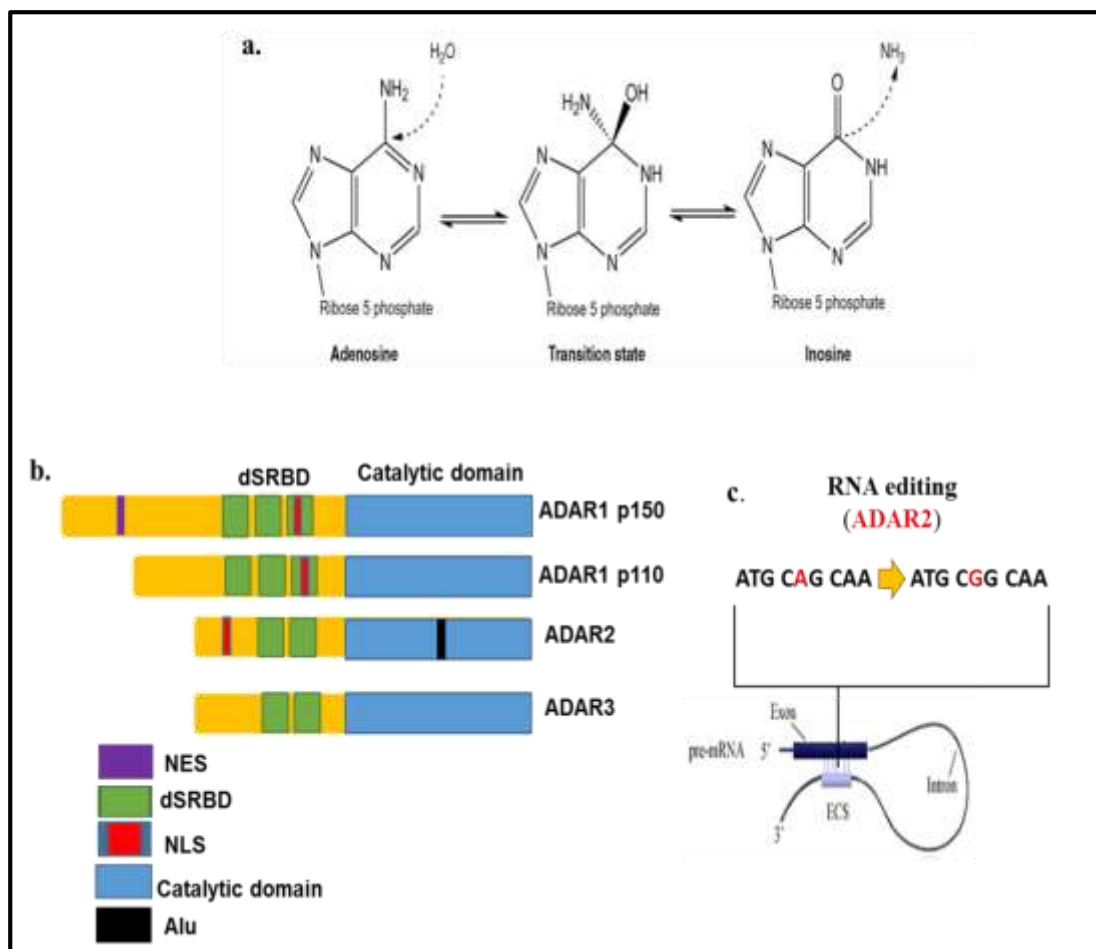


Figure 1.3: ADAR2 deamination of *GLUR2* at Q/R site.

(a) Hydrolytic deamination mediates A-I conversion. (b) Members of *ADAR* family showing catalytic domain required for editing, double stranded binding motifs (dsRBM), Nuclear export signal (NES), Nuclear localisation sequence (NLS), Alu sequences (Alu). (c) *ADAR2* catalyses of *GLUR2* at Q/R site (A-I conversion) within dsRNA in coding region consisting of intron 11 and exon 11 complementary sequence (ESC) in coding and non-coding region. Figure a. was obtained from (Farajollahi & Maas, 2010) with permission 3512491421010 (b) Figure b and c. was modified from (Hideyama & Kwak, 2011).

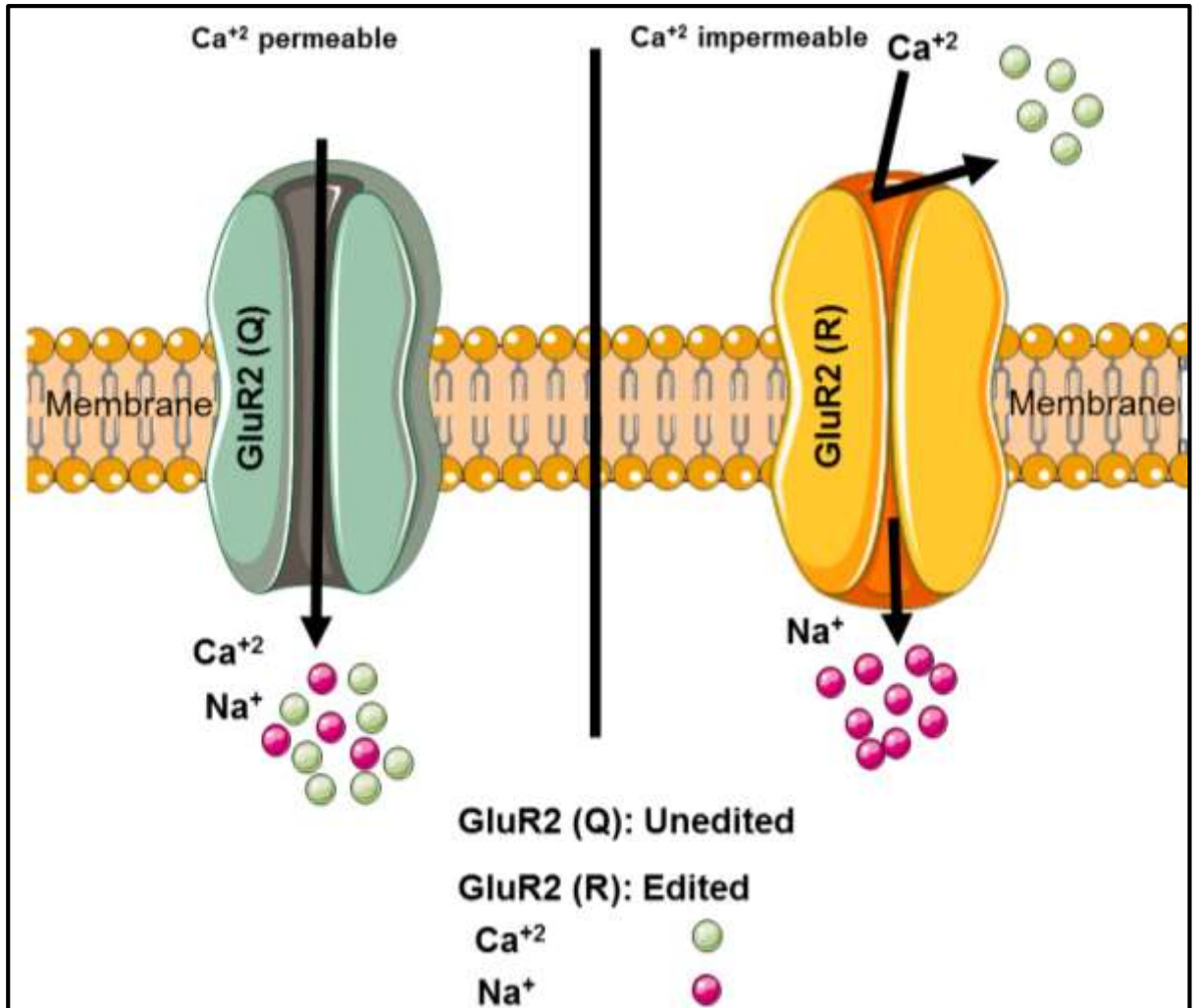


Figure 1.4: Permeability of *GLUR2* at Q/R site.

AMPA receptor subunit *GLUR2* located on the second transmembrane domain (M2) showing impermeable Ca²⁺ influx caused by edited *GLUR2* (R) at Q/R site. (a). Whereas unedited form of *GLUR2* within AMPA receptor is showing lack of edited *GLUR2* (Q) at Q/R site resulting in permeable AMPA receptor, modified from (Hideyama & Kwak, 2011).

1.6 Aims and Hypothesis

Glutamate excitotoxicity plays a key role in a range of neurodegenerative pathologies, including ALS. Possible explanations underlying excitotoxicity in motor neurons in ALS include (i) impaired RNA editing of glutamate receptors (ii) reduced *ADAR2* activity, responsible for editing of *GLUR2*, *GLUR5* and *GLUR6* at multiple sites, and (iii) aberrant transcripts of *EAAT2*. Therefore, the current study hypothesised that (i) altered glutamate receptor editing in motor neurons in ALS is relevant to pathogenesis. (ii) There is no relationship between mRNA expression of *ADAR2* and *ADAR3*. (iii) A decrease in *EAAT2* mRNA expression contributes to the excitotoxicity associated with ALS. (iv) MNs from *ALS/C9ORF72*-positive patients have more inclusions than *ALS/C9ORF72*-negative patients. (v) *GLUR2* protein levels do not contribute to *GLUR2* editing. (vi) Decreased *ADAR2* and *EAAT2* expression in ALS contributes to excitotoxicity mediated MN loss. (vii) Altered *ADAR3* expression is not linked to *ADAR2* and *GLUR2* editing. (viii) Use of next generation sequencing will allow in-depth analysis of the *GLUR2*, *GLUR5* and *GLUR6* as well as *ADAR2*, *ADAR3* and *EAAT2* RNA species.

The aims of this study were (i) to investigate RNA editing of *GLUR2*, *GLUR5* and *GLUR6* in the pathogenesis of ALS disease and determine the differences between edited RNA levels of glutamate receptors in controls compared to *ALS/C9ORF72*-positive and *ALS/C9ORF72*-negative patients. (ii) To determine the *ADAR2* and *ADAR3* gene expression in the spinal cord from ALS versus control cases. Because of the emerging roles of astrocytes in excitotoxic pathway leading to neurodegeneration this study also aimed (iii) to determine the normal and aberrant alternative transcripts particularly, exon 4 and 9 in *ALS/C9ORF72*-positive and *ALS/C9ORF72*-negative patients compared to controls. (iv) Identify the

neuropathological features of motor neurons and astrocytes in the thoracic spinal cord of a well characterised cohort of *ALS/C9ORF72*-positive and *ALS/C9ORF72*-negative compared to non-neurological controls. (v) To develop new methodology to look at different levels of expression that might exist in ALS.

Chapter 2
Materials and Methods

Chapter 2: Materials and Methods

2.1 Materials and their suppliers

Table 2.1: Equipment, chemicals and enzymes, antibodies and solutions.

Equipment	Suppliers
The Arcturus Laser Capture Microdissection System	Applied Biosystems Life Technologies
Antigen access unit	MenaPath
Nikon Eclipse Ni microscope	Nikon
Autostainer	Intellipath
Cryostat	Leica
Microscope slides	Leica, UK
Arcturus® CapSure® Macro LCM Caps	Applied Biosystems Life Technologies
Thermo Cycler	MJ Research
M3000P Qpcr	Agilent Technologies
Homogeniser	Kontes Glass, Anechem LTD.
Flash gel system	Lonza
NanoDrop 1000 Spectrophotometer	Labtech International, UK
DNA chip 1000	Agilent Technologies
BioAnalyser	Agilent
Geni box	Syngene
Next generation sequencing (Hi scan SQ system)	Illumina
Agencourt AMPure XP beads	cat number A63881, Beckman Coulter
Chemicals and enzymes	Suppliers
Ethylenediaminetetra- acetic acid (EDTA)	AnalaR, BDH Laboratory Supplies
Tri-sodium citrate (TSC)	Fisher Chemical
Access revelation TSC pH. 6	MenaPath
Xylene	Fisher scientific
Tris	Fisher scientific

Ethanol	Fisher scientific
Ethidium bromide	Fluka
DPX mounting media	Leica
The VECTASTAIN® Elite® ABC system	VECTOR Laboratories
Haematoxylin and eosin	Leica
Toluidine blue	Sigma
RNA PicoPure Isolation kit	Applied Biosystems Life Technologies
RNAqueous®-Micro Kit	Ambion
NucleoSpin kit	Macherey -Nagel
NEBNext mRNA second strand synthesis	NEB, cat number E6111, New England Biolabs
Nextera XT DNA sample preparation kit	Illumina
KAPA Illumina library quantification kit	cat number KK4824, Anachem
qscript™ cDNA supermix	Quanta Biosciences
QuantiTect reverse Transcription	QIAGEN
Dream Taq Green PCR master mix	Thermo Scientific
Brilliant III SYBR® Green qPCR Master Mix	Agilent Technologies;
QIAquick Gel Extraction	QIAGEN
RNase-free water	QIAGEN
Hyperladder V	Bioline
Agarose powder	Melford
Primers	Eurofins, mwg operon (Germany)
BbVI restriction enzyme	Fermentas
Affinity script cDNA synthesis	Agilent Technologies
MessageBOOSTER Whole Transcriptome cDNA Synthesis	Epicentre kit, cat number MBWT80510
Illumina Nextera XT kit	cat number 15031942, Illumina
Antibodies	Suppliers
p-TDP-43	CosmoBio (2B scientific)
p62	BD (610833)
Polyclonal Rabbit Anti-Glial Fibrillary Acidic Protein (GFAP)	DAKO cytotation

Polyclonal mouse Anti-RED1	Abcam
Polyclonal Rabbit Anti-ADARB2	Sigma
Monoclonal Mouse Anti-EAAT2	Leica Biosystems
AntiMouse IgG, VECTASTAIN Elite ABC Kit	Vector Laboratories
Antirabbit IgG, VECTASTAIN Elite ABC Kit	Vector Laboratories
Solutions	
Tris- acetate-EDTA (TAE) (1x) 40mM Tris base, 20mM acetic acid, 1mM EDTA, pH 8.0	
Tris-buffered saline (TBS) (1x) 50mM Tris, pH 7.6, 150mM NaCl	
Trisodium Citrate buffer (TSC) (1L) 11.6mM Na ₃ C ₆ H ₅ O ₇ , made up to 1L with deionized water, pH6	
Ethylenediaminetetra- acetic acid (EDTA) (1L) 1mM of C ₁₀ H ₁₆ N ₂ O ₈ , made up in 1L of dH ₂ O, pH to 8	
Avidin-biotin peroxidase complex Vectastain Elite ABC Kit in 50mM TBS	
Scotts Tap water (2.5L) 41mM of sodium bicarbonate (NaHCO ₃) and 166mM magnesium sulphate (MgSO ₄), made up in 2.5L deionized water	
Gill's haematoxylin 6g of haematoxylin, 4.2g of aluminium sulphate, 1.4g of citric acid 1.4g, 0.6g sodium iodate, 269ml of ethylene glycol, made up in 680ml of dH ₂ O.	

2.2 Human CNS tissue

Post-mortem human CNS tissue was obtained from the Sheffield Brain Tissue Bank located at the Royal Hallamshire Hospital, following ethical approval (MRC no.12/007) (see appendix I). Brain tissue of sporadic ALS patients and subjects free from neurological disorders were donated and consented by informed next of kin. Research was carried out in accordance with the approval of Ethics Committee of University of Sheffield.

Formalin fixed paraffin embedded (FFPE) tissue was obtained from readily available lumbar spinal cord sections of one familial ALS that carry *C9ORF72* repeat expansion (FALS/*C9ORF72*-positive case), thoracic spinal cord section of one apparently sporadic ALS patient which have subsequently been shown to carry *C9ORF72* repeat expansion (SALS/*C9ORF72*-positive case) and cervical spinal cord sections of one sporadic ALS case that do not carry any known genetic mutations associated with ALS (SALS case) (see table 2.2). For the purpose of this thesis, FALS/*C9ORF72*-positive, SALS/*C9ORF72*-positive case and SALS will be used.

Snap-frozen tissue was obtained from frontal cortex of 3 SALS cases and 5 controls free from neurological disease, motor cortex of 4 SALS cases and 3 non-neurological controls, thalamus, cerebellum, temporal cortex and motor cortex of one case with Pick's disease (see table 2.2). Snap-frozen readily available lower thoracic spinal cord (T11) from 5 apparently sporadic ALS patients which have subsequently been shown to carry *C9ORF72* repeat expansion (5 *C9ORF72*-related ALS (ALS/*C9ORF72*-positive) and 5 sporadic ALS patients that do not carry any known genetic mutations associated with ALS (ALS/*C9ORF72*-negative) and 5 non-neurological controls (see table 2.2). For the purpose of this thesis ALS/*C9ORF72*-positive and ALS/*C9ORF72*-

negative cases will be used throughout. Donated brains were dissected following a standard protocol (Ince *et al.*, 1995) and histologically blindly assessed by consultant neuropathologists. Detailed clinical information for all the cases, PMI, gender and age at onset and age at death was recorded (see Table 2.2).

Table 2.2: Detailed clinical information for ALS cases and controls.

FFPE thoracic spinal cord from ALS patients							
Case number	Clinical Diagnosis	Area/level	PMI in hours	Sex	Age at onset	Age at death	Length of illness
ALS							
273/99 (TBP0096)	FALS/C9ORF72	Bulbar	31	M	66	68	14 months
336/90 (TBP0048)	SALS/C9ORF72	Limb	6	M	63	64	11 months
113/08 (TBP0075)	SALS	Multifocal	9	F	68	70	31 months
Frozen frontal cortex from ALS patients and controls							
Case number	Clinical Diagnosis	Area/level	PMI in hours	Sex	Age at onset	Age at death	Length of illness
ALS							
TBP0074	SALS	Bulbar	19	M	71	75	37 months
113/08 (TBP0075)	SALS	Multifocal	9	F	68	70	31 months
136/97	SALS	n/a	16	F	76	78	13 months
Controls							
136/95	Control	n/a	10	F	n/a	87	n/a
147/95	Control	n/a	15	M	n/a	47	n/a
178/95	Control- Ischaemic Heart disease	n/a	24	F	n/a	63	n/a
35/96	Control	n/a	14	F	n/a	87	n/a
95/96	Control	n/a	n/a	n/a	n/a	n/a	n/a
Frozen motor cortex from ALS patients and controls							

Case number	Clinical Diagnosis	Area/level	PMI in hours	Sex	Age at onset	Age at death	Length of illness
ALS							
53/96 (TBP0070)	SALS/C9ORF72	Bulbar	7	F	61	64	40 months
159/96 (TBP0078)	SALS	Bulbar	20	M	41	43	23 months
137/96 (TBP0076)	SALS/UMN	Multifocal	9	F	56	65	99 months
57/97 (TBP0083)	SALS/PLS	Bulbar	18	F	76	78	26 months
Controls							
66/96 (TBP0071)	Control	Bulbar	10	F	70	73	37 months
144/96	Control	n/a	n/a	n/a	n/a	n/a	n/a
194/96	Control	n/a	n/a	n/a	n/a	n/a	n/a
Frozen tissue from different CNS regions of one case with PICK's disease							
Case number	Clinical Diagnosis	Area/level	PMI in hours	Sex	Age at onset	Age at death	Length of illness
10/96	Pick's disease	n/a	22	F	n/a	63	n/a
Temporal cortex							
Cerebellum							
Thalamus							
Motor cortex							
FFPE and frozen thoracic spinal cord from ALS cases and controls							
Case number	Block Number	Area/Level	Site of onset	PMI in hours	Sex	Age at onset	Age at death
ALS/C9ORF72-positive cases							
LP83/10	34	T11	Limb	13	Male	67	79
LP081/09	29	T11	Limb	60	Male	57	59

LP041/04 (TBP0110)	6	T11	Bulbar	48	Male	62	64
LP039/11	26	T11	Limb	96	Male	70	72
LP040/11	25	T11	Limb	10	Female	72	77
ALS/C9ORF72-negative cases							
LP014/11	24	T11	Limb	n/a	Male	49	51
LP005/11	30	T11	Limb	40	Female	62	67
LP023/10	7	T11	Limb	24	Female	34	42
LP005/10	23	T11	Limb	96	Male	38	40
LP094/09	25	T11	Bulbar	48	Male	62	63
Controls							
LP005/07	13	T11	n/a	12	Male	-n/a	64
LP085/07	25	T11	n/a	5	Female	-n/a	82
LP098/07	25	T11	n/a	63	Male	-n/a	67
035/96	8	T11	n/a	14	Female	-n/a	87
117/04	n/a	n/a	n/a	n/a	Male	-n/a	58

Available thoracic spinal cord, motor cortex and frontal cortex blocks were identified for the study and these cases were characterised by neuropathologists who were blind to any clinical information. Cases were categorised into FALS, SALS and apparently sporadic ALS with *C9ORF72* repeat expansion (ALS/*C9ORF72*-positive) and sporadic ALS without *C9ORF72* repeat expansion (ALS/*C9ORF72*-negative) and non-neurological controls. Cases were matched as closely as possible in their clinical diagnosis, PMI in hours, age and gender except for one patients with PICK disease that was initially identified as a control and later appeared to be a PICK patient. Abbreviation: N/A- not available.

2.3 RNA applications

2.3.1 FFPE and frozen tissue preparation

The post-mortem FFPE spinal cord was fixed in 10% formalin for 24 hours up to 48 hours then washed twice in 70% ethanol for 1hour, 80% ethanol for 1hour and 95% ethanol and finally washed three times in 100% ethanol for 1.5 hours to remove any water. Tissue blocks were then immersed three times in xylene for 1.5 hours and embedded in paraffin. The FFPE tissue blocks were sectioned into 7µm and collected on glass slides, dried overnight at 50°C and stored at room temperature. Whereas, the post-mortem frozen tissue blocks were embedded in mounting media (OCT) and sectioned (7µm) in a cryostat at -20°C. Sections were collected on uncoated, sterile microscope slides, and warmed to room temperature (RT) for approximately 30 seconds.

2.3.2 Histological staining of spinal cord for Laser Capture

Microdissection (LCM)

To visualise motor neurons for microdissection, FFPE and frozen spinal cord sections were stained with toluidine blue. FFPE sections were dewaxed twice in xylene for 5 minutes followed by rehydration of the material by graded alcohol: 100% ethanol ×2 for 3 minutes, 95% ethanol for 3 minutes and 70% ethanol for 3 minutes. Tissue sections were then immersed in toluidine blue for 40 seconds, washed in diethyl pyrocarbonate (DEPC)-treated water, dehydrated through graded series of ethanol for 30 seconds. Once tissue sections were dehydrated, sections were cleared twice in xylene for 5 minutes and air dried for 1 hour, making them ready for LCM.

The frozen spinal cord sections were fixed in acetone for 3 minutes, immersed in toluidine blue for 40 seconds, washed in DEPC-treated water, dehydrated through graded series of ethanol for 30 seconds each and cleared in xylene twice for 5 minutes before being air dried for 1 hour.

Approximately 200 motor neurons from each case were picked by LCM.

Astrocytes were isolated by LCM combined with a rapid immunoprotocol to identify astrocytes (Waller *et al.*, 2012). Following sectioning of the spinal cord to 7µm and its collection onto uncharged glass slides, tissue sections were warmed to RT for 30 seconds, then fixed in cold acetone for 3 minutes and blocked in 2% normal serum for 3 minutes at RT. Section were incubated with GFAP antibody (1:50 dilution), washed with TBS before being incubated with 5% biotinylated secondary antibody for 3 minutes at RT. Sections were washed with TBS then incubated with 4 % ABC-HRP reagent for 3 minutes at RT. Sections were washed with TBS then DAB was used to visualise where the antibody had bound. The reaction was quenched in water, and the sections dehydrated through increasing concentrations of alcohol for 30s, cleared in xylene twice for 5 minutes and air dried for at least 1 hour. Approximately 1000 astrocytes were picked followed by RNA extraction.

2.3.3 RNA extraction from FFPE tissue

RNA extractions from FFPE tissue sections were optimised using RNAqueous-Micro kit from Ambion. According to the manufacturer's protocol, a 100µl of lysis solution was added to the sample and incubated for 30 minutes at 42°C. Samples were briefly vortex and centrifuged to collect the fluid at the bottom of the tube. Micro Filter Cartridge was wet with 30µl of lysis solution and incubated for 5 minutes then centrifugation of the prewetted filter for ~30 seconds at top speed to remove liquid.

3µl of the LCM Additive solution was added to the lysate and mixed well by vortexing. 129µl of 100% ethanol was added to the lysate and mixed by gently vortexing. Lysate mixture was passed through Micro Filter Cartridge by centrifuge for 1 minute at 10,000 x g to bind the RNA to the filter. An 180µl of wash solution 1 was added to the filter and centrifuged for 1 minute at 10,000 x g. Followed by another two washes with wash solution 2 by adding 180µl to the filter and centrifuge for 1 minute at 13,000 x g. The flow-through was discarded and the filter was centrifuged for 1 minute at 13,000 x g. RNA was eluted in 10µl of preheated elution solution to 95°C, then incubate for 5 minutes at RT and centrifuged for 1 minute at 13,000 x g.

2.3.4 RNA extraction from frozen total spinal cord

RNA extractions were carried out on one section of a 20µm of spinal cords using NucleoSpin kit (Macherey -Nagel), according to the manufacturers` instructions. All centrifugation in the protocol was performed for 1 minute at 11,000xg, unless otherwise stated. 50µm tissue sections were suspended in 350µl of Guanidinium thiocyanate (RA1) and 3.5µl of B-mercaptoethanol. The cell suspension was added to a NucleoSpin® column and centrifuged. The flow through was mixed with 350µl of 70% ethanol and loaded into a NucleoSpin column, centrifuged and washed with 350µl of membrane desalting buffer (MBD) by centrifugation. The column was loaded with 95µl of the DNase reaction mixture and incubated at RT for 15 minutes. 200µl of the Guanidinihydrochloride-Ethanol buffer (RAW2) was added to the column and centrifuged. The column was washed twice in washing buffer (RA3), firstly with a volume of 600µl and then with 250µl. The column was dried by centrifugation for 2 minutes and the RNA eluted in 60µl of RNase-free water by centrifugation.

2.3.5 RNA extraction from LCM-isolated motor neurons and astrocytes

On average 200 motor neurons were picked from 10 frozen tissue sections by LCM and 1000 astrocytes were isolated from 7 frozen tissue sections of the spinal cord. The RNA was extracted from LCM isolated motor neurons or astrocytes using the RNA PicoPure (Arcturus) Isolation kit, according to the manufacturer's protocol. The film was carefully removed from the LCM cap using sterile tweezers and placed in a sterile 0.2 ml eppendorf. 50µl of extraction buffer was added to the captured cells and incubated at 42°C for 30 minutes on the thermocycler, followed by centrifugation at 800xg for 2 minutes at RT, at this stage the cell extracts could be stored at -80°C. To isolate RNA from the samples, RNA purification columns were pre-conditioned with 250µl of conditioning buffer for 5 minutes at RT, then centrifuged at 16,000xg for 1 minute. 50µl of 70% ethanol was added to the sample extract and mixed thoroughly by pipetting up and down. The mixture of sample extract and ethanol was added to the pre-conditioned purification column and centrifuged at 100xg for 2 minutes at RT, enabling RNA to bind to the column. The columns were centrifuged at 16000xg for 30 seconds and the flow through discarded. 100µl of wash buffer 1 was added to the purification column and centrifuged at 8000xg for 1 minute at RT. 100µl of wash buffer 2 was added to the purification column and centrifuged at 8000xg at 1 minute. An additional centrifugation step of 16,000xg for 1minute was performed to remove any remaining buffer from the column. The RNA column was transferred to a sterile 1.5 ml microcentrifuge tube, and the total RNA was eluted in 11µl of RNase-free water at 12,000xg for 1 minute.

2.3.6 RNA integrity and cDNA synthesis

The amount of total RNA was quantified using the NanoDrop 1000 Spectrophotometer and the RNA quality assessed on the Pico chip Bioanalyser. 50ng of RNA was added to 4µl qScript™ cDNA super mix (thawed on ice) and RNase-free water was added to make a total reaction volume of 20µl. The mixture was incubated in the thermal cycler to amplify cDNA for 5 minutes at 25°C, followed by 30 minutes at 42°C, and finally the reaction was deactivated for 5 minutes at 85°C.

2.4 Designing primers

The primer sequence for GLUR2, GLUR5 and GLUR6 was identified using National Centre for Biotechnology information website (NCBI) then inputted into the Primer3 plus website (<http://www.bioinformatics.nl/cgi-bin/primer3plus/primer3plus.cgi>). (see figure 2.1- 2.3). Forward and reverse primers were selected (see table 2.3).

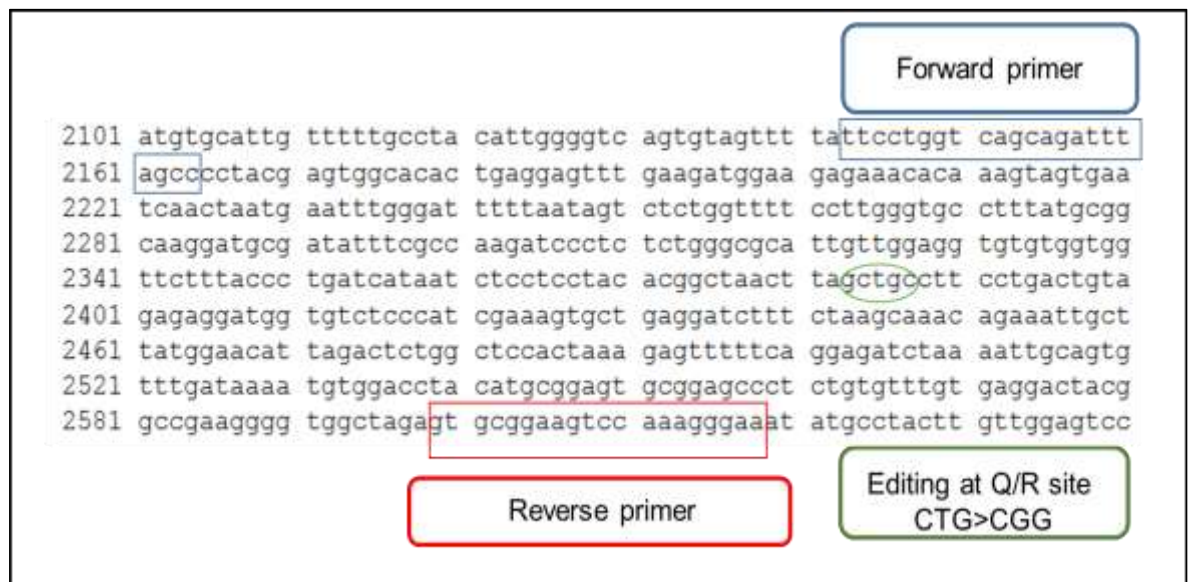


Figure 2.1:GLUR2 (NM-000826) sequence showing editing at Q/R site.

GLUR2, also called *GRIA2*, gene is located on chromosome 4q 32.1. Forward primers are highlighted in blue and reverse primers are highlighted in red. The *BbvI* (*BseXI*) highlighted in green recognizes GCAGC editing site and cut *GLUR2* at Q607 (CTG) to R (CGG).

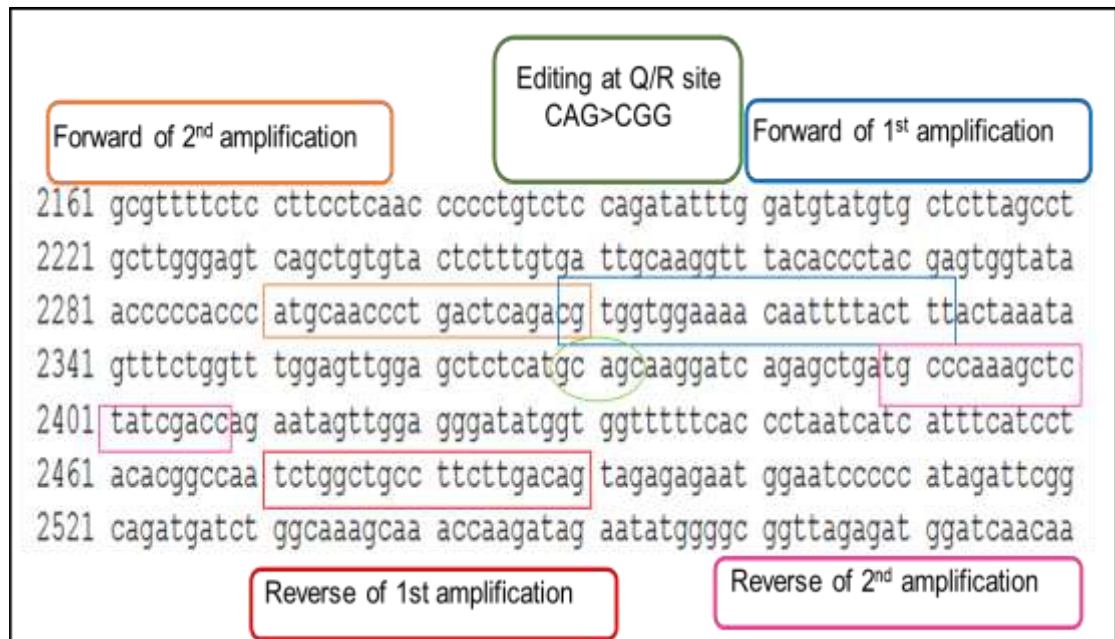


Figure 2.2: *GLUR5* (NM-000830) sequence showing editing at Q/R site.

GLUR5 also called *GRIKI* gene is located on chromosome 21q22.11, forward primers are highlighted in blue and reverse primers are highlighted in red. The *BbvI* (*BseXI*) highlighted in green recognizes GCAGC editing site and cut *GLUR5* at Q636 (CAG) to R (CGG).

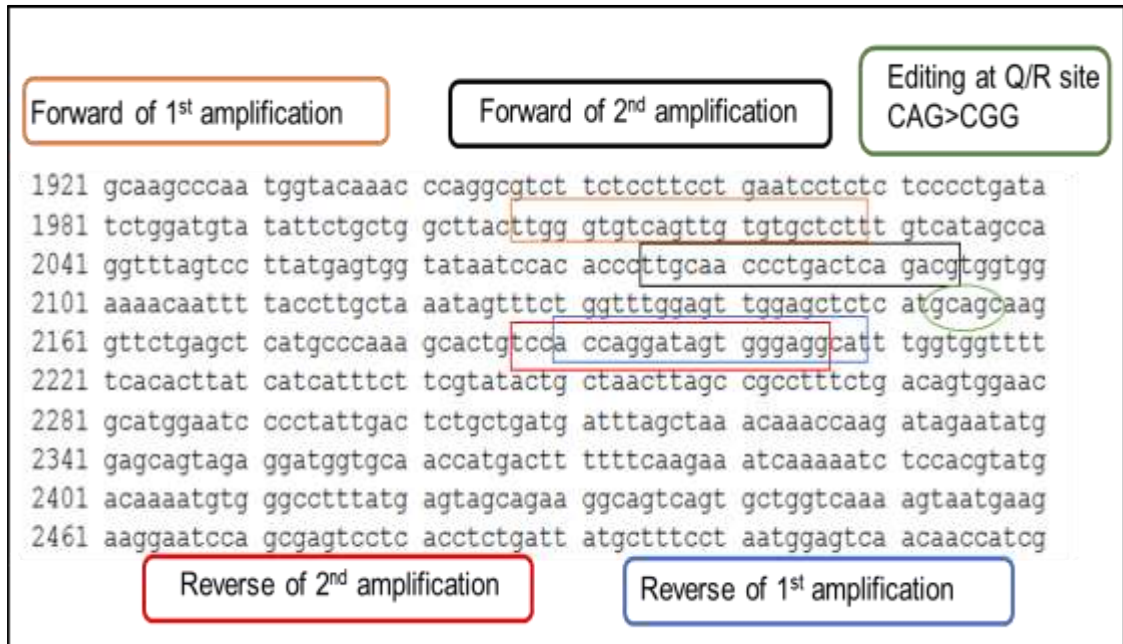


Figure 2.3: *GLUR6* (NM-021956) sequence showing editing at Q/R site.

GLUR6, also called *GRIK2*, gene is located on chromosome 6q16.3, forward primers are highlighted in blue and reverse primers are highlighted in red. The *BbvI* (*BseXI*) highlighted in green recognizes GCAGC editing site and cut *GLUR6* at Q621 (CAG) to R (CGG).

Table 2.3: Sequence of *GLUR2*, *GLUR5* and *GLUR6* primers used in the study.

Primers	Sequence reference	Position	Primer Sequence
External <i>GLUR2</i>	NM-000826.3	Forward	TTCCTGGTCAGCAGATTTAGCC
		Reverse	GTGCGGAAGTCCAAAGGGAA
External <i>GLUR5</i>	NM-000830.3	Forward	CGTGGTGGAAAACAATTTTACTTT
		Reverse	TCTGGCTGCCTTCTTGACAG
Nested <i>GLUR5</i>		Forward	ATGCAACCCTGACTCAGACG
		Reverse	TGCCCAAAGCTCTATCGACC
External <i>GLUR6</i>	NM-021956	Forward	TTGGGTGTCAGTTGTGTGCT
		Reverse	ACCAGGATAGTGGGAGGCAT
Nested <i>GLUR6</i>		Forward	TTGCAACCCTGACTCAGACG
		Reverse	TCCACCAGGATAGTGGGAGG

2.5 Reverse transcription-polymerase chain reaction (RT-PCR)

50ng of cDNA was added to 10µl of Dream Taq Green PCR master and 5pM of forward and reverse primers to give a final volume of 20µl. Primers concentrations were reduced from 10 pmol/µl to 5 pmol/µl to eliminate primer dimer formation that might interfere with the correct identification of the product of interest on DNA Chip BioAnalyser. Samples were run on the following thermal cycling conditions; initial denaturation at 95°C for 3 minutes followed by 40 cycles of denaturation at 95°C for 30 seconds, annealing at 60°C for 1 minute and extension at 72°C for 1 minutes. Final extension was at 72°C for 15 minutes. To visualise the product, samples were run on a 2% agarose gel for 40 minutes at 120V.

2.5.1 Gel purification

Following the manufacturer's protocol, DNA fragments were excised from the agarose gel with a clean scalpel, weighed and 3 volumes of QG buffer were added. The gel was incubated at 50°C for 10 minutes or until the gel completely dissolved. 1 gel volume of isopropanol was added to the sample and mixed before being added to a QLAquick spin column placed in 2 ml collection tube. The column was centrifuged for 1 minute at 17.900×g at RT and the flow through discarded. The QLAquick spin column was placed back in to the collection tube and 500µl of QC buffer was added then centrifuged for 1 minute at 17.900×g at RT. 750µl of PE buffer was added to the column, centrifuged for 1minute at 17.900×g, flow through was discarded. To ensure all the buffer was removed, the column was centrifuged for 1 minute at 17.900×g at

RT. DNA was eluted in 30 µl of dH₂O, centrifuged for 1 minute at 17.900×g, collected in a sterile tube.

An alternative method to purify PCR before digestion was flash gel system that enabled the purification of PCR products and removal of primer dimers without loss of DNA after band excision. There are two types of wells in the flash gel™ cassette: loading wells and recovery wells, which were both flooded with water prior to sample loading. 5µl of hyper ladder V and 10µl of PCR products were loaded into the flash gel cassette. The Flash gel™ cassette was placed on the flash gel™ dock and the light switched on to visualize running of the samples from the loading wells to the recovery wells. Samples were run for 5 minutes at 275 V and collected from the recovery wells. The flashGel™ Mask was placed under the recovery wells enabling sample visualization, then 10µl of water was loaded into recovery well to collect samples. Recovered samples were subsequently digested with restriction enzyme, as detailed below.

2.6 Restriction enzyme digest

The PCR product can be digested using *BbvI* or *BseXI* restriction enzymes (see figure 2.4). Both of these enzymes are able to digest double stranded DNA at a unique sequence of nucleotides in the DNA strand at the centre of the recognition sequence (GCAGC), different sized fragments, when compared to the full length PCR product, classified as edited and non-edited RNA, respectively. Briefly, 1 unit of *BbvI* restriction enzyme was used to digest 7 µl of PCR reaction by incubating at 37°C for 90 minutes, followed by inactivation at 65°C for 20 minutes. DNA cuts were visualised on DNA chip BioAnalyser.

The DNA chip was used to analyse and compare the RT-PCR products prior to digestion and restriction enzyme digests for the separation of nucleic acid fragments based on their sizes. Following manufacturer's protocol, the gel was prepared by adding 25 µl of dye concentrate to the DNA gel matrix, following centrifugation for 15 minutes at 2,400xg at 4°C. 9 µl of the gel was loaded into the G-well then pressure plunging was applied to distribute the gel. The DNA chip was placed into the priming station and the plunger was positioned at 1ml. Additional two 9 µl were loaded into the gel wells. 1 µl of sample (~50ng/µl) was loaded into each well, in addition to 5 µl of marker. The application running time was approximately 35 minutes. Samples were then detected by their absorbance and translated to standard gel-like images and electropherograms.

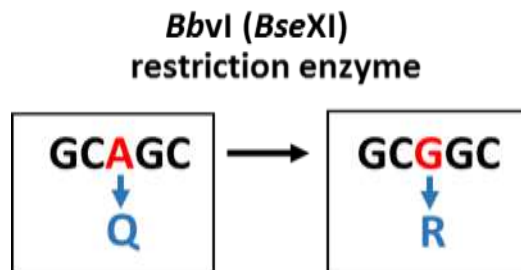


Figure 2.4: Restriction digest enzymes

BbvI and *BseXI* are restriction enzymes that recognizes the same site of GCAGC and both cut at the CAG (Q) site that result in CGG (R). Hence fully edited *GLUR2* will not be digested by the enzyme.

2.6.1 Quantification of editing levels

The editing level of *GLUR2*, *GLUR5* and *GLUR6* transcripts were quantified using Agilent 2100 expert DNA chip software. Analysis of electropherogram obtained from post digestion with restriction enzyme was performed. The percentage of editing was calculated as: concentration of edited transcripts/ sum of edited and non-edited

transcripts x100. The average of editing from each group was calculated in GraphPrism 6.

2.7 Quantitative PCR (qPCR) experiments

As previously stated, RNA was extracted from total spinal cord and from LCM-isolated motor neurons/astrocytes (see section 2.3.4-2.3.5). RNA was then converted to cDNA then primers were added (see section 2.4) and mixed in 2X Brilliant III SYBR® Green (see table 2.5). *ADAR2* and *ADAR3* primers were optimised to 10pmol and the cDNA concentration was optimised to 50ng/µl. All *EAAT2* primers (5pmol) and cDNA concentration (12ng/µl) were optimised previously. A qPCR was performed on the following genes; *ADAR2*, *ADAR3*, *EAAT2* (*EAAT2*⁺⁴ (exon 3-4), *EAAT2*⁺⁹ (exon 8-9) and *EAAT2*^{Δ4} (exon 3-5), *EAAT2*^{Δ9} (exon 8-10) (see figure 2.5)).

All reactions were performed in triplicate along with no template control for each of the primer pairs. The reaction conditions was as follows: initial denaturation at 95°C for 10 minutes, denaturation at 95°C for 30 seconds followed by at 60°C for 1 minute repeated in 40 cycles. At the end of those cycles, another cycle carried out at 95°C for 1 minute, 55°C for 30 seconds and 95°C for 30 seconds extension.

Exon 1	481	gctcctctta	aataccgctc	ccggccgcac	ttgcgctca	ccccggcgtc	cgctttctcc
	541	ctcgcccaca	gctgcccgat	agtgtggaag	aggagggggc	gttccccaga	ccatggcatc
	601	tacggaaggt	gccaacaata	tgcccagca	ggtggaagtg	cgaatgcacg	acagtcattc
Exon 2	661	tggtcagag	gaacccaagc	accggcacct	gggcctgcgc	ctgtgtgaca	agctggggaa
	721	gaatctgctg	ctcacctga	cggtgtttgg	tgatcctctg	ggagcagtgt	gtggagggct
	781	tcttcgcttg	gca tctccca	tccaccctga	tgt ggttatg	ttaatagcct	tcccagggga
Exon 3	841	tatactcatg	aggatgctaa	aaatgctcat	tctccctcta	a	ctccctctca
	901	gg ttgtca	ggcct ggatg	ctaaggctag	tggcc gcttg	ggcacgagag	ccatgggtga
	961	ttacatgtcc	acgaccatca	ttgctgcagt	actgggggtc	attctggtct	tggctatcca
Exon 4	1021	tccaggcaat	cccaagctca	agaagcagct	ggggcctggg	agaagaatg	atgaagtgtc
	1081	cagcctggat	gccttctctg	acottattcg	aaatctcttc	cctgaaaacc	ttgtccaagc
	1141	ctgctttcaa	cag attc aaa	cagtgcagaa	gaaagtcctg	gttgcaccac	cgccggacga
Exon 5	1201	ggaggccaac	gcaaccagcg	ctgttgcttc	tctggtgaac	gagactgtga	ctga ctccctctca
	1261	ctccctctca	ctccctctca	tggtta	tcaagaaggg	cctggagtcc	aaggatggga
	1321	aggtctgata	gggtttttca	ttgcttttgg	catcgctatg	gggaagatgg	gagatcaggc
Exon 6	1381	caagctgatg	gtggatttct	tcaacatttt	gaatgagatt	gtaatgaagt	tagtgatcat
	1441	gatcatgtgg	tactctccc	tgggtatcgc	ctgcctgac	tgtggaaaga	tcattgcaat
	1501	caaggactta	gaagtgggtg	ctaggcaact	ggggatgtac	atggtaacag	tgatcatagg
Exon 7	1561	cctcatcatc	cacgggggca	tctttctccc	cttgatttac	tttgtagtga	ccaggaaaaa
	1621	cccctctccc	ttttttgctg	gcattttcca	agcttggtac	actgccttgg	gcaccgcttc
	1681	cagtgtctgga	actttgcttg	tcacctttcg	ttgcttggaa	gaaaatctgg	ggattgataa
Exon 8	1741	gcgtgtgact	agattcgtcc	ttctgtttgg	agcaaccatt	aacatggatg	gtacagccct
	1801	ttatgaagcg	gt agccgcca	tctttatagc	cc aatgaat	ggtgtgttcc	tggatggagg
	1861	acagatt gtg	actgtaagcc	tcacagccac	cctggcaage	gtcggcgcgg	ccagtatccc
Exon 9	1921	cagtgcgggg	ctggtcacca	tgtctctcat	tctgacagcc	gtgggcctgc	caacagagga
	1981	catcagcctg	ctggtggctg	tggactggct	gct ggacagc	atgaga actt	cagtcaatgt
	2041	tgtgggtgac	tcttttgggg	ctgggatagt	ctatcacctc	tccaagtctg	agctggatac
Exon 10	2101	cattga ctcc	cagcatcgag	tgcatt gaaga	tattgaaatg	accaagactc	aatccattta

Figure 2.5: Primers of *EAAT2* transcripts (NM-004171); exon 4 and exon 9.

Exons are coloured differently in green and in black; Exon 4 and exon 9 containing sequences were labelled as EAAT2⁺4 and EAAT2⁺9, and primers that skip exon 4 and exon 9 were labelled as EAAT2^Δ4 and EAAT2^Δ9. Primer pairs highlighted in green are forward and reverse of exon 4^Δ and exon 9^Δ excluding sequences; forward primers contained bases across the exon boundaries of exon 4 and 9 and first few bases of exon 10 and exon 5 respectively. Exon boundaries marked in bold. The reverse primers of exon 4^Δ and 9^Δ were designed on exons 10 and 5 respectively. Primers highlighted in yellow are exon 4⁺ and exon 9⁺ including sequences covered segments of exon 3 to 4 and exon 8 to 9; spanning exon – exon junctions.

Table 2.4: Primers used.

Primers	Sequence reference	Position	Primer sequence
<i>ADAR2</i>	NM-001112	Forward	TCGCTAATCCCATCCTCAGA
		Reverse	GATGAAAGAGGAGCTGAGAGAAG
<i>ADAR3</i>	NM-018702	Forward	TGCTGTTTCACAGACTGGTAG
		Reverse	CATCCCGGCTCTGCAAG
<i>EAAT2^{Δ4} (exon 3-5)</i>	NM_004171.3	Forward	TCATCTCCAGCTTAATCACAGATTC
		Reverse	TCTTAGTCTCCTCCGGCACC
<i>EAAT2^{Δ9} (exon 8-10)</i>		Forward	GTGACTGTAAGGGACAGGATGAGA
		Reverse	ATGCACTCGATGCTGGGAG
<i>EAAT2⁺4 (exon 3-4)</i>		Forward	TCTCCCATCCACCCTGATGT
		Reverse	GGCCACTAGCCTTAGCATCC
<i>EAAT2⁺9 (exon 8-9)</i>		Forward	AGCCGCCATCTTTATAGCCC
		Reverse	GGCTGTCAGAATGAGGAGCA

Table 2.5: QPCR conditions.

Primers	cDNA Concentration	Primers Concentration	2X Brilliant III SYBR® Green	Total volume
<i>ADAR2</i>	50 ng	10 pM for forward and reverse primers	10µl	20µl
<i>ADAR3</i>				
<i>EAAT⁺4 (exon 3-4)</i>	12.5 ng	5 pM for forward and reverse primers		
<i>EAAT^{Δ4} (exon 3-5)</i>				
<i>EAAT⁺9 (exon 8-9)</i>				
<i>EAAT^{Δ9} (exon 8-10)</i>				

2.10.1 Statistical analysis

The threshold cycle number for product detection (Δ CT) was used to calculate the relative expression levels. Relative quantification ($\Delta\Delta$ Ct) was normalized to β -actin to determine differences in the targeted gene expression. Statistical analysis was performed using one way ANOVA (GraphPad Prism 6).

2.8 Immunohistochemistry (IHC)

Immunodetection of specific antigens was performed on FFPE material (see table 2.2). Brain blocks were fixed in 10% formalin for ~48h before being processed: 70% ethanol x2 for 1hour, 80% ethanol for 1hour and 95% ethanol for 1hour and absolute ethanol for 1.5 hours. The tissue was immersed in xylene three times for 1.5 hrs and embedded in paraffin. 5µm sections were collected on poly-L-lysine coated, charged glass slides, dried overnight at 50°C and stored at RT until required. Prior to staining sections were dewaxed in xylene twice and re-hydrated to water through a graded series of ethanol for 5 minutes; 100%, 95% then 70%. Sections were incubated in 3% hydrogen peroxide (H₂O₂) in methanol for 20 minutes to block endogenous peroxidase activity. Antigen unmasking was performed using an appropriate antigen retrieval method, either pressure cooker (high temperature and high pressure) or microwave (high temperature) (see table 2.6). Sections were washed in TBS and then blocked with 1.5% relevant normal serum diluted in TBS for 30 minutes at RT to prevent non-specific binding of the secondary antibody.

An optimized concentration of primary antibody diluted in blocking solution was applied to the sections for 1hour at RT. Negative controls were incubated in TBS in absence of primary antibody or with the relevant concentration of an IgG control. Sections were washed in TBS for 5 minutes at RT, and incubated with 0.5% biotinylated secondary antibody (either biotinylated anti-Mouse IgG or biotinylated anti-Rabbit IgG, depending on the species of the primary antibody) for 30 minutes at RT. Sections were washed thoroughly in TBS for 5 minutes, and incubated with 1.5% Avidin-Biotinylated horseradish peroxidase complex (ABC) for 30 minutes. ABC reagent was prepared 30 minutes prior to use by adding 2 drops of reagent A and 2

drops of reagent B to 10ml TBS. Then sections were washed in TBS for 5 minutes at RT. The antibody was visualized by incubating the sections with the peroxidase substrate DAB for 5 minutes at RT. To prepare DAB, 2 drops of buffer solution, 4 drops of DAB stock and 2 drops of hydrogen peroxide were mixed in 5ml of dH₂O. The reaction was quenched using water and the sections were counterstained for 1 minute with Gill's haematoxylin. Gill's haematoxylin was prepared by adding 6g of haematoxylin to 4.2g of aluminium sulphate, 1.4g of citric acid 1.4g, 0.6g sodium iodate, 269ml of ethylene glycol and mixed in 680ml of dH₂O. The slides were rinsed in tap water and blued in Scott's Water for 1 minute. Finally, the sections were dehydrated in a graded series of ethanol (70%, 95%, and 100%), cleared in xylene then cover slipped using DPX permanent mounting media.

Table 2.6: Antibodies used in the study, their antigen retrieval method and dilution of primary antibody.

Antibodies	Antigen retrieval method	Antibody dilution/Incubation time	Supplier
p-TDP-43	Pascal pressure chamber with TSC (pH6) buffer for 30 seconds at 125C and 22 psi	1:4000/30 minutes	Cosmobio (2B)
p62	Pascal pressure chamber with TSC (pH6) buffer for 30 seconds at 125C and 22 psi	1:200/30 minutes	BD (610833)
GLUR2	Pascal pressure chamber with TSC (pH6) buffer for 30 seconds at 125C and 22 psi	1:50 16 hours	Sigma
ADAR2	Pascal pressure chamber with TSC (pH6) buffer for 30 seconds at 125C and 22 psi	1:100/ 1hour	Abcam
ADAR3	Pascal pressure chamber with TSC (pH6) buffer for 30 seconds at 125C and 22 psi	1:200/ 1hour	Sigma
GFAP	Microwave with TSC (pH.6.5) buffer for 10 minutes	1:20/ 1 hour	Dako cytomation
EAAT2	Pascal pressure chamber with EDTA (pH.8) buffer for 30 seconds at 125C and 22 psi	1:2000/ 1 hour	Leica biosystems

2.8.1 Statistical analysis

Images were captured and analysed using an upright Olympus BX61 microscope and Cell^R imaging software. Five random images were taken from the grey matter of the spinal cords of each case using a Hamamatsu ORCA-ER digital camera. Analysis^{AD} software was used and the percentage area immunoreactivity in the area of interest in all cases was analysed using one-way ANOVA (GraphPad Prism 6).

2.9 Next generation sequencing

RNA extraction was carried out on dissected 200 motor neurons (7 μ m) using RNA PicoPure (Arcturus) Isolation kit (see section 2.3.5). RNA extraction was repeated 3 times to improve the RNA quality. Step 2.12.1 to 2.12.6 was repeated 3 times to optimise single stranded and double stranded RNA and then step 2.12.7 which is library preparation was repeated twice to get sufficient cDNA for sequencing. Samples were handed to the technical team for just running the experiments on the Illumina.

2.9.1 First-strand cDNA synthesis

10ng of total RNA in 3 μ l was added to 0.5 μ l of Message Booster Whole Transcriptome primers and 1.5 μ l of Rnase-Free Water. This was incubated at 65°C for 5 minutes in a thermocycler then chilled on ice for 1 minute and briefly centrifuged First-strand cDNA was prepared by mixing 1.25 μ l of Message Booster Reverse Transcriptase buffer, 0.25 μ l DTT, 0.25 μ l RiboGuard RNase Inhibitor and 0.25 μ l of MMLV-Reverse Transcriptase. This was added to the RNA plus primers mixture and incubated at RT for 10 minutes followed by a second incubation at 37°C for 60 minutes.

2.9.2 Second-strand cDNA synthesis

First-strand cDNA was added to 4.5µl of MessageBooster DNA Polymerase premix and 0.5µl of Message Booster DNA Polymerase. This mixture was incubated at 65°C for 10 minutes then 80°C for 3 minutes. 1µl of Message Booster cDNA finishing solution was added to the reaction and then incubated at 37 °C for 10 minutes followed by another incubation at 80°C then centrifugation for 1 minute.

2.9.3 *In vitro* transcription

The following reagents were mixed: 2µl of MessageBooster T7 Transcription buffer, 14µl of NTP premix, 2µl of DTT and 2µl of Message Booster T7 RNA Polymerase. Then, the mixture was added to the reaction and incubated at 42°C for 4 hours and 2µl of RNase-Free DNase 1 was added to the reaction and incubated at 37°C for 15 minutes.

2.9.4 Round one, RNA purification

1µl of Poly (I) was added to each reaction and RNA was purified and eluted in 8µl of RNase-Free water.

2.9.5 Round-two, first-strand cDNA synthesis

To each purified RNA sample, 2µl of the random primers was added, incubated at 65°C for 5 minutes, chilled on ice for 1 minute and briefly centrifuged. 1.5µl of the Message Booster Reverse Transcription, 0.25µl and 0.25µl of MMLV-RT were added to the reaction and incubated at 37°C for 60 minutes.

2.9.6 Second strand cDNA synthesis

The first strand cDNA synthesis (20 µl) generated by MessageBooster was heat inactivated on ice and 48µl of Nuclease-Free Water was added to the reaction. To this was added 8µl of 10X second strand synthesis reaction and 4µl of second strand synthesis enzyme mix from the NEBNext mRNA second strand synthesis kit. The total volume for the reaction was 80µl. The reaction was mixed thoroughly and incubated for 2.5 hours at 16°C. The cDNA was purified using a PCR column purification from New England Biolabs and eluted in 20µl elution buffer. Samples were cleaned up using the basic Agencourt magnetic beads. 36µl of magnetic beads were added to the cDNA, then the reaction was mixed and incubated for 5 minutes at RT. The reaction was placed on Agencourt SPRIPlate 96 Super Magnet Plate for 2 minutes to separate the reaction from beads. While the reaction plate is situated on the magnet plate, the supernatant was discarded leaving 5µl of supernatant behind to avoid disturbing the beads. This was followed by washing the reaction with 200µl of 70% ethanol then the reaction was incubated for 30 seconds at RT before the supernatant containing ethanol was discarded. The reaction plate was removed from the magnet plate and 40µl of elution buffer was added to each sample then incubated for 2 minutes at RT. The reaction plate was placed back on the magnet plate for 1 minute to separate beads from the solution and the eluted reaction was transferred away in to new plate. 1µl of the reaction was measured by NanoDrop.

2.9.7 Library preparation

2.9.7.1 Tagmentation of genomic DNA

The sample DNA was fragmented and tagged with adaptor sequences to the ends using Nextera XT DNA sample preparation kit. The following mix was prepared and loaded

into Nextera XT Tagment Amplicon plate: 10µl of Tagment DNA Buffer, 5µl of input cDNA at 1ng/µl and 5µl of Amplicon Tagment Mix. The reaction plate covered with microseal and centrifuge at 280xg at 20°C for 1 minute. The reaction was then placed in a thermocycler and incubated at 55°C for 5 minutes and hold at 10°C. Then, 5µl of Neutralize Tagment Buffer was added to each well of the reaction plate. The reaction samples were mixed and centrifuged at 280xg at 20°C for 1 minute then reaction plate was incubated at RT for 5 minutes.

2.9.7.2 PCR amplification

A TruSeq Index Plate was used and index primers were arranged as follows: index 1 (i7) primers were arranged in order horizontally (orange caps), so that N701 is in column 1 and N712 is in column 12. Index 2 (i5) primers (white caps) were arranged in order vertically, so that S501 (Seq-TAGATCGC) is in row A and S508 (Seq-CTAAGCCT) is in row H. These positions were recorded. Then, 15µl Nextera PCR master mix was added to the reaction plate followed by adding 5µl of index primer 1 and 5µl of index primer 2 to the plate. The sample plate was covered with a microseal film and centrifuged at 280xg at 20°C for 1 minute. Then, PCR was performed on the following program: one step of initial denaturation at 72°C for 3 minutes followed by denaturation at 95°C for 30 seconds then 12 cycles of denaturation at 95°C for 10 seconds, annealing at 55°C for 30 seconds and extension at 72°C for 30 seconds and a final extension at 72°C for 5 minutes.

2.9.7.3 PCR clean up

Following the PCR amplification, the reaction was centrifuged at 280xg for 1 minute and library DNA was purified using AMPure XP beads. 50µl of the PCR product was

transferred to new plate and 30µl of beads were added and PCR reaction was mixed on shaker plate at 1.800 rpm for 2 minutes then incubated at RT for 5 minutes. The reaction plate was placed on magnet plate for 2 minutes. The supernatant was discarded, the beads were washed with 200µl of 80% of ethanol then the supernatant containing ethanol was discarded after incubation for 30 seconds. While the plate is on the magnet plate, beads were air dried for 15 minutes then sample plate was removed from the magnet stand and 52.5µl of resuspension buffer was added to the beads. Following incubation at RT for 2 minutes then sample plate was placed on the magnet stand for 2 minutes. 50µl of the purified PCR products were transferred to new plate and 1µl of NGS library was measured in NanoDrop, Bioanlyser High sensitivity DNA chip and qPCR using KAPA library quantification kit and samples were run on Illumina Hi scan SQ system by the in-house technical team..

Chapter 3

***RNA editing of glutamate
receptors in SALS patients***

Chapter 3: RNA editing of glutamate receptors in SALS patients

3.1 Introduction

As discussed in the Introduction while some of the key mechanisms that contribute to ALS have been identified, very little is known about the basis for the selective loss of motor neurons. The co-existence of neurons with other cell types in the central nervous system suggests that their survival depends on a complex interplay of intrinsic cellular attributes and extrinsic environmental factors. So the question remains why are motor neurons selectively vulnerable to death, possibly by excitotoxicity, in ALS? One explanation may be due to the excitotoxicity caused by an increased proportion of Ca^{+2} -permeable ion channels, which are activated upon rapid release of presynaptic glutamate (Heath & Shaw, 2002). In addition inefficient glutamate re-uptake may partly contribute to the accumulation of excitotoxic Ca^{+2} . Previous studies have implicated the AMPA and kainate receptors in ALS (Heath & Shaw, 2002; Van Den Bosch *et al.*, 2006b). This suggests the hypothesis that AMPA and kainate receptors contribute to the pathogenesis of ALS, despite the fact that AMPA and kainate receptors in certain conformations are generally less permeable to Ca^{2+} than the NMDAR (Van Den Bosch *et al.*, 2006b). The AMPA and kainate receptors are thought to mediate motor neuron injury in a subpopulation of central neurons which are directly permeable to Ca^{2+} (Kwak & Kawahara, 2005). In normal situations the AMPA receptors are composed of heteromeric complexes of four receptor subunits: GLUR1, GLUR2, GLUR3 and GLUR4. In contrast, hetero-multimeric kainate receptors (KA) are composed of GLUR5-7 and KA1-KA2 which have distinct role at the synapse

compare to other glutamate receptors (Lerma *et al.*, 2001). The GLUR5-7 subunits have low affinity to glutamate and are capable of forming functional homomeric channels. In contrast to GLUR5-7 subunits, KA1-KA2 have high affinity to glutamate but require co-assembly with one or more GLUR5-7 subunits to form functional channels. Like many other ion channels the hetero-multimeric assembly leads to the formation of receptors with unique pharmacological and functional properties, also through their action at both pre- and postsynaptic sites. KARs have also been shown to modulate synaptic transmission and neuronal excitability through their action at both pre- and postsynaptic sites (Lerma *et al.*, 2001).

The physiologic properties of AMPA and KA receptors are controlled by post-transcriptional mechanisms such as RNA editing, which modifies one or more translation codons, thus leading to functionally distinct proteins from a single gene (Seeburg *et al.*, 1998; Barbon *et al.*, 2003). The predominant type of RNA editing in mammals is adenosine-to-inosine (A-I) catalyzed by the adenosine deaminase acting on RNA (ADAR). In particular, the GLUR2 subunit of the AMPA receptor and the GLUR5 and GLUR6 subunits of KA receptor are subject to RNA editing at the Q/R site, which results in glutamine being substituted by arginine at a position located in the channel pore (Caracciolo *et al.*, 2013). The Q/R site in GLUR2, GLUR5 and GLUR6 is in different positions for each receptor; 607Arg, 636Arg and 621Arg, respectively. For instance, when edited GLUR2 (R) is present in the AMPA receptor complex, AMPA receptors become impermeable to Ca^{+2} . Whereas, AMPA receptors containing the unedited form of GLUR2 (Q) have high Ca^{+2} permeability (Hollmann *et al.*, 1991). Normally, this editing process occurs with virtually 100% efficiency from the embryonic stage onwards. It has been demonstrated that motor neurons express relatively lowered quantities of GLUR2 in ALS patients (Shaw *et al.*, 1999; Van

Damme *et al.*, 2002). A study using laser microdissection showed that single motor neurons had an editing efficiency that was approximately 56 % incomplete in sporadic ALS patients compared to 100% editing efficiency observed in controls (Kawahara *et al.*, 2004). This incomplete editing of motor neurons in SALS patients at Q/R site correlates with decreased ADAR2 activity (Aizawa *et al.*, 2010; Hideyama *et al.*, 2012b; Yamashita *et al.*, 2012b; Yamashita & Kwak, 2013; Kubota-Sakashita *et al.*, 2014).

RNA editing can also occur at other sites in the mRNA of glutamate receptor subunits including the R/G site of *GLUR2*, where arginine can be substituted for glycine, and two positions prone to mRNA editing have been identified in the M1 segment of *GLUR6*: the I/V site, where a valine can be substituted for an isoleucine and the Y/C site, where a tyrosine can be substituted for a cysteine. Therefore, editing at these positions modulates the effect of editing at the Q/R site in calcium flow such that the fully edited subunit inhibit Ca^{+2} entry to anion channel. However, further studies are required to determine the mechanism of interaction among these three sites (Köhler *et al.*, 1993; Barbon *et al.*, 2003).

Previous work has also shown that ADAR2 itself is regulated post-translationally by peptidyl-prolyl isomerase NIMA interacting protein 1 (Pin1) and WW domain-containing protein 2 (WWP2). Pin1 is a positive regulator for ADAR2 that causes conformational changes to ADAR2 that alters the catalytic stability and subcellular localisation. ADAR2 without Pin1 translocate to the cytoplasm where it is unable to edit pre-mRNA of *GLUR2* at the Q/R or R/G site. WWP2 is a negative regulator for ADAR2 where the binding results in ADAR2 ubiquitination and subsequent degradation, therefore, increased expression of WWP2 leads to decreased ADAR2 protein levels (Marcucci *et al.*, 2011).

Like *ADAR2*, *ADAR3* has all the key residues required for catalysis however, it lacks the motif for deamination activity on double-stranded RNA (dsRNA) on specific substrates such as *GLUR2* (Melcher *et al.*, 1996; Chen *et al.*, 2000). *ADAR3* has the ability to bind not only dsRNA but also single-stranded RNA (ssRNA) in the N-terminus, through an arginine rich domain, making it distinct from the other members of *ADAR* family (Chen *et al.*, 2000). The function of *ADAR3* is unknown however, it has been speculated that *ADAR3* is a negative regulator for *ADAR1* and *ADAR2* *in vitro* when *ADAR3* has appeared to inhibit the activities of RNA editing enzymes of the *ADAR* gene family (Chen *et al.*, 2000). *ADAR3* might compete for dsRNA substrates preventing the binding of the other *ADAR* enzymes (Tomaselli *et al.*, 2013). A recent study had shown that *ADAR3* does not compete with *ADAR2* in its binding to dsRNA substrates at least for certain edited mRNAs. For instance, it has been shown that *ADAR3* binds to *Lam-2* and *pop-1* mRNAs, which are known edited mRNA, in the presence or absence of *ADAR2*. It has been suggested that *ADAR3* might function to promote *ADAR2* editing by binding to mRNA and then either alter binding of the *ADAR2* to specific regions and/or regulate the catalytic activity of *ADAR2* (Washburn, 2014).

As previously mentioned, the loss of EAAT2 protein in ALS might be explained by aberrant alternative splicing and production of truncated mRNA of exon 4 and exon 9 found in motor cortex but not in the cerebellum or hippocampus of ALS patients (Lin *et al.*, 1998). Evidence has shown that aberrant EAAT2 protein was not detected in the motor cortex or the spinal cord of ALS patients which may be caused by rapid degradation of truncated proteins (Lin *et al.*, 1998), but later studies also identified these mRNA splice variants in control tissue (Meyer *et al.*, 1999; Flowers *et al.*, 2001).

Defect in the astrocytic glutamate re-uptake system of EAAT2 leads to excitotoxicity that may contribute to neuronal injury in ALS (Ferraiuolo *et al.*, 2011).

Hypothesis:

- Altered glutamate receptor editing in motor neurons in ALS is relevant to disease pathogenesis
- There is no relationship between mRNA expression of *ADAR2* and *ADAR3*
- A decrease in *EAAT2* mRNA expression contributes to the excitotoxicity associated with ALS

Aims:

- To investigate RNA editing of *GLUR2*, *GLUR5* and *GLUR6* in the pathogenesis of ALS disease and the differences between edited RNA levels of glutamate receptors in controls compared to *ALS/C9ORF72*-positive and *ALS/C9ORF72*-negative patients.
- To determine the *ADAR2* and *ADAR3* gene expression in the spinal cord from ALS versus control cases
- To determine the aberrant expression of *EAAT2* transcripts in the astrocytes of the spinal cord of ALS cases and controls

3.2 Results

3.2.1 Optimisation development

The laser capture microdissection (LCM) of MNs was optimised in in FFPE sections of spinal cord tissue of 3 ALS patients; FALS/*C9ORF72*-positive, SALS/*C9ORF72*-positive and SALS (see table 3.1). In order to visualise MNs for LCM, sections were stained with toluidine blue and ~400 MNs were picked. RNA extraction was carried out using RNA aqueous micro kit from Ambion and the RNA concentration was measured by Nanodrop (see table 3.2). Nanodrop data showed an RNA concentration of ~234-340ng/μl. RNA was converted to a cDNA and RT-PCR was performed. However, RT-PCR of ALS case did not show any peaks in the DNA chip bioanalyser because of the low RNA quality (see figure 3.1). The expected RT-PCR sized 270bp.

Table 3.1: FFPE sections obtained from spinal cord of ALS patients

Case number	Clinical Diagnosis	Area/level	PMI in hours	Sex	Age at onset	Age at death	Length of illness
273/99G (TBP0096)	FALS/ <i>C9ORF72</i>	Bulbar	31	M	66	68	14 months
336/90J (TBP0048)	SALS/ <i>C9ORF72</i>	Limb	6	M	63	64	11 months
113/08AC	SALS	Multifocal	9	F	68	70	31 months

The FFPE spinal cord sections was obtained from different spinal cord regions; Case no.273/99G was obtained from lumbar spinal cord, case no. 336/90J was obtained from thoracic spinal cord and case no. 113/08A was obtained from cervical spinal cord.

Table 3.2: Nanodrop of spinal cord sections of ALS patients

Sample ID	RNA concentration	A260	A280	260/280	260/230
273/99G (TBP0096)	234ng/ μ l	5.850	12.424	0.47	0.91
336/90J (TBP0048)	340ng/ μ l	8.0504	15.966	0.53	3.01
113/08AC	244 ng/ μ l	6.124	13.020	0.47	1.19

Nanodrop data showed RNA concentration of 3 ALS patients. A260: The absorbance reading at 260nm, A280: The absorbance reading at 280nm, 260/280: A ratio for pure RNA is \sim 2 and 260/230: A ratio for pure RNA is \sim 2-2.2.

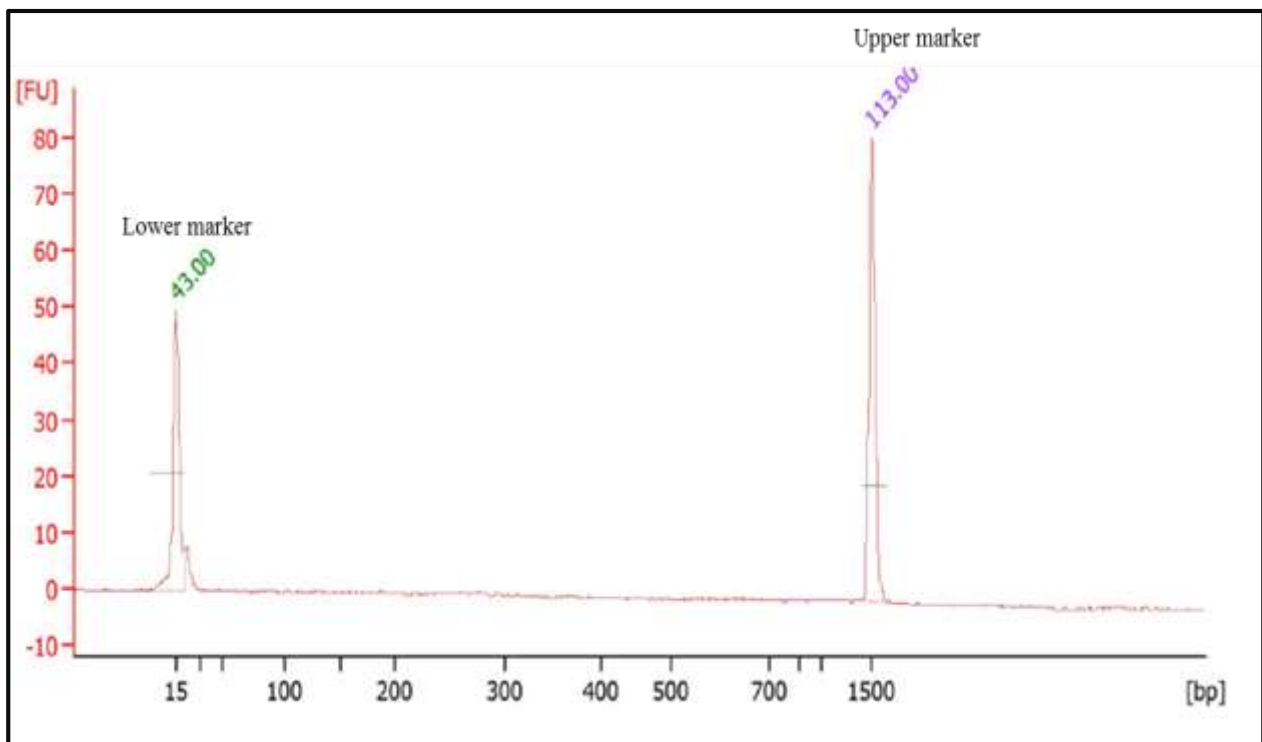


Figure 3.1: DNA chip bioanalyser of PCR of ALS

DNA chip bioanalyser of PCR reaction of ALS case did not show any DNA product. The expected DNA product sized 270bp.

MNs dissection by LCM was also optimised in frozen spinal cord tissue because of the low quality of the extracted RNA from FFPE tissue (0.47/260/280 see table 3.2). In order to visualise MNs for LCM, sections were stained with toluidine blue and varying numbers of MNs were isolated (see figure 3.2). The first attempt to isolate RNA in frozen tissue was carried out with 10 MNs and then 20 MNs, which gave a low RNA concentration and quality as measured by Nanodrop (data are not shown) and Picochip (see figure 3.3). However, increasing the number of isolated MNs to 200 gave an increased RNA concentration of 22.7pg/μl (see figure 3.3).

The PCR reactions for *GLUR2*, *GLUR5* and *GLUR6* were optimised using human universal reference RNA as well as optimising the digestion of PCR product to identify the editing efficacy of glutamate receptors at the Q/R site. Prior to digestion with the restriction enzyme *BseXI*, RT-PCR of the three glutamate receptors was expected to produce PCR products sized 240bp for *GLUR2* (see figure 3.4a), 227bp for *GLUR5* (see figure 3.4b) and 117bp for *GLUR6* (see figure 3.4c). *GLUR2*, *GLUR5* and *GLUR6* were first amplified by RT-PCR with a temperature gradient from 52°C to 60°C. However, *GLUR2* annealing temperature was increased to 67°C to eliminate primer dimer formation. *GLUR2* was optimally amplified at 67°C as demonstrated by a single clear band without the expression of a primer dimer compared to the other annealing temperatures (see figure 3.4a). The optimal annealing temperature for *GLUR5* was determined to be 55°C, as this temperature increased the purity of the single product compared to other temperatures tested (see figure 3.4b). The annealing temperature for *GLUR6* was optimised at 60°C, because at this temperature there was increased product and reduced non-specific bands relative to other temperatures tested (see figure 3.4c). Increasing the annealing temperature was associated with reduced primer

dimer formation. Minimising primer dimer formation was vital to determine RNA editing levels.

In order to distinguish between the edited and unedited *GLUR2* mRNA at the Q/R site the restriction enzyme *BseXI* was used to cut *GLUR2* cDNA once, creating two fragments sized 191bp and 49bp. In addition, *BseXI* cuts -unedited *GLUR2* into three fragments sized 100, 91, and 49bp (see figure 3.5a). The fragments were analysed using a DNA chip bioanalyser, which showed complete editing (100%) of *GLUR2* at the Q/R site in the universal reference tissue (see figure 3.5b). *GLUR5* RNA editing was also optimised using restriction digest *BseXI* that cuts the PCR product of *GLUR5* at Q/R site. The DNA chip bioanalyser showed three peaks; the first two peaks were sized 93bp and 143bp and were the edited *GLUR5* whereas, the third peak was sized 227bp and was the non-edited form of *GLUR5* (see figure 3.6b). In addition to the optimisation of *GLUR2* and *GLUR5* restriction digests, *GLUR6* digestion resulted in three peaks; the first two peaks were sized 31bp and 88bp representing the edited form (R) and the 117bp representing the non-edited form (Q) of *GLUR6* in the universal reference RNA (see figure 3.7b).

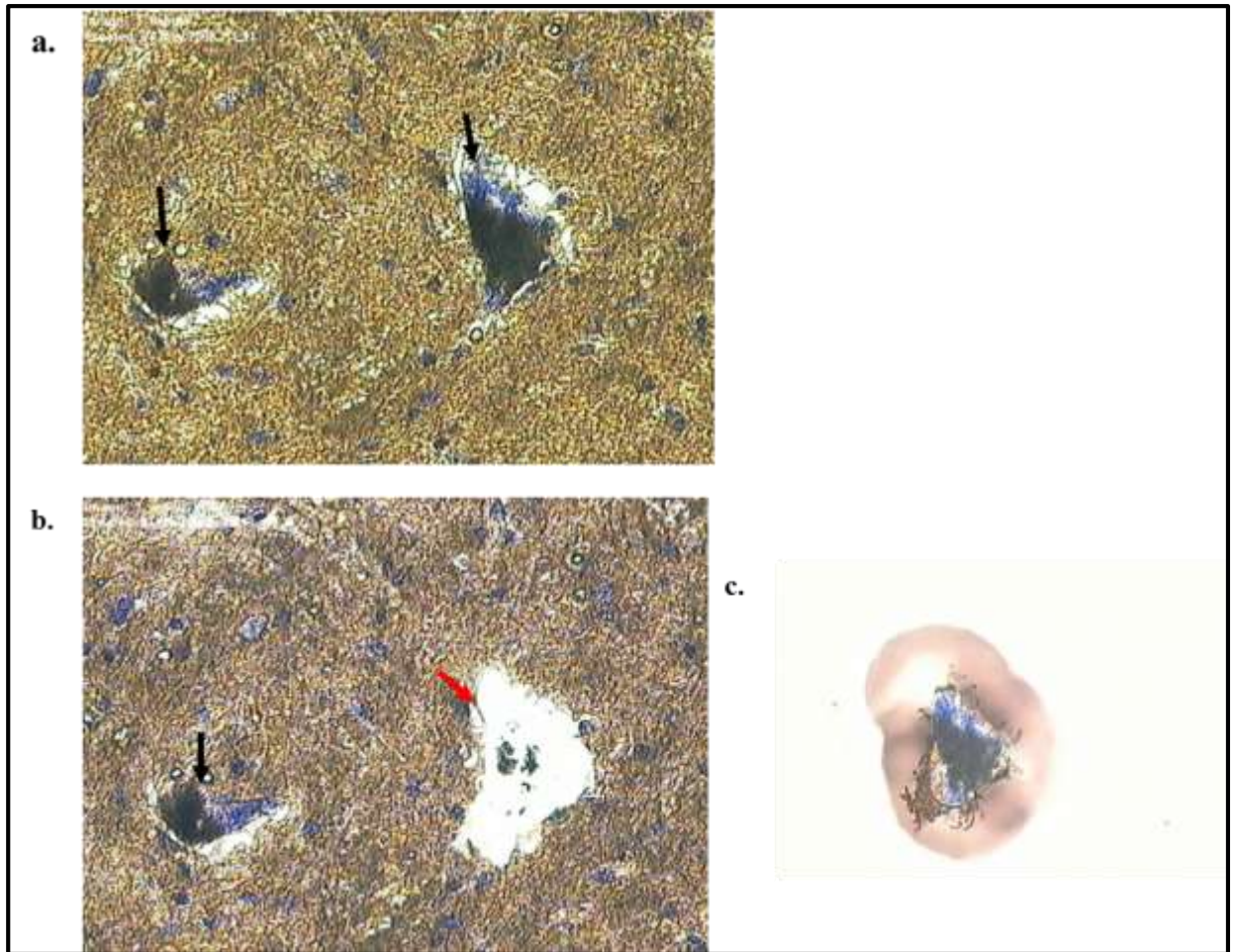


Figure 3.2: Microdissection of MNs by LCM.

Panel a. shows MN stained with toluidine blue prior LCM. Panel b. shows MN after LCM (red arrow). Panel c. shows isolated MNs on cap scale bar= 50 μ m.

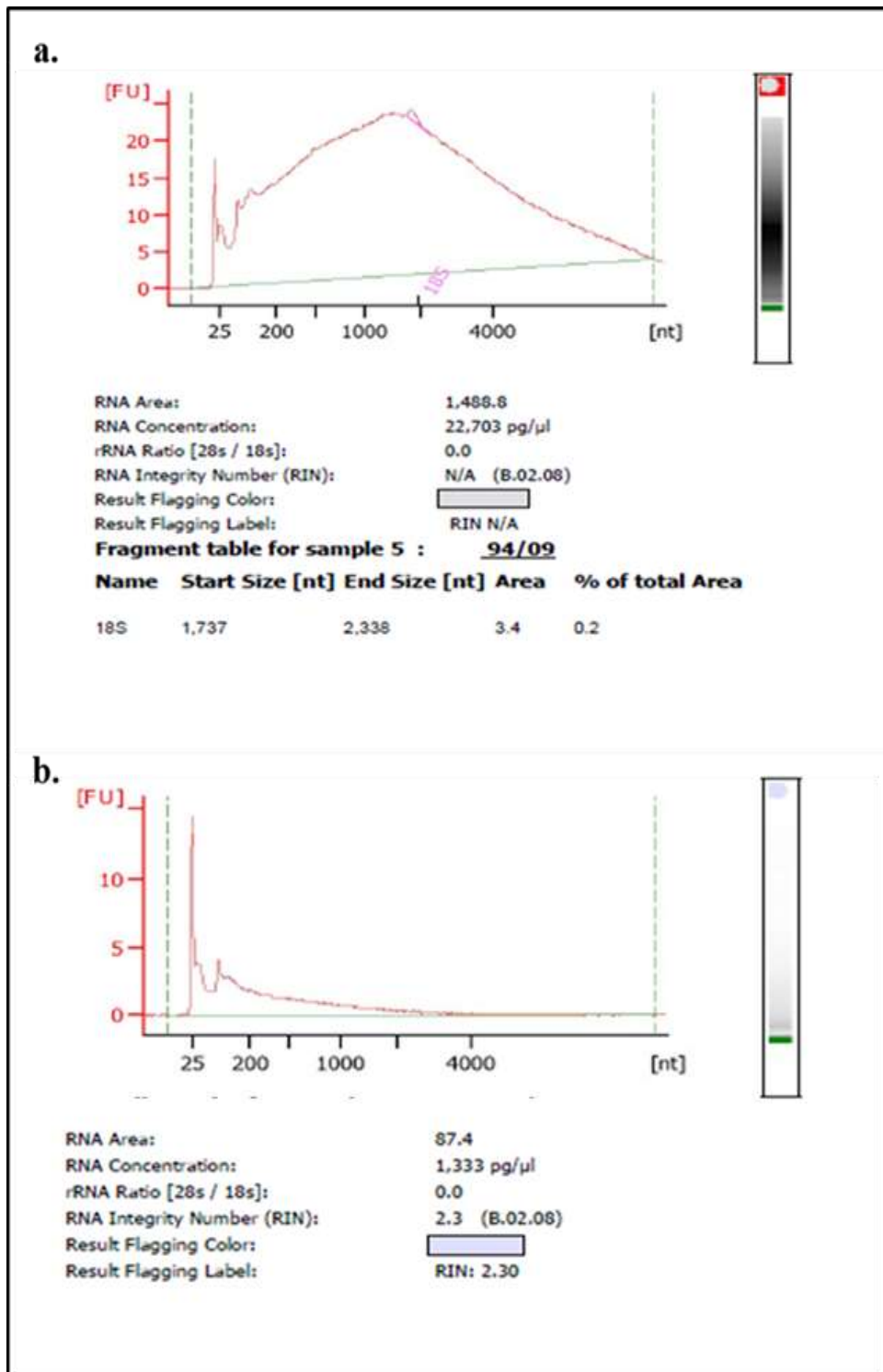


Figure 3.3: RNA concentration of MNs of ALS patients.

Pico chip bioanalyser showed RNA concentration of 200 MNs from one ALS patient with high RNA concentration of 22.7pg/ μ l (a). Another SALS patient sample was used to isolate 20 MNs and showed low RNA concentration of 1.3pg/ μ l (b).

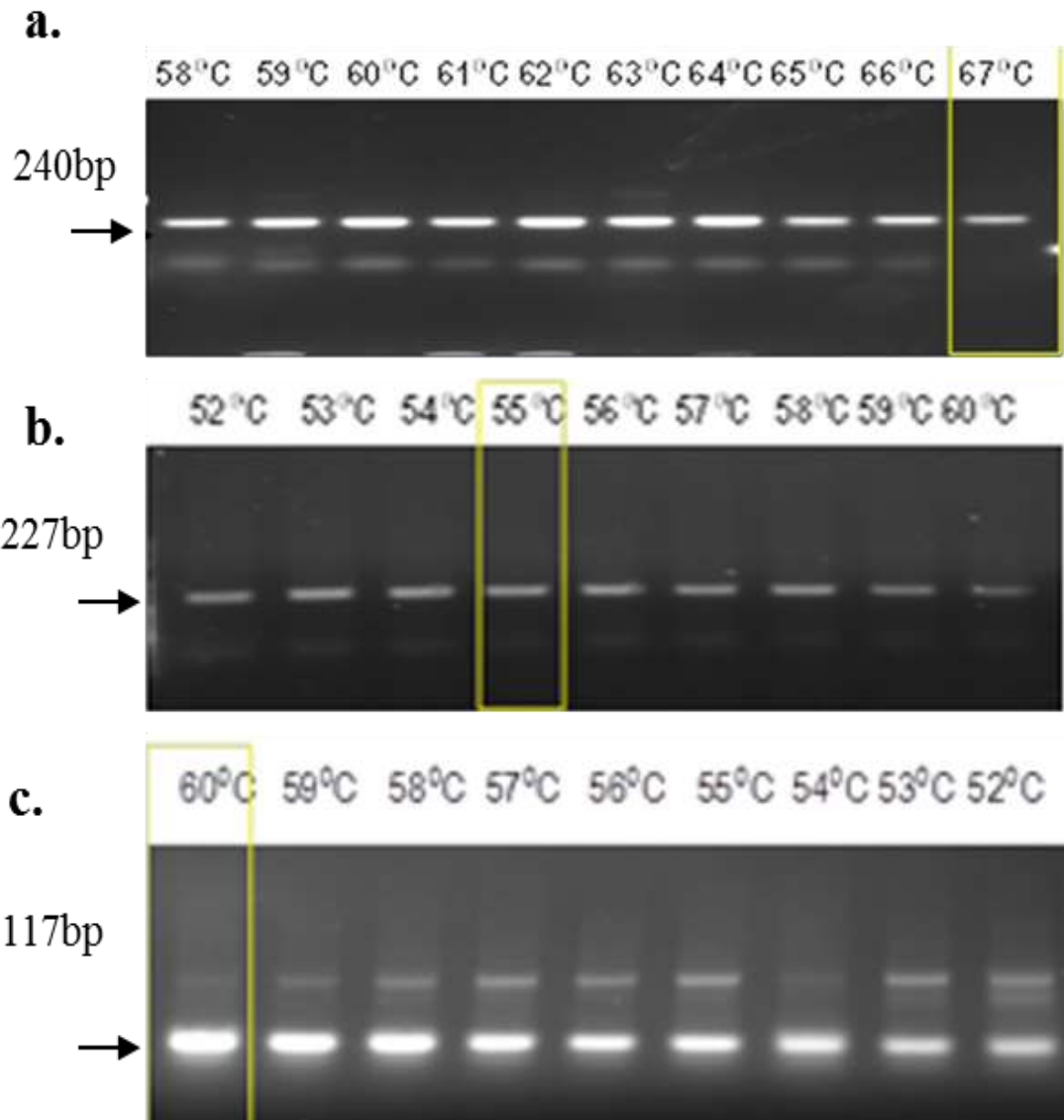


Figure 3.4: PCR optimisation of *GLUR2*, *GLUR5* and *GLUR6* primers.

Agarose gel electrophoresis analysis of PCR optimisation products using the human universal reference RNA *GLUR2* (a), *GLUR5* (b) and *GLUR6* (c). PCR products were observed in all the indicated temperatures. The optimal annealing temperature which gave a single PCR product was 67 °C for *GLUR2* (a), 55 °C for *GLUR5* and (b) 60 °C for *GLUR6* (c).

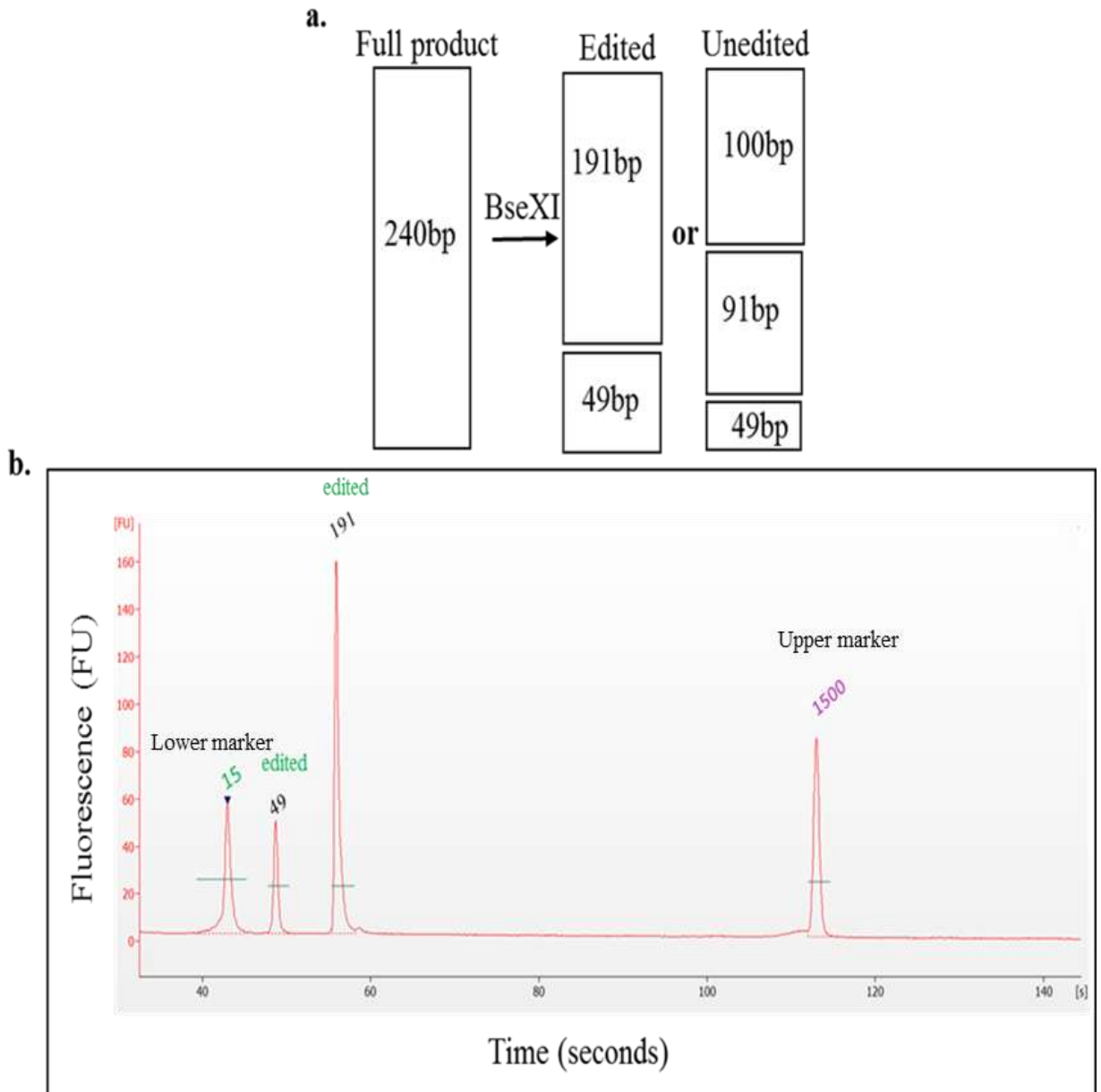


Figure 3.5: Restriction digest analysis of *GLUR2* editing.

A schematic representation of *BseXI* restriction enzyme digests to differentiate between edited and unedited *GLUR2* mRNA at Q/R site (a). DNA chip bioanalyser showed two peaks of edited *GLUR2* (191bp, 49bp) in human universal reference RNA (b).

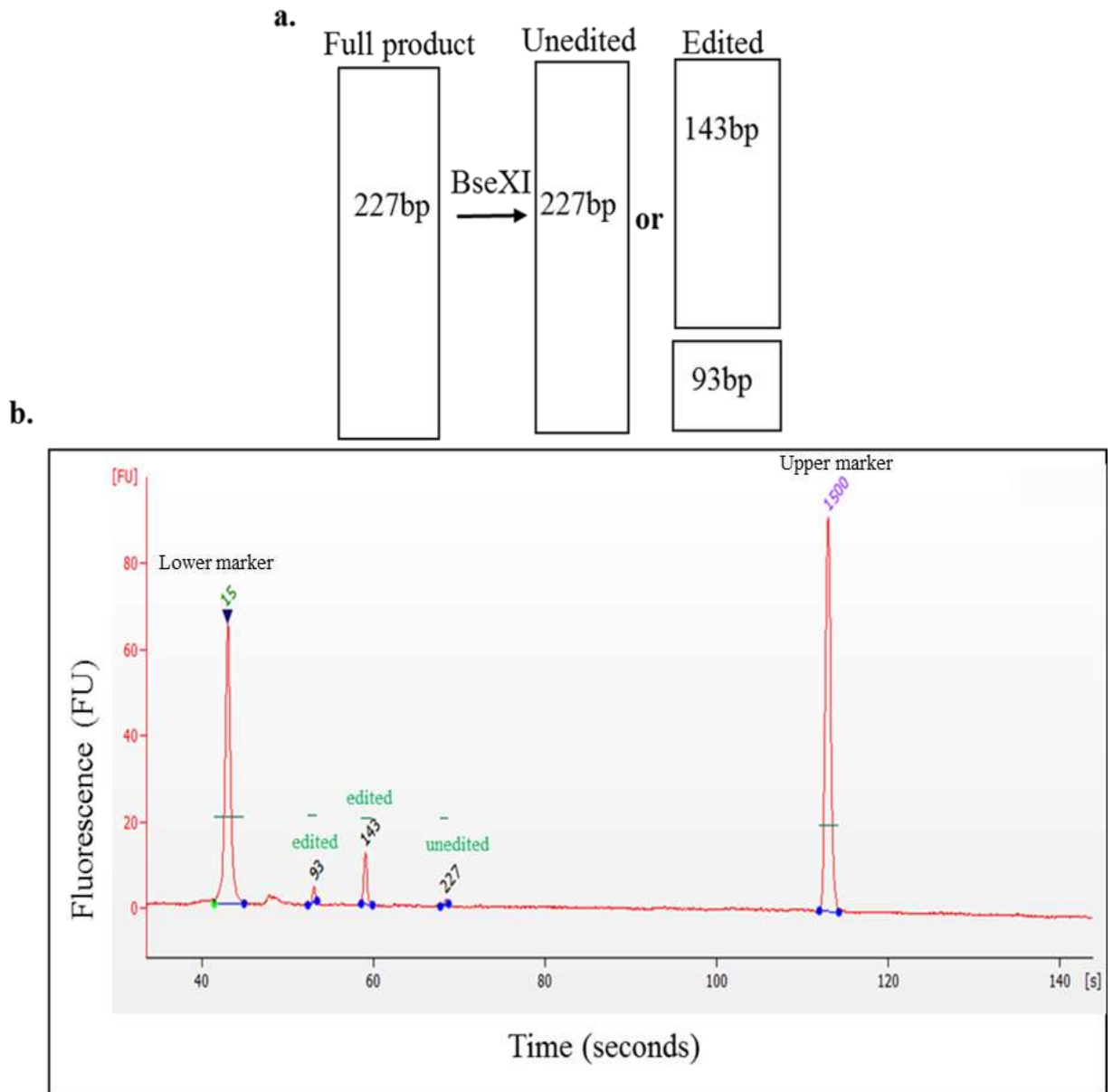


Figure 3.6: Restriction digest analysis of *GLUR5* editing.

A schematic representation of *BseXI* restriction enzyme digests to differentiate between edited and unedited *GLUR5* mRNA at Q/R site (a). DNA chip bioanalyser showed two peaks of edited (93bp and 143bp) and a single peak of unedited (227bp) *GLUR5* in human universal RNA (b).

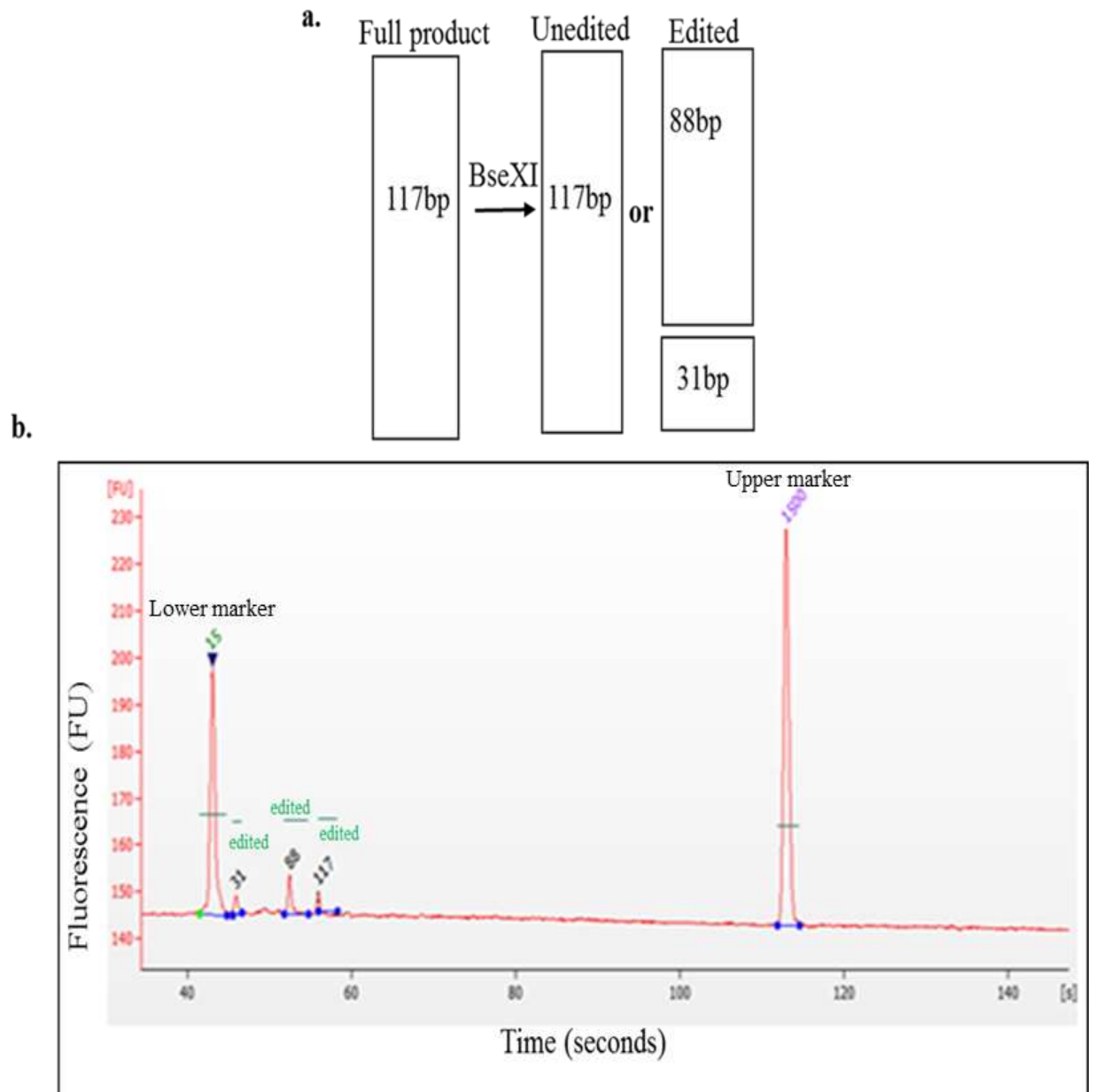


Figure 3.7: Restriction digest analysis of *GLUR6* editing.

A schematic representation of *BseXI* restriction enzyme digests to differentiate between edited and unedited *GLUR6* mRNA at Q/R site (a). DNA chip bioanalyser showed two peaks of edited (31bp and 88bp) and a single peak of unedited (117bp) *GLUR6* in human universal RNA (b).

3.2.2 RNA editing of glutamate receptor subunits in different CNS regions

RNA editing levels of *GLUR2*, *GLUR5* and *GLUR6* were determined in the motor cortex of 4 SALS patients and in 3 control subjects. *GLUR2*, *GLUR5* and *GLUR6* RNA editing levels were also studied in the frontal cortex of 3 SALS cases in comparison to 5 controls (see table 3.3). Additionally, *GLUR2*, *GLUR5* and *GLUR6* RNA editing was examined in temporal cortex, cerebellum, and thalamus and in motor cortex of one patient of PICK disease.

Table 3.3: Multiple CNS regions of several ALS patients and one PICK patient

Frozen motor cortex from ALS patients and controls							
Case number	Clinical Diagnosis	Area/level	PMI in hours	Sex	Age at onset	Age at death	Length of illness
TBP0070 (53/96)	SALS/ <i>C9ORF72</i>	Bulbar	7	F	61	64	40 months
TBP0078 (159/96)	SALS	Bulbar	20	M	41	43	23 months
TBP0076 (137/96)	SALS/UMN	Multifocal	9	F	56	65	99 months
TBP0083 (57/97)	SALS/PLS	Bulbar	18	F	76	78	26 months
TBP0071 (66/96)	Control	Bulbar	10	F	70	73	37 months
144/96	Control	n/a	n/a	n/a	n/a	n/a	n/a
194/96	Control	n/a	n/a	n/a	n/a	n/a	n/a
Frozen frontal cortex from ALS patients and controls							
Case number	Clinical Diagnosis	Area/level	PMI in hours	Sex	Age at onset	Age at death	Length of illness

TBP0074	SALS	Bulbar	19	M	71	75	37 months
TBP0075	SALS	Multifocal	9	F	68	70	31 months
136/97	SALS	n/a	16	F	76	78	13 months
136/95	Control	n/a	10	F	n/a	87	n/a
147/95	Control	n/a	15	M	n/a	47	n/a
178/95	Control- Ischaemic Heart disease	n/a	24	F	n/a	63	n/a
35/96	Control	n/a	14	F	n/a	87	n/a
95/96	Control	n/a	n/a	n/a	n/a	n/a	n/a
Frozen tissue from different CNS regions of one case with PICK's disease							
Case number	Clinical Diagnosis	Area/level	PMI in hours	Sex	Age at onset	Age at death	Length of illness
Temporal cortex	Pick's disease	n/a	22	F	n/a	63	n/a
Cerebellum							
Thalamus							
Motor cortex							

New primers had to be designed because of the PCR reaction that showed evidence of contamination as evidenced by the presence of a band in the negative control. Since the intensity of this product decreased with lower primer concentration it was concluded that the primers had become contaminated. The new primers were designed to be larger than the contaminated product. RT-PCR of *GLUR2*, *GLUR5* and *GLUR6* showed PCR products sized 487bp for *GLUR2* (see figure 3.8), 114bp for *GLUR5* (see figure 3.9) and 132bp for *GLUR6* (see figure 3.10). *GLUR2*, *GLUR5*, *GLUR6* were optimised at 60°C, which showed increased PCR products and reduced non-specific bands. Some PCR products had strong primer dimer that had to be removed by cleaning the PCR product prior to digestion with restriction enzymes. Instead of using agarose gel extraction method an alternative approach was used which is a flash gel system that allowed isolation of cleaned PCR product without cutting the gel from available recovery wells on the flash gel (see section 2.8.1).

In order to distinguish between the edited and non-edited mRNA at Q/R site, the restriction enzyme BbVI was used because it has a similar cut site as *BseXI* but was found to be more efficient (see figure 2.4). DNA chip bioanalyser showed a single peak representing predigest RT-PCR (see figure 3.11b) and two peaks (252bp and 235bp) representing fully edited *GLUR2* at Q/R site in the motor cortex of the SALS patient (see figure 3.11c).

Editing of the kainate receptor subunits *GLUR5* and *GLUR6* were calculated after digestion with restriction enzyme BbVI. When it is edited, BbVI cuts *GLUR5* digest into two fragments (82bp and 32bp) compared to the unedited *GLUR5* sized 114bp (see figure 3.12c). *GLUR6* has similar fragments sized 102bp and 30bp if edited and one fragment sized 132bp when it is unedited (see figure 3.13c).

The analysis of *GLUR2* RNA editing in the frontal cortex of SALS cases (n=3) and in the motor cortex of SALS cases (n=4) compared to controls showed 100% editing at Q/R site (see figure 3.14a). *GLUR5* RNA editing of the same SALS cases (n=3) in the frontal cortex was $83 \pm 9\%$ similar to controls (n=5) that had $82 \pm 7\%$ editing at Q/R site. Whereas, the analysis of *GLUR5* editing in the motor cortex had shown $79 \pm 11\%$ editing in 4 SALS cases and $66 \pm 21\%$ editing in 3 controls (see figure 3.15a). *GLUR6* RNA editing of *GLUR6* was also analysed in the frontal cortex of 3 SALS cases and 5 controls, both groups had shown $88 \pm 9\%$ and $86 \pm 6\%$ editing, respectively. Additionally, RNA editing of the *GLUR6* in the motor cortex of SALS cases (n=4) and in controls (n=3) both had shown similar editing values of $90 \pm 4\%$ and $90 \pm 8\%$, respectively (see figure 3.16a).

RNA editing was also studied in *GLUR2*, *GLUR5* and *GLUR6* of one case with Pick's disease in the motor cortex, temporal cortex, cerebellum and thalamus (see table 3.3). Editing of *GLUR2* in the motor cortex of this case decreased from 100% to 84% editing efficiency. Both the thalamus and temporal cortex had higher *GLUR2* editing of 91% compared to 22% in the cerebellum and 84% in the motor cortex (see figure 3.14b). Like *GLUR2*, *GLUR5* had also variable levels of RNA editing in cerebellum, thalamus, temporal cortex and motor cortex, ranging from 71% to 33% (see figure 3.15b). This patient also had a similar editing profile in the *GLUR6* of these CNS regions, ranging from 66% to 50% (see figure 3.16b). This case was originally included as a control but subsequently characterised as a Pick's case. As shown in figure 3.14b, 3.15b and 3.16b, data did not have error bars because it represent only one case with PICK disease.

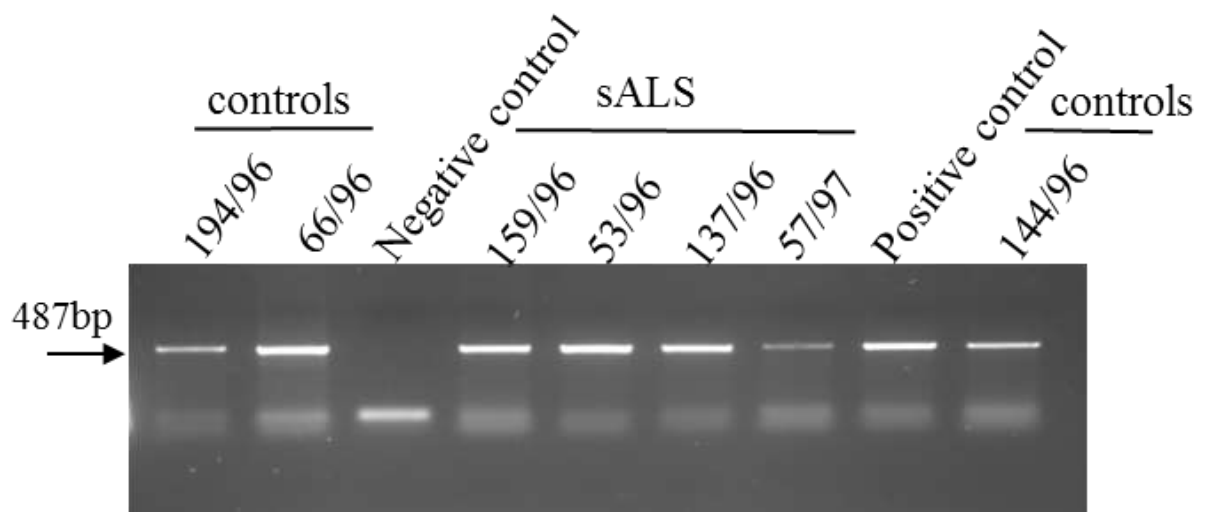


Figure 3.8: Screening *GLUR2* RNA in the motor cortex of SALS patients

Agarose gel electrophoresis of PCR products obtained from motor cortex of SALS patients and controls using *GLUR2* primer sequence, see sequence information in methods figure 2.1. Positive control was whole spinal cord of control case and the negative control was the PCR mixture lacking DNA. Primer dimer was seen. 4 SALS patients and 3 controls were used.

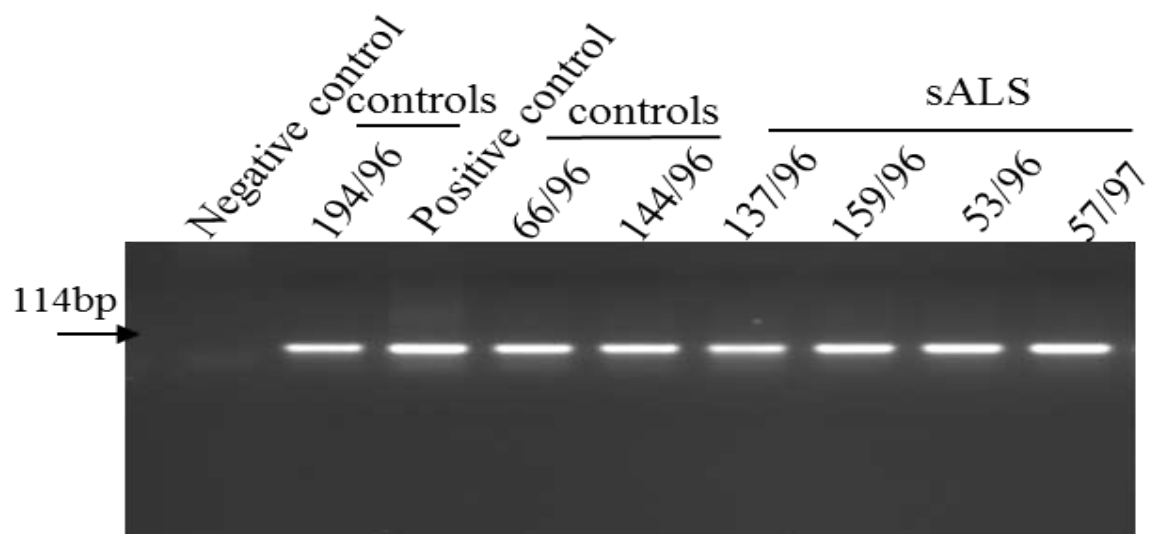


Figure 3.9: Screening *GLUR5* RNA in the motor cortex of SALS patients.

Agarose gel electrophoresis of PCR products obtained from motor cortex of SALS patients and controls using *GLUR5* primer sequence, see sequence information in methods figure 2.2. Positive control was whole spinal cord of control case and the negative control was the PCR mixture lacking DNA. 4 SALS patients and 3 controls were used.

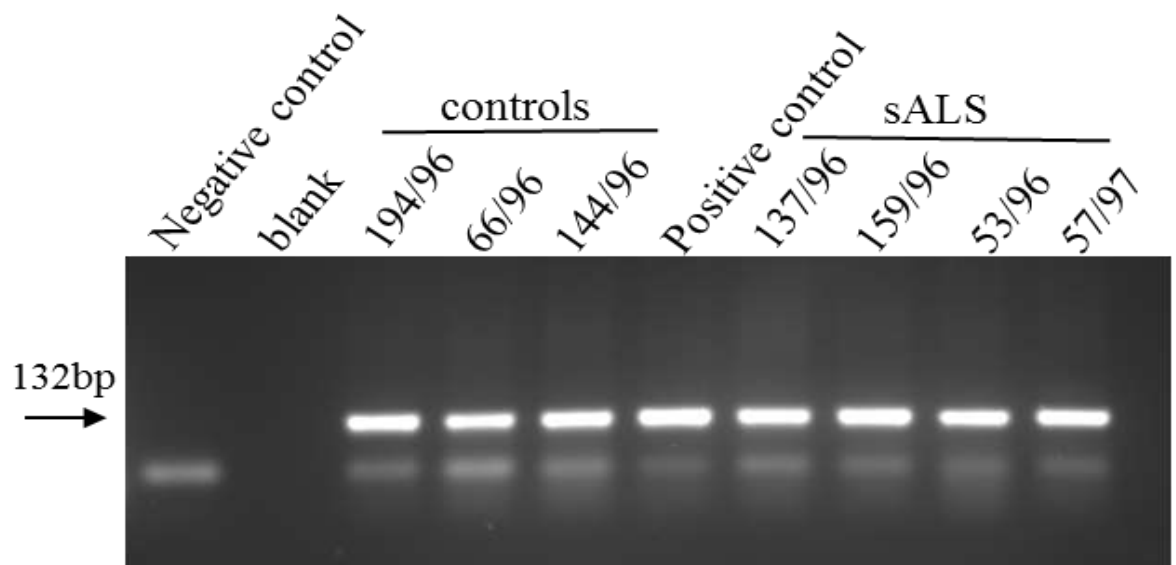


Figure 3.10: Screening *GLUR6* RNA in the motor cortex of SALS patients.

Agarose gel electrophoresis of PCR products obtained from motor cortex of SALS patients and controls using *GLUR6* primer sequence, see sequence information in methods figure 2.3. Positive control was whole spinal cord of control case and the negative control was the PCR mixture lacking DNA. Primer dimer was seen. Cases were 4 SALS patients and 3 controls.

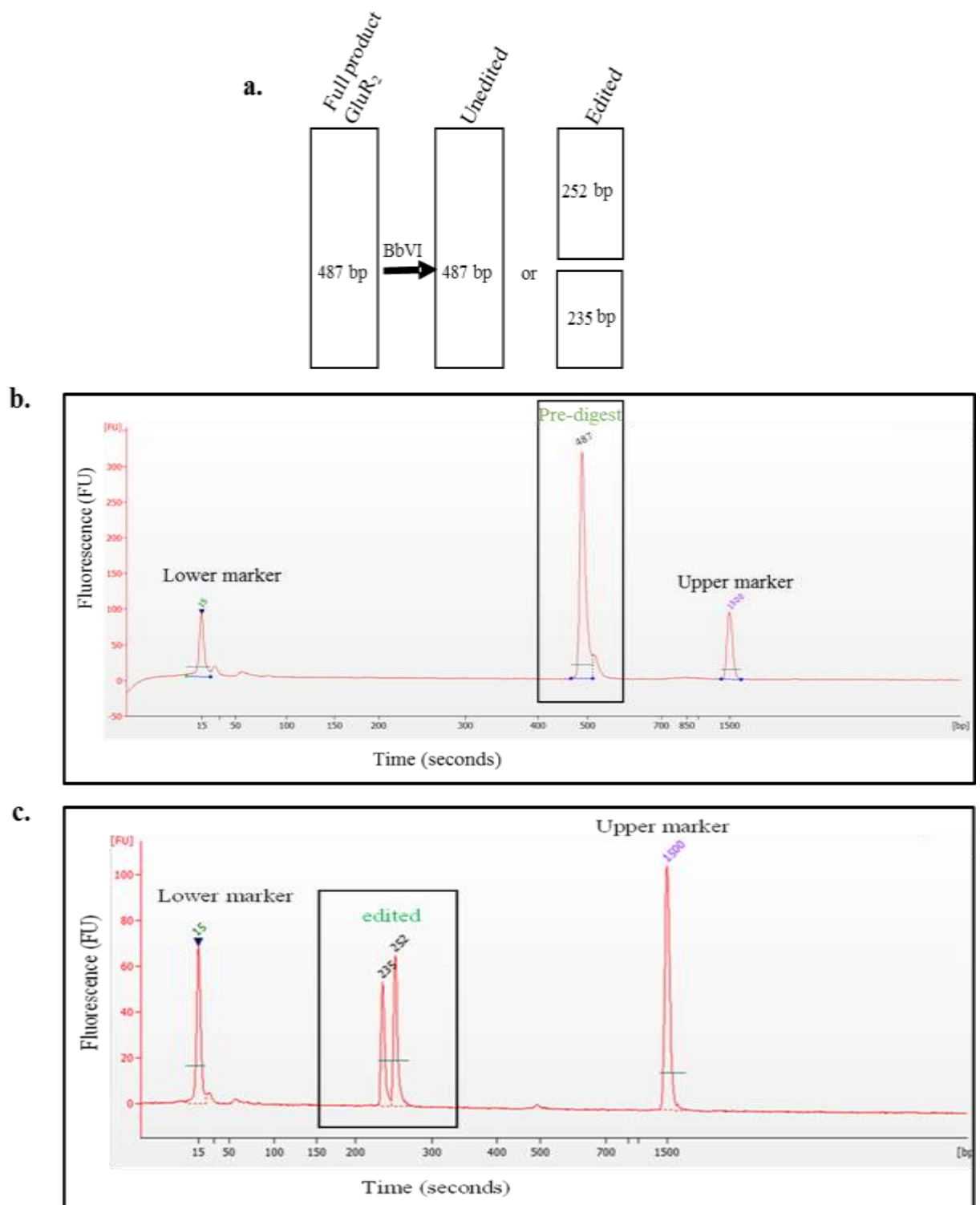


Figure 3.11: Restriction digest analysis of *GLUR2* editing.

A schematic representation of BbVI restriction enzyme digests to differentiate between edited and unedited *GLUR2* mRNA at Q/R site (a). DNA chip bioanalyser showed a single peak *GLUR2* predigest sized 487bp (b). *GLUR2* edited at 252bp and 235bp in motor cortex of SALS patients and controls (c).

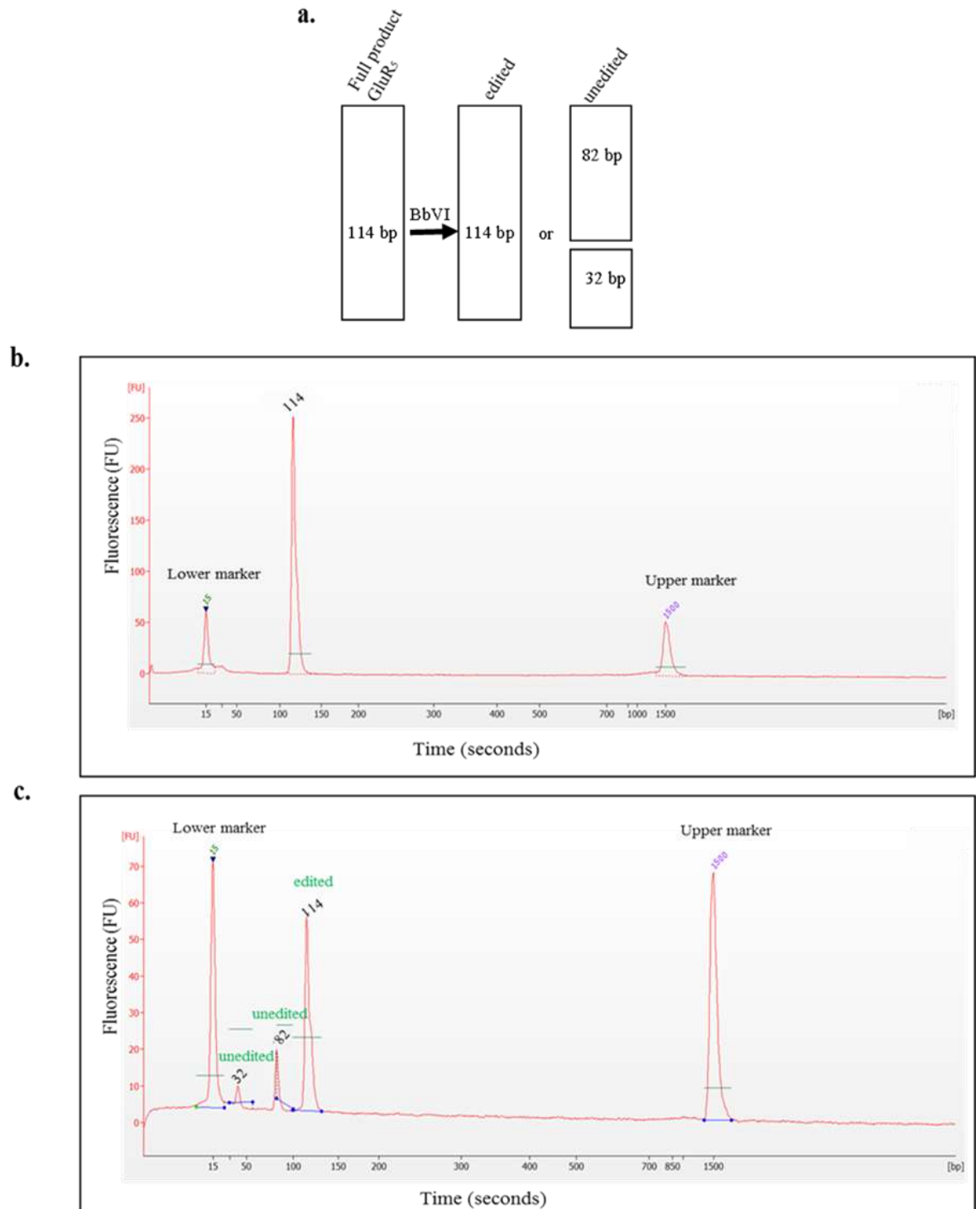


Figure 3.12: Restriction digest analysis of *GLUR5* editing.

A schematic representation of BbVI restriction enzyme digests to differentiate between edited and unedited *GLUR5* mRNA at Q/R site (a). DNA chip bioanalyser showed a single peak of *GLUR5* predigest sized 114bp (b), two peaks of non-edited (82bp and 32bp) and edited (114bp) *GLUR5* in the motor cortex of SALS patients and controls (c).

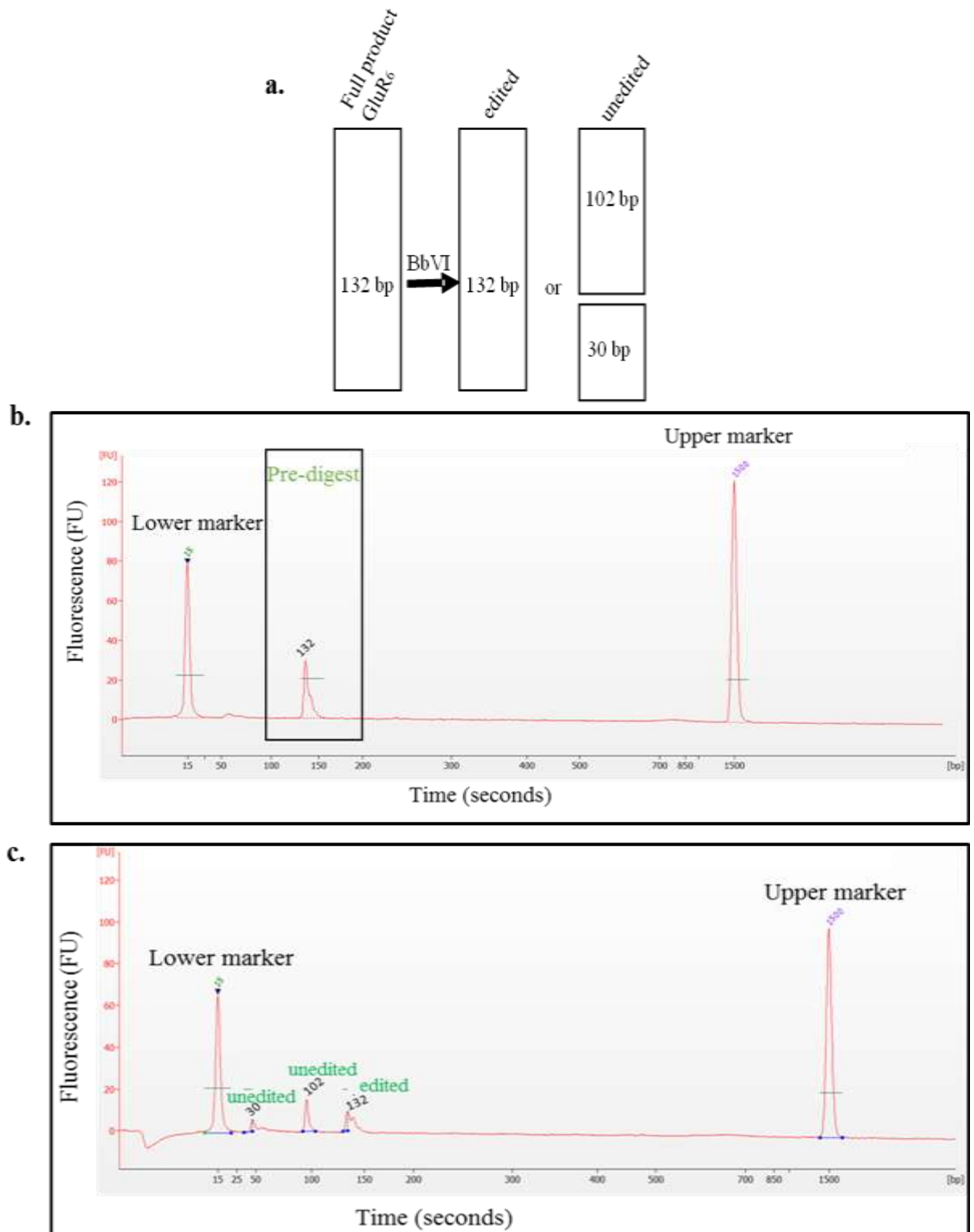


Figure 3.13: Restriction digest analysis of *GLUR6* editing.

A schematic representation of BbVI restriction enzyme digests to differentiate between edited and unedited *GLUR6* mRNA at Q/R site (a). DNA chip bioanalyser showed a single peak of *GLUR6* predigest sized 132bp (b), two peaks of non-edited (102bp and 30bp) and edited (132bp) *GLUR6* in the motor cortex of SALS patients and controls (c).

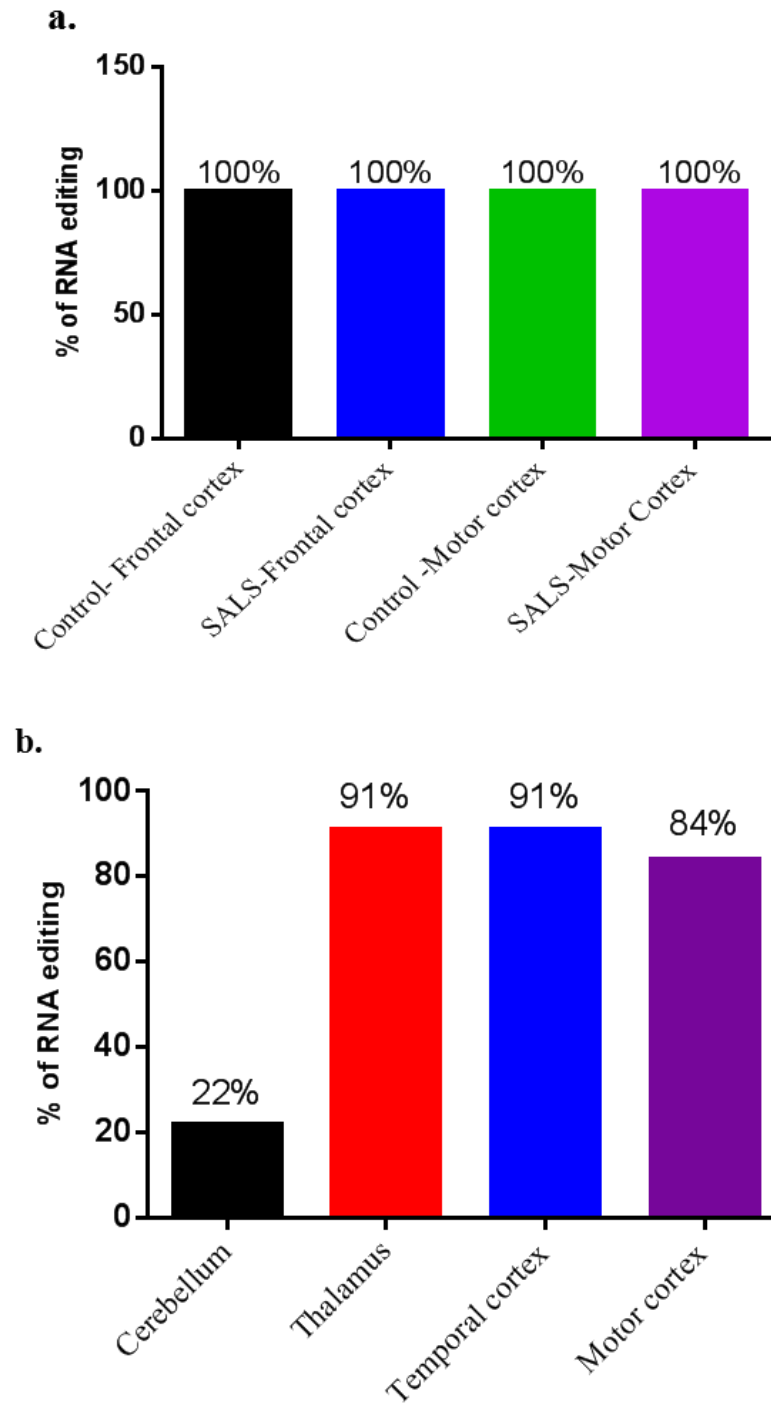


Figure 3.14: Percentage of *GLUR2* RNA editing.

RNA editing of *GLUR2* in frontal and motor cortex of controls and SALS patients (a), RNA editing of different CNS regions in one patient with PICK's disease (b).

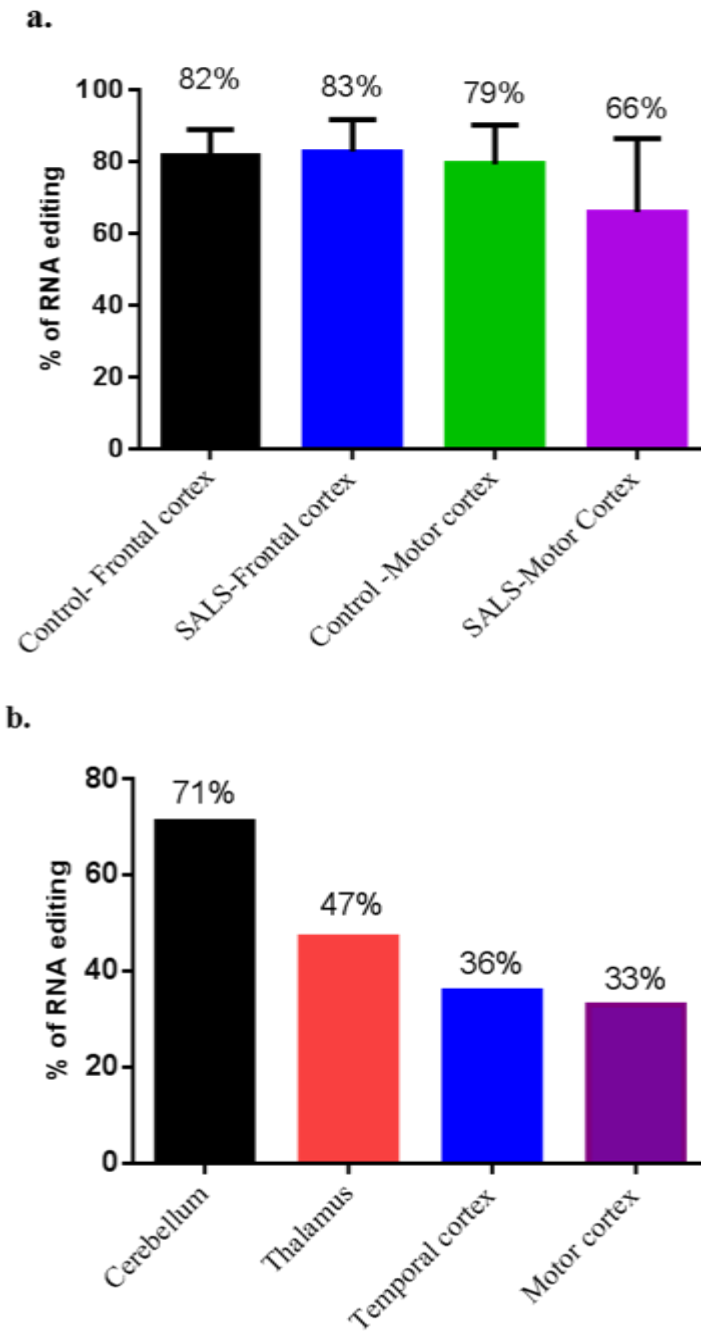


Figure 3.15: Percentage of *GLUR5* RNA editing.

RNA editing of *GLUR5* in frontal and motor cortex of controls and SALS patients (a), RNA editing of different CNS regions in one patient with PICK's disease (b).

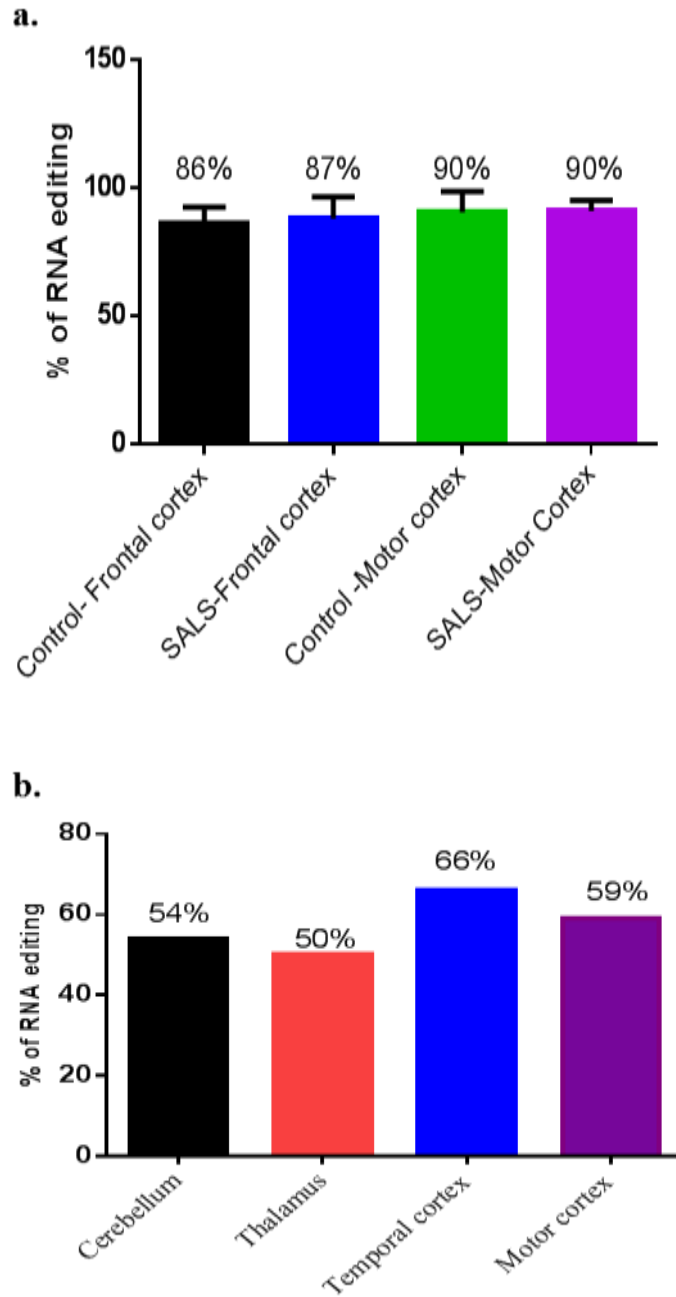


Figure 3.16: Percentage of *GLUR6* RNA editing.

RNA editing of *GLUR6* in frontal and motor cortex of controls and SALS patients (a), RNA editing of different CNS regions in one patient with PICK's disease (b).

3.2.3 RNA editing of glutamate receptors in MNs of ALS

This study aimed to investigate the level of mRNA editing of *GLUR2*, *GLUR5* and *GLUR6* in whole tissue of frozen thoracic spinal cord and in laser captured motor neurons of ALS/*C9ORF72*-positive patients, ALS/*C9ORF72*-negative patients and controls (n=15) (see table 3.4).

Table 3.4: Frozen thoracic spinal cord from ALS cases and controls

Case number	Block Number	Area/Level	Site of onset	PMI in hours	Sex	Age at onset	Age at death
ALS/<i>C9ORF72</i>-positive cases00							
LP83/10	34	T11	Limb	13	Male	67	79
LP081/09	29	T11	Limb	60	Male	57	59
LP041/04	6	T11	Bulbar	48	Male	62	64
LP039/11	26	T11	Limb	96	Male	70	72
LP040/11	25	T11	Limb	10	Female	72	77
ALS/<i>C9ORF72</i>-negative cases							
LP014/11	24	T11	Limb	n/a	Male	49	51
LP005/11	30	T11	Limb	40	Female	62	67
LP023/10	7	T11	Limb	24	Female	34	42
LP005/10	23	T11	Limb	96	Male	38	40
LP094/09	25	T11	Bulbar	48	Male	62	63
Controls							
LP005/07	13	T11	n/a	12	Male	n/a	64
LP085/07	25	T11	n/a	5	Female	n/a	82
LP098/07	25	T11	n/a	63	Male	n/a	67
035/96	8	T11	n/a	14	Female	n/a	87
70/96	2	C7	n/a	n/a	n/a	n/a	n/a

The RNA editing of *GLUR2* at Q/R site showed 100% editing in the spinal cord and in MNs of controls, ALS/*C9ORF72*-positive cases and ALS/*C9ORF72*-negative cases (see figure 3.17 & 3.18).

The RNA editing of *GLUR5* in the spinal cord of ALS cases and controls showed similar levels of RNA editing of $38 \pm 24\%$ (mean \pm SD) and $21 \pm 26\%$, respectively (see figure 3.19a). The RNA editing of *GLUR5* was also determined in the spinal cord of ALS/*C9ORF72*-positive cases and ALS/*C9ORF72*-negative cases compared to controls showing $21 \pm 26\%$ in controls, $41 \pm 20\%$ in *C9ORF72* negative cases and $35 \pm 29\%$ in *C9ORF72*-positive cases (see figure 3.19b).

The RNA editing of *GLUR5* in MNs of ALS cases and controls showed $48 \pm 19\%$ in ALS cases and $30 \pm 25\%$ in controls (see figure 3.20a). The editing efficiency of *GLUR5* in MNs was $39 \pm 17\%$ in ALS/*C9ORF72*-positive cases, $57 \pm 19\%$ editing in ALS/*C9ORF72*-negative cases and $30 \pm 25\%$ in controls (see figure 3.20b).

The RNA editing levels of *GLUR6* in the spinal cord showed $33 \pm 9.4\%$ in ALS patients to $32 \pm 18\%$ in controls (see figure 3.21a). Additionally, the editing efficiency of *GLUR6* in the spinal cord of ALS/*C9ORF72*-positive cases and ALS/*C9ORF72*-negative cases was $36 \pm 8\%$ and $30 \pm 1\%$, respectively compared to controls that showed $32 \pm 18\%$ editing (see figure 3.21b).

The RNA editing of *GLUR6* in MNs showed $81 \pm 36\%$ editing in ALS and $72 \pm 42\%$ in controls (see figure 3.22a). Furthermore, the editing levels of *GLUR6* in MNs were increased from $77 \pm 43\%$ editing in ALS/*C9ORF72* -negative cases to $86 \pm 32\%$ editing in ALS/*C9ORF72*-positive cases compared to $72 \pm 42\%$ in controls (see figure 3.22b).

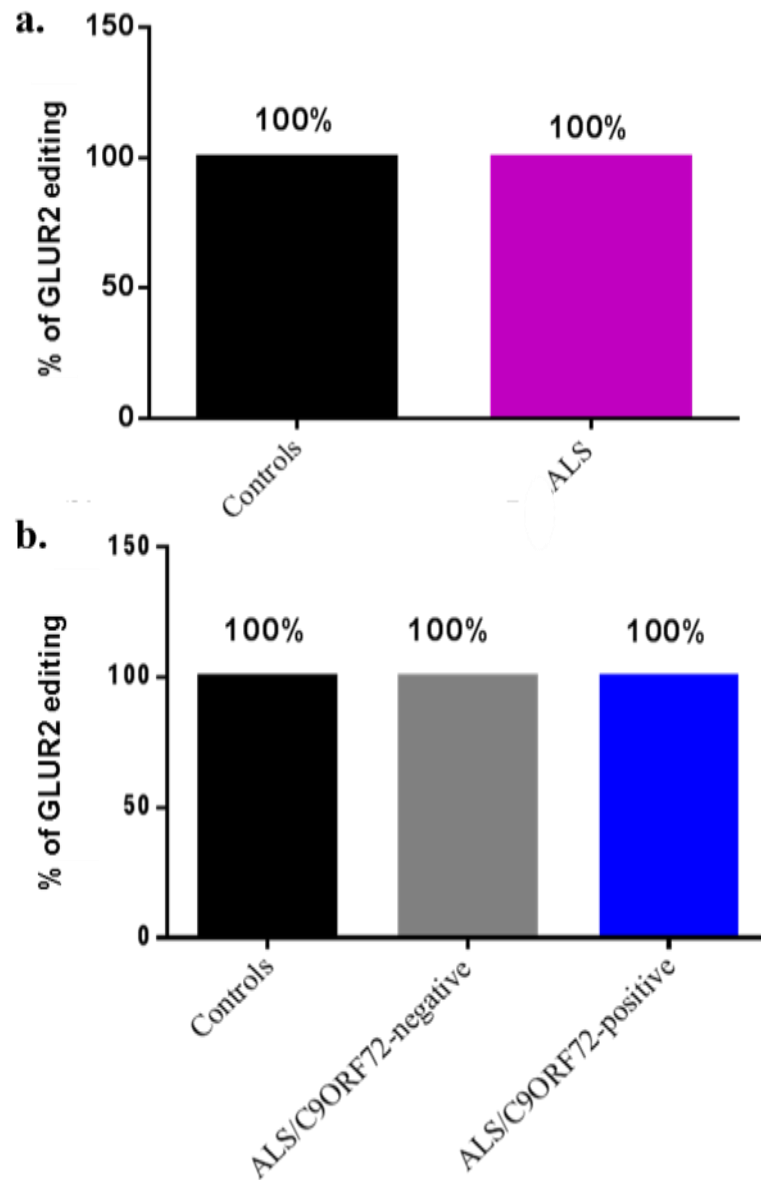


Figure 3.17: RNA editing of *GLUR2* in the spinal cord of ALS cases.

RNA editing efficiency of *GLUR2* in the spinal cord of controls and ALS patients (a) in controls, ALS/ *C9ORF72*-negative cases and ALS/*C9ORF72*-positive cases (b).

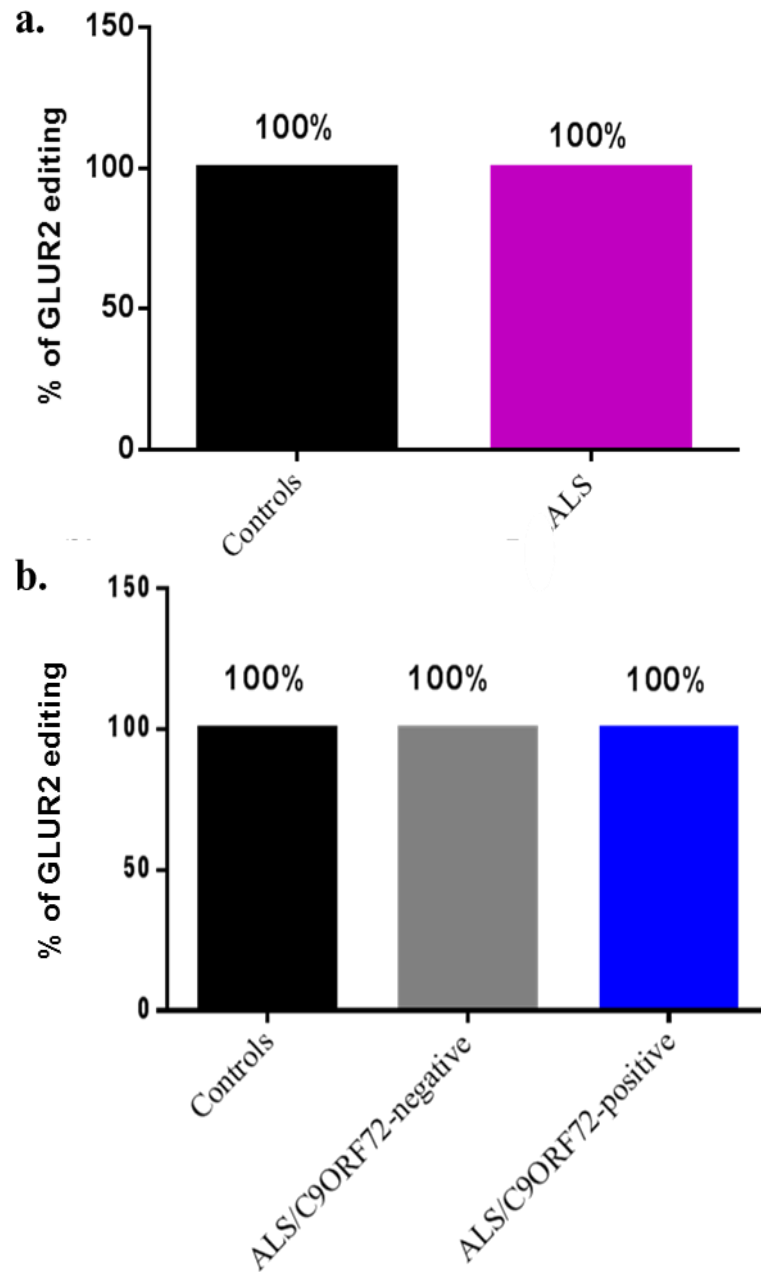


Figure 3.18: RNA editing of *GLUR2* in MNs of ALS

Percentage of RNA editing of *GLUR2* in MNs of controls and ALS cases (a) in controls, ALS/*C9ORF72*-negative cases and ALS/*C9ORF72*-positive cases (b).

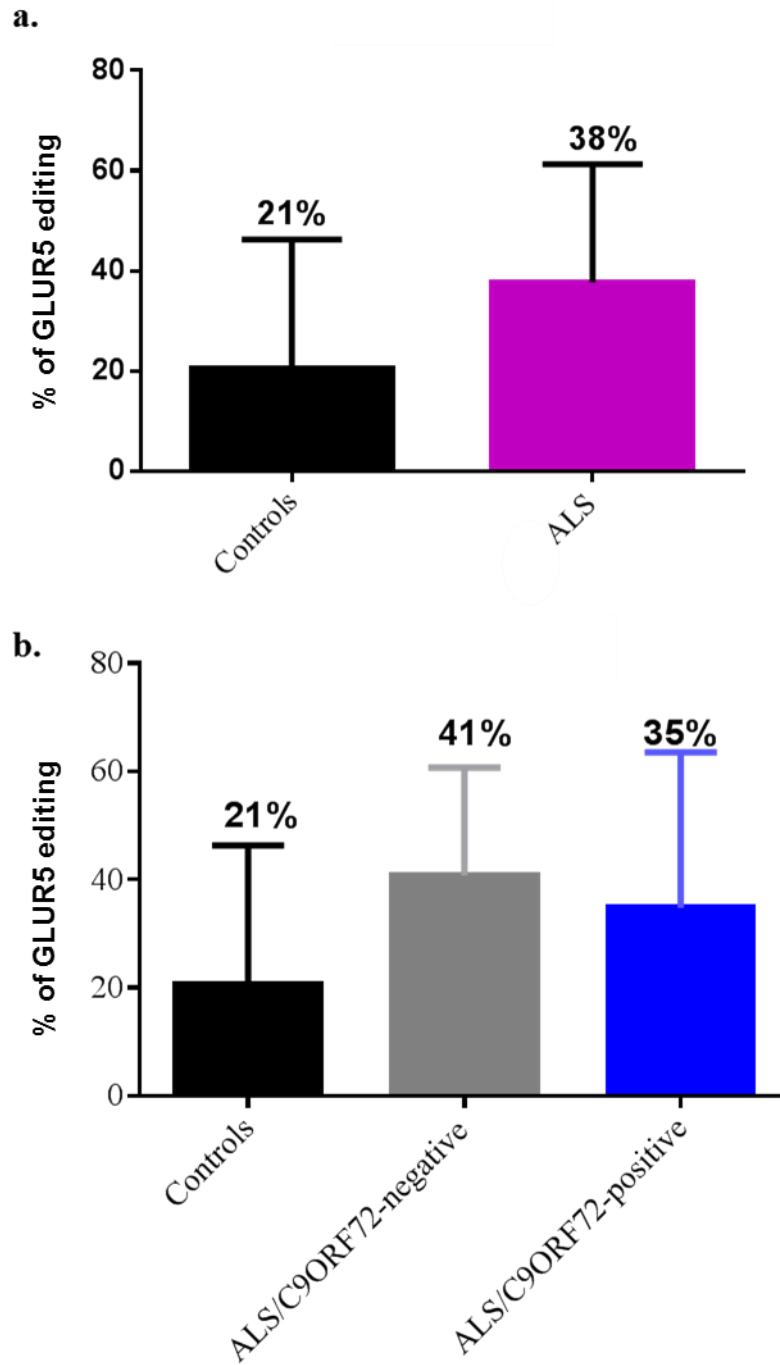


Figure 3.19: RNA editing of *GLUR5* in the spinal cord of ALS cases.

RNA editing efficiency of *GLUR5* in the spinal cord of controls and ALS patients (a) in controls, ALS/ *C9ORF72*-negative cases and ALS/*C9ORF72*-positive cases (b).

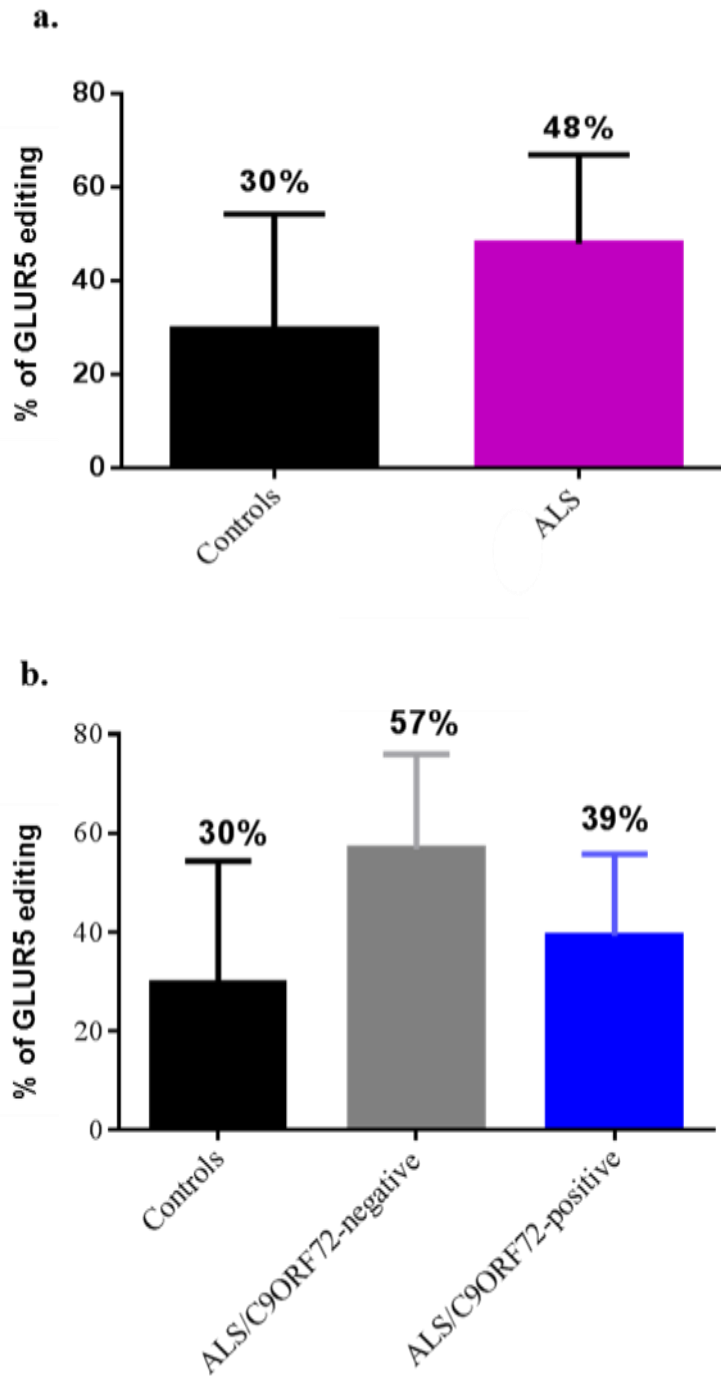


Figure 3.20: RNA editing of *GLUR5* in MNs of ALS

Percentage of RNA editing of *GLUR5* in MNs of controls and ALS cases (a) in controls, ALS/*C9ORF72*-negative cases and ALS/*C9ORF72*-positive cases (b).

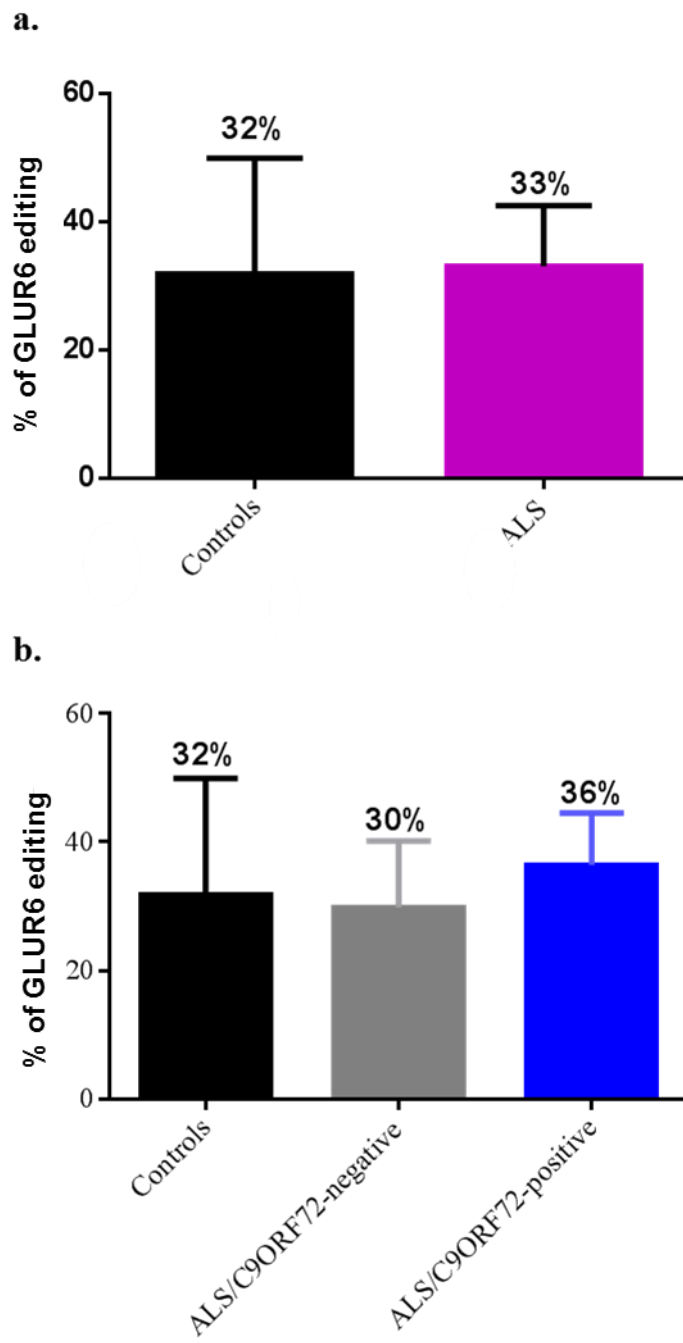


Figure 3.21: RNA editing of *GLUR6* in the spinal cord of ALS cases.

RNA editing efficiency of *GLUR6* in the spinal cord of controls and ALS patients (a) in controls, ALS/ *C9ORF72*-negative cases and ALS/*C9ORF72*-positive cases (b).

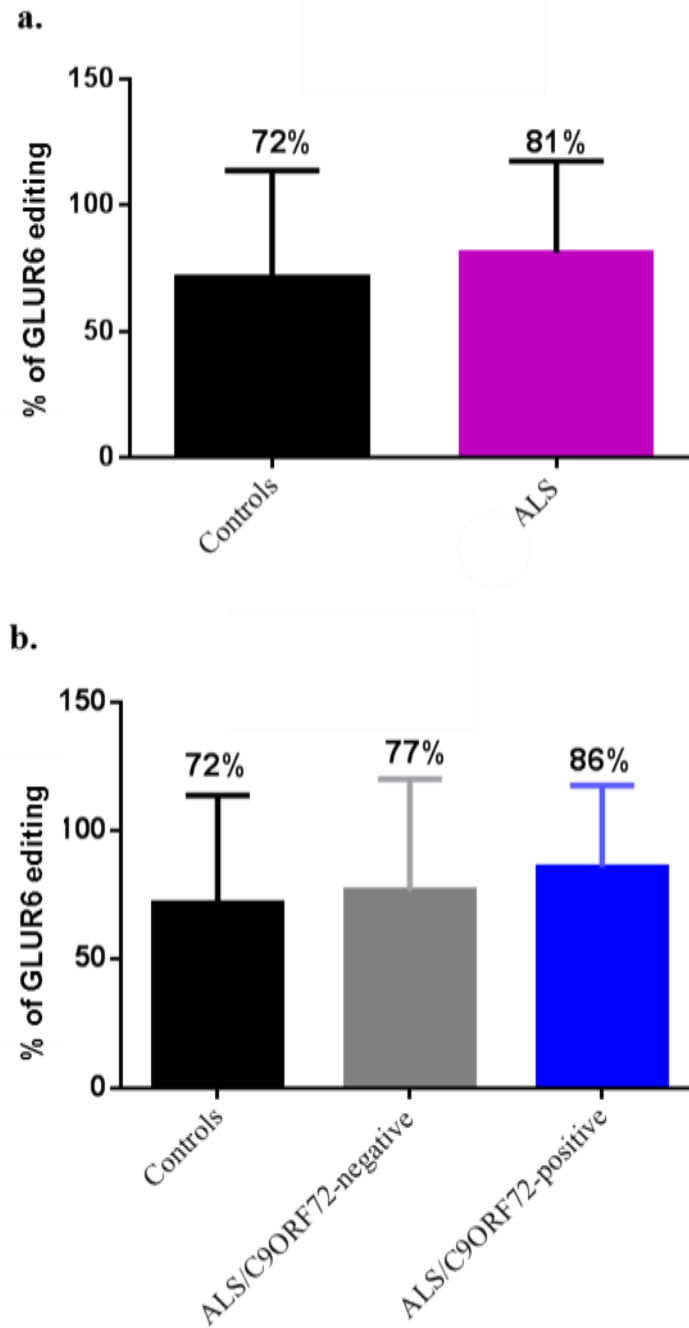


Figure 3.22: RNA editing of *GLUR6* in MNs of ALS

Percentage of RNA editing of *GLUR6* in MNs of controls and ALS cases (a) in controls, ALS/*C9ORF72*-negative cases and ALS/*C9ORF72*-positive cases (b).

Table 3.5: *GLUR* editing at Q/R site of ALS patients.

<i>Percentage (%) of editing of one patient with PICK'S disease at Q/R site</i>													
		<i>GLUR2</i>				<i>GLUR5</i>				<i>GLUR6</i>			
Regions	Number of patients	SALS											
Temporal	1	91				36				66			
Thalamus		91				47				50			
Motor cortex		84				33				59			
Cerebellum		22				22				54			
<i>Percentage (%) of editing of SALS patients at Q/R site</i>													
		<i>GLUR2</i>				<i>GLUR5</i>				<i>GLUR6</i>			
Regions	No of patients	Cntr		SALS		Cntr		SALS		Cntr		SALS	
Frontal cortex	3	100	100	82 ± 7		83 ± 9		86 ± 6		88 ± 9			
Motor cortex	4	100	100	79 ± 11		66 ± 21		90 ± 8		90 ± 4			
<i>Percentage (%) of editing in ALS/C9ORF72-negative and ALS/C9ORF72-positive patients at Q/R site</i>													
		<i>GLUR2</i>				<i>GLUR5</i>				<i>GLUR6</i>			
	No of patients	Cntr	ALS	<i>C9ORF72</i> ⁻	<i>C9ORF72</i> ⁺	Cntr	ALS	<i>C9ORF72</i> ⁻	<i>C9ORF72</i> ⁺	Cntr	ALS	<i>C9ORF72</i> ⁻	<i>C9ORF72</i> ⁺
Spinal cord	5	100	100	100	100	21 ± 26	38 ± 24	41 ± 20	35 ± 29	32 ± 18	33 ± 9.4	30 ± 1	36 ± 8
MNs	5	100	100	100	100	30 ± 25	48 ± 19	57 ± 19	39 ± 17	72 ± 42	81 ± 36	77 ± 43	86 ± 32

The percentage of the RNA editing of *GLUR2*, *GLUR5* and *GLUR6* was calculated using this formula [% of RNA editing= non-edited/edited+ non-edited concentrations]. The mean and SD were analysed using One-way ANOVA and student T-Test. Abbreviations: Cntr - control, *C9ORF72*⁻- *C9ORF72*-negative, *C9ORF72*⁺- *C9ORF72*- positive, MNs-motor neurons, *GLUR*- glutamate receptors, SD- standard deviation

3.2.4 *ADAR* mRNA expression in ALS

This study investigated the correlation between the expression of *ADAR2* and *ADAR3* in spinal cord of ALS/*C9ORF72*-positive cases and ALS/*C9ORF72*-negative cases compared to controls. Quantitative real-time PCR was used to determine the mRNA expression of *ADAR2* and *ADAR3* relative to an internal reference *GAPDH* mRNA. The data was further analysed using student T-test and one-way ANOVA.

The mRNA expressions of *ADAR2* in the spinal cord of ALS cases was increased (2.1 ± 0.87) (mean \pm SD) compared to controls (1 ± 0.1) however, this data did not reach statistical significance ($p=0.1151$) (see figure 3.23a). *ADAR2* expression was also examined in the spinal cord of ALS/*C9ORF72*-positive cases and ALS/*C9ORF72*-negative cases, it showed increased *ADAR2* expression of $1.7 \pm 0.7\%$ in ALS/*C9ORF72*-positive cases and $2.2 \pm 0.5\%$ in ALS/*C9ORF72*-negative cases compared to $1 \pm 0.1\%$ in controls. However, the relative expression of *ADAR2* between ALS and controls did not reach statistical significance ($p=0.9177$) (see figure 3.23b).

The mRNA expressions of *ADAR3* in the spinal cord of ALS cases was similar to controls (1 ± 0.3) with no statistical significance between ALS cases and controls, ($p=0.8038$) (see figure 3.24a). The expression of *ADAR3* in ALS cases in particular ALS/*C9ORF72*-positive cases (1 ± 0.2), ALS/*C9ORF72*-negative cases (1 ± 0.3) and controls (1 ± 0.2) did not show any statistical significance ($p=0.9498$) (see figure 3.24b).

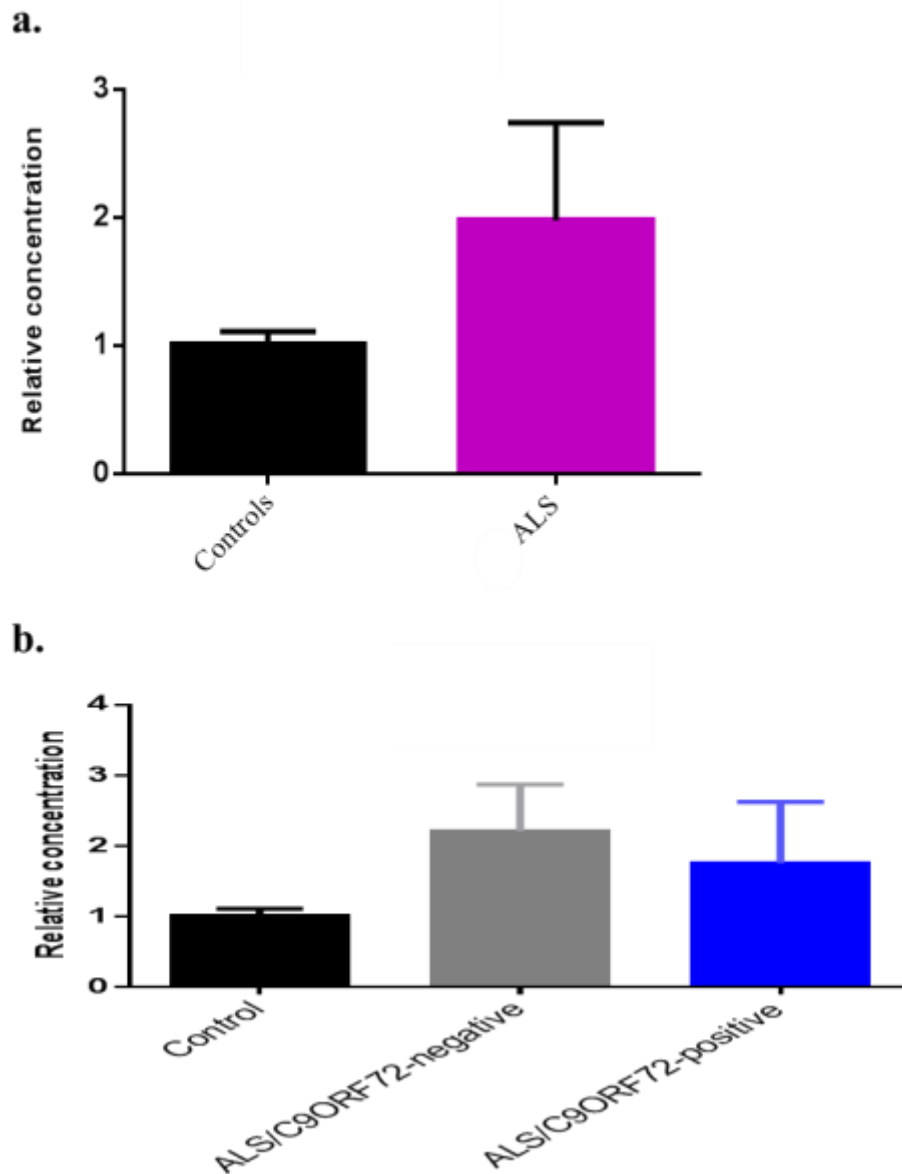


Figure 3.23: The relative expression of *ADAR2* in spinal cord of ALS cases.

The analysis of *ADAR2* mRNA expression in spinal cord of ALS patients and controls (a) and ALS/*C9ORF72*-positive cases and ALS/*C9ORF72*-negative cases compared to controls (b). Student T-Test revealed non statistical significance between ALS cases and controls of *ADAR2*, $p=0.1151$. One-way ANOVA showed no significant difference in the expression of *ADAR2*, $p=0.1977$ across the 3 groups.

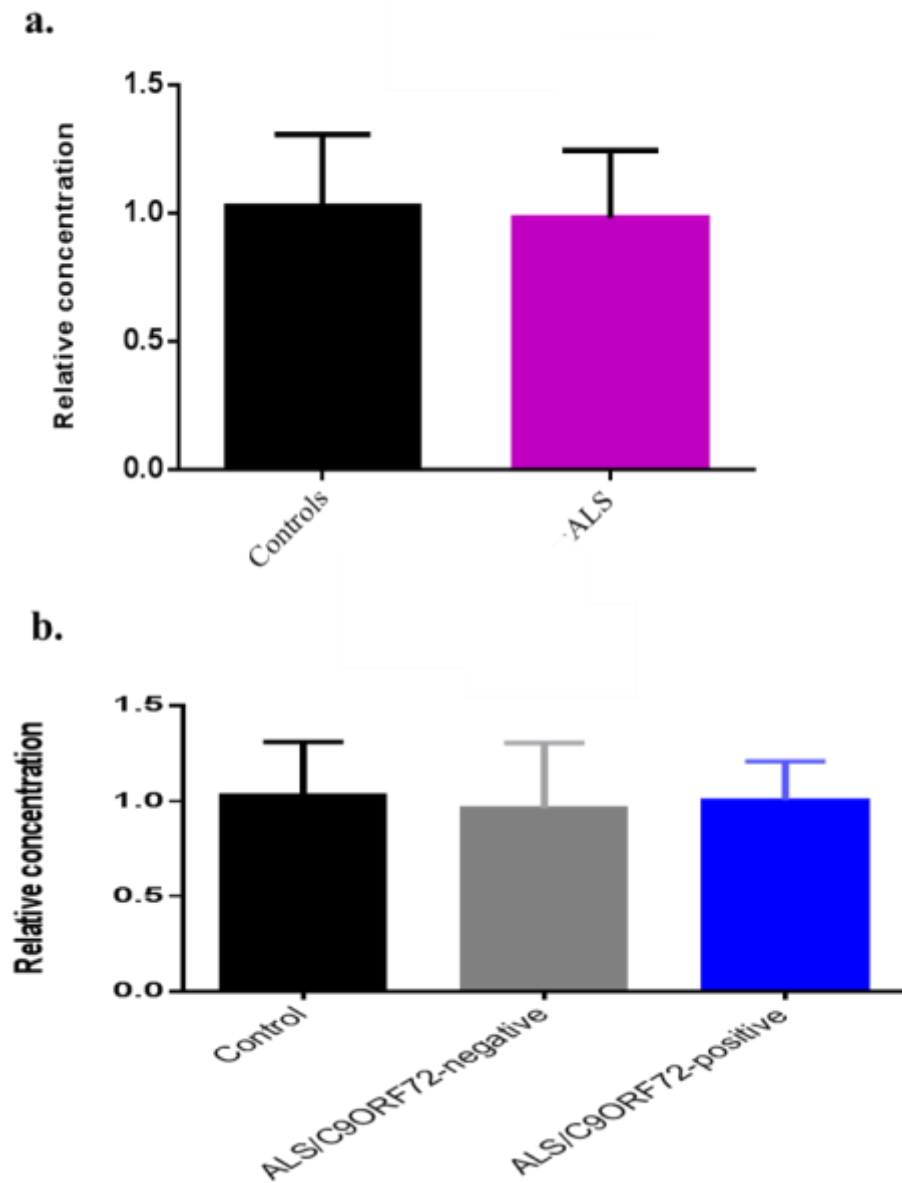


Figure 3.24: The relative expression of *ADAR3* in spinal cord of ALS cases

The analysis of *ADAR3* mRNA expression in the spinal cord of ALS patients and in controls (a) ALS/*C9ORF72*-positive cases and ALS/*C9ORF72*-negative cases compared to controls (b). Student T-Test revealed non statistical significance between ALS cases and controls of *ADAR3*, $p= 0.8038$. One-way ANOVA showed no significant difference in the expression of *ADAR3*, $p= 0.9498$ across the 3 groups.

3.2.5 The potential role of normal and aberrant alternative transcripts of *EAAT2* in astrocytes

To investigate the alternatively spliced variants of *EAAT2*, exon 4 and exon 9 retaining and skipping transcripts in controls and in ALS patients. The normal *EAAT2* transcripts (also called *EAAT2* retaining transcripts) are $EAAT2^{+4}$ and $EAAT2^{+9}$. Whereas, the aberrant *EAAT2* transcripts (also called *EAAT2* skipping transcripts) are $EAAT2^{\Delta 4}$ and $EAAT2^{\Delta 9}$. All *EAAT2* transcripts were measured by quantitative real-time PCR. The mRNA of these normal and aberrant *EAAT2* transcripts were normalised to an internal reference *GAPDH* mRNA and analysed using student T-test and one-way ANOVA.

Examining the relative expression of the $EAAT2^{+4}$ in the astrocytes of all ALS cases versus controls showed 3.25 ± 2.36 (mean \pm SD) in ALS cases compared to 1.69 ± 1.4 in controls (see figure 3.25a). Additionally, the expression of $EAAT2^{+4}$ transcript in astrocytes showed 4 ± 3.7 in ALS/*C9ORF72*-positive and 2.7 ± 0.6 in ALS/*C9ORF72*-negative cases relative to 1.6 ± 1.4 in controls (see figure 3.25b). An increase in the $EAAT2^{+4}$ expression was observed in ALS patients to controls ($p=0.3151$) or ALS/*C9ORF72*-negative cases and ALS/*C9ORF72*-positive cases compared to controls ($p=0.533$), though this was not significant.

Examining the relative expression of the $EAAT^{\Delta 4}$ in the astrocytes of ALS cases versus controls showed 2.70 ± 1.9 in ALS cases compared to 2.1 ± 1.66 in controls (see figure 3.26a). The expression of the $EAAT^{\Delta 4}$ transcript was 3 ± 2.6 in ALS/*C9ORF72*-positive cases and 2.1 ± 0.1 in ALS/*C9ORF72*-negative cases relative to 2.1 ± 1.5 in controls (see figure 3.26b). The difference between the expression of $EAAT^{\Delta 4}$ transcript of ALS cases and controls did not reach statistical significance

($p=0.6663$). The expression of EAAT^{Δ4} transcripts was increased in ALS cases with and without *C9ORF72* expansion compared to controls ($p=0.8205$), though this was not significant.

The relative expression of EAAT2⁺⁹ in the astrocytes of all ALS cases versus controls showed 1.86 ± 0.9 in ALS cases compared to 1.21 ± 0.4 in controls (see figure 3.27a). An increase in the expression of EAAT2⁺⁹ transcript of ALS cases compared to controls was observed, $p=0.2818$, though this was not significant. The relative expression of EAAT2⁺⁹ transcript was also examined in the astrocytes of ALS/*C9ORF72*-positive cases (2 ± 3.7) and in ALS/*C9ORF72*-negative cases (1.7 ± 0.7), compared to controls (1.2 ± 0.4), $p=0.244$ (see figure 3.27b). However, the difference in EAAT^{Δ9} transcript of ALS cases particularly between ALS cases with and without *C9ORF72* expansion relative to controls did not reach statistical significance, $p=0.4376$. EAAT2⁺⁹ transcripts in the astrocyte of ALS/*C9ORF72*-positive cases exhibited a large error due to variability in cases and RNA quality.

The relative expression of EAAT2^{Δ9} in the astrocytes of ALS cases versus controls showed 2.8 ± 3.5 in ALS cases compared to 1.14 ± 0.5 in controls (see figure 3.28a). Furthermore, the expression of EAAT2^{Δ9} transcript in the astrocytes was 4 ± 5 in ALS/*C9ORF72*- positive cases, 1.7 ± 1.9 in ALS/*C9ORF72*-negative cases and 1.1 ± 0.4 in controls (see figure 3.28b). Overall expression of EAAT2^{Δ9} transcripts in ALS and controls ($p=0.4376$) or in ALS/*C9ORF72*- positive cases, ALS/*C9ORF72*-negative cases and controls did not show any statistical significance ($p=0.5092$).

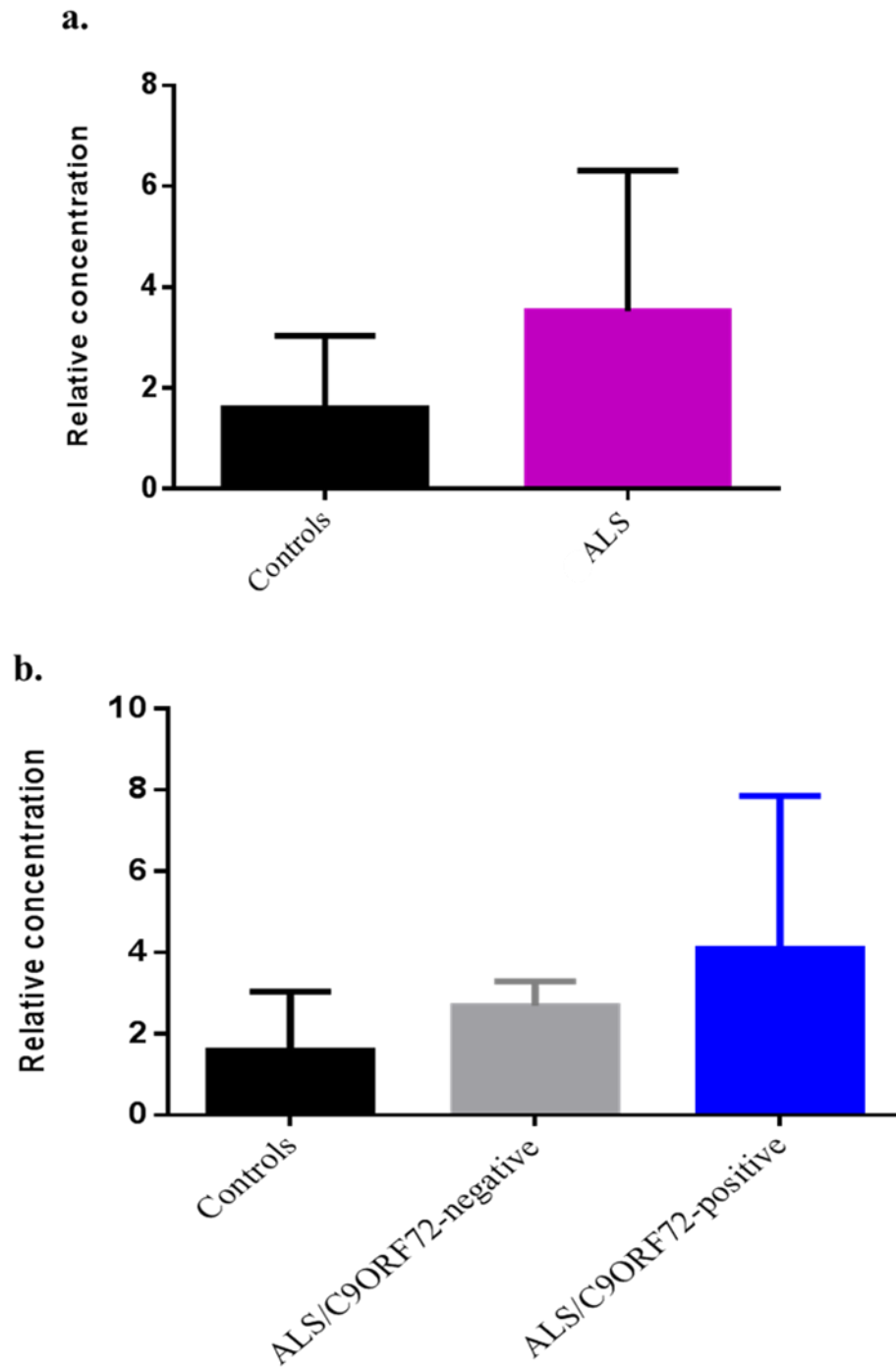


Figure 3.25: The mRNA expression of EAAT⁺4 in the grey matter of the spinal cord of ALS cases.

The expression of EAAT⁺4 transcript showed non statistical significance between ALS cases and controls ($p=0.3151$) (a). This test was carried out by student T-Test. Using one-way ANOVA, the expression of EAAT⁺4 was also analysed in controls, ALS/*C9ORF72*-negative cases and ALS/*C9ORF72*-positive cases. It showed no statistical significance between ALS cases with and without *C9ORF72* expansion and controls ($p=0.533$).

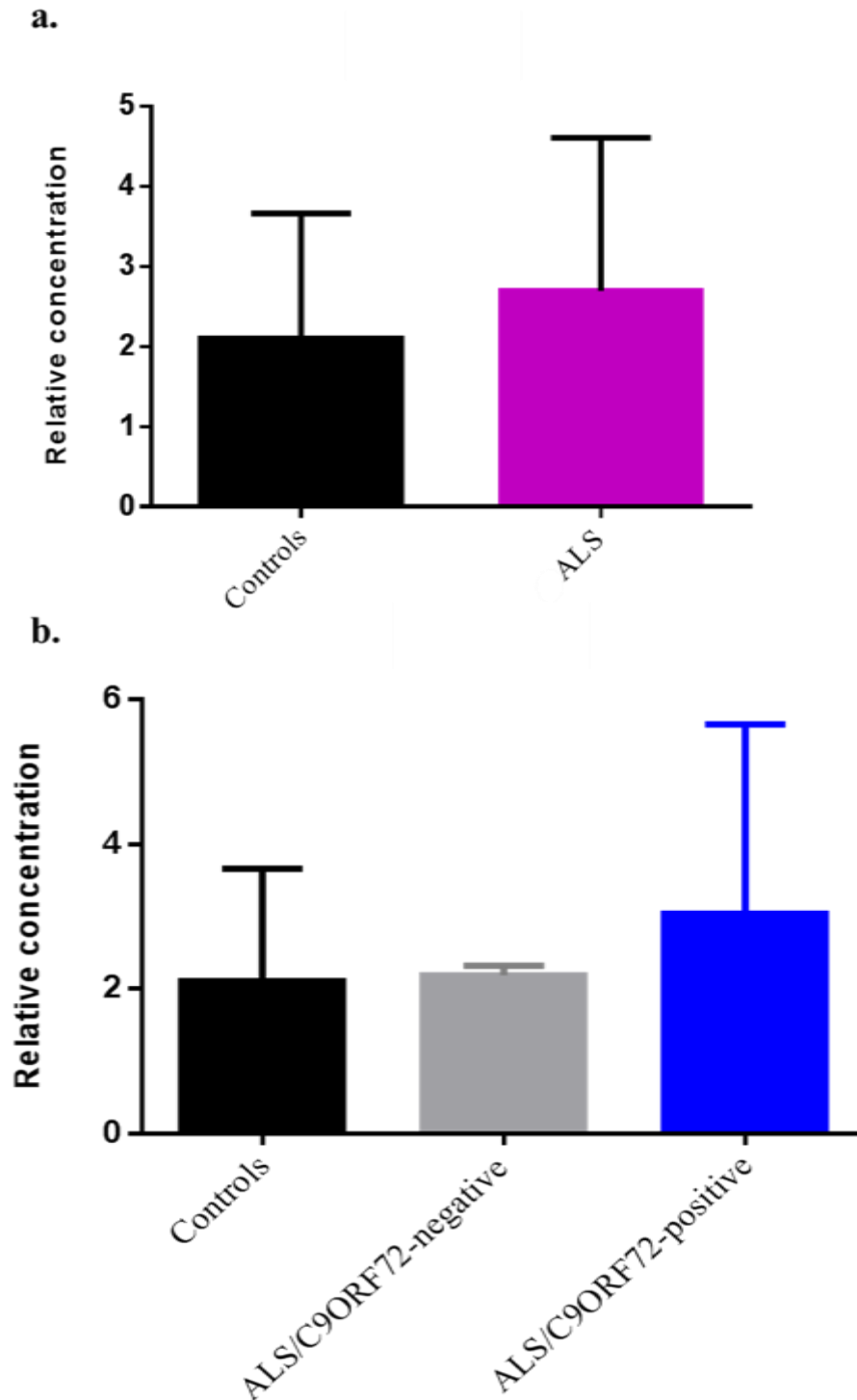


Figure 3.26: The mRNA expression of EAAT⁴ skipping in the grey matter of the spinal cord of ALS cases.

The expression of EAAT⁴ showed non statistical significance between ALS cases and controls ($p=0.6663$) (a). This test was carried out by student T-Test. Using one-way ANOVA, the expression of EAAT⁴ was also analysed in controls, ALS/C9ORF72-negative cases and ALS/C9ORF72-positive cases. It showed no statistical significance between ALS cases with and without C9ORF72 expansion and controls ($p= 0.8205$).

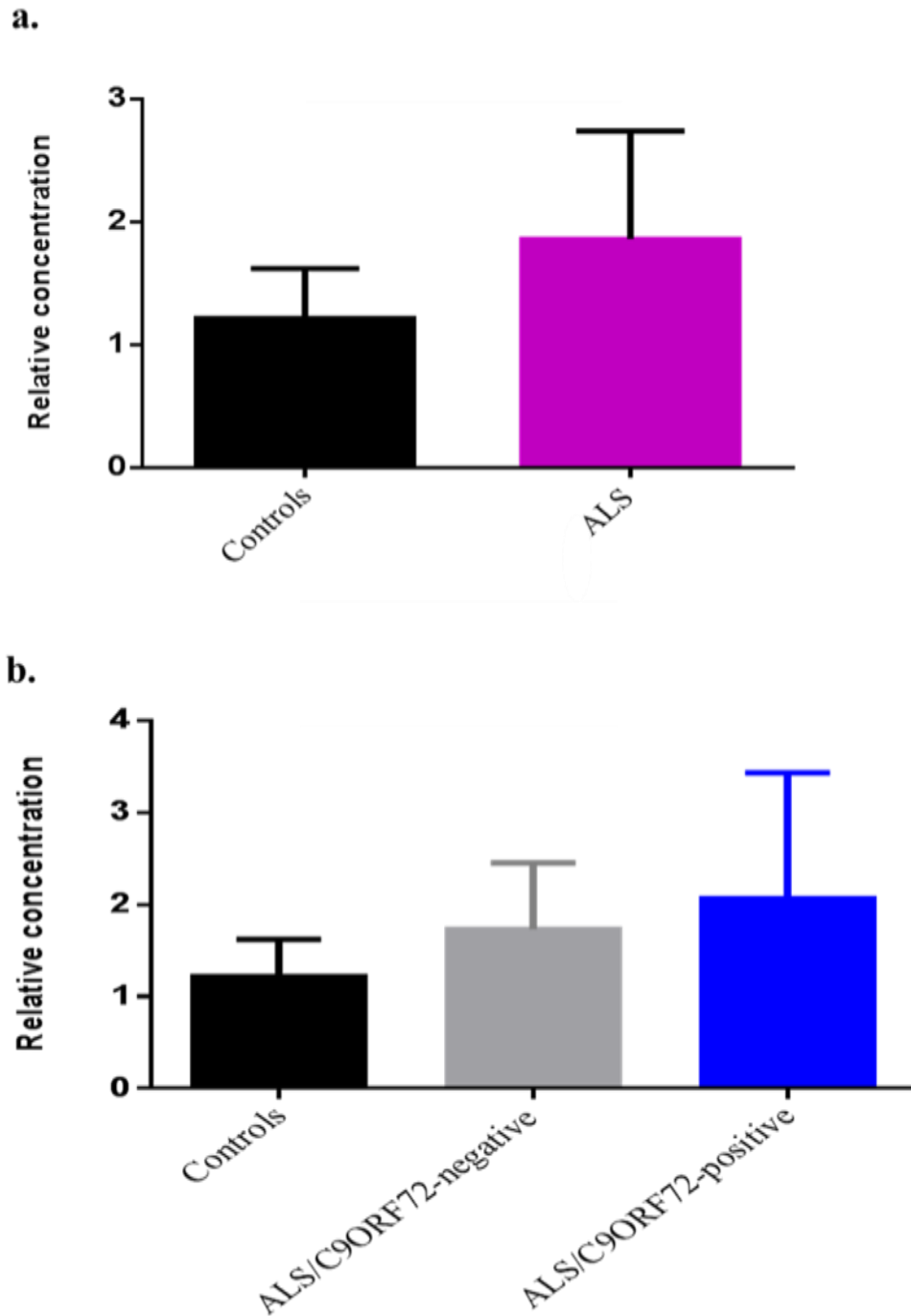


Figure 3.27: The mRNA expression of EAAT⁺9 in the grey matter of the spinal cord of ALS cases.

A student T-test revealed an increase in the EAAT⁺9 of ALS patients compared to controls ($p=0.2818$), though this was not significant. Using one-way ANOVA, there was no statistical significance between controls, ALS/C9ORF72-negative cases and ALS/C9ORF72-positive cases ($p=0.244$) (b).

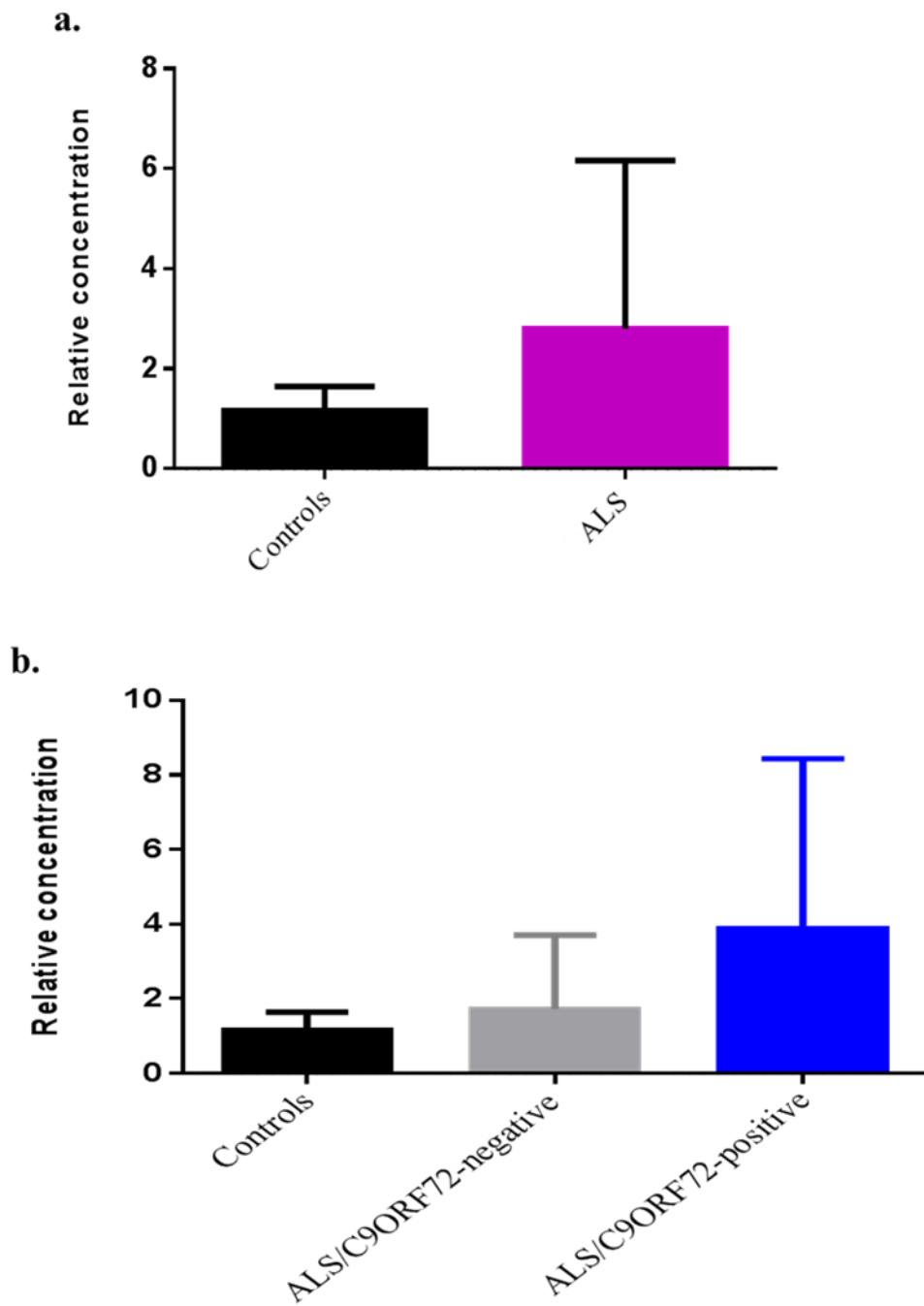


Figure 3.28: The mRNA expression EAAT⁹ in the grey matter of the spinal cord of ALS cases.

A student T-test revealed an increase in the expression of EAAT⁹ in ALS patients compared to controls ($p=0.4376$), though this was not significant. Using one-way ANOVA, there was no statistical significance between controls, ALS/C9ORF72-negative cases and ALS/C9ORF72-positive cases in the expression of EAAT⁹ ($p=0.5092$) (b).

3.3 Discussion

The current study determined the levels of RNA editing in *GLUR2*, *GLUR5* and *GLUR6* in ALS patients compared to controls. The RNA editing of *GLUR2* at Q/R site was 100% edited in the frontal cortex, motor cortex, spinal cord and in MNs of ALS cases and controls. Whereas, RNA editing efficiency of *GLUR5* at Q/R site was less in the frontal cortex, motor cortex, spinal cord and in MNs of both ALS/*C9ORF72*-negative and ALS/*C9ORF72*-positive cases compared controls. Similarly, *GLUR6* RNA editing at Q/R site showed similar levels of editing to *GLUR5* in the frontal cortex, motor cortex, spinal cord and in MNs of ALS/*C9ORF72*-negative and ALS/*C9ORF72*-positive compared controls.

Several lines of evidence support the theory that MNs in the spinal cord of SALS are differentially more vulnerable to AMPA receptor-mediated excitotoxicity than other neuronal subsets, both *in vitro* (Rothstein *et al.*, 1993; Carriedo *et al.*, 1996) and *in vivo* (Nakamura *et al.*, 1994; Kwak & Nakamura, 1995). Studies have suggested that increased Ca^{+2} influx through Ca^{+2} -permeable AMPA receptor not containing subunit *GLUR2* might be the mechanism by which these effects occur (Carriedo *et al.*, 1996; Van Den Bosch *et al.*, 2000). It has been shown that AMPA receptors lacking *GLUR2* have high levels of Ca^{+2} influx whereas, AMPA receptor containing *GLUR2* have a low Ca^{+2} influx (Hollmann *et al.*, 1991; Verdoorn *et al.*, 1991). Particularly, those AMPA receptors containing edited *GLUR2* at Q/R site, since when edited *GLUR2* (R) is present in the AMPA receptor complex, AMPA receptors become impermeable to Ca^{+2} . Whereas, when AMPA receptors contain the unedited form of *GLUR2* (Q), their Ca^{+2} permeability remains high (Sommer *et al.*, 1991). Therefore, both deficiency in

GLUR2 expression and abnormal editing levels of *GLUR2* mRNA can induce AMPA receptor-mediated neuronal death (Hollmann *et al.*, 1991; Wright & Vissel, 2012).

Although most attention has been focused on the *GLUR2* of the AMPA receptor subunit, the involvement of other glutamate receptors such as KA receptor subunits *GLUR5* and *GLUR6* in ALS has been reported (Heath & Shaw, 2002). Studies had shown that KA receptors are thought to mediate motor neuron injury when they become permeable to Ca^{2+} (Carriedo *et al.*, 1996; Vincent & Mulle, 2009). These subunits are also subject to RNA editing by *ADAR2* on a dsRNA structure, usually formed between the exonic editing site and a downstream intron sequence (Lomeli *et al.*, 1994; Higuchi *et al.*, 2000).

In attempt to study a control case when we were blinded to any clinical information, we studied RNA editing of one case which was later reported as a case of Pick's disease. Pick's disease is a form of frontotemporal dementia characterized by shrinking of the frontal and temporal anterior lobes of the brain and progressive deterioration of social skills leading to impairment of intellect, memory, and language (Gustafson, 1987). Pick's disease is characterised by loss of neurons and gliosis of white matter in the frontal cortex and temporal cortex (Yamakawa *et al.*, 2006), and abnormal accumulation of tau protein resulting in Pick bodies. (Mimuro *et al.*, 2010). It has been demonstrated that these Pick bodies are immunoreactive for HO-1, an oxidative stress marker, in the cerebellar cortex compared to controls. The damage caused by oxidative stress and free radicals may further lead to excitotoxicity which have been implicated in wide range of neurodegenerative diseases including Alzheimer's disease, Pick's disease and ALS (Castellani *et al.*, 1995; Van Den Bosch *et al.*, 2006a). Pick cases have not been previously examined in *GLUR2* editing and

future work would require increasing number of cases and studying RNA editing of *GLUR2* in other editing sites.

GLUR2 was fully edited at Q/R site in the motor cortex, frontal cortex, and spinal cord and in MNs of a series ALS cases and controls. This finding is in agreement with previous studies that showed complete *GLUR2* editing in various CNS regions of the cerebellum, hippocampus, MNs, motor cortex and temporal cortex of control groups (Kwak *et al.*, 2008; Zhu *et al.*, 2012) (see table 3.6).

Table 3.6: Summary of *GLUR* editing at Q/R site of various diseases.

<i>Percentage (%) of editing of GLUR2 at Q/R</i>								
	Purkenji cells	MNs	Motor cortex	Hippocampus	Cerebellum	Temporal cortex	Frontal cortex	References
Control	100	100	100	100	100	100	100	(Kwak <i>et al.</i> , 2008; Zhu <i>et al.</i> , 2012)
SALS	100	0-100	100	N/A	N/A	N/A	N/A	(Kwak & Kawahara, 2005; Kawahara <i>et al.</i> , 2006; Kwak <i>et al.</i> , 2008)
SBMA	N/A	100	N/A	N/A	N/A	N/A	N/A	
Epilepsy	N/A	N/A	N/A	100	N/A	100%	N/A	(Kortenbruck <i>et al.</i> , 2001)
<i>Percentage (%) of editing of GLUR5 at Q/R</i>								
			Motor cortex	Hippocampus	Cerebellum	Temporal cortex	Frontal cortex	
Control			57-70	N/A	43	60	60	(Zhu <i>et al.</i> , 2012)
Epilepsy			N/A	33-66	N/A	49-75	N/A	(Kortenbruck <i>et al.</i> , 2001; Vissel <i>et al.</i> , 2001)
<i>Percentage (%) of editing of GLUR6 at Q/R</i>								
			Motor cortex	Hippocampus	Cerebellum	Temporal cortex	Frontal cortex	
Control			80	N/A	81	81	81	(Zhu <i>et al.</i> , 2012)
Epilepsy			N/A	41-80	N/A	65-84	N/A	(Kortenbruck <i>et al.</i> , 2001; Vissel <i>et al.</i> , 2001)

RNA editing levels of *GLURs* in SALS patients and other neurodegenerative diseases such as epilepsy and spinal muscular atrophy. Abbreviation: N/A-not available, *GLUR*- glutamate receptors, Q/R site- glutamate/arginine, MNs-motor neurons, SBMA-spinal and bulbar muscular atrophy, SALS-sporadic ALS.

The observed complete editing of ALS/*C9ORF72*-positive patients and ALS/*C9ORF72*-negative patients are in agreement with previous reports that show complete *GLUR2* editing in motor cortex of SALS (Kwak *et al.*, 2008). However, the level of *GLUR2* editing in the MNs of ALS patients is in disagreement with previous report indicating that altered *GLUR2* editing was specific to MNs of SALS patients (Takuma *et al.*, 1999; Kawahara *et al.*, 2004). Different data might be because of the following (i) these reports had focused on *GLUR2* editing in the spinal cord specifically the ventral and dorsal horn of the grey matter of the spinal cord as whole tissue in SALS cases and controls (ii) they also examined less number of MNs (n=10 to 17 cells) from 5 cases (iii) their SALS cohort was not well defined (Takuma *et al.*, 1999; Kawahara *et al.*, 2004). However, we were able provide a consistent levels of a complete *GLUR2* editing in more ALS patients, characterised ALS cases with and without *C9ORF72* expansion, more MNs were also isolated (n=200 cells). All these factors may contribute to different *GLUR2* editing quantification.

Studies had also reported complete *GLUR2* editing at Q/R site of non-ALS diseases such as spinal and bulbar muscular Atrophy (SBMA) and epileptic patients (Kwak *et al.*, 2008). In disagreement with previous studies, our findings showed less edited *GLUR2* of 84% in the motor cortex of a Pick's disease patient. We have also shown less edited *GLUR2* in other CNS regions including thalamus, temporal and cerebellum of this patient however, these data demonstrate a single PCR of one patient. Future work of an increased number of Pick's cases is required to confirm editing levels of *GLUR2* as well as investigating *GLUR2* editing in spinal cord and in MNs to determine whether this data is reproduced.

In the study of *GLUR5* and *GLUR6*, variable RNA editing levels were observed in the spinal cord and in MNs of *ALS/C9ORF72*-positive and *ALS/C9ORF72*-negative patients and in controls. The observed variability within RNA editing of *GLUR5* and *GLUR6* in our data were also reported in the hippocampus of epileptic patients showing 33-66% editing and 41-80% editing respectively (Kortenbruck *et al.*, 2001; Zhu *et al.*, 2012) (see table 3.6). This might be explained by variations from tissue to tissue and/or variations between cases. However, *GLUR5* and *GLUR6* RNA editing found in epilepsy had similar levels to ALS, suggesting that these subunits are not specifically linked to certain region or ALS disease nor it is linked to excitotoxicity in ALS.

Studies have suggested that deficient *ADAR2* activity in MNs of SALS patients occurs before abnormal *GLUR2* RNA editing at the Q/R site, consequently resulting in Ca⁺² permeable AMPA receptor- mediated mechanisms (Aizawa *et al.*, 2010; Hideyama *et al.*, 2012a; Yamashita & Kwak, 2013; Kubota-Sakashita *et al.*, 2014). In the current study the mRNA expression of *ADAR2* in spinal cord was increased in the ALS cases, which might be due to faulty regulation in ALS to compensate for a reduced level of *ADAR2* expression by the editing of its own pre mRNA. Auto-editing of *ADAR2* has been proposed to be a mechanism for *ADAR2* to balance its own expression (Rueter *et al.*, 1999; Feng *et al.*, 2006; Wahlstedt *et al.*, 2009). Studies have shown that *ADAR2* editing its own pre-mRNA at a site within intron 4 that creates an alternative splice site (Rueter *et al.*, 1999) and the splicing at this alternative site (-1) resulted in loss of *ADAR2* protein, *ADAR2* auto-edits itself to regulate and control protein expression (Wahlstedt *et al.*, 2009).

Interestingly, the expression levels of *ADAR3* were not altered in SALS with and without *C9ORF72* expansion compared to controls. One possible reason maybe that *ADAR3* is mainly expressed in the thalamus and amygdala and less expressed in the spinal cord (Chen *et al.*, 2000). Another possible reason is the small numbers of cases used in this study. This may suggest that *ADAR3* does not compete or enhance *ADAR2* expression (Savva *et al.*, 2012; Tomaselli *et al.*, 2013; Washburn, 2014). Therefore, *ADAR3* does not appear to play a role in RNA editing of *GLUR2*, *GLUR5* and *GLUR6* and that there is no obvious relationship between mRNA expression of *ADAR2* or *ADAR3*.

Aberrant alternative splicing of *EAAT2* may contribute to glutamate-mediated excitotoxicity in ALS. In a previous study, truncated mRNA species of exon 4 and exon 9 have been detected in the motor cortex of ALS patients (Lin *et al.*, 1998). However, later studies have shown these aberrant transcripts detected in both ALS patients and control samples (Meyer *et al.*, 1999; Flowers *et al.*, 2001). In support of these findings, exon skipping and exon retention were present in astrocytes of the grey matter of the spinal cord, in both control and SALS patients (Meyer *et al.*, 1999; Flowers *et al.*, 2001). The normal *EAAT2* transcripts (*EAAT2*⁺⁴ and *EAAT2*⁺⁹) and the aberrant *EAAT2* transcripts (*EAAT2*^{Δ4} and *EAAT2*^{Δ9}), both showed a trend of increased expression in ALS patients with the *C9ORF72* expansion. The lack of a significant association might be due to the small number of samples in each group and the case-to-case variation within the SALS cases in expression of the *C9ORF72* gene. The aberrant RNA metabolism of *EAAT2* in ALS *C9ORF72* expansion carriers, might provide early evidence for aberrant RNA metabolism to occur as part of the pathogenic mechanism (Lin *et al.*, 1998; Renton *et al.*, 2011).

Since the C9ORF72 repeat is known to sequester HnRNPs (Cooper-knock *et al.*, 2014), it is likely to influence splicing behaviour in some way and hence there may be an impact on previous results where the distinction was not made between ALS/C9ORF72-positive and ALS/C9ORF72-negative cases.

The LCM-isolated MNs required optimisation of the techniques for RNA preparation, RT-PCR and their restriction digests. Initially, *GLUR2*, *GLUR5* and *GLUR6* RT-PCRs were optimised on a commercially available universal human reference RNA (UHRR). The use of UHRR helped to conserve the valuable human RNA samples from the brain bank and assisted the optimisation of RT-PCR experiments especially when working with very low-input quantities of RNA as is required with patient samples (Novoradovskaya *et al.*, 2004). Once the PCR conditions for the glutamate receptor were optimised on the UHRR, experiments were repeated on FFPE spinal cord sections of SALS patients. FFPE material was used because of its superior histology, greater availability and the neuropathology of the archive material was well characterised. However, tissue fixation reduces the efficiency of PCR because of protein cross-linking and RNA degradation. Therefore, RNA isolated from FFPE material was found to be a challenge for further molecular analyses (Ludyga *et al.*, 2012). As a result, frozen spinal cord tissues were used because of its improved RNA quality (Ludyga *et al.*, 2012).

The RNA editing levels of *GLUR2*, *GLUR5* and *GLUR6* at Q/R site were quantified using restriction digest to determine editing levels of *GLURs* at Q/R site because of its speed and efficiency. An alternative method is to sub-clone PCR products into vectors obtained from the PCR products and the editing transcripts analysed by sequencing. However, this method is expensive and time consuming because it requires many

sequence analyses to perform a reliable statistical analysis (Barbon *et al.*, 2003). A more precise and sensitive method to quantify the efficiency of editing is to use qPCR. This method discriminates between edited and unedited transcripts in a more precise and sensitive manner compared to the other two methods because of time and resource restraints (Lyddon *et al.*, 2012).

In summary, the current study demonstrates that *GLUR2* is fully edited in MNs of SALS and controls, highlighting that not all SALS cases have abnormal *GLUR2* editing and suggesting other factors contribute to excitotoxicity in ALS. In contrast to *GLUR2*, *GLUR5* and *GLUR6* had lower levels of RNA editing in all tissue examined suggesting that these editing levels were not only found in ALS but also in other neurological diseases. Other factors contributing to excitotoxicity may include the abnormal regulation of *ADAR2* and/or aberrant *EAAT2* transcripts. *ADAR3* neither competes with *ADAR2* nor is found to be linked to RNA editing of *GLUR2*, *GLUR5* and *GLUR6*. Although these data were not statistically significant owing to the small number of cases (n=15) and variation in post-mortem tissue, however, it may give a clue to understand some of the key mechanisms in ALS. Future work to examine RNA editing in a larger cohort as well as studying the expression of *GLUR2* and *ADAR2* in MNs is required.

Chapter 4
***Neuropathological
characterisation of ALS
tissue***

Chapter 4: Neuropathological characterisation of ALS tissue

4.1 Introduction

One of the proposed pathogenic mechanisms of ALS is selective motor neuron (MN) death mediated by excitotoxicity resulting from an AMPA receptor subunit with deficient or unedited *GLUR2* (Carriedo *et al.*, 1996; Kwak & Kawahara, 2005; Kawahara *et al.*, 2006). *GLUR2* editing is catalysed by *ADAR2*, and is believed to be complete at birth. However, it is suggested that incomplete *GLUR2* editing might be linked to sporadic ALS disease (Kwak & Kawahara, 2005; Kawahara *et al.*, 2006).

As discussed earlier, *GLUR2* editing is mediated by the ADAR family of enzymes specifically *ADAR2*. Whereas, *ADAR3* has shown to be catalytically inactive however, studies have suggested that *ADAR3* might have a role in ALS with *C9ORF72* expansion repeats in iPSNs. A group has found *ADAR3* within the complex of the *C9ORF72* repeats in the iPSNs tissue of ALS *C9ORF72* without further characterisation of the role of *ADAR3* in ALS with *C9ORF72* nor its relation to RNA editing (Almeida *et al.*, 2013; Donnelly *et al.*, 2013; Todd & Paulson, 2013). Additionally, *ADAR3* has been suggested to compete with *ADAR1* and *ADAR2* for binding substrates thereby changing the editing profile (Savva *et al.*, 2012).

Studies have demonstrated that expression of *ADAR1* and *ADAR2* are associated with the nucleolus and *ADAR3* is localised in the nucleolus and cytoplasm of human tissue (Desterro *et al.*, 2003; Sansam *et al.*, 2003; Savva *et al.*, 2012). The localisation of *ADAR2* has been shown to be exclusively in the nuclear fraction of human cortex tissue, and is further supported by the nucleolar *ADAR2* immunoreactivity observed in the nuclei of motor neurons of control human spinal cord (Aizwa *et al.*, 2010). It

should be noted that ALS patients' neurons which displayed ADAR2 nuclear immunoreactivity were devoid of TDP-43 inclusions. (Aizawa *et al.*, 2010). Conversely ADAR2-negative neurons contained TDP-43 positive inclusions, suggesting that reduced ADAR2 activity is linked to the formation of TDP-43 inclusions by altering GLUR2 Q/R site-editing or some other editing behaviour in motor neurons of SALS patients (Aizawa *et al.*, 2010; Hideyama *et al.*, 2012a; Yamashita & Kwak, 2013). TDP-43 is cleared from the nucleus to form inclusions in the cytoplasm under the following stress conditions: (i) over expression, (ii) interference with its nuclear localisation signal, and (iii) when the individual has a pathogenic TDP43 mutation. These TDP-43 cytoplasmic inclusions are typical for the phenotype of ALS (Neumann *et al.*, 2006a; Lagier-Tourenne & Cleveland, 2009; Ince *et al.*, 2011a) and FTLN. Abnormal TDP-43 cytoplasmic inclusions are associated with both ubiquitin positive and tau-negative cortical neurons of FTLN patients and motor neurons of SALS patients (Arai *et al.*, 2006). TDP-43 and p62 compact and skein-like inclusions have also been demonstrated in the spinal cord of ALS and in FTLN cases, both with and without the C9ORF72 mutation (Al-Sarraj *et al.*, 2011; Cooper-Knock *et al.*, 2012).

A further contributory factor in the potential excitotoxic cascade that leads to ALS may include dysfunction of EAAT2 which plays an important role in regulating glutamate at the synapse (Rothstein *et al.*, 1990; Lin *et al.*, 1998). Studies have demonstrated dramatic increases in glutamate levels in the cerebrospinal fluid of ALS patients and reduced EAAT2 in isolated synaptosomes from the motor cortex and the spinal cord (Rothstein *et al.*, 1992). In support of these findings, immunohistochemical and western blot analysis has revealed a significant loss of EAAT2 protein both in the motor cortex and spinal cord of ALS patients (Rothstein *et al.*, 1995). In contrast no

significant difference in either EAAT1 or glial fibrillary acidic protein (GFAP) has been detected in ALS patients, indicating that the defective change is specific to EAAT2 glutamate transporter expression (Bristol & Rothstein, 1996). Although some studies have suggested that aberrant transcripts of EAAT2 play critical roles in the downregulation of EAAT2 protein levels in ALS patients (Lin *et al.*, 1998; Meyer *et al.*, 1998; Meyer *et al.*, 1999), others have shown that these aberrant transcripts are also present in neurologically normal controls (Honig *et al.*, 2000; Flowers *et al.*, 2001). The EAAT2 alternatively spliced variants that have been described are exon 4 (EAAT2^{Δ4}) and exon 9 (EAAT2^{Δ9}) skipping. Normally, exon 4 and exon 9 encode regions of EAAT2 involved in the trafficking of glutamate from the extracellular space into the cytosol of astrocytes (Yernool *et al.*, 2004; Reyes *et al.*, 2009). The literature is currently lacking investigations on exon 9 and 4 excluded transcripts (EAAT2^{Δ9}, EAAT2^{Δ4}); both encoding crucial motifs, in relation to a deficient or total loss of EAAT2 expression in ALS/*C9ORF72*-positive compared to ALS/*C9ORF72*-negative ALS patients. Such an investigation may identify changes in excitotoxic pathways which contribute to neurodegenerative pathology.

Hypothesis

- MNs from *ALS/C9ORF72*-positive patients have more inclusions than *ALS/C9ORF72*-negative patients.
- GLUR2 protein levels do not contribute to GLUR2 editing.
- Decreased ADAR2 and EAAT2 expression in ALS contributes to excitotoxicity mediated MN loss.
- Altered ADAR3 expression is not linked to ADAR2 and GLUR2 editing.

Aim

Identify the neuropathological features of motor neurons and astrocytes in the thoracic spinal cord of a well characterised cohort of *ALS/C9ORF72*-positive and *ALS/C9ORF72*-negative compared to non-neurological controls.

4.2 Results

4.2.1 Cases used in this study

In this chapter FFPE ALS tissue with and without *C9ORF72* repeat expansion (n=10) and non-neurological controls (n=5) were used to study the following proteins; p-TDP-43, p62, GLUR2, ADAR2, ADAR3, GAFF and EAAT2 (see table 4.1).

Table 4.1: FFPE thoracic spinal cord tissue of ALS cases.

Case number	Block Number	Area/Level	Site of onset	PMI in hours	Sex	Age at onset	Age at death
ALS/<i>C9ORF72</i>-positive cases							
LP83/10	34	T11	Limb	13	Male	67	79
LP081/09	29	T11	Limb	60	Male	57	59
LP041/04	6	T11	Bulbar	48	Male	62	64
LP039/11	26	T11	Limb	96	Male	70	72
LP040/11	25	T11	Limb	10	Female	72	77
ALS/<i>C9ORF72</i>-negative cases							
LP014/11	24	T11	Limb	n/a	Male	49	51
LP005/11	30	T11	Limb	40	Female	62	67
LP023/10	7	T11	Limb	24	Female	34	42
LP005/10	23	T11	Limb	96	Male	38	40
LP094/09	25	T11	Bulbar	48	Male	62	63
Controls							
LP005/07	13	T11	n/a	12	Male	n/a	64
LP085/07	25	T11	n/a	5	Female	n/a	82
LP098/07	25	T11	n/a	63	Male	n/a	67
035/96	8	T11	n/a	14	Female	n/a	87

Available FFPE thoracic spinal cord of ALS/*C9ORF72*-positive and ALS/*C9ORF72*-negative cases and controls free from neurological disease. Cases were matched closely as possible in their clinical information, spinal cord location. The p-TDP-43, p62, GLUR2, ADAR2, ADAR3, GAFF and EAAT2 proteins were characterised by immunohistochemistry. Abbreviation: n/a-not available.

4.2.2 p-TDP43 and p62 pathology in ALS patients

Detailed analysis of MN pathology in the anterior horn of human thoracic spinal cord sections was compared between non-neurological control cases, *ALS/C9ORF72*-positive and *ALS/C9ORF72*-negative cases (see table 4.1).

Proteasomal degradation marker (p62) and p-TDP-43 proteins were assessed blinded to any clinical information using a semi-quantitative manual scoring system based on the distribution and immunoreactive pattern of protein expression. Negative and isotype antibody controls confirmed the specificity of the immunostaining profile. No inclusions were observed in any of the 5 controls (see figure 4.1a & 4.2a).

MNs of ALS cases contained p62⁺ and p-TDP-43⁺ cytoplasmic inclusions. These included compact round (see figure 4.1c & 4.2d) or filamentous skein-like bodies (see figure 4.1d). Compact inclusions were occasionally observed in the cytosol of small oval shaped glia (see figure 4.1e & 4.2d).

p62⁺ inclusions were only observed in ALS cases, $p=0.0102$. One out of 5 *ALS/C9ORF72*-negative cases contained p62⁺ inclusions (1.67 ± 3.73) (mean \pm SD). All *ALS/C9ORF72*-positive cases (5 out of 5) examined had p62⁺ inclusions in MNs (11.80 ± 10.94). *ALS/C9ORF72*-positive cases contained significantly more MNs with p62⁺ inclusions than MNs in *ALS/C9ORF72*-negative patients, $p=0.0016$ (see figure 4.4a).

3 out of 5 of the *ALS/C9ORF72*-negative cases had MNs containing TDP-43⁺ inclusions (8.61 ± 15.75), in contrast to the other 2 cases of the same *ALS/C9ORF72*-negative cohort which did not contain any inclusions. All *ALS/C9ORF72*-positive cases also displayed MNs containing inclusions (5 out of 5) (11.80 ± 10.94). The

number of MNs with p-TDP-43⁺ inclusions was significantly different in ALS cases compared to controls $p= 0.0378$ (see figure 4.3b), but did not significantly differ between ALS/*C9ORF72*-negative and ALS/*C9ORF72*-positive patients ($p=0.0633$) (see figure 4.4b).

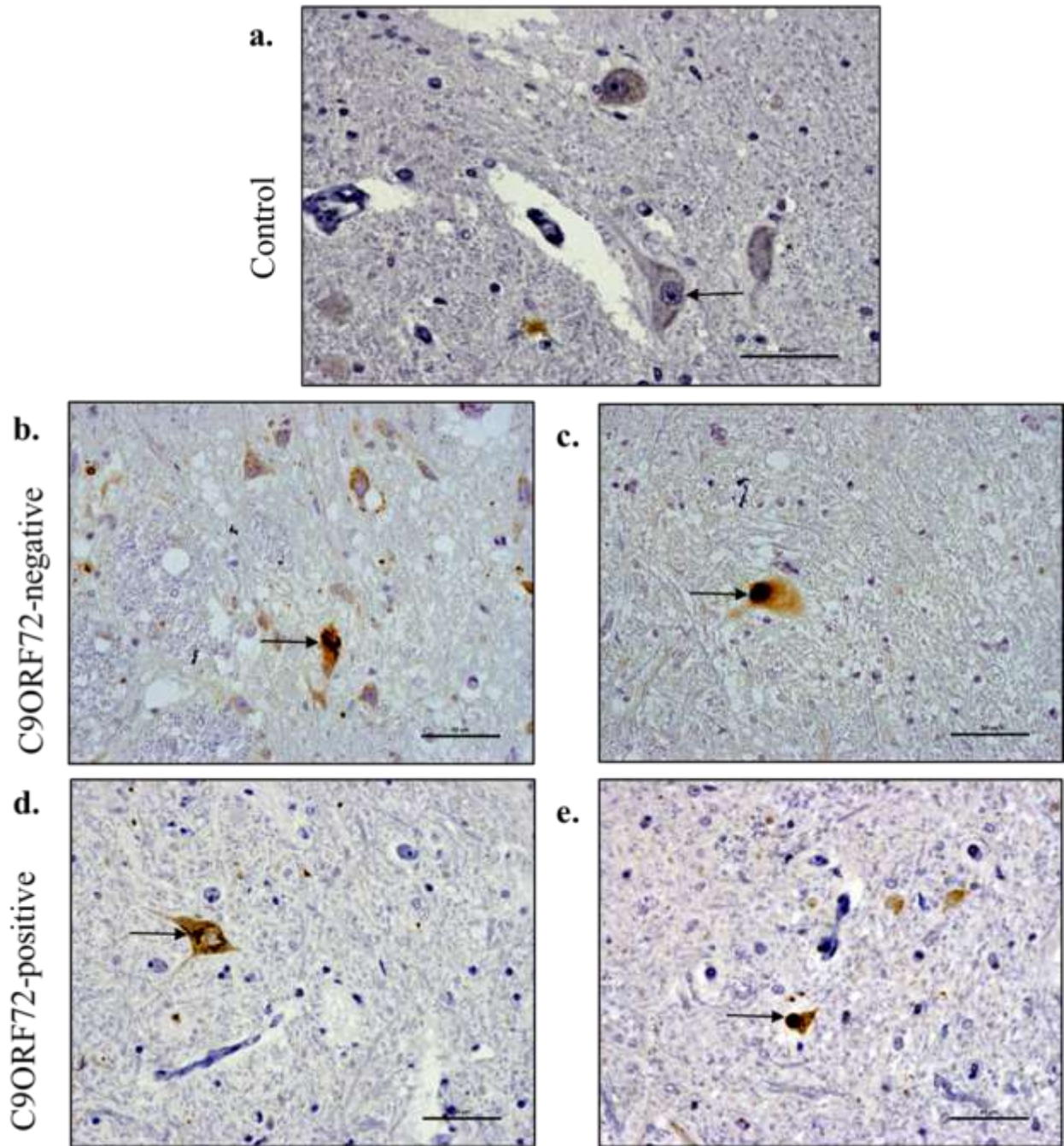


Figure 4.1: p62 reactivity in MNs of the spinal cord of ALS patients.

MN in non-neurological control cases did not contain p62 inclusions (a), in contrast to both ALS/C9ORF72-negative cases (b-c) and ALS/C9ORF72-positive cases (d-e). MNs contained skein-like bodies (b, d) and compact inclusions (c). Compact inclusions were also detected in some glia (e), scale bars =50 μ m.

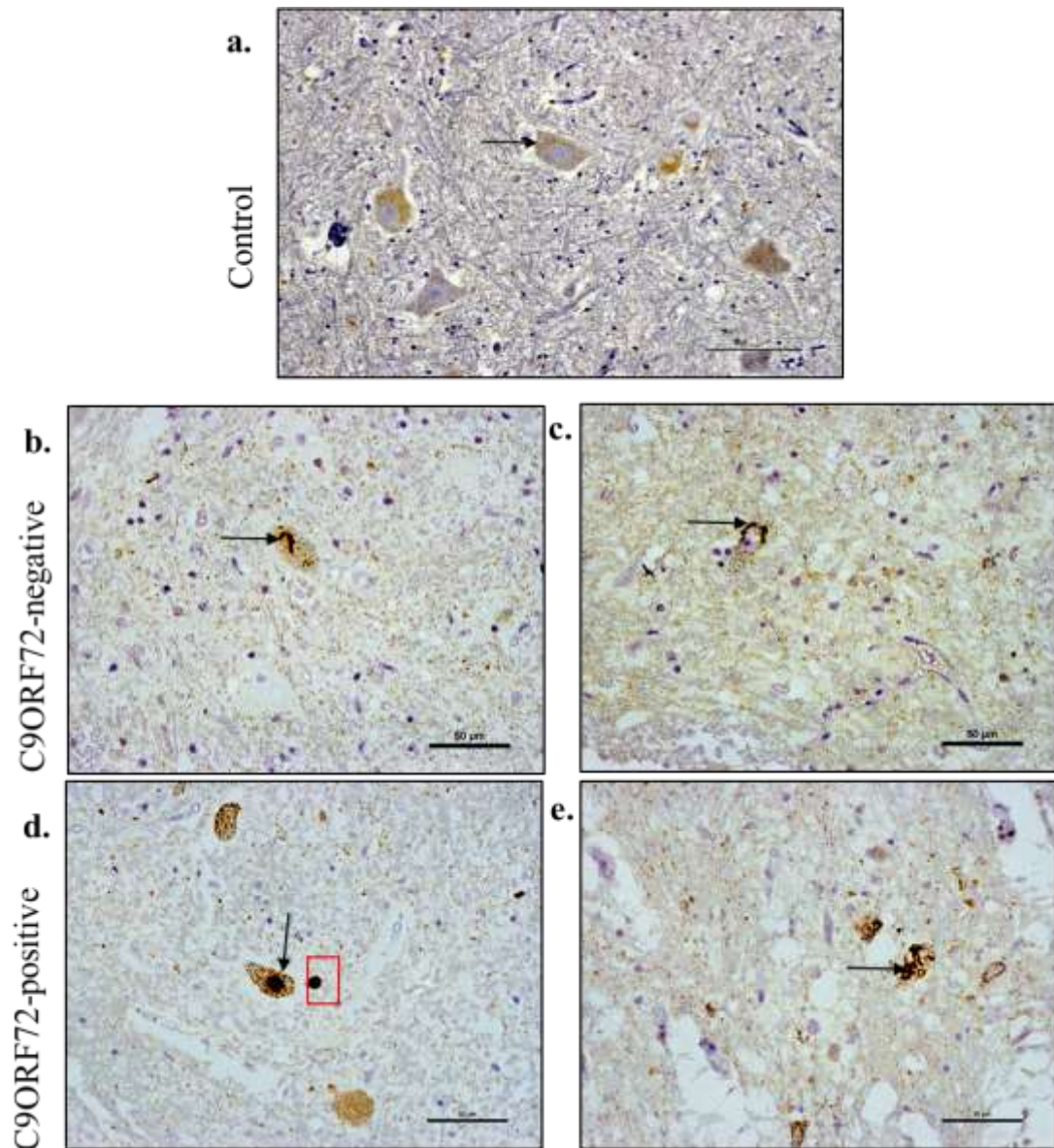


Figure 4.2: p-TDP-43 reactivity in MNs of the spinal cord of ALS patients.

MN in non-neurological control cases did not display any immunoreactivity for phosphorylated- TDP-43⁺, the pale cytoplasmic staining represents non-specific lipofuscin granules (a) in contrast to both ALS/*C9ORF72*-negative (b-c), ALS/*C9ORF72*-positive cases (d-e). MNs contained dense skin-like bodies (b-c, e) and compact inclusions (arrow) (d). Glia containing compact inclusions were also observed (box) (d), scale bar =50 μm.

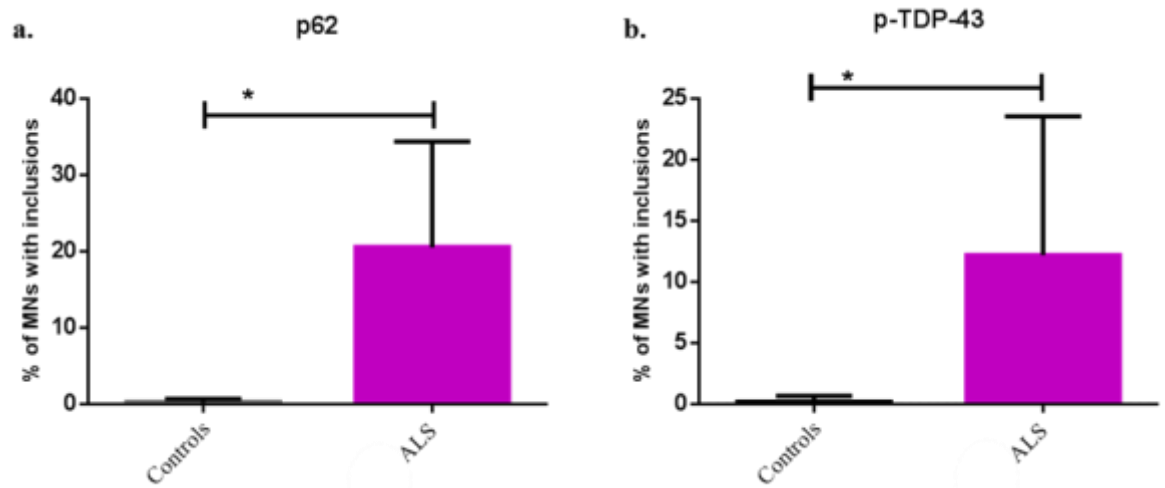


Figure 4.3: p62 and p-TDP-43 inclusions in MNs of ALS cases.

Analysed immunohistochemical staining of the spinal cord of ALS patients and controls. The percentage of MNs with inclusions was significantly higher in ALS patients compared to control samples, both for p62⁺ ($p=0.0102$) and p-TDP-43⁺ inclusions ($p=0.0378$). * denotes statistical difference using student T-Test ($p<0.05$).

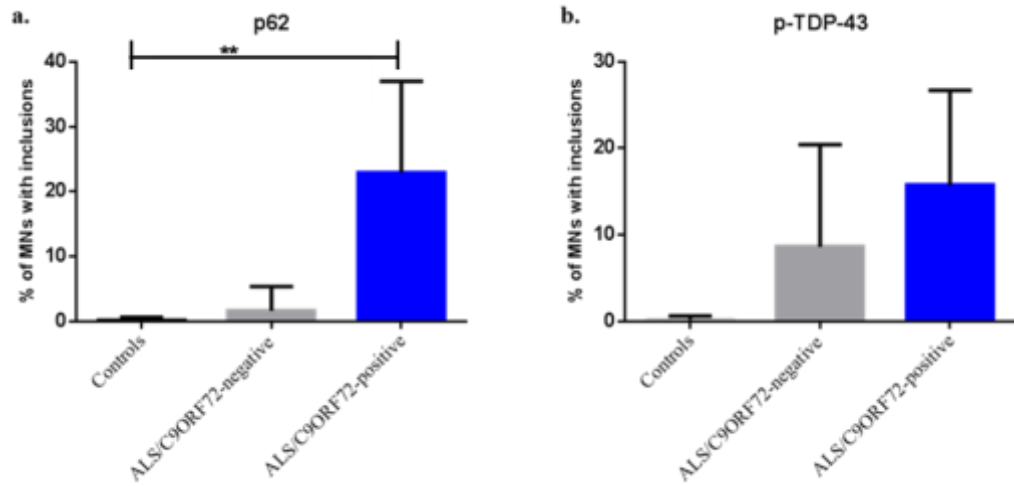


Figure 4.4: p62 and p-TDP-43 inclusions in MNs of ALS with and without *C9ORF72* expansion.

ALS/*C9ORF72*-positive cases displayed a significantly greater proportion of MNs with inclusions compared to ALS/*C9ORF72*-negative patients $p=0.0016$. (a), No difference in TDP43 pathology was observed between the 2 ALS groups (b), Data measured by one-way ANOVA.

4.2.3 The expression of GLUR2 in ALS patients

The expression of GLUR2 in MNs was investigated using immunohistochemistry. The optimal working dilution of GLUR2 antibody which gave a highly specific staining pattern and minimal background staining was 1:50 (see figure 4.5a). Negative controls displayed no immunoreactivity, thereby confirming the specificity of the staining.

Intense punctate immunopositive GLUR2 was observed in the endoplasmic reticulum (see figure 4.6 a-b), and the membranes of MN (see figure 4.6a-c). Occasionally, non-specific pale granule staining of lipofuscin in the cytoplasm was observed, but was easily distinguishable from specific GLUR2 immunoreactivity (see figure 4.6b).

MNs displaying no GLUR2 immunoreactivity were detected in ALS cases (mean \pm SD: 1.73 ± 0.71) and in controls (2 ± 0.72). However, there was no statistical significance in the number of GLUR2⁻ MN between ALS patients and controls ($p=0.5884$). ALS cases and controls showed similar levels of GLUR2⁺ staining in the membrane of 1.53 ± 1.14 and 1.53 ± 1.27 ($p>0.999$), respectively. In contrast, MNs with GLUR2⁺ immunoreactivity associated with the ER were higher in controls (5.73 ± 1.96) compared to ALS cases (2.4 ± 1.69) ($p=0.0127$) (see figure 4.7).

GLUR2 expression in ALS cases was further interrogated and any differences in staining between ALS/*C9ORF72*-negative and ALS/*C9ORF72*-positive cases was assessed. GLUR2-negative MNs were a feature of both controls (2 ± 0.72), ALS/*C9ORF72*-negative cases (1.6 ± 0.69) and in ALS/*C9ORF72*-positive cases (1.84 ± 0.79), $p=0.7769$. MNs with positive GLUR2⁺ membranes were observed in controls (1.53 ± 1.27), ALS/*C9ORF72*-negative patients (1.45 ± 1.02) and ALS/*C9ORF72*-positive patients (1.6 ± 1.2). Similarly, MNs with GLUR2⁺

endoplasmic reticulum were also a feature of control cases (5.73 ± 1.86), ALS/*C9ORF72*-negative cases (1.75 ± 1.59) and ALS/*C9ORF72*-positive cases (2.92 ± 1.5594). There was no significant difference between controls, ALS/*C9ORF72*-negative and ALS/*C9ORF72*-positive groups, either in the number of GLUR2 negative MN ($p=0.7769$) or in the number of MN with GLUR2⁺ positive membrane staining ($p=0.9836$). In contrast, the number of MN with GLUR2⁺ positive endoplasmic reticulum significantly differed between controls, ALS/*C9ORF72*-negative patients and ALS/*C9ORF72*-positive patients, $p=0.0313$ (see figure 4.8).

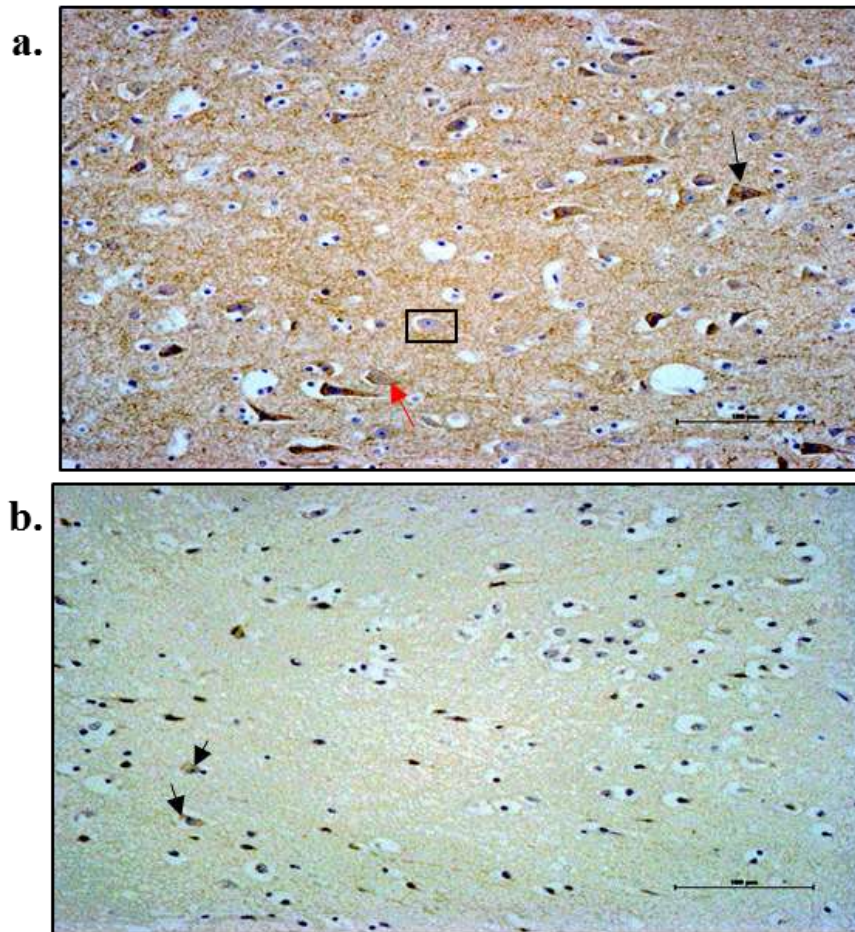


Figure 4.5: Optimisation of GLUR2 staining in the cingulate gyrus of a non-neurological control case.

The antibody against GLUR2 was used at the optimal dilution of 1:50, which gave positive GLUR2⁺ staining of both the endoplasmic reticulum (black arrow) and the membrane (red arrow) of neurons, with some GLUR2 negative neurons also observed (in box) (a). This pattern of staining reduced as the dilution factor of the GLUR2 antibody increased, giving a very weak signal in neurons when used at a dilution of 1:400, which was difficult to distinguish from the non-specific staining of lipofuscin (black arrow) (b), scale bar=100µm.

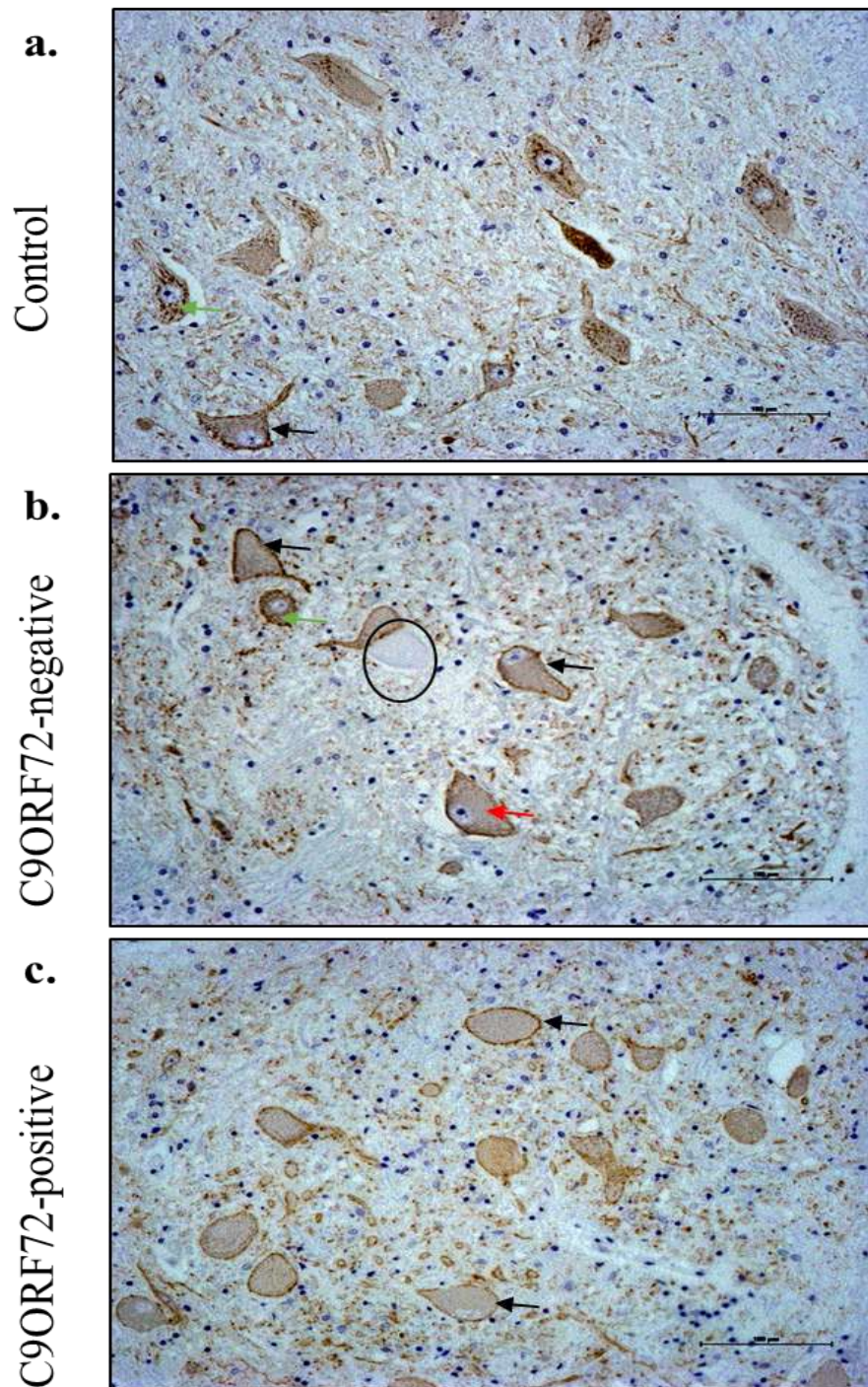


Figure 4.6:GLUR2 staining of MNs in the anterior horn of spinal cord of ALS. Two patterns of GLUR2 immunoreactivity were detected in MNs, intense staining of the membrane (black arrow) and punctate, granular staining of the endoplasmic reticulum (green arrow) (a-c). MN negative for GLUR2 (in circle) as well as lipofuscin staining in the cytoplasm (red arrow) was also seen (b), scale bar=100µm.

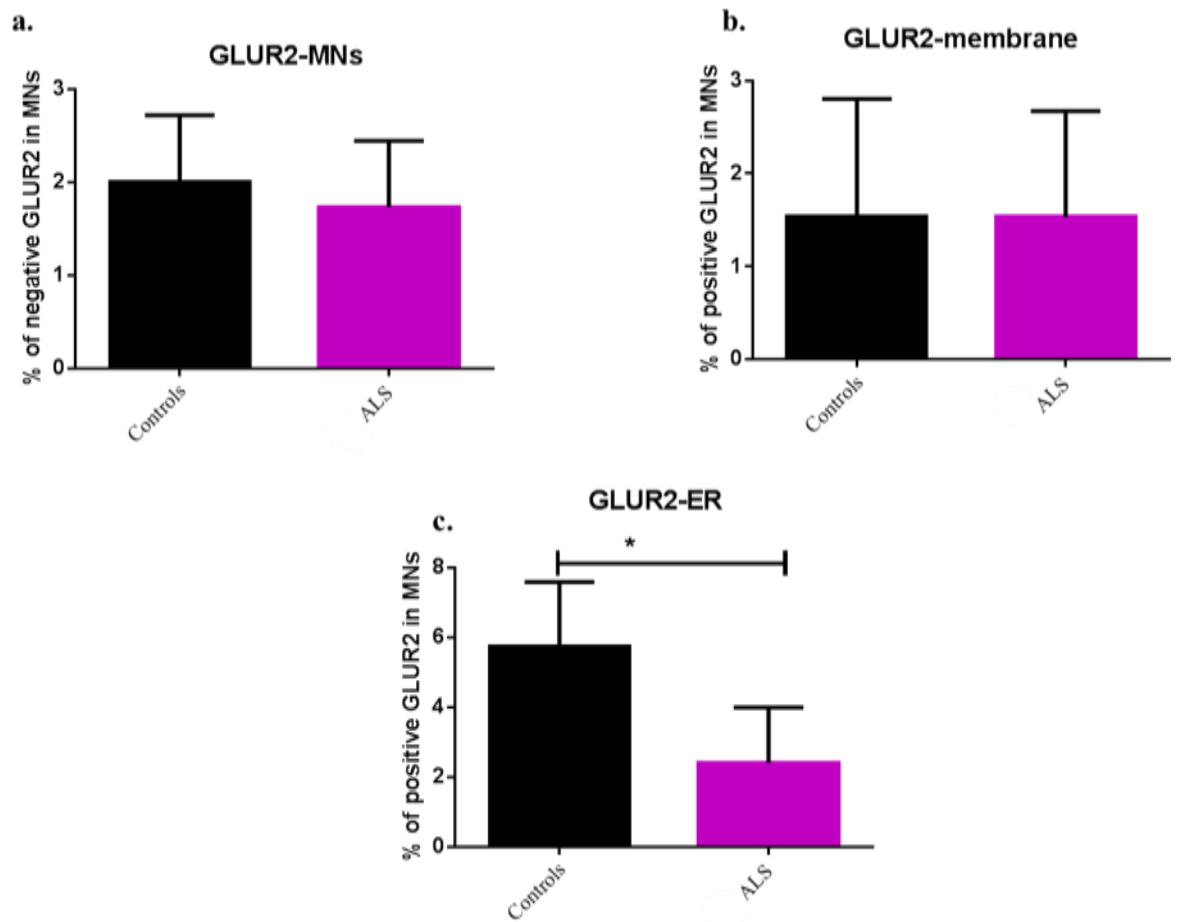


Figure 4.7: The expression of GLUR2 in MNs of ALS.

Panel (a) shows negative GLUR2 staining in MNs and panels (b) shows positive staining in the membrane. Panel (c) shows positive staining in the ER. No significant difference in the proportion of GLUR2⁻ MNs was observed between ALS patients and controls ($p=0.5884$). GLUR2 staining in the membrane of MNs did not show any statistical significance in ALS and controls ($p>0.999$). Whereas GLUR2 staining in ER was significantly higher in controls than ALS patients ($p=0.0127$). The statistical analysis was carried out by student T-Test.

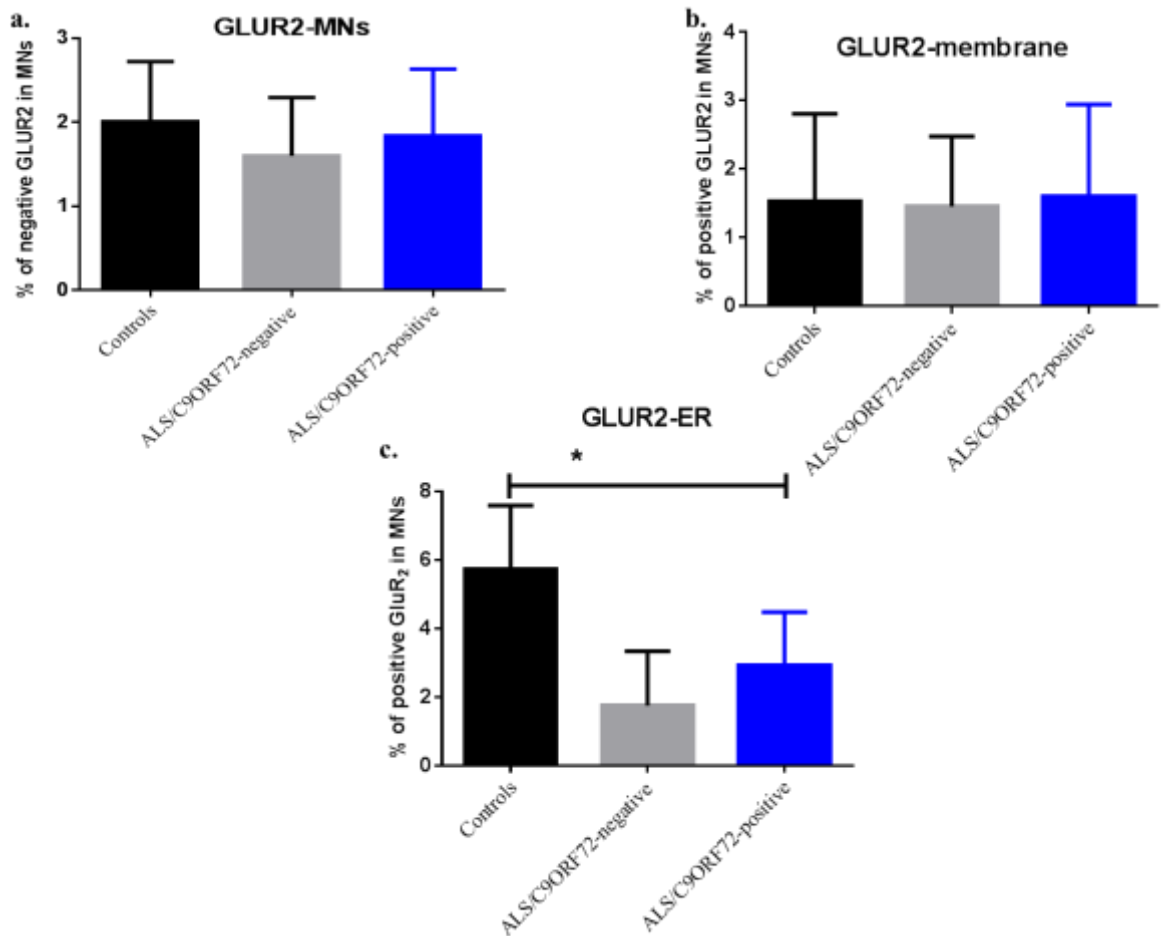


Figure 4.8: The expression of GLUR2 in MNs of ALS with and without *C9ORF72* expansion.

Neither the proportion of GLUR2⁻ (a), nor MN with GLUR2⁺ membrane immunoreactivity showed any significant difference across the three groups (b). In contrast, only GLUR2⁺ endoplasmic reticulum showed statistical significance between controls, ALS/*C9ORF72*-negative and ALS/*C9ORF72*-positive cases $p=0.0313$ (c), as measured by one-way ANOVA.

4.2.4 ADAR2 and ADAR3 localisation in ALS

Expression of ADAR2 and ADAR3 was investigated using immunohistochemistry. ADAR2 and ADAR3 antibodies were optimised to 1:100 and 1:200 respectively, selected because of the high specificity of the staining pattern and minimal background (see figure 4.9a & 4.10a). Negative controls confirmed the specificity of the staining pattern observed. ADAR2 immunoreactivity was exclusively associated with the nucleolus of MN. In contrast ADAR3 was predominantly detected in the cytosol, in addition to some nucleolar immunoreactivity. ADAR2 and ADAR3 were assessed semi-quantitatively and differences in the staining pattern analysed by student T-test. Weak and non-specific staining of lipofuscin was present in all cases, but was easily distinguished from the intense ADAR2 specific immunoreactivity. ADAR2 positive (see figure 4.11a) and negative (see figure 4.11e) nucleoli were observed in MNs throughout all controls (n=5) and ALS groups (n=10).

ADAR3 displayed an intense punctate staining in the cytoplasm (see figure 4.12a) and/or positive staining in the nucleolus (see figure 4.12d) of MNs in both controls and ALS groups. Interestingly, ADAR3 was occasionally observed in the axons of MN (see figure 4.12f). 3 out of 5 of controls had ADAR3⁺ staining in the nucleolus of MNs (mean \pm SD: 1.43 \pm 1.65) while 2 out of 5 of these cases were devoid of ADAR3⁺ staining. In 10 SALS patients compared to 5 controls, the expression of positive ADAR2 ($p=0.9468$) and ADAR3 staining ($p=0.0834$) in the nucleolus or ADAR3⁺ staining in the cytosol ($p=0.6965$) did not reach statistical significance (see figure 4.13).

In controls, the total number of MN which had ADAR2 immunopositive nucleoli was 25.19 ± 10.43 . Similar to controls, ALS/*C9ORF72*-negative patients had also positive ADAR2⁺ nucleoli in MN (31.97 ± 11.58). ALS/*C9ORF72*-positive patients also had ADAR2⁺ in 19.28 ± 15.14 of MNs, except one case which lacked any ADAR2⁺ nucleoli. The difference in ADAR2 expression between all groups did not reach significance ($p=0.3974$) (see figure 4.14a).

All ALS/*C9ORF72*-negative cases (4.12 ± 3.32) and ALS/*C9ORF72*-positive cases (8.27 ± 5.70) had ADAR3⁺ in the nucleolus. ADAR3⁺ positive staining was seen in the cytosol of controls (48.42 ± 10.63), in ALS/*C9ORF72*-negative patients (37.08 ± 42.64) and in ALS/*C9ORF72*-positive patients (71.69 ± 28.96). There was no significant difference between controls, ALS/*C9ORF72*-negative and ALS/*C9ORF72*-positive groups in either the number of MN with ADAR3⁺ nucleoli ($p=0.0879$) or cytosolic staining ($p=0.2595$) (see figure 4.14b & c).

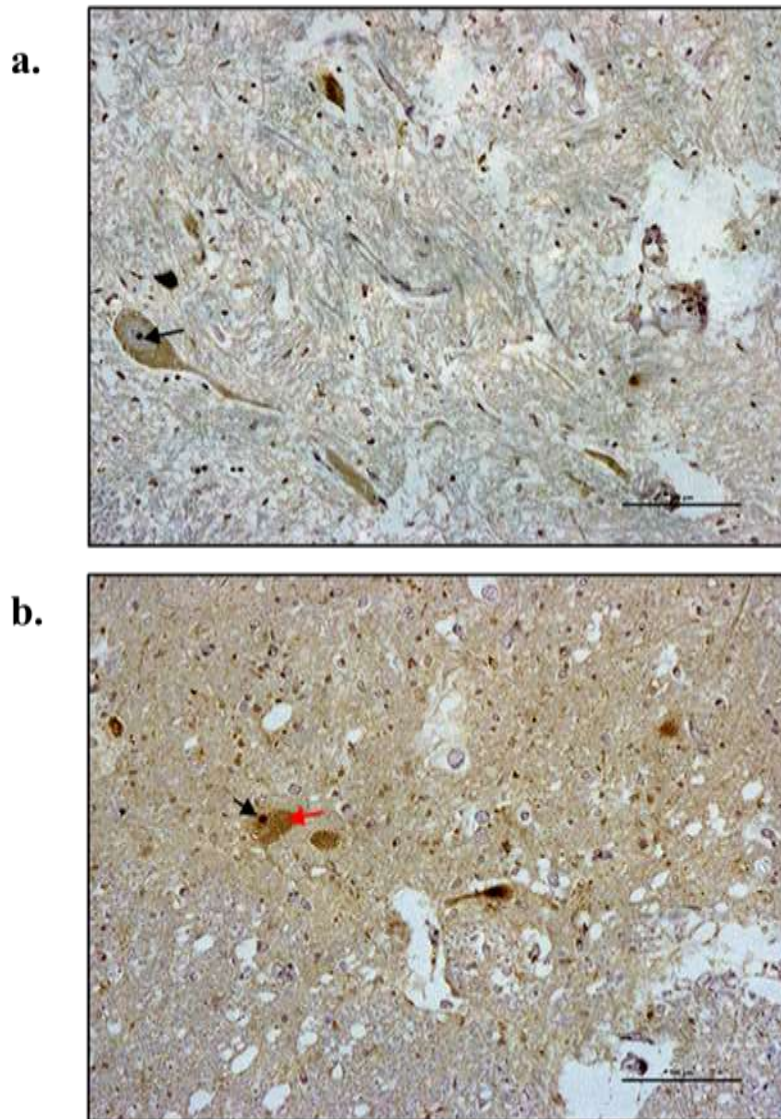


Figure 4.9: Optimisation of ADAR2 antibody dilution.

ADAR2 antibody was best optimised at a dilution of 1:100 using a microwave for the antigen retrieval. Positive nucleolar staining of MN (black arrow) (a). A similar pattern of staining was observed using an alternative method of antigen retrieval, ADAR2⁺ nucleolar staining was detected (black arrow) and non-specific lipofuscin staining was observed (red arrow) with non-specific staining in the back ground staining when the sections were pressure cooked, antibody 1: 100 dilution (b), scale bar=100µm

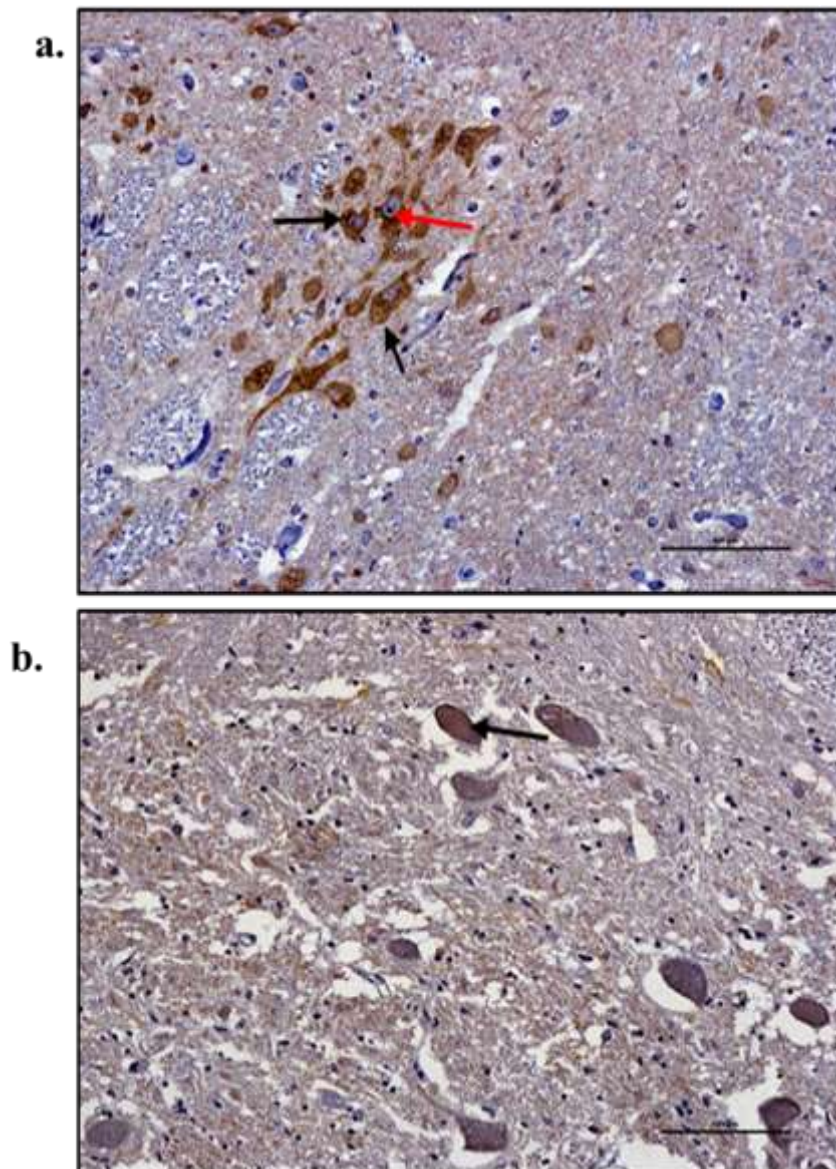


Figure 4.10: Optimisation of ADAR3 antibody dilution.

ADAR3 antibody was best optimised at a dilution of 1: 200 and using a pressure cooker for the antigen retrieval. Punctate immunoreactivity was observed in the cytosol (black arrow), with no staining of the nucleolus (red arrow) (a). In contrast, a reduced intensity of staining and increased non-specific lipofuscin staining was observed in MNs using the microwave for the antigen retrieval (b), scale bar= 100µm.

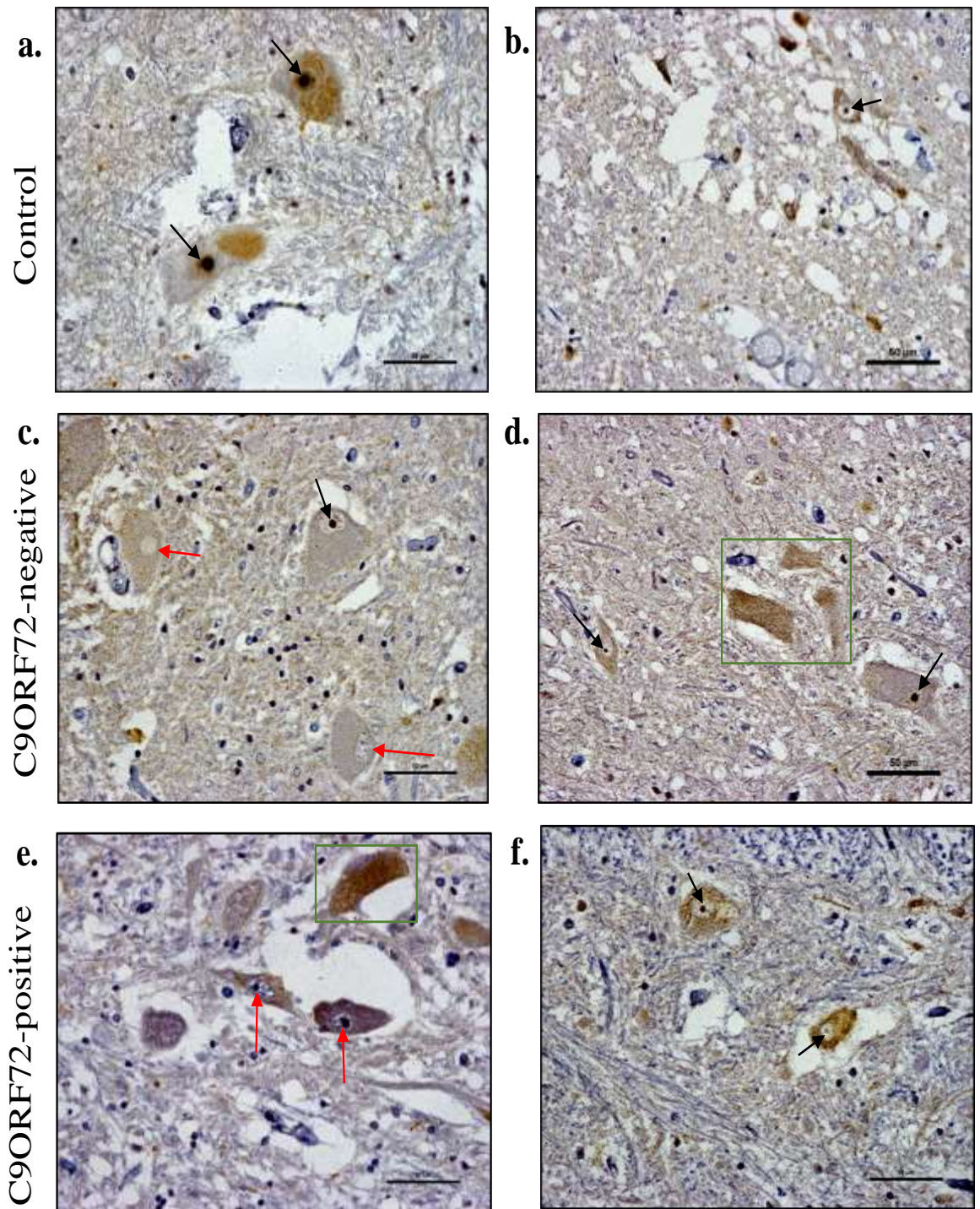


Figure 4.11: Pattern of ADAR2 reactivity associated with MNs of spinal cord.

ADAR2 was associated with nucleoli in MNs in non-neurological control cases (black arrow) (a-b), ALS/*C9ORF72*-negative (c-d) and ALS/*C9ORF72*-positive (e-f). Non-specific lipofuscin was observed in the cytoplasm (box), but was easily distinguished from specific immunoreactivity (d-e). MNs contained ADAR2 positive (black arrow) (a-d, f) and ADAR2 negative nucleoli (red arrow) (c, e-f), scale bar= 50 μ m.

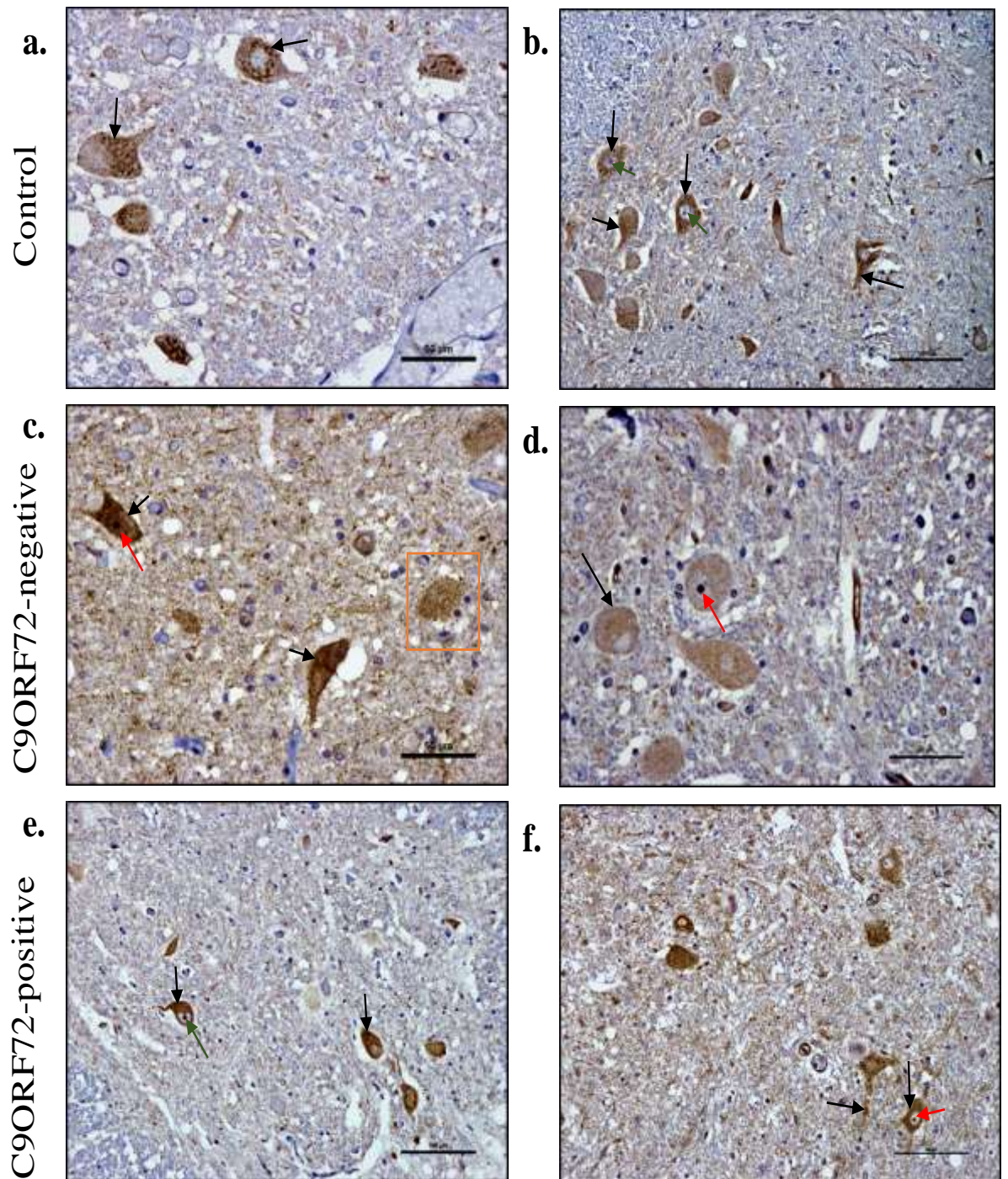


Figure 4.12: Pattern of ADAR3 reactivity associated with MNs of spinal cord.

Non-neurological controls (a-b), ALS/*C9ORF72*-negative (c-d) and ALS/*C9ORF72*-positive (e-f) displayed punctate cytoplasmic staining positive for ADAR3 (black arrow) and negative nucleoli (green arrow) in these MNs. Lipofuscin was observed in the anterior horn of spinal cord (box) (c). ADAR3 immunopositive staining extending to the axons of MNs (f), scale bar represents 100um in b, e-f and 50um in a, c-d.

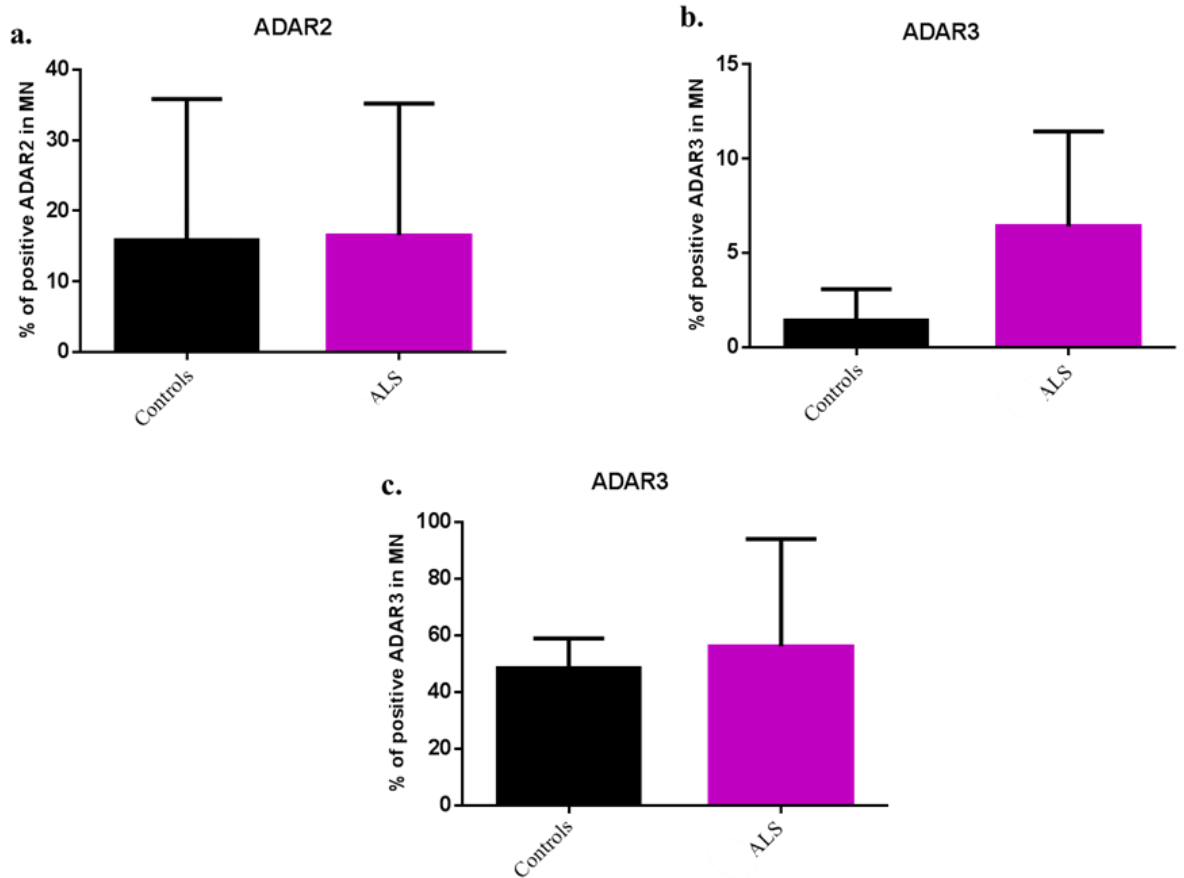


Figure 4.13: Expression levels of ADAR2 and ADAR3 in MNs of ALS patients.

There was no statistical significance between ALS patients and controls in the proportion of ADAR2 ($p=0.9468$) and ADAR3 immunoreactive nucleoli ($p=0.0834$) (a-b) or ADAR3 immunoreactivity in the cytosol ($p=0.6965$) (c). The statistics was carried out using student T-test.

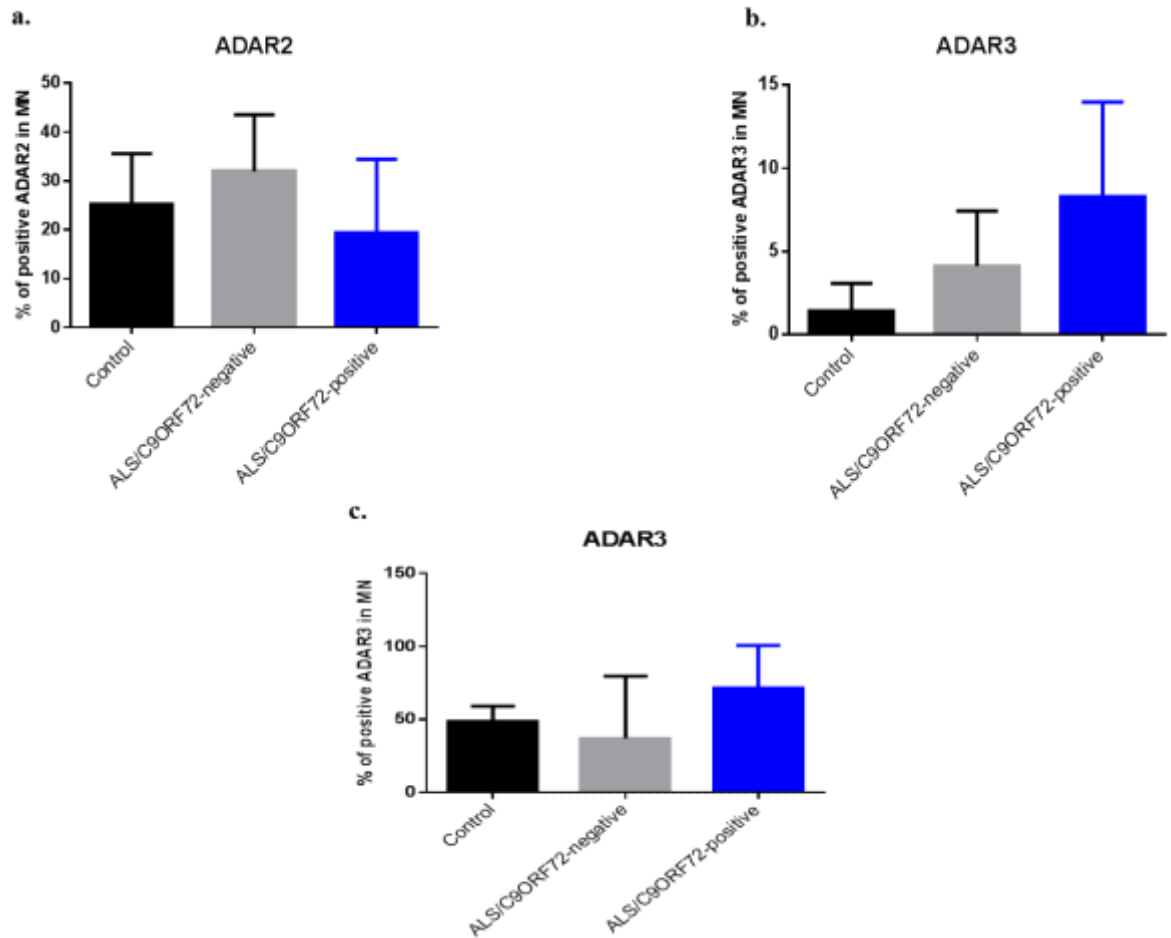


Figure 4.14: Expression levels of ADAR2 and ADAR3 in MNs of ALS patients with and without *C9ORF72* expansion.

No significant differences in the proportion of MNs positive for ADAR2 were detected in the nucleoli of controls, ALS/*C9ORF72*-negative and ALS/*C9ORF72*-positive cases, $p=0.3974$ (a). Similarly, the proportion of ADAR3 positive MNs in the nucleoli (b) and in the cytosol (c) did not differ across the 3 groups, $p=0.0879$ and $p=0.2595$, respectively as measured by one-way ANOVA.

4.2.5 Expression of glutamate transporter EAAT2 in astrocytes of ALS cases

Detailed characterisation of the astrocyte phenotype was performed to assess changes in astrocyte gliosis and function between the controls, ALS/C9ORF72-positive and ALS/C9ORF72-negative cases. GFAP and EAAT2 expression were quantified using image analysis.

GFAP⁺ astrocytes were present throughout both the grey and white matter in both controls and ALS cases (see figure 4.15 & 4.16). GFAP immunolabelled distinct astrocyte cell bodies and processes throughout the grey matter (see figure 4.15). Loss of motor neurons and dense astrogliosis were observed in the grey matter of ALS cases (see figure 4.15b-c), while the white matter displayed a denser immunoreactive profile (see figure 4.16), with few individual astrocyte cell bodies readily identifiable in control cases (see figure 4.16a).

EAAT2 immunolabelled delicate astrocyte processes in the grey matter of controls and ALS groups (see figure 4.17). Whereas, white matter showed weak staining of astrocyte process in controls (see figure 4.17a) and negative staining of EAAT2 in the ALS groups (see figure 4.17b-c). Loss of EAAT2⁺ astrocytes surrounding motor neurons was observed in the grey matter of ALS cases compared to controls (figure. 4.17b-c). Very little staining of EAAT2 was observed in the white matter of ALS cases compared to controls (see figure 4.18).

GFAP immunoreactivity was assessed in ALS patients (n=10) compared to controls (n=5), and analysed using student T-Test. Levels of GFAP⁺ immunoreactivity were significantly higher in ALS patients compared to controls, both in the grey matter

($p=0.0393$) and the white matter ($p=0.0198$) (see figure 4.19 a-b). A decrease in EAAT2 protein was observed in both the grey matter of ALS patients ($n=10$) compared to controls ($n=5$) ($p=0.4140$) and in the white matter of these cases ($p=0.7157$), though this was not significant (see figure 4.19 c-d).

GFAP expression in ALS cases was further interrogated and any differences in staining between ALS/*C9ORF72*-negative and ALS/*C9ORF72*-positive cases was assessed. There was no significant difference in GFAP immunoreactive profiles in either the grey ($p=0.1291$) or white matter between controls, ALS/*C9ORF72*-negative and ALS/*C9ORF72*-positive cases ($p=0.0742$) (see figure 4.20a-b). Like GFAP, EAAT2 staining showed no statistically significant difference between controls, ALS/*C9ORF72*-negative and ALS/*C9ORF72*-positive cases in either the grey ($p=0.4584$) or white matter of the spinal cord ($p=0.4734$) (see figure 4.20 c-d).

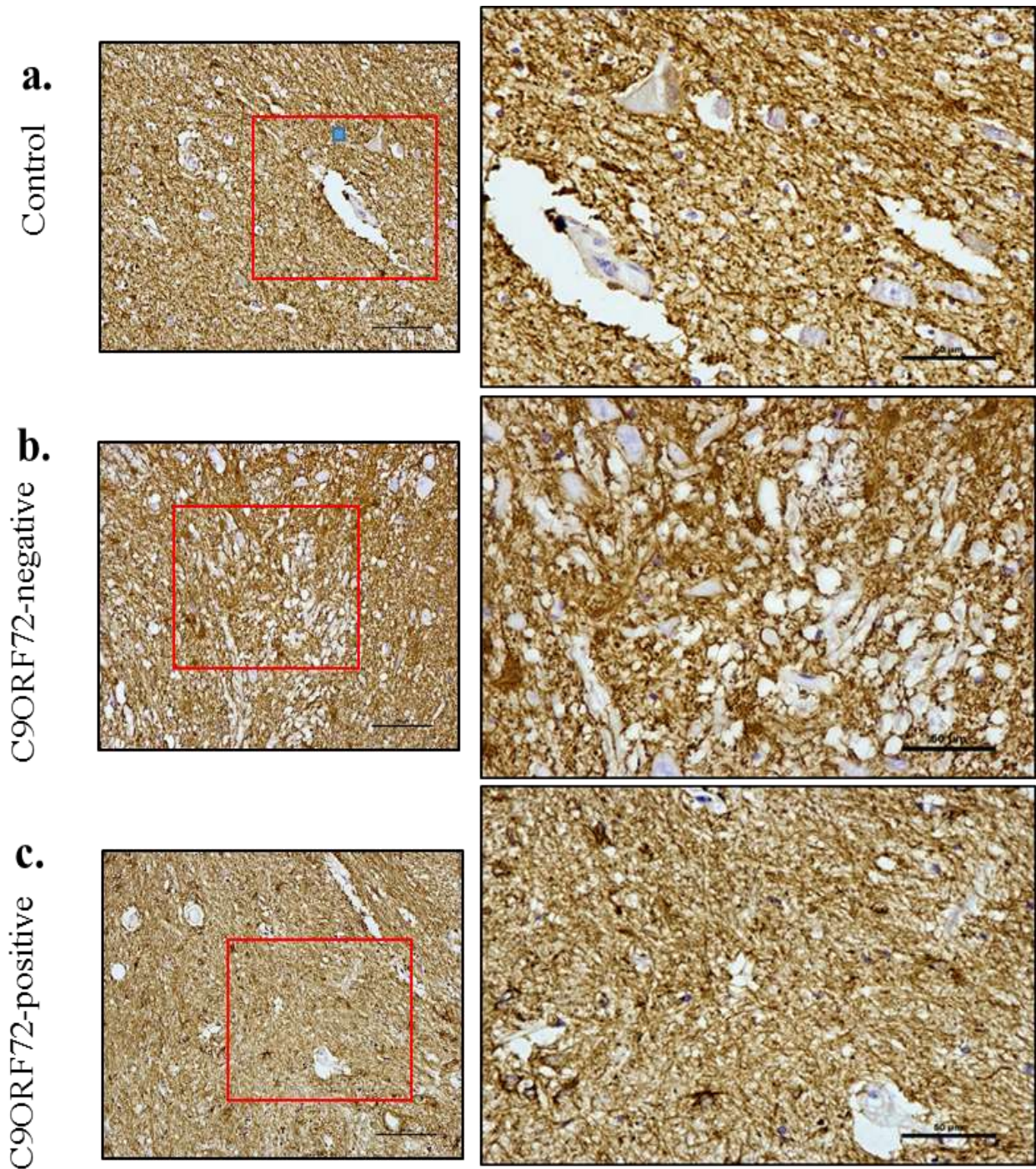


Figure 4.15: GFAP reactivity in the grey matter of spinal cord of ALS patients. Control cases displayed intense GFAP immunoreactivity surrounding motor neurons (a). GFAP immunolabelled distinct astrocyte cell bodies and process in both ALS/*C9ORF72*-negative and ALS/*C9ORF72*-positive cases (b-c). The scale bar represents 100 μm on the left panels and 50 μm on the right.

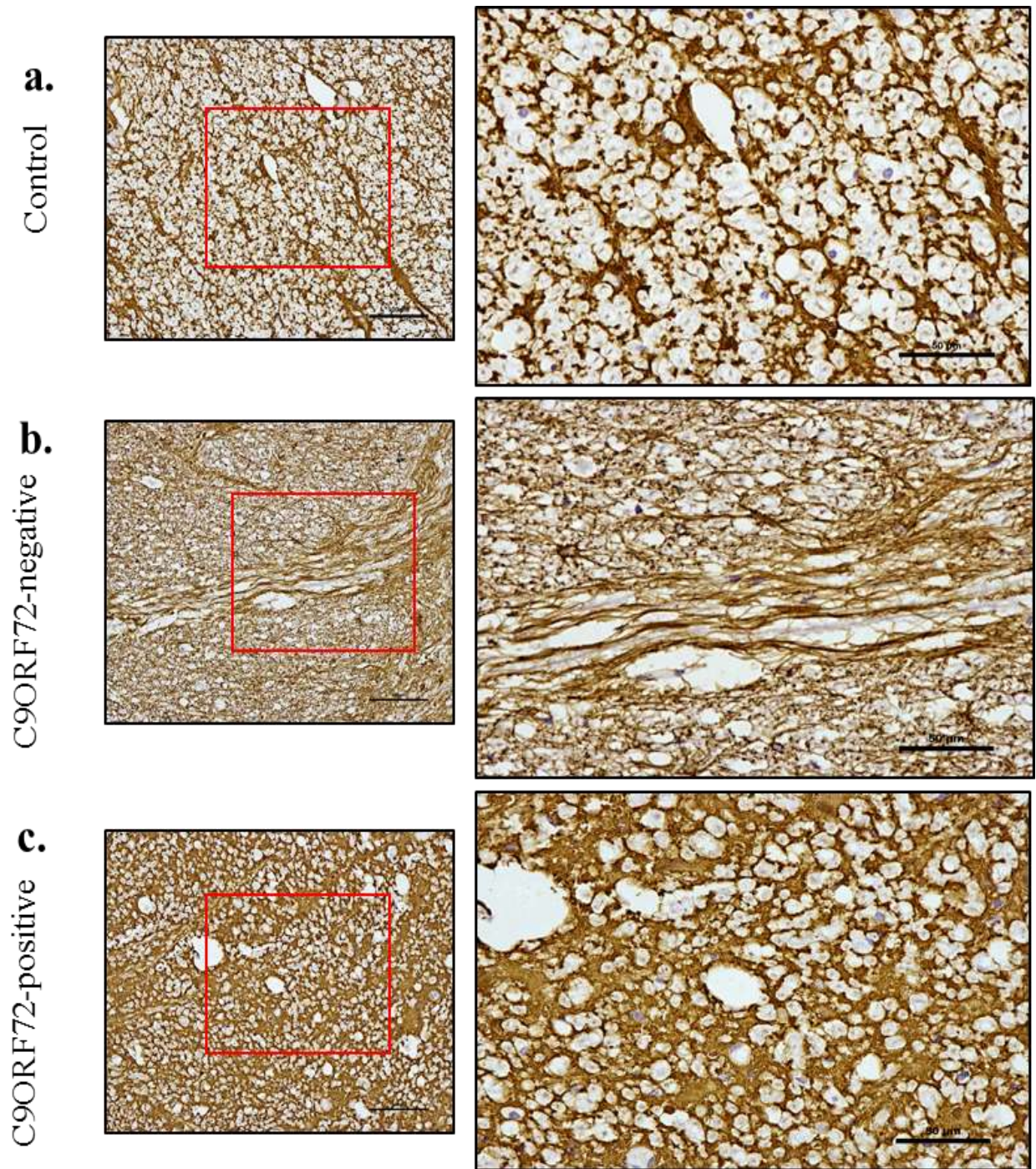


Figure 4.16: GFAP reactivity in the white matter of spinal cord of ALS patients. Dense astroglial staining was observed in the white matter of control (a), ALS/*C9ORF72*-negative (b) and ALS/*C9ORF72*-positive cases (c). A 100 μm scale bar prospective is presented on the left panels and a 50 μm scale bar prospective is presented on the right.

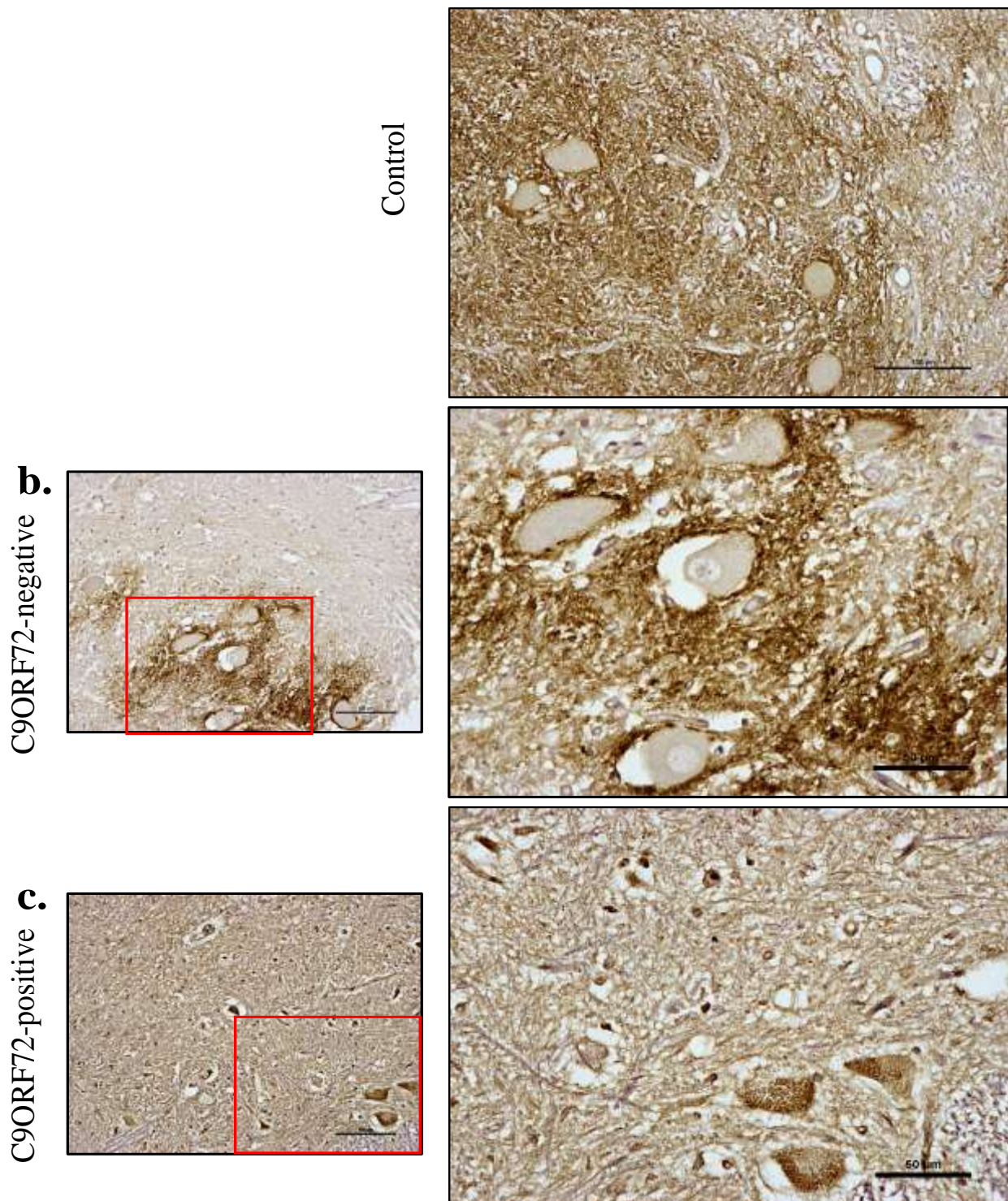


Figure 4.17: EAAT2 reactivity in the grey matter of spinal cord of ALS patients
 Control cases displayed a confluent pattern of EAAT2 throughout the grey matter (a). ALS/*C9ORF72*-negative cases displayed intense patchy, distinct EAAT2 staining surrounding motor neurons (b). ALS/*C9ORF72*-positive sections contained little EAAT2 staining, lipofuscin was observed in motor neurons (c), scale bar=100µm

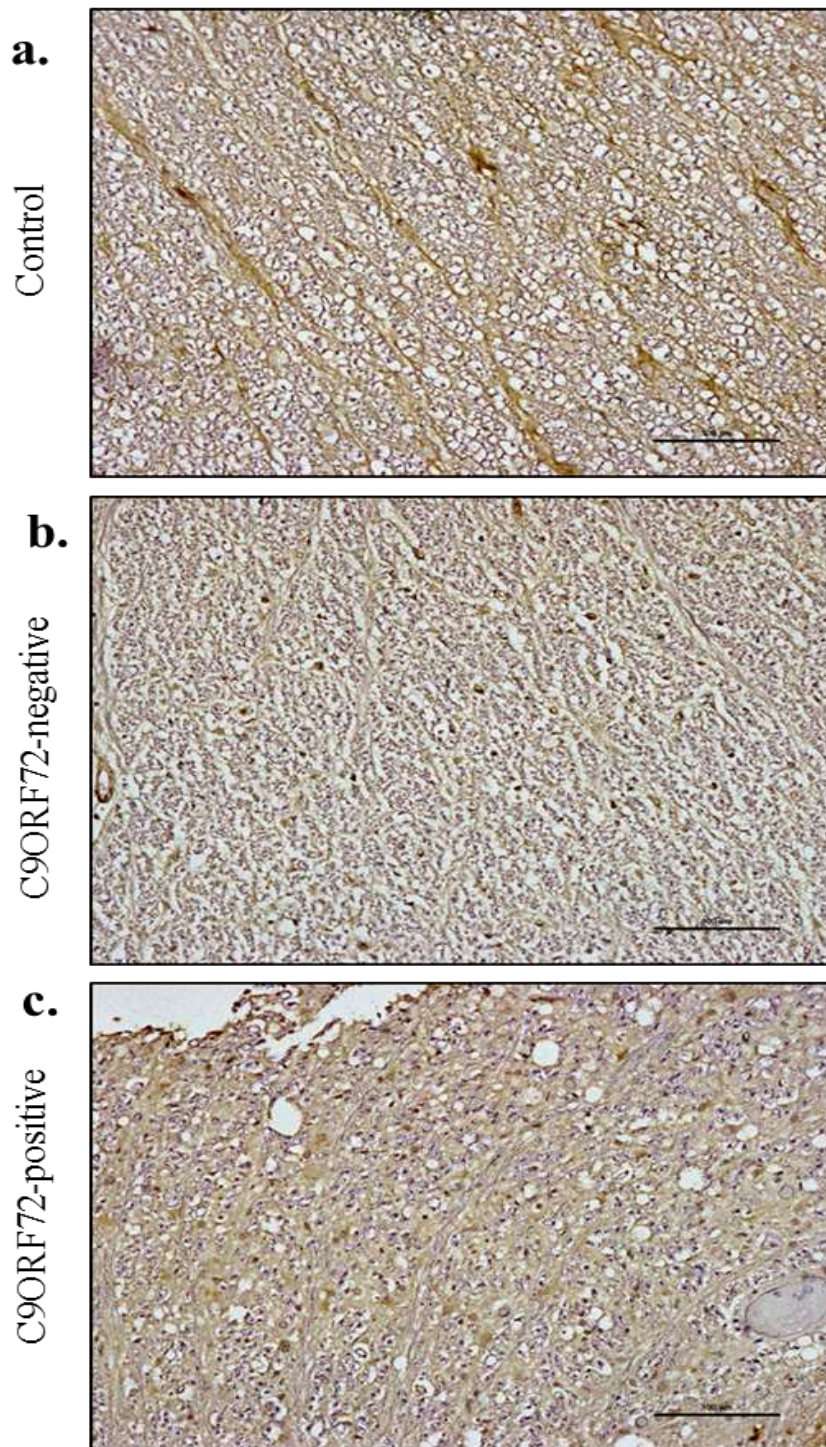


Figure 4.18: EAAT2 reactivity in white matter of spinal cord of ALS patients
 Control group depicting of weak immunoreactive EAAT2 staining (a). Both ALS/*C9ORF72*-negative and ALS/*C9ORF72*-positive groups exhibiting almost non-reactive white matter to EAAT2 (b-c), scale bar =100µm

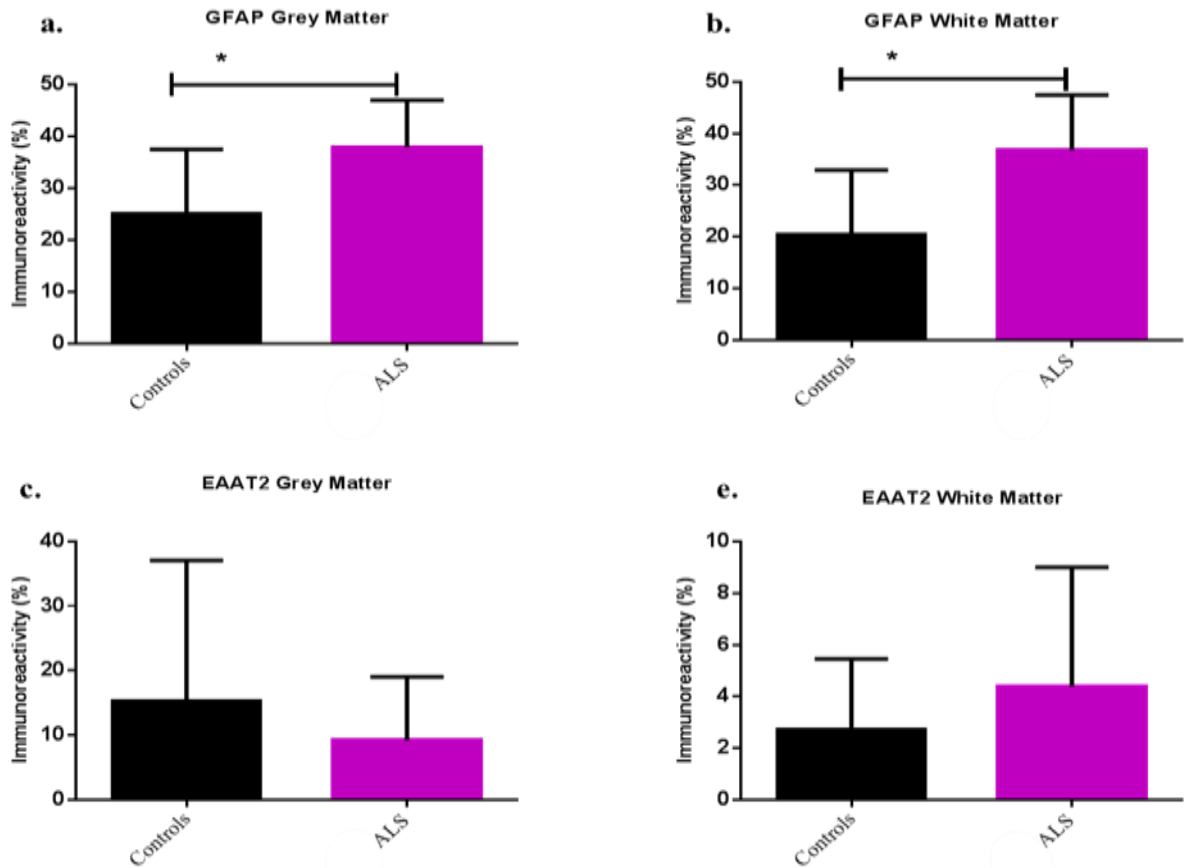


Figure 4.19: GFAP and EAAT2 reactivity in the grey and white matter of ALS patients.

In the grey matter of spinal cord sections, GFAP immunoreactivity in the grey matter was significantly higher in ALS cases compared to controls ($p=0.0393$). Similarly, in the white matter of the spinal cord, GFAP immunoreactivity was significantly higher in ALS patients compared to controls ($p=0.0198$). In contrast, EAAT2 immunoreactivity in both the grey and white matter of the spinal cord did not show any significant difference between the two groups ($p=0.4585$ and $p=0.4734$, respectively). The data was analysed using student T-Test.

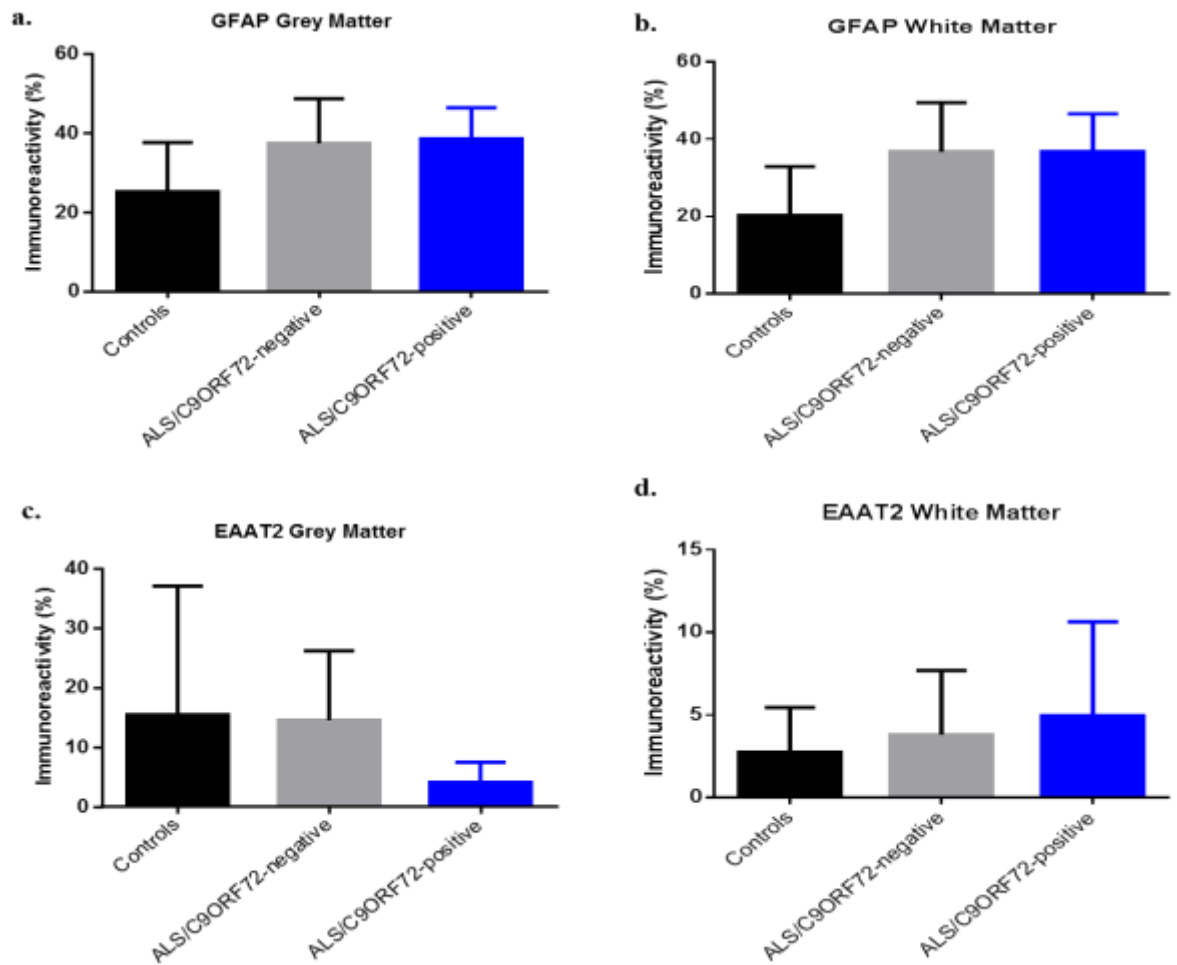


Figure 4.20: GFAP and EAAT2 reactivity in the grey and white matter of ALS patients with and without *C9ORF72* expansion.

Levels of GFAP immunoreactivity between the 3 groups did not significantly differ in either the grey matter ($p=0.1291$) or the white matter of the spinal cord ($p=0.0742$) (a-b). Similarly, levels of EAAT2 immunoreactivity did not significantly differ between the three groups in either the grey ($p=0.4140$) or white matter ($p=0.7157$), as measured by one-way ANOVA (c-d).

4.3 Discussion

The present study describes the detailed characteristics of MN pathology in the anterior horn of spinal cord of ALS patients, both with and without the *C9ORF72* mutation, in comparison to non-neurological controls. ALS cases contained significantly higher numbers of MN containing p62 and p-TDP43 inclusions than controls. In contrast controls contained greater expression of GLUR2 associated with the ER. ALS cases were associated with increased astrogliosis and a reduction in EAAT2 immunoreactivity.

TDP-43 is a DNA/RNA binding protein that is predominantly found in the nucleus. TDP-43 is involved in RNA regulation mechanisms including mRNA transport, stability, and splicing. However, the role of TDP-43 in the brain is poorly understood (Mackenzie *et al.*, 2014). The formation of TDP-43 inclusion bodies is associated with the substantial reduction in the normal physiological TDP-43 nuclear staining. Additionally, pathological forms of TDP-43 undergo abnormal post-translational modifications including ubiquitination, N-terminal truncation and hyperphosphorylation (Neumann *et al.*, 2006a; Neumann *et al.*, 2009). Moreover, TDP-43 contributes to cell death via loss-of-function and gain-of-function mechanisms (Mackenzie *et al.*, 2014). Any mutations or disruption of many ALS-linked genes involved in protein homeostasis pathways such as p62 lead to TDP-43 mislocalisation forming inclusions in the cytoplasm of MNs of ALS patients (Seelaar *et al.*, 2007; Cooper-Knock *et al.*, 2012; Stewart *et al.*, 2012).

In line with previous studies, the results of the current study demonstrate the pathology of ALS patients with *C9ORF72* expansion (ALS/*C9ORF72*⁺) is indistinguishable from typical sporadic ALS patients (ALS/*C9ORF72*⁻), with

predominant MN degeneration and TDP-43 positive neuronal and glial cells inclusions. These pathological inclusions are consistently seen in the MNs of the spinal cord as well as upper motor neurons and lower brainstem (Mackenzie *et al.*, 2014). Evidence has shown TDP-43 pathology in a wide range of neuroanatomical regions including frontal and temporal cortex, hippocampus, thalamus, striatum, midbrain and substantia nigra (Murray *et al.*, 2011; Hsiung *et al.*, 2012). Interestingly, the current study demonstrates ALS/*C9ORF72*-positive patients have significantly higher levels of p62 positive inclusions compared to ALS/*C9ORF72*-negative patients, which confirms reports that this is a feature of cases containing the *C9ORF72* repeat expansion where higher levels of p62 were detected in neurons and glia in the anterior horn of the spinal cord, cranial nerve motor nuclei and motor cortex (Cooper-Knock *et al.*, 2012). These p62 positive inclusions were not only found in the cytoplasm of neurons but also in glial cell of ALS patients with the *C9ORF72* repeat expansion (Al-Sarraj *et al.*, 2011; Mackenzie *et al.*, 2014). In 5 ALS/*C9ORF72*-negative cases, only one case showed p62 immunoreactivity in the thoracic spinal cord suggesting p62 inclusions. However, upon further analysis this case might be explained by the fact that the area of onset might be different.

Although levels of p-TDP-43 were significantly increased in ALS cases compared to controls, in contrast to p62 the current study did not demonstrate any significant difference in the TDP-43 expression between ALS/*C9ORF72*-positive and ALS/*C9ORF72*-negative cases, which might reflect the presence of TDP-43 in an immature form which has not yet been sequestered in to inclusions, and/or possible abnormality in autophagy (Boillée *et al.*, 2006; Cruits *et al.*, 2013). p62 plays an important role in protein degradation by ubiquitin-proteasome system and autophagosome-lysosome pathways. When autophagy functions at normal rates, the

role of p62 is to deliver ubiquitylated proteins for autophagosomal damage. However, when autophagy is compromised under pathological conditions, including neurodegenerative diseases, p62 binds non-selectively to ubiquitylated proteins and prevents their delivery to the proteasome for degradation. Therefore, the accumulation of p62 makes it difficult to serve as a substrate for the proteasome with its narrow catalytic pore (Korolchuk *et al.*, 2010). In the current study, MN of ALS patients with the *C9ORF72* expansion contain higher levels of p62 inclusions compared to those SALS cases without the expansion. This may be in part explained by three pathogenic mechanisms: (i) haploinsufficiency where loss of function occurs as a result of the *C9ORF72* repeats, (ii) the expression of mutant *C9ORF72* protein results in a gain of protein toxicity or (iii) RNA toxicity caused by the production of RNA repeats (La Spada & Taylor, 2010). Additional pathogenic mechanisms caused by the *C9ORF72* expansion might occur due to complementary repeat containing RNA produced by bidirectional transcription or dipeptide-repeat proteins resulted from non-ATG (RAN) translation (Ling *et al.*, 2013; Mann *et al.*, 2013) eventually leading to the production of potential toxic RNA and protein species.

As previously mentioned, ADAR2 edits the double-stranded RNA of *GLUR2* in a site-specific manner (Bass, 2002; Keegan *et al.*, 2004). Several lines of evidence have shown that decreased ADAR2 activity correlates with reduced *GLUR2* editing at Q/R site in MNs of SALS patients and in mouse models of disease (Higuchi *et al.*, 2000; Aizawa *et al.*, 2010; Hideyama *et al.*, 2010; Hideyama *et al.*, 2012a; Yamashita & Kwak, 2013; Kubota-Sakashita *et al.*, 2014). In agreement with these findings, the current study demonstrates that *GLUR2* is significantly decreased in the endoplasmic reticulum of MNs of ALS/*C9ORF72*-negative and ALS/*C9ORF72*-positive cases compared to control cases. The present study did not find any significant difference in

ADAR2 and ADAR3 levels between control and SALS cases, which may reflect the small number of cases used (n=15). Extending the study to include a larger cohort would provide more insight.

Recent studies have demonstrated a link between a reduction or absence of ADAR2 in the nucleus of MNs and the formation of cytoplasmic TDP-43 inclusions in ALS (Aizawa *et al.*, 2010; Hideyama *et al.*, 2012a; Yamashita & Kwak, 2013). It has been suggested that TDP-43 is not an upstream event of inefficient GLUR2 RNA editing at Q/R site in the MNs of SALS patients but that deficient ADAR2 in these MNs occurs before abnormal GLUR2 editing and TDP-43 pathology (Hideyama *et al.*, 2012b). TDP-43 over expression, TDP-43 knockdown and TDP-43 C- terminal fragments or TDP-43 mutations do not alter ADAR2 expression (Yamashita *et al.*, 2012b). Interestingly, our data showed that the expression of ADAR3 protein was increased in the nucleolus and cytoplasm of MNs in ALS cases with the C9ORF72 expansion, this requires further investigation since the role of ADAR3 is not clear it is difficult to predict what effect it might have. As yet there is no literature on the subject.

ADAR3 was found to colocalize with C9ORF72 repeats in induced pluripotent stem cells (iPSCs) that were derived from ALS/FTD patients with C9ORF72 repeats and mutant SOD1-ALS patients. Moreover, knocking-down ADAR3 expression results in the decrease of RNA foci, which implies that there is a functional interaction between ADAR3 and RNA repeats *in vivo* (Almeida *et al.*, 2013; Donnelly *et al.*, 2013; Todd & Paulson, 2013). Together these findings may provide a clue for the mechanism by which a member of the RNA editing enzyme family, namely ADAR3, may contribute to ALS pathology, in particular in ALS/C9ORF72-positive cases.

In line with previous reports, the grey matter in the spinal cord of ALS patients exhibited astrogliosis and increased of GFAP content were associated with loss of

MNs (Vargas & Johnson, 2010). These features of astrocytic response to injury have been observed in neurodegenerative diseases including ischaemia and Alzheimer's disease (Simpson *et al.*, 2010; Vargas & Johnson, 2010).

Glutamate transporter dysfunction plays an important role in excitotoxicity-mediated MN degeneration. In the current study we demonstrate a reduction of EAAT2 expression in the spinal cord of ALS patients, though this was not significant. This is in agreement with previous reports of the decreased EAAT2 expression in the spinal cord and motor cortex of ALS patients, and in the hSOD1 mouse model (Rothstein *et al.*, 1995; Milton *et al.*, 1997; Vargas & Johnson, 2010). The non-significant difference in EAAT2 expression between controls and SALS groups likely reflects the small number of cases tested (n=15). Future experiments would require increased number of cases.

The presence of p62 and p-TDP-43 inclusions in MNs in the grey matter of spinal cord is hallmark for ALS disease. The loss of EAAT2 surrounding MNs in the SALS cases is clear feature of excitotoxicity and neuronal death in ALS. ADAR2 protein was not associated with reduced GLUR2 protein in SALS cases however, sufficient GLUR2 has to be edited to impact anion channel permeability. Data did not suggest if there is any interaction between ADAR2 and ADAR3. Future investigation of the detailed neuropathology of a larger cohort may help to elucidate the mechanism of MN injury in SALS.

Chapter 5
Next generation
sequencing

Chapter 5: Next generation sequencing

5.1 Introduction

Illumina sequencing by synthesis (SBS) derived from the original work of Balasubramanian and Klenerman (Illumina). They used fluorescently labelled nucleotides to visualise the movement of DNA polymerase at a single molecule resolution. The synthesised DNA was immobilised to a solid substrate.

This technology led to the formation of Solexa which was derived from the first SBS machines and was used to sequence the whole genome of the bacteriophage phiX-174 in 2005, as a result, sequencing more than 3 million bases in a single run. The SBS technology was further developed by Illumina and is now able to generate gigabytes of data in a single run and sequence the entire genome in matter of days (<http://www.illumina.com/technology/next-generation-sequencing/sequencing-technology.html>).

The fundamental architecture of this technology consists of flow cells that are composed of a series of channels running through a glass slide. The inside of the channels are arrayed with single stranded oligonucleotides that are the binding site for the material to be sequenced. The library is derived from a fragmented double stranded DNA sequence, which may be fragments of DNA isolated using short nucleotide bait sequences, native genomic DNA or cDNA.

The fragmentation is achieved by sonication or enzymatically when it is termed tagmentation. The double-stranded molecules are fragmented to sizes of around 150 to 300 bases and have attached to each end a short index or barcode sequence and the complementary strand to the adapters that are arrayed on the flow cell. The index sequence is unique to each sample to allow the identification of samples in the

analysis. The library is applied in flow cell lane by lane followed by hybridisation using a piece of technology called the C-bot which enhances binding between target DNA and adaptor. The density of the hybridisation is critical and requires each strand to be distinct from its neighbour.

As can be seen in figure 5.1, the Illumina system involves single-stranded DNA fragments to be ligated to adaptors, which then attach to glass surface flow cells. The process by which hybridization of DNA to the oligonucleotides on the flow cell occurs is by the active heating and cooling system. This is followed by and incubation with reactants and an isothermal PCR to amplify the fragments in a cluster on the surface. Within the sequencer, the flow cell is placed onto a movable stage and supplied with polymerase and distinct fluorophores for each labelled nucleotide. Labelled nucleotides are attached at a 3'-OH modified to ensure single base incorporation. This is followed by imaging to determine the incorporated nucleotides at each cluster and removing the fluorophore and the 3'-OH end at the beginning of the next cycle. The obtained data is analysed by filtering the low quality reads between 32 and 40bp, with each run yields yielding 40-50 million sequences (Mardis, 2008).

The benefit of using this system allows production of large volumes of data in a time efficient manner. It enables sequencing small genomes without aligning to a reference sequence (also called *de novo* sequencing). However, *de novo* sequencing creates short single read sequencing that if continued leads to increased number of gaps in the data where no reads align. Consequently, fragmentation of sequence reads leads to data being obtained from a poor quality sample.

Paired-end (PE) sequencing overcomes some of the issues encountered in *de novo* sequencing since it reads from both ends of a DNA fragment, thereby enabling greater

alignment especially in repetitive sequences. It yields longer fragments and fills gaps in sequences resulting in complete overall coverage (see figure 5.2) (Mardis, 2008; Fullwood *et al.*, 2009). Additionally, little input DNA is sufficient to produce a library and sequence the paired ends of a given fragment. In this manner each molecule generates many reads that are dependent upon the amount of material in the original sample. In order to gain valuable information the right amount of sample must be determined.

Short molecules require a small number of reads, while longer molecules need an increased number of reads. These longer molecules will have a number of possible variations including very rare occurrences, therefore an increased number of reads is necessary to determine the levels of all variants.

Herein, RNA extraction was repeated three times to improve the RNA concentration. RNA was extracted from 200 MNs of 9 samples (4 ALS/*C9ORF72*-positive cases, 3 ALS/*C9ORF72*-negative cases and 2 controls). The improved RNA concentration varied from 2ng/μl to 7ng/μl. 10ng of RNA was cleaned up to remove ribosomal RNA using MessageBooster whole transcriptome kit. RNA was sequenced and appeared to be read accurately and an appropriate depth was reached in a single lane. A read depth of greater than 30x for each sample was expected to be generated using paired end sequencing which should increase confidence in the accuracy of the data.

The data is analysed as soon as it is generated by the sequencing analysis viewer software, (Illumina), which allowed real time monitoring of the quality control. Afterwards, the image files (BCL) is converted into usable format by another Illumina software bcl2fastq. The obtained sequences in the fastq text format are aligned to the known human sequence to determine variations and their levels.

Previously, we have explored the levels of RNA editing of *GLUR2*, *GLUR5* and *GLUR6* in the spinal cord and MNs of SALS patients using restriction digests. We found complete editing of *GLUR2* in both MNs and spinal cord in all sample groups. Whereas, *GLUR5* and *GLUR6* were found to be less edited in spinal cord and MNs of controls and patient groups. In this chapter, it was hoped to assess the levels of RNA editing with an independent method using next generation sequencing.

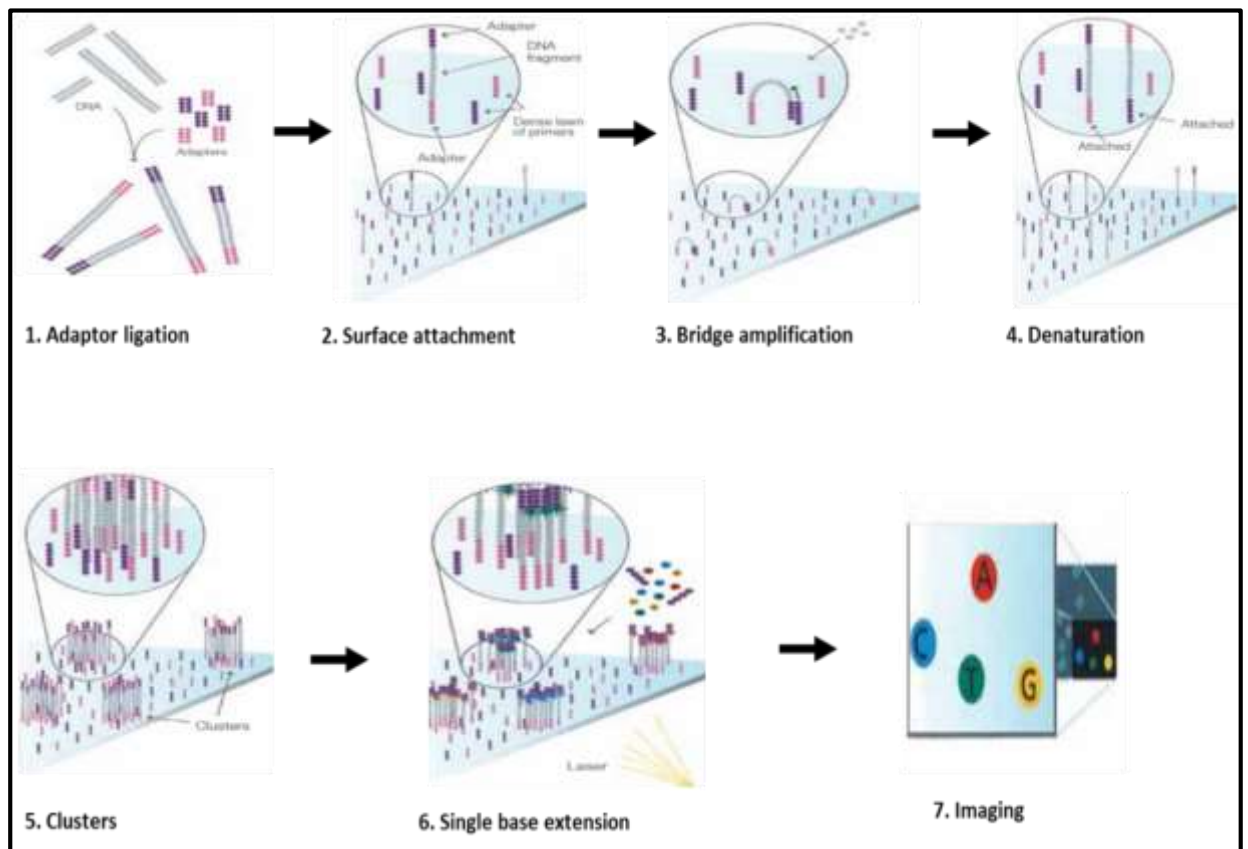


Figure 5.1: The workflow of Illumina genome analyser.

The workflow consists of single stranded hybridisation, bridge formation and cluster generation. One strand is cleaved and the other strand is sequenced via the adaptor by the addition of fluorescent nucleotides. The sequencing data is obtained by recording many images throughout the flow cell with every cycle or nucleotide added. This figure was obtained from (Mardis, 2008) with permission 3501860851558.

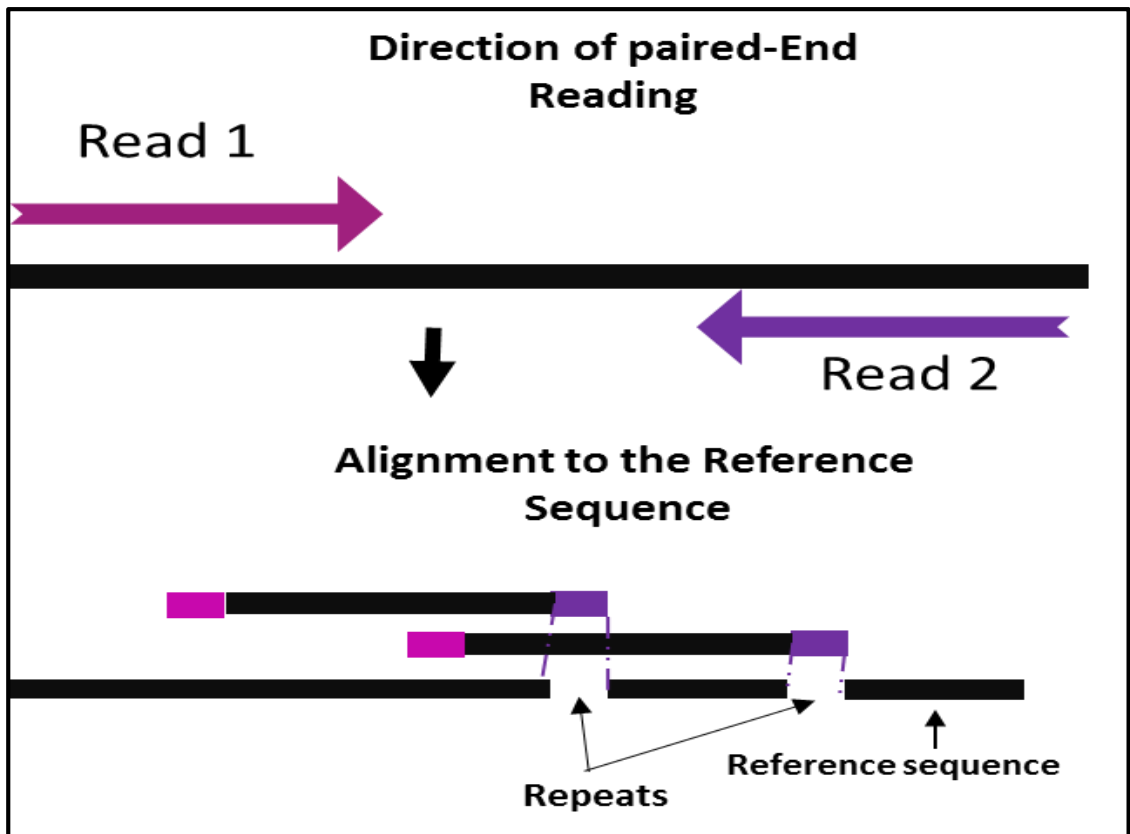


Figure 5.2: Sequencing of Paired-End libraries.

This method enables the read of sequences from both ends to accurately align repetitive regions that are difficult to sequence, modified from Illumina, 2013

Hypothesis

Use of next generation sequencing will allow in-depth analysis of the *GLUR2*, *GLUR5* and *GLUR6* as well as *ADAR2*, *ADAR3* and *EAAT2* RNA species.

Aim

To develop new methodology to look at different levels of expression that might exist in ALS.

5.2 Results

To accurately quantify editing status of *GLUR2*, *GLUR5* and *GLUR6*, a DNA library was prepared from 9 cases; 3 ALS/*C9ORF72*-positive and 3 ALS/*C9ORF72*-negative and 2 controls (see table 5.1). The DNA library was quantified by qPCR and DNA chip bioanalyser. The qPCR did not show any results whereas, DNA chip bioanalyser was able to examine the library (see figure 5.3). In this study we are going to focus on two libraries that was believed to be prepared at a different DNA concentration; 10pmol and 5pmol. Library of 10pmol library was loaded in lane 7 and half of the same library of 5pmol DNA concentration was loaded in lane 8.

Table 5.1: Cases used in the study

Case number	Block Number	Area/Level	Site of onset	PMI in hours	Sex	Age at onset	Age at death
ALS/<i>C9ORF72</i>-positive cases							
LP081/09	29	T11	Limb	60	Male	57	59
LP041/04	6	T11	Bulbar	48	Male	62	64
LP039/11	26	T11	Limb	96	Male	70	72
LP040/11	25	T11	Limb	10	Female	72	77
ALS/<i>C9ORF72</i>-negative cases							
LP014/11	24	T11	Limb	n/a	Male	49	51
LP005/10	23	T11	Limb	96	Male	38	40
LP094/09	25	T11	Bulbar	48	Male	62	63
Controls							
LP005/07	13	T11	n/a	12	Male	n/a	64
117/04	n/a	n/a	n/a	n/a	Male	n/a	58

Available thoracic spinal cord of ALS/*C9ORF72*-positive and ALS/*C9ORF72*-negative patients and controls. Abbreviation: N/A- not available

As shown in figure 5.4, the flow cell containing library formed clusters. Using sequence analysis viewer software from Illumina, each nucleotide base (A, T, C, G) were coloured with a distinctive colour to differentiate between bases. The intensity signal read these bases separately in the 1st DNA strand. The laser loses energy after 50 cycles where a sharp peak was shown (see figure 5.5). When the reading of the 1st DNA strand was finished, Illumina sequencing software reads the 2nd DNA strand at 100 cycles and more chemicals were added to boost the reading for the 2nd DNA strand (see figure 5.5). As shown in figure 5.6, the intensity signal of library number 7 and library number 8.

The Phrd quality score (Q30) assess the accuracy of each step in the process including library preparation and reading alignment. It reveals how much of the data is usable and sequencing data with low Q30 means increased portion of the reads being unusable, which is likely to contain more errors. The percentage of \geq Q30 yield of bases with Q30 or higher from clusters passing filter divided by total yield of clusters passing filter. The Q30 for the total number of 9 libraries were 82.2% (see figure 5.7).

The signal density and passing filter (PF) did not overlap between signal density and PF in lane 7. However, the signal density and PF were almost overlapped in lane 8 (see figure 5.8). Additionally, the intensity signal of the 4 bases in lane 7 only were less separated and an overlapping between bases were seen in figure 5.9. The Q30 score of the total samples in lane 7 was 57.2% (see figure 5.10). Bcl2fastq-1.8.4 software showed 9 samples that had a different adaptors (index sequence). Each sample of ALS and controls produced quality control data of Q30 score of $> 41\%$ and index reads of $> 33\%$ in library number 7 on the flow cell (see table 5.2). This library was less diluted library with a decreased index values and Q30. Whereas, library number 8 on the flow cell had a more diluted library that showed higher Q30 of $> 42\%$

and index reads of > 93% (see table 5.3). The percentage of index reads in both libraries had 1 mismatch to given index.

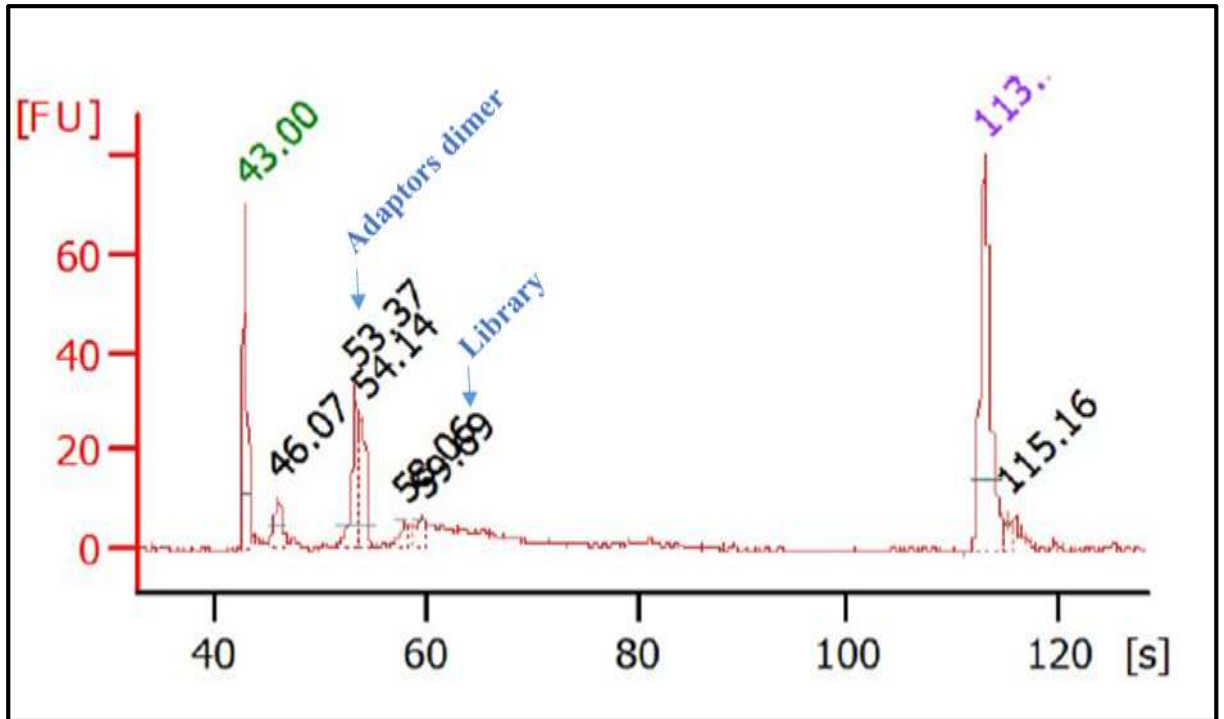


Figure 5.3: DNA chip bioanalyser for DNA library.

DNA library was quantified using DNA chip bioanalyser and each peak represent different variables; the first peak is a primer dimer, the second peak is an adaptors and the third peak is the library.

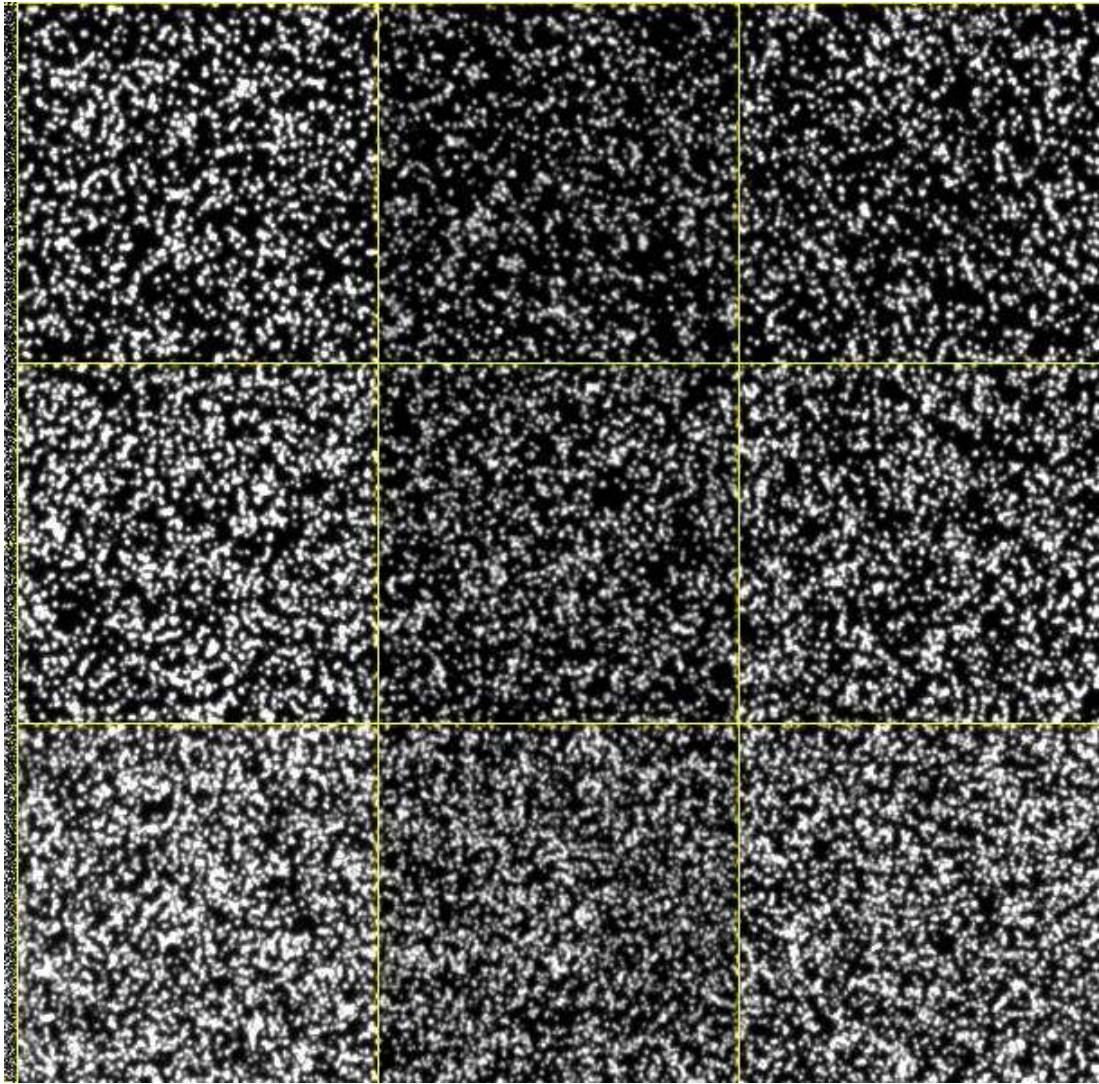


Figure 5.4: Flow cell containing clusters.

Libraries in flow cells formed clusters, the reading was in two direction vertically and horizontally.

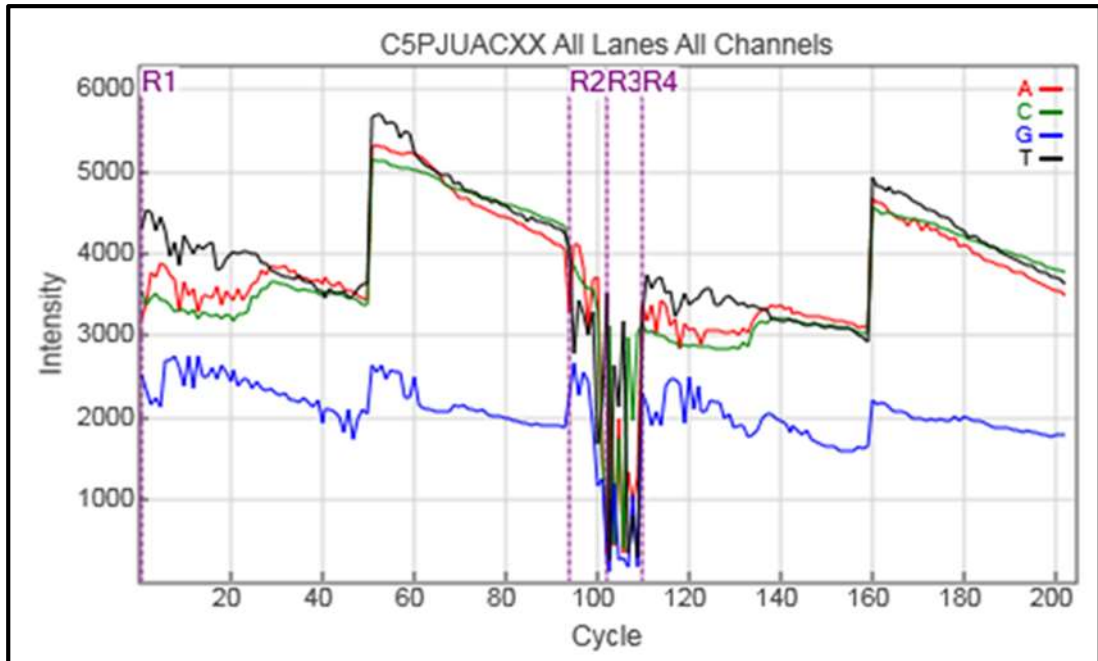


Figure 5.5: The base call quality of all libraries.

The intensity signal of 9 libraries were viewed using sequence analysis viewer software. The average quality reads of the first, second, third and the fourth base degrades over the course of the sequence.

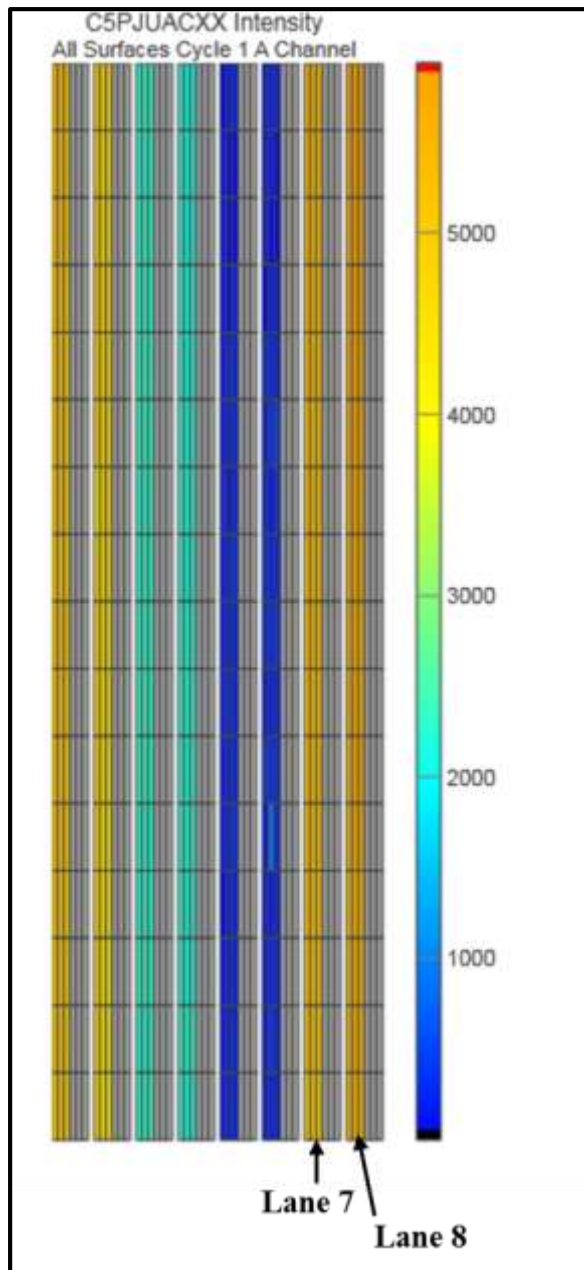


Figure 5.6: The quality call of library 7 and library 8.
The average quality of the 4 bases over the course of the sequence showing high intensity signal.

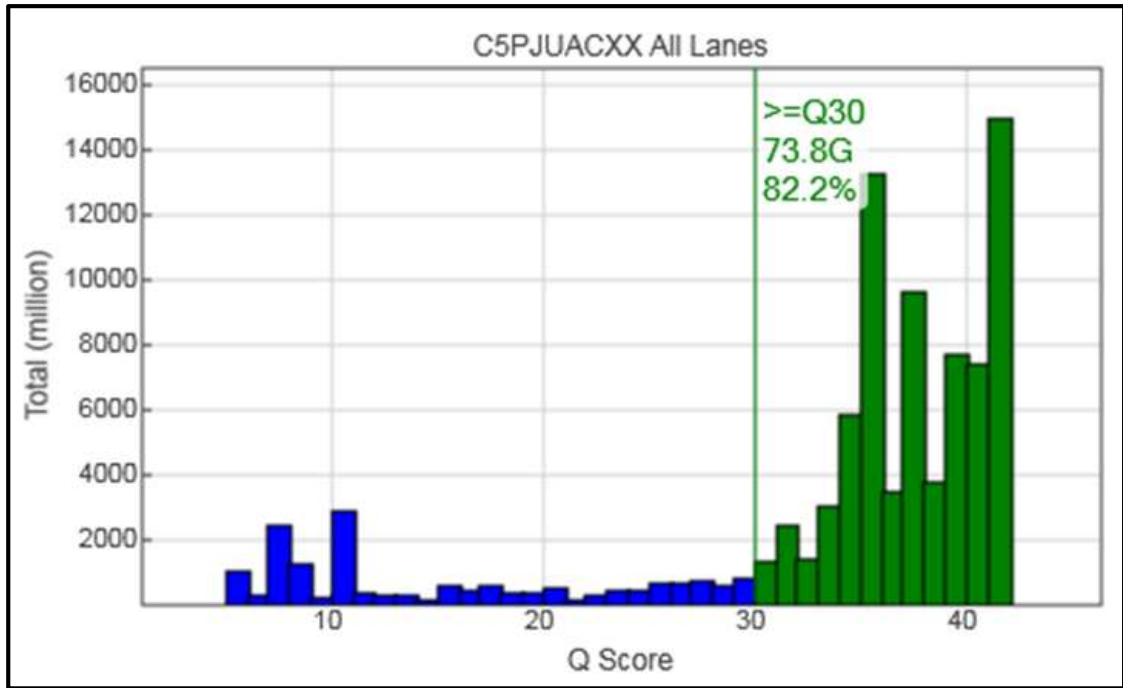


Figure 5.7: Q score heat map of libraries.

The flow cell had 9 libraries that were run on Illumina Hi scan SQ system. The quality control of libraries were assessed by Q30. The green smear represented a high score of Q30 of 82.2% in the total number of libraries.

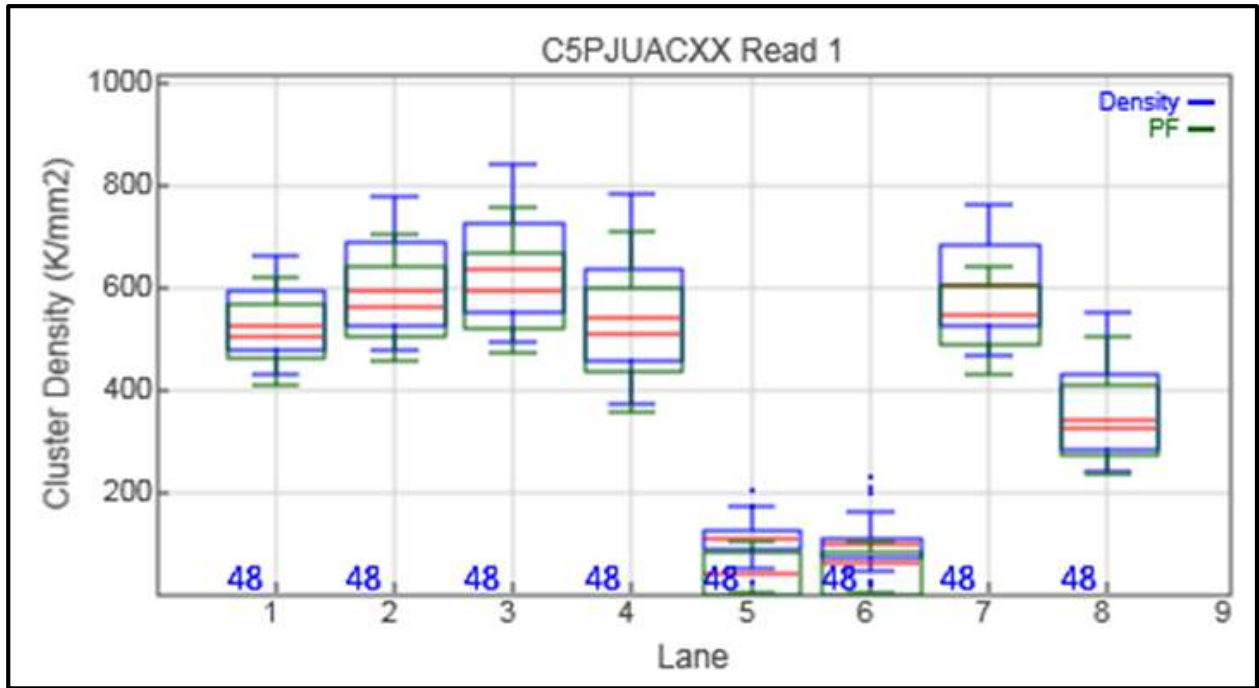


Figure 5.8: The level of cluster density and PF in each lane.

The flow cell showed 9 lanes containing 9 different libraries, our samples are library 7 (10pmol) and library 8 (5pmol). Cluster density in library 7 did not overlap with PF. Whereas, library 8 was almost overlapped between density and PF.

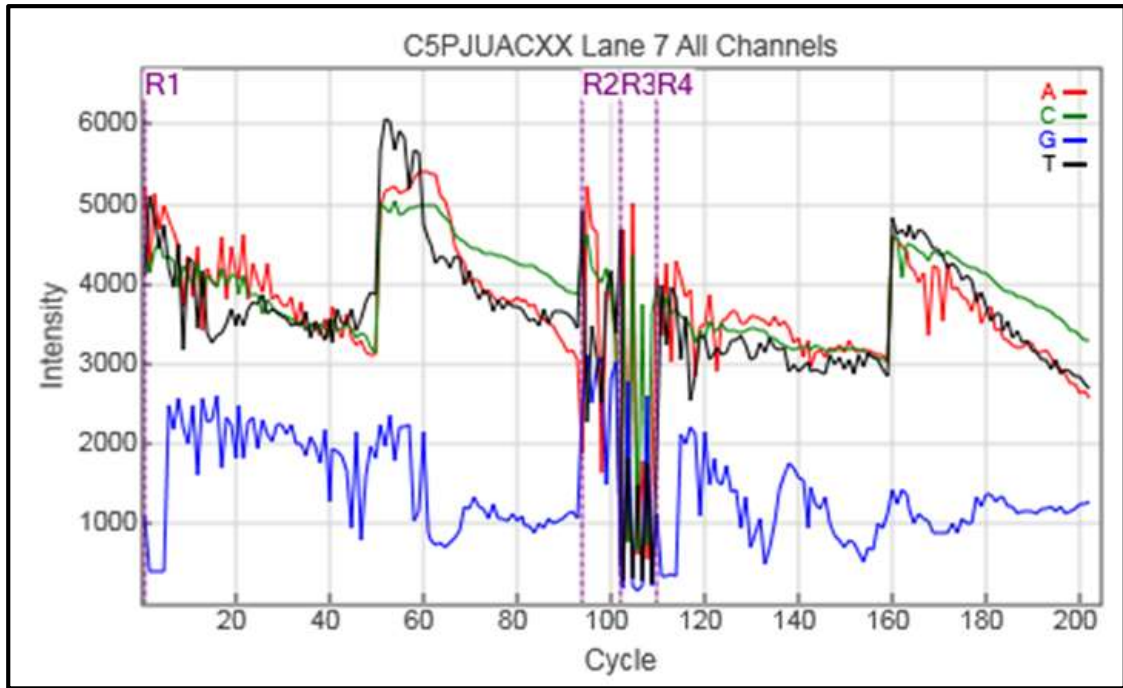


Figure 5.9: The base quality call of library number 7.

The intensity signal of the first, second, third and the fourth nucleotides were less separated. This intensity signal was viewed using sequence analysis viewer software.

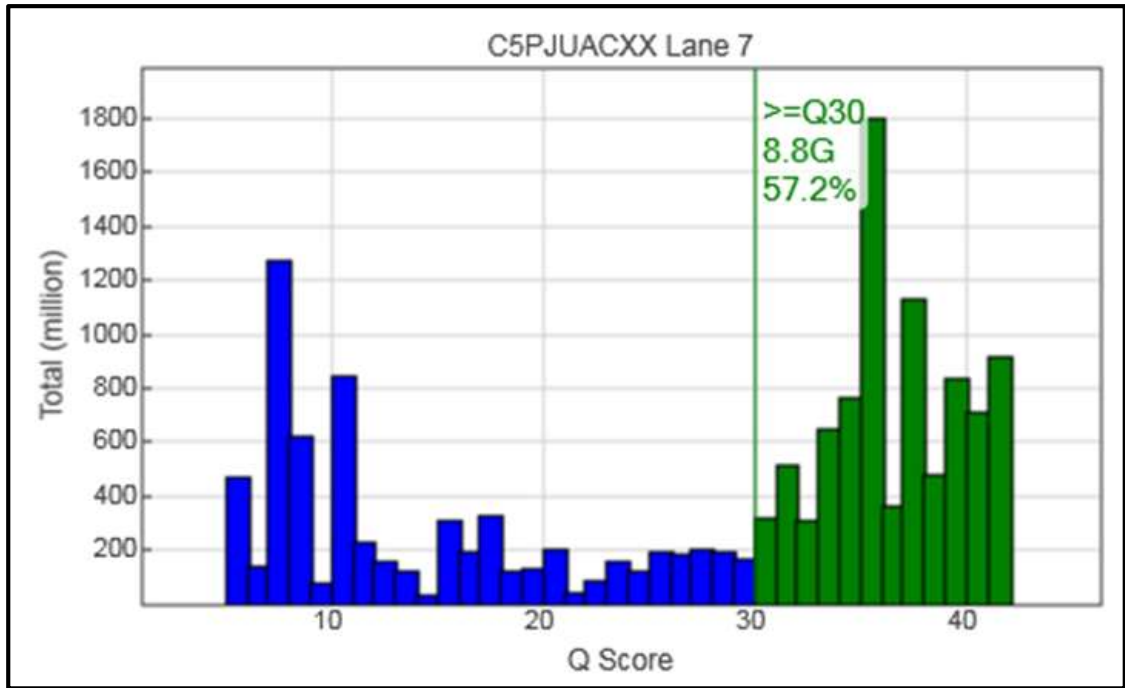


Figure 5.10: Q score heath map of library 7.

Q30 score assessed quality control of sequencing that was viewed in Illumina Hi scan SQ system. Library 7 Q score heat map represented a drop in quality from 100% to 57.2%

Table 5.2: Quantitation statistics of the sequencing run for less dilute library

Lane	Sample ID	Sample Ref	Index	Control	Yield (Mbases)	% PF	Reads	% of raw clusters per lane	% Perfect Index Reads	% One Mismatch Reads (Index)	% of \geq Q30 Bases (PF)	Mean Quality Score (PF)
7	005-07	Human	TAGGCATG-TAGATCGC	N	1,496	100.00	16,090,152	10.59	34.00	63.64	56.60	26.39
7	005-10	Human	CAGAGAGG-TAGATCGC	N	1,169	100.00	12,570,684	8.28	33.69	64.09	66.14	28.83
7	014-11	Human	CGTACTAG-TAGATCGC	N	1,662	100.00	17,872,240	11.77	33.61	63.97	50.54	24.42
7	039-11	Human	TCCTGAGC-TAGATCGC	N	567	100.00	6,095,050	4.01	33.61	62.65	47.43	23.90
7	041-04	Human	CGAGGCTG-TAGATCGC	N	2,280	100.00	24,521,456	16.15	34.17	63.92	69.09	29.95
7	040-11	Human	TAAGCGA-TAGATCGC	N	2,547	100.00	27,384,980	18.03	34.09	63.48	54.96	26.00
7	081-09	Human	CTCTCTAC-TAGATCGC	N	932	100.00	10,020,296	6.60	33.67	64.01	55.19	25.66
7	094-09	Human	GCTACGCT-TAGATCGC	N	1,323	100.00	14,227,020	9.37	33.32	63.56	46.40	23.41
7	117-04	Human	GGACTCCT-TAGATCGC	N	1,055	100.00	11,339,190	7.47	33.17	63.06	41.04	22.11
7	unknown	Undetermined	Clusters with unmatched barcodes for lane 7	N	Undetermined_indices	1,093	100.00	11,755,642	7.74	0.00	0.00	50.00

The quality data produced from library number 7 on the flow cell. The most important values are index reads that were $> 33\%$ and the Q30 that were $> 41\%$. The less dilute library had a decreased index values and Q30 suggesting it formed less cluster density.

Table 5.3: Quantitation statistics of the sequencing run for more dilute library.

Lane	Sample ID	Sample Ref	Index	Control	Yield (Mbases)	% PF	Reads	% of raw clusters per lane	%Perfect Index Reads	% One Mismatch Reads (Index)	% of >= Q30 Bases (PF)	Mean Quality Score (PF)
8	005-07	Human	TAGGCATG-TAGATCGC	N	1,051	100.00	11,298,434	11.73	95.04	4.92	63.55	27.96
8	005-10	Human	CAGAGAGG-TAGATCGC	N	784	100.00	8,430,244	8.76	95.40	4.56	75.69	31.01
8	014-11	Human	CGTACTAG-TAGATCGC	N	1,184	100.00	12,728,112	13.22	95.27	4.69	56.92	25.73
8	039-11	Human	TCCTGAGC-TAGATCGC	N	391	100.00	4,204,490	4.37	93.78	6.15	50.97	24.61
8	041-04	Human	CGAGGCTG-TAGATCGC	N	1,539	100.00	16,551,410	17.19	95.40	4.56	78.79	32.29
8	040-11	Human	TAAGGCGA-TAGATCGC	N	1,673	100.00	17,990,488	18.68	95.00	4.96	61.43	27.47
8	081-09	Human	CTCTCTAC-TAGATCGC	N	635	100.00	6,828,498	7.09	95.24	4.71	62.69	27.29
8	094-09	Human	GCTACGCT-TAGATCGC	N	795	100.00	8,544,190	8.87	93.62	6.27	50.03	24.05
8	117-04	Human	GGACTCCT-TAGATCGC	N	679	100.00	7,306,320	7.59	93.64	6.27	42.78	22.29
8	Unknown	Undetermined	Clusters with unmatched barcodes for lane 8	N	224	100.00	2,406,288	2.50	0.00	0.00	50.51	24.41

The quality data produced from library number 8 on the flow cell. The most important values are index reads that were > 93% and the Q30 that were > 42%. For these it appears that the more dilute library has generated better values suggesting it had a better cluster density and that this allowed cleaner sequencing.

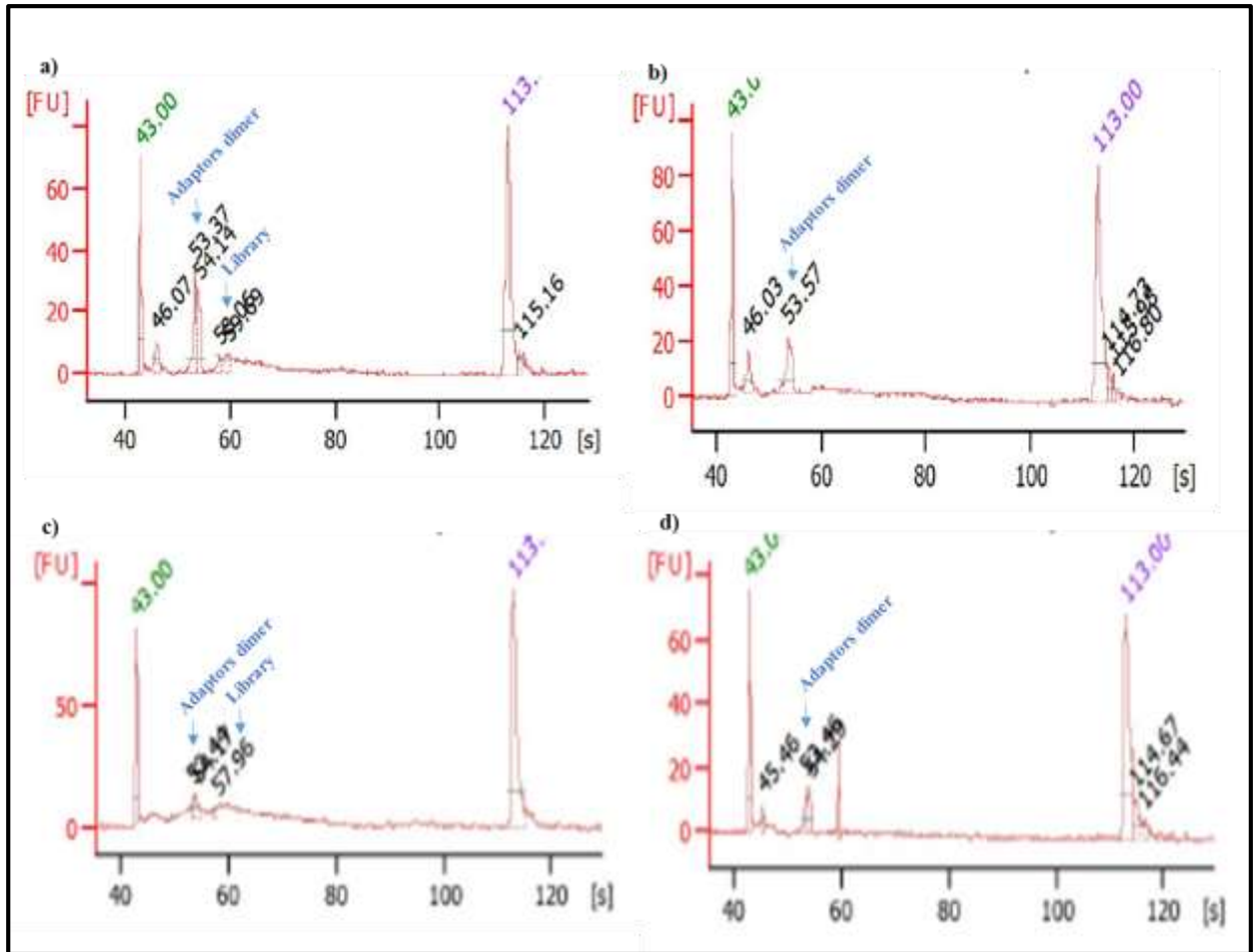


Figure 5.11: DNA chip bioanalyser of library samples.

Panel a. is sample 05/07 & panel c. is sample 81/09, both had shown two peaks; one is adaptor dimer and the second is a library. Whereas, panel b. is sample 40/11 and panel d. is 14/11, both showed only adaptor dimer with no library detected.

Reads were mapped to the human genome UCSC hg19 using Bowtie (Langmead *et al.*, 2009). Expression values for transcripts were generated using Bitseq (Glaus *et al.*, 2012). In particular, we utilised an implementation of transcript expression inference utilising Variational Bayes algorithmics within Bitseq (<http://arxiv.org/pdf/1308.5953.pdf>).

The percentage of mapped reads was very low, <0.1% for most samples; however in certain cases the number was higher. The reason for this is unclear, perhaps the degraded RNA extracted from post-mortem laser captured neurons was too degraded to provide accurate mapping. The samples with mapped reads were 40/11 (5.4%), 14/11 (21%), 81/09 (25%) and 05/07 (10%) samples however, only samples 05/07 and 81/09 had shown a library to be mapped to the human genome whereas, samples 41/11 and 14/11 did not show a library therefore the percentage of mapping reads were not accurate and maybe mapped to adaptor dimers (see figure 5.11).

As can be seen in table 5.4, *ENST00000529637* is transcript from *ENSG00000090686* gene which is an ubiquitin specific peptidase 48. *ENST00000270722* is also transcript for *ENSG00000142611* gene which is a PR domain containing 16. Both transcripts were mapped to human genome and demonstrated high reads similar to the comparative data set (see appendix II). Most of the data showed very similar levels of expression for all transcripts including those of interest. However, some transcripts as indicated in figure 5.11 were variable demonstrating a low level of differential expression.

Table 5.4: Mapping reads to the human genome.

Gene	005-07 Control	014-11 ALS/C9ORF72 negative	041-11 ALS/C9ORF72 positive	081/09 ALS/C9ORF72 positive	Comparative data set
<i>ENST00000529637</i>	6.36E-07	2.93E-07	4.38E-07	6.68E-05	6.68E-05
<i>ENST00000270722</i>	6.36E-07	4.40E-07	7.00E-07	4.38E-07	6.12E-07

5.3 Discussion

Next generation sequencing was used in order to try and study the differential expression of *GLUR2*, *GLUR5* and *GLUR6* editing and *ADAR2*, *ADAR3* in ALS tissue. However, this approach was not successful due to poor quality and quantity of RNA that were used which did not allow generation of full data set. The methodology found to be valid in other libraries but optimisation of the conditions to generate more accurate data sets was needed. There might be a number of reasons for unsuccessful reads in next generation sequencing. (i) The production of adapter dimer led to unsuccessful alignment to the human genome. (ii) Very short reads were also observed and paired-end sequencing was not successful in some of the samples. (iii) Small number of MNs and degraded RNA tissue is likely to have contributed to the unsuccessful experiment. Future studies require repetition of the experiment with better library preparation. Other potential quality control that could be performed prior to running the experiment is align trimmer that removes aligned sequences of adaptors, primers and barcode indexes in both ends of sequence reads. Such alien sequences improve the quality of results for downstream analyses (Criscuolo & Brisse 2013).

To conclude, there was no differential gene expression in *GLUR2*, *GLUR5* and *GLUR6* or in *ADAR2*, *ADAR3* and *EAAT2*. However, the fact that some differential expression was observed indicated that the methodology might be valid in a future experiment with greater optimisation.

Chapter 6

General Discussion

Chapter 6: General Discussion

6.1 Discussion

The vulnerability of MNs to injury in sporadic ALS may result from excitotoxicity mediated by abnormal Ca^{+2} -permeable AMPA receptors. Abnormal RNA editing of AMPA receptor *GLUR2* at the Q/R site is a plausible pathogenic mechanism leading to MNs death in ALS (Kwak & Kawahara, 2005). Therefore, the current research tested the hypothesis that altered glutamate receptor editing in MNs is relevant to the pathogenesis of ALS. Whilst *GLUR2* mRNA editing was 100% in MNs, the protein levels were reduced in the ER of these MNs in ALS cases, both with and without the *C9ORF72* expansion, demonstrating that RNA editing of *GLUR2* is not linked to the observed reduction of *GLUR2* protein.

These findings are in contrast to reports of abnormal *GLUR2* editing in MNs of SALS cases (Takuma *et al.*, 1999; Kawahara *et al.*, 2004; Kwak & Kawahara, 2005), which likely reflect the pre-mortem hypoxia-associated *ADAR2* changes arising from prolonged duration on a respiratory machine (Nevo-Caspi *et al.*, 2011). Furthermore, these studies investigated RNA editing of small number of MNs, which may not represent the dominant status of *GLUR2*, *GLUR5* and *GLUR6* editing in the MN population. Moreover, these reports also studied *GLUR2* editing in the spinal cord, specifically the ventral and dorsal horn of the grey matter of the spinal cord as whole tissue in SALS cases and controls. Additionally, they have also examined MNs from 5 SALS cases of a cohort that was not well defined (Takuma *et al.*, 1999; Kawahara *et al.*, 2004). In contrast to these reports, the current study clearly and consistently

demonstrates complete *GLUR2* editing in SALS patients, both with and without the *C9ORF72* expansion.

The RNA editing levels of *GLUR5* and *GLUR6* in MNs of SALS cases, both with and without the *C9ORF72* expansion, were also examined since they too are catalysed by *ADAR2*. The RNA editing levels in *GLUR5* and *GLUR6* were not consistent in MNs, spinal cord, frontal cortex and motor cortex and/or in multiple ALS cohort including ALS cases with and without *C9ORF72* expansion.

Whilst *GLUR5* and *GLUR6* editing has, to date, not been investigated in ALS, the observed variability of RNA editing levels within our cohort are similar to those reported in the hippocampus from epileptic patients (Kortenbruck *et al.*, 2001), suggesting that a mixed level of editing of these subunits is not specifically linked to certain anatomical brain regions or specific disease entities.

ADAR2 edits the double-stranded RNA of *GLUR2* (Bass, 2002; Keegan *et al.*, 2004). Elevated expression of *ADAR2* mRNA was detected in the spinal cord of SALS cases, both with and without *C9ORF72* expansion, compared to controls. In contrast, MNs showed reduced *ADAR2* protein in SALS cases with *C9ORF72* expansion, which may reflect faulty regulation of *ADAR2* to compensate for a reduced level of *ADAR2* protein by the editing of its own pre mRNA (Rueter *et al.*, 1999; Feng *et al.*, 2006; Wahlstedt *et al.*, 2009). It is not clear why *ADAR2* levels are reduced in MN of SALS cases with the *C9ORF72* expansion and not in those cases without the expansion, but this observation might be amenable to further examination.

ADAR2 interact with the RNA binding protein hnRNP (Garncarz *et al.*, 2013). Thus, it has been shown that hnRNP colocalizes with RNA foci in motor neurons of ALS/*C9ORF72*-positive cases, suggesting sequestration of RNA binding proteins,

inhibition of mRNA splicing as a result of depleted RNA processing proteins and tagging of expanded *C9ORF72* pre-mRNA for nuclear export leading to cytoplasmic repeat associated non-ATG translation and potentially formation of toxic dipeptide repeat protein. (Cooper-Knock *et al.*, 2014).

The mRNA expression levels of *ADAR3* did not show any change in SALS cases, either with or without *C9ORF72* expansion, compared to controls. This finding may reflect low expression levels of *ADAR3* in the spinal cord (Chen *et al.*, 2000), and may also reflect the small number of cases used in the study (n=15). However, in contrast the mRNA expression, *ADAR3* protein levels were increased in the MNs of SALS cases with *C9ORF72* mutation compared to both SALS cases without the mutation and controls. The function of *ADAR3* is as yet unknown, however, it has been suggested that *ADAR3* may play a role in ALS with *C9ORF72* expansion repeats. A recent study has demonstrated the interaction between *ADAR3* and ALS *C9ORF72* repeats in iPSNs of ALS/FTD which results in RNA foci formation. This is validated with knockdown studies of *ADAR3* which show reduction of RNA foci (Donnelly *et al.*, 2013). However, this report did not characterise the role of *ADAR3* specifically in ALS with *C9ORF72* and its relationship with RNA editing. Future studies are required to fully elucidate the role of *ADAR3* in ALS cases with the *C9ORF72* expansion.

In an attempt to investigate *ADAR2* and *ADAR3* mRNA expressions in MNs, qPCR was used. However, this approach was not successful likely due to the poor RNA quality in post-mortem tissue as well as the small number of MNs used in the study (n=15). It was hoped that using an alternative method, next generation sequencing, would overcome this problem. However, on this occasion the next generation sequencing approach proved unsuccessful.

The protein levels of ADAR2 in the nucleolus of MNs are decreased and ADAR3 levels in the nucleolus are increased in ALS cases with *C9ORF72* expansion. The inverse correlation between the protein levels of ADAR2 and ADAR3 suggests a competitive interaction or a novel role of ADAR3 in RNA editing of *GLUR2*, *GLUR5* and *GLUR6* (Savva *et al.*, 2012; Tomaselli *et al.*, 2013; Washburn, 2014). Therefore, it was suggested that there is a relationship between ADAR2 and ADAR3 protein. Future studies should elucidate the link between ADAR2 and ADAR3.

Several studies have demonstrated a link between a reduction of ADAR2 in the nucleus of MNs and the formation of cytoplasmic TDP-43 inclusions in ALS (Aizawa *et al.*, 2010; Hideyama *et al.*, 2012a; Yamashita & Kwak, 2013). It has been shown that increased Ca^{+2} influx from the Ca^{+2} -permeable AMPA receptor activates calpain, Ca^{+2} -dependent cysteine protease, which cleaves TDP-43 into aggregation-prone fragments (Yamashita *et al.*, 2012a).

In the current study, SALS cases contained significantly higher numbers of MN containing p62 and p-TDP43 inclusions than non-neurological controls which have been shown previously. Interestingly, ALS cases with the *C9ORF72* expansion contain significantly higher levels of p62 positive inclusions compared to ALS cases without *C9ORF72* expansion, supporting a previous report that increased p62 inclusions in MNs and glia is a feature of ALS cases with the expansion. (Cooper-Knock *et al.*, 2012). It is still unknown yet whether the formation of TDP-43 aggregation is a cause or a consequence of MNs degeneration in ALS.

The grey matter in the spinal cord of ALS patients exhibited astrogliosis, a reduction in EAAT2 protein and increased mRNA expression of aberrant *EAAT2* transcripts. This is in agreement with previous reports that found reduced EAAT2 protein in the

motor cortex SALS cases linked to the presence of intron 7 retention and exon 9 skipping in astrocytes of the grey matter in the spinal cord (Rothstein *et al.*, 1995; Milton *et al.*, 1997; Meyer *et al.*, 1999; Flowers *et al.*, 2001; Vargas & Johnson, 2010). Increased extracellular glutamate and loss of EAAT2 were shown to be a characteristic feature of at least 40% of sporadic ALS patients. It has been shown that changes in astroglia including downregulation of EAAT2 expression occurs before MNs degeneration (Howland *et al.*, 2002). Astrogliosis surrounding MNs may not be ALS-specific and arise from long hypoxic distress in some terminal patients (Vargas & Johnson, 2010). This feature has been observed in other neurological diseases including Alzheimer's disease (Simpson *et al.*, 2010). The loss of EAAT2 can cause excitotoxic MN degeneration and lead to the formation of free radicals which in itself causes oxidative stress and excitotoxicity (Rothstein *et al.*, 1996). Oxidative stress can also damage DNA encoding *EAAT2* or damage DNA repair proteins and eventually lead to alterations of EAAT2 in sporadic ALS (Howland *et al.*, 2002).

In an attempt to examine the RNA editing levels of one SALS in different region of the CNS using different treated tissue; FFPE spinal cord and frozen frontal cortex. These two regions could not be compared due to low RNA quality in the FFPE tissue. Whereas, the frozen frontal cortex showed fully edited GLUR2 and reduced levels of GLUR5 and GLUR6 editing. Similarly, fully editing GLUR2 was also observed in the frontal cortex and in spinal cord of control case. Also, reduced GLUR5 and GLUR6 editing in both regions.

However, our data did not reach statistical significance which may reflect the small number of samples in each group, as well as the case-to-case variation within the SALS cases in the expression of *C9ORF72* gene. Future experiments would require increased number of cases and using mass spectrometry as an alternative method

because it is more sensitive and quantitative method compared to immunohistochemistry. Western blot might be another cheaper approach to quantitate protein levels in the tissues. However, the disadvantage of these techniques was that it does not show protein localization within the tissue therefore, immunohistochemistry was used in our study as a better option to quantify proteins and also show its localization in MNs.

LCM proteomic is another method that and it has been attempted by Professor Ros Banks at University of Leeds (personal communication). However, it was concluded that this approach is far more labor intensive to be used successfully.

In conclusion, immunohistochemistry was used in this study to determine the protein levels of the following; ADAR2, ADAR3, GLUR2, EAAT2. The editing enzyme *ADAR2* showed increased mRNA and reduced protein in ALS cases with *C9ORF72* expansion. The ADAR3 protein was inversely related to ADAR2. Additionally, RT-PCR was performed in *GLUR2*, *GLUR5*, and *GLUR6*, *ADAR2*, *ADAR3* and *EAAT2* transcripts. The *GLUR2* was fully edited in MN of ALS cases and in controls and *EAAT2* alternative transcripts were increased in ALS cases with the *C9ORF72* expansion. Next generation sequencing was used to supplement these findings but were not appropriately successful.

6.2 Future Work

Future work will investigate *ADARI* as it is the other editing enzyme to edit *GLUR2*. Increasing sample size to enable analysis within specific groups of patients as well as using the same patients throughout experiments to allow the data to be combined from all sections. Repeating the use of next generation sequencing and troubleshoot the library DNA concentration to ensure better amplification.

Chapter 7

References

References

- Aizawa, H., Sawada, J., Hideyama, T., Yamashita, T., Katayama, T., Hasebe, N., Kimura, T., Yahara, O. & Kwak, S. (2010) TDP-43 pathology in sporadic ALS occurs in motor neurons lacking the RNA editing enzyme ADAR2. *Acta neuropathologica*, **120**, 75-84.
- Akbarian, S., Smith, M.A. & Jones, E.G. (1995) Editing for an AMPA receptor subunit RNA in prefrontal cortex and striatum in Alzheimer's disease, Huntington's disease and schizophrenia. *Brain research*, **699**, 297-304.
- Al-Sarraj, S., King, A., Troakes, C., Smith, B., Maekawa, S., Bodi, I., Rogelj, B., Al-Chalabi, A., Hortobágyi, T. & Shaw, C.E. (2011) p62 positive, TDP-43 negative, neuronal cytoplasmic and intranuclear inclusions in the cerebellum and hippocampus define the pathology of C9orf72-linked FTL and MND/ALS. *Acta neuropathologica*, **122**, 691-702.
- Al-Saif, A., Al-Mohanna, F. & Bohlega, S. (2011) A mutation in sigma-1 receptor causes juvenile amyotrophic lateral sclerosis. *Annals of neurology*, **70**, 913-919.
- Almeida, S., Gascon, E., Tran, H., Chou, H.J., Gendron, T.F., DeGroot, S., Tapper, A.R., Sellier, C., Charlet-Berguerand, N. & Karydas, A. (2013) Modeling key pathological features of frontotemporal dementia with C9ORF72 repeat expansion in iPSC-derived human neurons. *Acta neuropathologica*, **126**, 385-399.
- Andersen, J.K. (2004) Oxidative stress in neurodegeneration: cause or consequence?
- Armon, C. (2009) Smoking may be considered an established risk factor for sporadic ALS. *Neurology*, **73**, 1693.
- Armon, C., Kurland, L.T., Daube, J.R. & O'Brien, P.C. (1991) Epidemiologic correlates of sporadic amyotrophic lateral sclerosis. *Neurology*, **41**, 1077-1077.
- Atkin, J.D., Farg, M.A., Turner, B.J., Tomas, D., Lysaght, J.A., Nunan, J., Rembach, A., Nagley, P., Beart, P.M. & Cheema, S.S. (2006) Induction of the unfolded protein response in familial amyotrophic lateral sclerosis and association of protein-disulfide isomerase with superoxide dismutase 1. *Journal of Biological Chemistry*, **281**, 30152.
- Atkin, J.D., Farg, M.A., Walker, A.K., McLean, C., Tomas, D. & Horne, M.K. (2008) Endoplasmic reticulum stress and induction of the unfolded protein response in human sporadic amyotrophic lateral sclerosis. *Neurobiology of disease*, **30**, 400-407.

- Banati, R.B., Gehrmann, J., Schubert, P. & Kreutzberg, G.W. (1993) Cytotoxicity of microglia. *Glia*, **7**, 111-118.
- Bannwarth, S., Ait-El-Mkadem, S., Chausseot, A., Genin, E.C., Lacas-Gervais, S., Fragaki, K., Berg-Alonso, L., Kageyama, Y., Serre, V. & Moore, D.G. (2014) A mitochondrial origin for frontotemporal dementia and amyotrophic lateral sclerosis through CHCHD10 involvement. *Brain*, **137**, 2329-2345.
- Barbon, A., Vallini, I., La Via, L., Marchina, E. & Barlati, S. (2003) Glutamate receptor RNA editing: a molecular analysis of GLUR2, GLUR5 and GLUR6 in human brain tissues and in NT2 cells following in vitro neural differentiation. *Molecular brain research*, **117**, 168-178.
- Bass, B.L. (2002) RNA editing by adenosine deaminases that act on RNA. *Annual review of biochemistry*, **71**, 817.
- Bäumer, D., Hilton, D., Paine, S., Turner, M., Lowe, J., Talbot, K. & Ansorge, O. (2010) Juvenile ALS with basophilic inclusions is a FUS proteinopathy with FUS mutations. *Neurology*, **75**, 611-618.
- Beaulieu, J.-M., Nguyen, M.D. & Julien, J.-P. (1999) Late onset death of motor neurons in mice overexpressing wild-type peripherin. *The Journal of cell biology*, **147**, 531-544.
- Beleza-Meireles, A. & Al-Chalabi, A. (2009) Genetic studies of amyotrophic lateral sclerosis: controversies and perspectives. *Amyotrophic Lateral Sclerosis*, **10**, 1-14.
- Bezprozvanny, I. (2009) Calcium signaling and neurodegenerative diseases. *Trends in molecular medicine*, **15**, 89-100.
- Bilsland, L.G., Sahai, E., Kelly, G., Golding, M., Greensmith, L. & Schiavo, G. (2010) Deficits in axonal transport precede ALS symptoms in vivo. *Proceedings of the National Academy of Sciences*, **107**, 20523.
- Boillée, S., Vande Velde, C. & Cleveland, D.W. (2006) ALS: a disease of motor neurons and their nonneuronal neighbors. *Neuron*, **52**, 39-59.
- Bristol, L.A. & Rothstein, J.D. (1996) Glutamate transporter gene expression in amyotrophic lateral sclerosis motor cortex. *Annals of neurology*, **39**, 676-679.

- Brooks, B.R. (1994) El Escorial World Federation of Neurology criteria for the diagnosis of amyotrophic lateral sclerosis. *Journal of the neurological sciences*, **124**, 96-107.
- Bruijn, L., Becher, M., Lee, M., Anderson, K., Jenkins, N., Copeland, N., Sisodia, S., Rothstein, J., Borchelt, D. & Price, D. (1997) ALS-linked SOD1 mutant G85R mediates damage to astrocytes and promotes rapidly progressive disease with SOD1-containing inclusions. *Neuron*, **18**, 327-338.
- Brusa, R., Zimmermann, F., Koh, D.-S., Feldmeyer, D., Gass, P., Seeburg, P.H. & Sprengel, R. (1995) Early-onset epilepsy and postnatal lethality associated with an editing-deficient GluR-B allele in mice. *Science*, **270**, 1677-1680.
- Caracciolo, L., Fumagalli, F., Carelli, S., Madaschi, L., La Via, L., Bonini, D., Fiorentini, C., Barlati, S., Gorio, A. & Barbon, A. (2013) Kainate receptor RNA editing is markedly altered by acute spinal cord injury. *Journal of molecular neuroscience*, **51**, 903-910.
- Carriedo, S.G., Yin, H.Z. & Weiss, J.H. (1996) Motor neurons are selectively vulnerable to AMPA/kainate receptor-mediated injury in vitro. *The Journal of neuroscience*, **16**, 4069-4079.
- Castellani, R., Smith, M., Richey, P., Kalaria, R., Gambetti, P. & Perry, G. (1995) Evidence for oxidative stress in Pick disease and corticobasal degeneration. *Brain research*, **696**, 268-271.
- Cermelli, C., Vinceti, M., Beretti, F., Pietrini, V., Nacci, G., Pietrosevoli, P., Bartoletti, A., Guidetti, D., Sola, P. & Bergomi, M. (2003) Risk of sporadic amyotrophic lateral sclerosis associated with seropositivity for herpesviruses and echovirus-7. *European journal of epidemiology*, **18**, 123-127.
- Chancellor, A. & Warlow, C. (1992) Adult onset motor neuron disease: worldwide mortality, incidence and distribution since 1950. *Journal of Neurology, Neurosurgery & Psychiatry*, **55**, 1106.
- Chen, C., Cho, D., Wang, Q., Lai, F., Carter, K.C. & Nishikura, K. (2000) A third member of the RNA-specific adenosine deaminase gene family, ADAR3, contains both single- and double-stranded RNA binding domains. *Rna*, **6**, 755-767.
- Chen, H., Richard, M., Sandler, D.P., Umbach, D.M. & Kamel, F. (2007) Head injury and amyotrophic lateral sclerosis. *American journal of epidemiology*, **166**, 810.
- Chen, Y.Z., Bennett, C.L., Huynh, H.M., Blair, I.P., Puls, I., Irobi, J., Dierick, I., Abel, A., Kennerson, M.L. & Rabin, B.A. (2004) DNA/RNA helicase gene mutations in a form of

juvenile amyotrophic lateral sclerosis (ALS4). *The American Journal of Human Genetics*, **74**, 1128-1135.

Chow, C.Y., Landers, J.E., Bergren, S.K., Sapp, P.C., Grant, A.E., Jones, J.M., Everett, L., Lenk, G.M., McKenna-Yasek, D.M. & Weisman, L.S. (2009) Deleterious Variants of *FIG4*, a Phosphoinositide Phosphatase, in Patients with ALS. *The American Journal of Human Genetics*, **84**, 85-88.

Cleveland, D.W. & Rothstein, J.D. (2001) From Charcot to Lou Gehrig: deciphering selective motor neuron death in ALS. *Nat Rev Neurosci*, **2**, 806-819.

Cooper-Knock, J., Hewitt, C., Highley, J.R., Brockington, A., Milano, A., Man, S., Martindale, J., Hartley, J., Walsh, T. & Gelsthorpe, C. (2012) Clinico-pathological features in amyotrophic lateral sclerosis with expansions in C9ORF72. *Brain*, **135**, 751-764.

Cooper-Knock, J., Walsh, M.J., Higginbottom, A., Highley, J.R., Dickman, M.J., Edbauer, D., Ince, P.G., Wharton, S.B., Wilson, S.A. & Kirby, J. (2014) Sequestration of multiple RNA recognition motif-containing proteins by C9orf72 repeat expansions. *Brain*, awu120.

Criscuolo, A. & Brisse, S. (2013) AlienTrimmer: a tool to quickly and accurately trim off multiple short contaminant sequences from high-throughput sequencing reads. *Genomics*, **102**, 500-506.

Cruts, M., Gijselinck, I., Van Langenhove, T., van der Zee, J. & Van Broeckhoven, C. (2013) Current insights into the C9orf72 repeat expansion diseases of the FTL/ALS spectrum. *Trends in neurosciences*, **36**, 450-459.

De Vos, K.J., Chapman, A.L., Tennant, M.E., Manser, C., Tudor, E.L., Lau, K.F., Brownlees, J., Ackerley, S., Shaw, P.J., McLoughlin, D.M., Shaw, C.E., Leigh, P.N., Miller, C.C. & Grierson, A.J. (2007) Familial amyotrophic lateral sclerosis-linked SOD1 mutants perturb fast axonal transport to reduce axonal mitochondria content. *Hum Mol Genet*, **16**, 2720-2728.

DeJesus-Hernandez, M., Mackenzie, I.R., Boeve, B.F., Boxer, A.L., Baker, M., Rutherford, N.J., Nicholson, A.M., Finch, N.A., Flynn, H. & Adamson, J. (2011) Expanded GGGGCC Hexanucleotide Repeat in Noncoding Region of *C9ORF72* Causes Chromosome 9p-Linked FTD and ALS. *Neuron*, **72**, 245-256.

DeJesus-Hernandez, M., Kocerha, J., Finch, N.C., Crook, R., Baker, M., Desaro, P., Johnston, A., Rutherford, N., Wojtas, A. & Kennelly, K. (2010) De novo truncating FUS gene

mutation as a cause of sporadic amyotrophic lateral sclerosis. *Human mutation*, **31**, E1377-E1389.

Deng, H.-X., Hentati, A., Tainer, J.A., Iqbal, Z., Cayabyab, A., Hung, W.-Y., Getzoff, E.D., Hu, P., Herzfeldt, B. & Roos, R.P. (1993) Amyotrophic lateral sclerosis and structural defects in Cu, Zn superoxide dismutase. *Science*, **261**, 1047-1051.

Deng, H.X., Chen, W., Hong, S.T., Boycott, K.M., Gorrie, G.H., Siddique, N., Yang, Y., Fecto, F., Shi, Y. & Zhai, H. (2011) Mutations in UBQLN2 cause dominant X-linked juvenile and adult-onset ALS and ALS/dementia. *Nature*, **477**, 211-215.

Desterro, J.M., Keegan, L.P., Lafarga, M., Berciano, M.T., O'Connell, M. & Carmo-Fonseca, M. (2003) Dynamic association of RNA-editing enzymes with the nucleolus. *Journal of cell science*, **116**, 1805-1818.

Doble, A. (1999) The role of excitotoxicity in neurodegenerative disease: implications for therapy. *Pharmacology & therapeutics*, **81**, 163-221.

Dong, X.-x., Wang, Y. & Qin, Z.-h. (2009) Molecular mechanisms of excitotoxicity and their relevance to pathogenesis of neurodegenerative diseases. *Acta pharmacologica Sinica*, **30**, 379-387.

Donnelly, C.J., Zhang, P.-W., Pham, J.T., Heusler, A.R., Mistry, N.A., Vidensky, S., Daley, E.L., Poth, E.M., Hoover, B. & Fines, D.M. (2013) RNA Toxicity from the ALS/FTD C9ORF72 Expansion Is Mitigated by Antisense Intervention. *Neuron*, **80**, 415-428.

Dormann, D., Rodde, R., Edbauer, D., Bentmann, E., Fischer, I., Hruscha, A., Than, M.E., Mackenzie, I.R.A., Capell, A. & Schmid, B. (2010) ALS-associated fused in sarcoma (FUS) mutations disrupt Transportin-mediated nuclear import. *The EMBO Journal*, **29**, 2841-2857.

Duan, W., Li, X., Shi, J., Guo, Y., Li, Z. & Li, C. (2010) Mutant TAR DNA-binding protein-43 induces oxidative injury in motor neuron-like cell. *Neuroscience*, **169**, 1621-1629.

Dykens, J.A. (1994) Isolated cerebral and cerebellar mitochondria produce free radicals when exposed to elevated CA²⁺ and Na⁺: implications for neurodegeneration. *Journal of neurochemistry*, **63**, 584-591.

Engelhardt, J.I. & Appel, S.H. (1990) IgG reactivity in the spinal cord and motor cortex in amyotrophic lateral sclerosis. *Archives of neurology*, **47**, 1210.

- Elden, A.C., Kim, H.-J., Hart, M.P., Chen-Plotkin, A.S., Johnson, B.S., Fang, X., Aramkola, M., Geser, F., Greene, R. & Lu, M.M. (2010) Ataxin-2 intermediate-length polyglutamine expansions are associated with increased risk for ALS. *Nature*, **466**, 1069-1075.
- Farajollahi, S. & Maas, S. (2010) Molecular diversity through RNA editing: a balancing act. *Trends in Genetics*, **26**, 221-230.
- Fecto, F., Yan, J., Vemula, S.P., Liu, E., Yang, Y., Chen, W., Zheng, J.G., Shi, Y., Siddique, N. & Arrat, H. (2011) SQSTM1 mutations in familial and sporadic amyotrophic lateral sclerosis. *Archives of neurology*, **68**, 1440-1446.
- Feng, Y., Sansam, C.L., Singh, M. & Emeson, R.B. (2006) Altered RNA editing in mice lacking ADAR2 autoregulation. *Molecular and cellular biology*, **26**, 480-488.
- Ferraiuolo, L., Kirby, J., Grierson, A.J., Sendtner, M. & Shaw, P.J. (2011) Molecular pathways of motor neuron injury in amyotrophic lateral sclerosis. *Nature Reviews Neurology*, **7**, 616-630.
- Ferrari, R., Kapogiannis, D., Huey, E.D. & Momeni, P. (2011) FTD and ALS: a tale of two diseases. *Current Alzheimer Research*, **8**, 273.
- Flowers, J.M., Powell, J.F., Leigh, P.N., Andersen, P. & Shaw, C.E. (2001) Intron 7 retention and exon 9 skipping EAAT2 mRNA variants are not associated with amyotrophic lateral sclerosis. *Annals of neurology*, **49**, 643-649.
- Forman, M.S., Trojanowski, J.Q. & Lee, V.M. (2007) TDP-43: a novel neurodegenerative proteinopathy. *Current opinion in neurobiology*, **17**, 548-555.
- Fratia, P., Mizielinska, S., Nicoll, A.J., Zloh, M., Fisher, E.M., Parkinson, G. & Isaacs, A.M. (2012) C9orf72 hexanucleotide repeat associated with amyotrophic lateral sclerosis and frontotemporal dementia forms RNA G-quadruplexes. *Scientific reports*, **2**.
- Fullwood, M.J., Wei, C.-L., Liu, E.T. & Ruan, Y. (2009) Next-generation DNA sequencing of paired-end tags (PET) for transcriptome and genome analyses. *Genome research*, **19**, 521-532.
- Garnarcz, W., Tariq, A., Handl, C., Pusch, O. & Jantsch, M.F. (2013) A high-throughput screen to identify enhancers of ADAR-mediated RNA-editing. *RNA biology*, **10**, 192-204.
- Gendron, T.F., Bieniek, K.F., Zhang, Y.-J., Jansen-West, K., Ash, P.E., Caulfield, T., Daugherty, L., Dunmore, J.H., Castanedes-Casey, M. & Chew, J. (2013) Antisense transcripts of

the expanded C9ORF72 hexanucleotide repeat form nuclear RNA foci and undergo repeat-associated non-ATG translation in c9FTD/ALS. *Acta neuropathologica*, **126**, 829-844.

Glaus, P., Honkela, A. & Rattray, M. (2012) Identifying differentially expressed transcripts from RNA-seq data with biological variation. *Bioinformatics*, **28**, 1721-1728.

Gonzalez-Scarano, F. & Baltuch, G. (1999) Microglia as mediators of inflammatory and degenerative diseases. *Annual review of neuroscience*, **22**, 219-240.

Greenway, M.J., Andersen, P.M., Russ, C., Ennis, S., Cashman, S., Donaghy, C., Patterson, V., Swingler, R., Kieran, D. & Prehn, J. (2006) ANG mutations segregate with familial and 'sporadic' amyotrophic lateral sclerosis. *Nature genetics*, **38**, 411-413.

Gros-Louis, F., Gaspar, C. & Rouleau, G.A. (2006) Genetics of familial and sporadic amyotrophic lateral sclerosis. *Biochimica et Biophysica Acta (BBA)-Molecular Basis of Disease*, **1762**, 956-972.

Gubbay, S.S., Kahana, E., Zilber, N., Cooper, G., Pintov, S. & Leibowitz, Y. (1985) Amyotrophic lateral sclerosis. A study of its presentation and prognosis. *Journal of neurology*, **232**, 295-300.

Gurney, M.E., Pu, H., Chiu, A.Y., Dal Canto, M.C., Polchow, C.Y., Alexander, D.D., Caliendo, J., Hentati, A., Kwon, Y.W. & Deng, H.-X. (1994) Motor neuron degeneration in mice that express a human Cu, Zn superoxide dismutase mutation. *Science*, **264**, 1772-1775.

Gustafson, L. (1987) Frontal lobe degeneration of non-Alzheimer type. II. Clinical picture and differential diagnosis. *Archives of gerontology and geriatrics*, **6**, 209-223.

Hall, E.D., Oostveen, J.A. & Gurney, M.E. (1998) Relationship of microglial and astrocytic activation to disease onset and progression in a transgenic model of familial ALS. *Glia*, **23**, 249-256.

Hand, C.K., Khoris, J., Salachas, F., Gros-Louis, F., Lopes, A.A.S., Mayeux-Portas, V., Brown Jr, R.H., Meininger, V., Camu, W. & Rouleau, G.A. (2002) A novel locus for familial amyotrophic lateral sclerosis, on chromosome 18q. *The American Journal of Human Genetics*, **70**, 251-256.

Harms, M.B., Cady, J., Zaidman, C., Cooper, P., Bali, T., Allred, P., Cruchaga, C., Baughn, M., Libby, R.T. & Pestronk, A. (2013) Lack of C9ORF72 coding mutations supports

a gain of function for repeat expansions in amyotrophic lateral sclerosis. *Neurobiology of aging*, **34**, 2234. e2213-2234. e2219.

Haugeto, Ø., Ullensvang, K., Levy, L.M., Chaudhry, F.A., Honoré, T., Nielsen, M., Lehre, K.P. & Danbolt, N.C. (1996) Brain glutamate transporter proteins form homomultimers. *Journal of Biological Chemistry*, **271**, 27715-27722.

Haverkamp, L.J., Appel, V. & Appel, S.H. (1995) Natural history of amyotrophic lateral sclerosis in a database population Validation of a scoring system and a model for survival prediction. *Brain*, **118**, 707-719.

Heath, P.R. & Shaw, P.J. (2002) Update on the glutamatergic neurotransmitter system and the role of excitotoxicity in amyotrophic lateral sclerosis. *Muscle & nerve*, **26**, 438-458.

Hewitt, C., Kirby, J., Highley, J. & et al. (2010) NOvel fus/tls mutations and pathology in familial and sporadic amyotrophic lateral sclerosis. *Archives of Neurology*, **67**, 455-461.

Hideyama, T. & Kwak, S. (2011) When does ALS start? ADAR2–GluA2 hypothesis for the etiology of sporadic ALS. *Frontiers in molecular neuroscience*, **4**.

Hideyama, T., Teramoto, S., Hachiga, K., Yamashita, T. & Kwak, S. (2012a) Co-occurrence of TDP-43 mislocalization with reduced activity of an RNA editing enzyme, ADAR2, in aged mouse motor neurons. *PloS one*, **7**, e43469.

Hideyama, T., Yamashita, T., Aizawa, H., Tsuji, S., Kakita, A., Takahashi, H. & Kwak, S. (2012b) Profound downregulation of the RNA editing enzyme ADAR2 in ALS spinal motor neurons. *Neurobiology of disease*, **45**, 1121-1128.

Hideyama, T., Yamashita, T., Suzuki, T., Tsuji, S., Higuchi, M., Seeburg, P.H., Takahashi, R., Misawa, H. & Kwak, S. (2010) Induced loss of ADAR2 engenders slow death of motor neurons from Q/R site-unedited GLUR2. *The Journal of Neuroscience*, **30**, 11917.

Higuchi, M., Maas, S., Single, F.N., Hartner, J., Rozov, A., Burnashev, N., Feldmeyer, D., Sprengel, R. & Seeburg, P.H. (2000) Point mutation in an AMPA receptor gene rescues lethality in mice deficient in the RNA-editing enzyme ADAR2. *Nature*, **406**, 78-81.

Hollmann, M., Hartley, M. & Heinemann, S. (1991) Ca²⁺ permeability of KA-AMPA-gated glutamate receptor channels depends on subunit composition. *Science*, **252**, 851-853.

- Honig, L., Chambliss, D., Bigio, E., Carroll, S. & Elliott, J. (2000) Glutamate transporter EAAT2 splice variants occur not only in ALS, but also in AD and controls. *Neurology*, **55**, 1082-1088.
- Hoppitt, T., Pall, H., Calvert, M., Gill, P., Yao, L., Ramsay, J., James, G., Conduit, J. & Sackley, C. (2011) A systematic review of the incidence and prevalence of long-term neurological conditions in the UK. *Neuroepidemiology*, **36**, 19-28.
- Hough, R.F. & Bass, B.L. (1994) Purification of the *Xenopus laevis* double-stranded RNA adenosine deaminase. *Journal of Biological Chemistry*, **269**, 9933-9939.
- Howland, D.S., Liu, J., She, Y., Goad, B., Maragakis, N.J., Kim, B., Erickson, J., Kulik, J., DeVito, L. & Psaltis, G. (2002) Focal loss of the glutamate transporter EAAT2 in a transgenic rat model of SOD1 mutant-mediated amyotrophic lateral sclerosis (ALS). *Proceedings of the National Academy of Sciences*, **99**, 1604-1609.
- Hsiung, G.-Y.R., DeJesus-Hernandez, M., Feldman, H.H., Sengdy, P., Bouchard-Kerr, P., Dwosh, E., Butler, R., Leung, B., Fok, A. & Rutherford, N.J. (2012) Clinical and pathological features of familial frontotemporal dementia caused by C9ORF72 mutation on chromosome 9p. *Brain*, awr354.
- Hutton, M., Lendon, C.L., Rizzu, P., Baker, M., Froelich, S., Houlden, H., Pickering-Brown, S., Chakraverty, S., Isaacs, A. & Grover, A. (1998) Association of missense and 5'-splice-site mutations in tau with the inherited dementia FTDP-17. *Nature*, **393**, 702-705.
- Ince, P.G., Highley, J.R., Kirby, J., Wharton, S.B., Takahashi, H., Strong, M.J. & Shaw, P.J. (2011a) Molecular pathology and genetic advances in amyotrophic lateral sclerosis: an emerging molecular pathway and the significance of glial pathology. *Acta neuropathologica*, **122**, 657-671.
- Ince, P.G., Highley, J.R., Kirby, J., Wharton, S.B., Takahashi, H., Strong, M.J. & Shaw, P.J. (2011b) Molecular pathology and genetic advances in amyotrophic lateral sclerosis: an emerging molecular pathway and the significance of glial pathology. *Acta neuropathologica*, 1-15.
- Ince, P.G., Lowe, J. & Shaw, P.J. (1998a) Amyotrophic lateral sclerosis: current issues in classification, pathogenesis and molecular pathology. *Neuropathol Appl Neurobiol*, **24**, 104-117.
- Ince, P.G., McArthur, F.K., Bjertness, E., Torvik, A., Candy, J. & Edwardson, J. (1995) Neuropathological Diagnoses in Elderly Patients in Oslo: Alzheimers Disease, Lewy

Body Disease, Vascular Lesions. *Dementia and Geriatric Cognitive Disorders*, **6**, 162-168.

Ince, P.G., Tomkins, J., Slade, J.Y., Thatcher, N.M. & Shaw, P.J. (1998b) Amyotrophic lateral sclerosis associated with genetic abnormalities in the gene encoding Cu/Zn superoxide dismutase: molecular pathology of five new cases, and comparison with previous reports and 73 sporadic cases of ALS. *J Neuropathol Exp Neurol*, **57**, 895-904.

Johnson, B.S., Snead, D., Lee, J.J., McCaffery, J.M., Shorter, J. & Gitler, A.D. (2009) TDP-43 is intrinsically aggregation-prone, and amyotrophic lateral sclerosis-linked mutations accelerate aggregation and increase toxicity. *Journal of Biological Chemistry*, **284**, 20329-20339.

Johnson, J.O., Mandrioli, J., Benatar, M., Abramzon, Y., Van Deerlin, V.M., Trojanowski, J.Q., Gibbs, J.R., Brunetti, M., Gronka, S. & Wu, J. (2010) Exome sequencing reveals VCP mutations as a cause of familial ALS. *Neuron*, **68**, 857-864.

Johnson, J.O., Pioro, E.P., Boehringer, A., Chia, R., Feit, H., Renton, A.E., Pliner, H.A., Abramzon, Y., Marangi, G. & Winborn, B.J. (2014) Mutations in the Matrin 3 gene cause familial amyotrophic lateral sclerosis. *Nature neuroscience*, **17**, 664-666.

Johnston, C.A., Stanton, B.R., Turner, M.R., Gray, R., Blunt, A.H.-M., Butt, D., Ampong, M.-A., Shaw, C.E., Leigh, P.N. & Al-Chalabi, A. (2006) Amyotrophic lateral sclerosis in an urban setting. *Journal of neurology*, **253**, 1642-1643.

Jubelt, B. (1992) Motor neuron diseases and viruses: poliovirus, retroviruses, and lymphomas. *Current opinion in neurology and neurosurgery*, **5**, 655.

Kawahara, Y., Ito, K., Sun, H., Aizawa, H., Kanazawa, I. & Kwak, S. (2004) Glutamate receptors: RNA editing and death of motor neurons. *Nature*, **427**, 801-801.

Kawahara, Y., Kwak, S., Sun, H., Ito, K., Hashida, H., Aizawa, H., Jeong, S.Y. & Kanazawa, I. (2003) Human spinal motoneurons express low relative abundance of GLUR2 mRNA: an implication for excitotoxicity in ALS. *Journal of neurochemistry*, **85**, 680-689.

Kawahara, Y., Sun, H., Ito, K., Hideyama, T., Aoki, M., Sobue, G., Tsuji, S. & Kwak, S. (2006) Underediting of GLUR2 mRNA, a neuronal death inducing molecular change in sporadic ALS, does not occur in motor neurons in ALS1 or SBMA. *Neuroscience research*, **54**, 11-14.

- Keegan, L.P., Gallo, A. & O'Connell, M.A. (2001) The many roles of an RNA editor. *Nature Reviews Genetics*, **2**, 869-878.
- Keegan, L.P., Leroy, A., Sproul, D. & O'Connell, M.A. (2004) Adenosine deaminases acting on RNA (ADARs): RNA-editing enzymes. *Genome Biol*, **5**, 209.
- Kieran, D., Hafezparast, M., Bohnert, S., Dick, J.R.T., Martin, J., Schiavo, G., Fisher, E.M.C. & Greensmith, L. (2005) A mutation in dynein rescues axonal transport defects and extends the life span of ALS mice. *The Journal of cell biology*, **169**, 561-567.
- Kiernan, M.C., Vucic, S., Cheah, B.C., Turner, M.R., Eisen, A., Hardiman, O., Burrell, J.R. & Zoing, M.C. (2011) Amyotrophic lateral sclerosis. *The Lancet*, **377**, 942-955.
- Kim, U., Garner, T.L., Sanford, T., Speicher, D., Murray, J.M. & Nishikura, K. (1994) Purification and characterization of double-stranded RNA adenosine deaminase from bovine nuclear extracts. *Journal of Biological Chemistry*, **269**, 13480-13489.
- Kim, H.J., Kim, N.C., Wang, Y.-D., Scarborough, E.A., Moore, J., Diaz, Z., MacLea, K.S., Freibaum, B., Li, S. & Molliex, A. (2013) Mutations in prion-like domains in hnRNPA2B1 and hnRNPA1 cause multisystem proteinopathy and ALS. *Nature*, **495**, 467-473.
- Kino, Y., Washizu, C., Aquilanti, E., Okuno, M., Kurosawa, M., Yamada, M., Doi, H. & Nukina, N. (2011) Intracellular localization and splicing regulation of FUS/TLS are variably affected by amyotrophic lateral sclerosis-linked mutations. *Nucleic acids research*, **39**, 2781-2798.
- Köhler, M., Burnashev, N., Sakmann, B. & Seeburg, P.H. (1993) Determinants of calcium permeability in both TM1 and TM2 of high affinity kainate receptor channels: Diversity by RNA editing. *Neuron*, **10**, 491-500.
- Korolchuk, V.I., Menzies, F.M. & Rubinsztein, D.C. (2010) Mechanisms of cross-talk between the ubiquitin-proteasome and autophagy-lysosome systems. *FEBS letters*, **584**, 1393-1398.
- Kortenbruck, G., Berger, E., Speckmann, E.-J. & Musshoff, U. (2001) RNA editing at the Q/R site for the glutamate receptor subunits GLUR2, GLUR5, and GLUR6 in hippocampus and temporal cortex from epileptic patients. *Neurobiology of disease*, **8**, 459-468.
- Kubota-Sakashita, M., Iwamoto, K., Bundo, M. & Kato, T. (2014) A role of ADAR2 and RNA editing of glutamate receptors in mood disorders and schizophrenia. *Age*, **39**, 43.45-13.46.

- Kurtzke, J.F. (1991) Risk factors in amyotrophic lateral sclerosis. *Advances in neurology*, **56**, 245.
- Kwak, S., Hideyama, T., Yamashita, T. & Aizawa, H. (2010) AMPA receptor-mediated neuronal death in sporadic ALS. *Neuropathology*, **30**, 182-188.
- Kwak, S. & Kawahara, Y. (2005) Deficient RNA editing of GLUR2 and neuronal death in amyotrophic lateral sclerosis. *Journal of molecular medicine*, **83**, 110-120.
- Kwak, S. & Nakamura, R. (1995) Acute and late neurotoxicity in the rat spinal cord in vivo induced by glutamate receptor agonists. *Journal of the neurological sciences*, **129**, 99-103.
- Kwak, S., Nishimoto, Y. & Yamashita, T. (2008) Newly identified ADAR-mediated A-to-I editing positions as a tool for ALS research. *RNA Biol*, **5**, 193-197.
- Kwiatkowski, T., Bosco, D., Leclerc, A., Tamrazian, E., Vanderburg, C., Russ, C., Davis, A., Gilchrist, J., Kasarskis, E. & Munsat, T. (2009) Mutations in the FUS/TLS gene on chromosome 16 cause familial amyotrophic lateral sclerosis. *Science*, **323**, 1205.
- La Spada, A.R. & Taylor, J.P. (2010) Repeat expansion disease: progress and puzzles in disease pathogenesis. *Nature Reviews Genetics*, **11**, 247-258.
- Laake, J.H., Slyngstad, T.A., Haug, F.M.Š. & Ottersen, O.P. (1995) Glutamine from glial cells is essential for the maintenance of the nerve terminal pool of glutamate: immunogold evidence from hippocampal slice cultures. *Journal of neurochemistry*, **65**, 871-881.
- Lagier-Tourenne, C., Baughn, M., Rigo, F., Sun, S., Liu, P., Li, H.-R., Jiang, J., Watt, A.T., Chun, S. & Katz, M. (2013) Targeted degradation of sense and antisense C9orf72 RNA foci as therapy for ALS and frontotemporal degeneration. *Proceedings of the National Academy of Sciences*, **110**, E4530-E4539.
- Lagier-Tourenne, C. & Cleveland, D.W. (2009) Rethinking als: The fus about tdp-43. *Cell*, **136**, 1001-1004.
- Langmead, B., Trapnell, C., Pop, M. & Salzberg, S.L. (2009) Ultrafast and memory-efficient alignment of short DNA sequences to the human genome. *Genome Biol*, **10**, R25.

- Law, A., Gauthier, S. & Quirion, R. (2001) Say NO to Alzheimer's disease: the putative links between nitric oxide and dementia of the Alzheimer's type. *Brain Research Reviews*, **35**, 73-96.
- Lee, A., Anderson, A.R., Stevens, M.G. & Pow, D.V. (2011) Exon 4-skipping GLT-1: a new form of an abundantly expressed glutamate transporter. *Neuroscience letters*, **504**, 228-231.
- Lee, Y.-B., Chen, H.-J., Peres, J.N., Gomez-Deza, J., Attig, J., Štalekar, M., Troakes, C., Nishimura, A.L., Scotter, E.L. & Vance, C. (2013) Hexanucleotide repeats in ALS/FTD form length-dependent RNA foci, sequester RNA binding proteins, and are neurotoxic. *Cell reports*, **5**, 1178-1186.
- Leigh, P.N. & Ray-Chaudhuri, K. (1994) Motor neuron disease. *Journal of Neurology, Neurosurgery & Psychiatry*, **57**, 886.
- Lerma, J., Paternain, A.V., Rodríguez-Moreno, A. & López-García, J.C. (2001) Molecular physiology of kainate receptors. *Physiological Reviews*, **81**, 971-998.
- Lewis, M. & Gordon, P.H. (2007) Lou Gehrig, rawhide, and 1938. *NEUROLOGY-MINNEAPOLIS*, **68**, 615.
- Lillo, P. & Hodges, J.R. (2009) Frontotemporal dementia and motor neurone disease: overlapping clinic-pathological disorders. *Journal of Clinical Neuroscience*, **16**, 1131-1135.
- Lin, C.-L.G., Bristol, L.A., Jin, L., Dykes-Hoberg, M., Crawford, T., Clawson, L. & Rothstein, J.D. (1998) Aberrant RNA processing in a neurodegenerative disease: the cause for absent EAAT2, a glutamate transporter, in amyotrophic lateral sclerosis. *Neuron*, **20**, 589-602.
- Ling, S.-C., Polymenidou, M. & Cleveland, D.W. (2013) Converging mechanisms in ALS and FTD: disrupted RNA and protein homeostasis. *Neuron*, **79**, 416-438.
- Liu, J., Lillo, C., Jonsson, P.A., Velde, C.V., Ward, C.M., Miller, T.M., Subramaniam, J.R., Rothstein, J.D., Marklund, S. & Andersen, P.M. (2004) Toxicity of familial ALS-linked SOD1 mutants from selective recruitment to spinal mitochondria. *Neuron*, **43**, 5-17.
- Logroscino, G., Traynor, B.J., Hardiman, O., Chiò, A., Mitchell, D., Swingler, R.J., Millul, A., Benn, E. & Beghi, E. (2010) Incidence of amyotrophic lateral sclerosis in Europe. *Journal of Neurology, Neurosurgery & Psychiatry*, **81**, 385-390.

- Lomeli, H., Mosbacher, J., Melcher, T., Hoyer, T., Kuner, T., Monyer, H., Higuchi, M., Bach, A. & Seeburg, P. (1994) Control of kinetic properties of AMPA receptor channels by nuclear RNA editing. *Science*, **266**, 1709-1713.
- Ludyga, N., Grünwald, B., Azimzadeh, O., Englert, S., Höfler, H., Tapio, S. & Aubele, M. (2012) Nucleic acids from long-term preserved FFPE tissues are suitable for downstream analyses. *Virchows Archiv*, **460**, 131-140.
- Luty, A.A., Kwok, J.B., Dobson-Stone, C., Loy, C.T., Coupland, K.G., Karlström, H., Sobow, T., Tchorzewska, J., Maruszak, A. & Barcikowska, M. (2010) Sigma nonopioid intracellular receptor 1 mutations cause frontotemporal lobar degeneration–motor neuron disease. *Annals of neurology*, **68**, 639-649.
- Lyddon, R., Navarrett, S. & Dracheva, S. (2012) Ionotropic glutamate receptor mRNA editing in the prefrontal cortex: no alterations in schizophrenia or bipolar disorder. *Journal of psychiatry & neuroscience: JPN*, **37**, 267.
- Mackenzie, I.R., Bigio, E.H., Ince, P.G., Geser, F., Neumann, M., Cairns, N.J., Kwong, L.K., Forman, M.S., Ravits, J. & Stewart, H. (2007) Pathological TDP-43 distinguishes sporadic amyotrophic lateral sclerosis from amyotrophic lateral sclerosis with SOD1 mutations. *Annals of neurology*, **61**, 427-434.
- Mackenzie, I.R., Frick, P. & Neumann, M. (2014) The neuropathology associated with repeat expansions in the C9ORF72 gene. *Acta neuropathologica*, **127**, 347-357.
- Mackenzie, I.R.A., Rademakers, R. & Neumann, M. (2010) TDP-43 and FUS in amyotrophic lateral sclerosis and frontotemporal dementia. *The Lancet Neurology*, **9**, 995-1007.
- Mahoney, C.J., Beck, J., Rohrer, J.D., Lashley, T., Mok, K., Shakespeare, T., Yeatman, T., Warrington, E.K., Schott, J.M. & Fox, N.C. (2012) Frontotemporal dementia with the C9ORF72 hexanucleotide repeat expansion: clinical, neuroanatomical and neuropathological features. *Brain*, **135**, 736-750.
- Manfredi, G. & Xu, Z. (2005) Mitochondrial dysfunction and its role in motor neuron degeneration in ALS. *Mitochondrion*, **5**, 77-87.
- Mann, D., Rollinson, S., Robinson, A., Bennion Callister, J., Thompson, J.C., Snowden, J.S., Gendron, T., Petrucelli, L., Masuda-Suzukake, M. & Hasegawa, M. (2013) Dipeptide repeat proteins are present in the p62 positive inclusions in patients with frontotemporal lobar degeneration and motor neurone disease associated with expansions in C9ORF72. *Acta Neuropathol Commun*, **1**, 68.

- Marcucci, R., Brindle, J., Paro, S., Casadio, A., Hempel, S., Morrice, N., Bisso, A., Keegan, L.P., Del Sal, G. & O'Connell, M.A. (2011) Pin1 and WWP2 regulate GLUR2 Q/R site RNA editing by ADAR2 with opposing effects. *The EMBO journal*, **30**, 4211-4222.
- Mardis, E.R. (2008) The impact of next-generation sequencing technology on genetics. *Trends in genetics*, **24**, 133-141.
- Maruyama, H., Morino, H., Ito, H., Izumi, Y., Kato, H., Watanabe, Y., Kinoshita, Y., Kamada, M., Nodera, H. & Suzuki, H. (2010) Mutations of optineurin in amyotrophic lateral sclerosis. *Nature*, **465**, 223-226.
- McGuire, V., Longstreth, W., Koepsell, T.D. & van Belle, G. (1996) Incidence of amyotrophic lateral sclerosis in three counties in western Washington state. *Neurology*, **47**, 571-573.
- McKhann, G.M., Albert, M.S., Grossman, M., Miller, B., Dickson, D. & Trojanowski, J.Q. (2001) Clinical and pathological diagnosis of frontotemporal dementia: report of the Work Group on Frontotemporal Dementia and Pick's Disease. *Archives of neurology*, **58**, 1803-1809.
- Melcher, T., Maas, S., Herb, A., Sprengel, R., Higuchi, M. & Seeburg, P.H. (1996) RED2, a brain-specific member of the RNA-specific adenosine deaminase family. *Journal of Biological Chemistry*, **271**, 31795-31798.
- Menzies, F.M., Ince, P.G. & Shaw, P.J. (2002) Mitochondrial involvement in amyotrophic lateral sclerosis. *Neurochemistry international*, **40**, 543-551.
- Meyer, T., Fromm, A., Münch, C., Schwalenstöcker, B., Fray, A.E., Ince, P.G., Stamm, S., Grön, G., Ludolph, A.C. & Shaw, P.J. (1999) The RNA of the glutamate transporter EAAT2 is variably spliced in amyotrophic lateral sclerosis and normal individuals. *Journal of the neurological sciences*, **170**, 45-50.
- Meyer, T., Münch, C., Knappenberger, B., Liebau, S., Völkel, H. & Ludolph, A. (1998) Alternative splicing of the glutamate transporter EAAT2 (GLT-1). *Neuroscience letters*, **241**, 68-70.
- Miller, R.G., Munsat, T.L., Swash, M. & Brooks, B.R. (1999) Consensus guidelines for the design and implementation of clinical trials in ALS. *Journal of the neurological sciences*, **169**, 2-12.

- Milton, I.D., Banner, S.J., Ince, P.G., Piggott, N.H., Fray, A.E., Thatcher, N., Horne, C. & Shaw, P.J. (1997) Expression of the glial glutamate transporter EAAT2 in the human CNS: an immunohistochemical study. *Molecular brain research*, **52**, 17-31.
- Mimuro, M., Yoshida, M., Miyao, S., Harada, T., Ishiguro, K. & Hashizume, Y. (2010) Neuronal and glial tau pathology in early frontotemporal lobar degeneration-tau, Pick's disease subtype. *Journal of the neurological sciences*, **290**, 177-182.
- Mitchell, J., Paul, P., Chen, H.-J., Morris, A., Payling, M., Falchi, M., Habgood, J., Panoutsou, S., Winkler, S. & Tisato, V. (2010) Familial amyotrophic lateral sclerosis is associated with a mutation in D-amino acid oxidase. *Proceedings of the National Academy of Sciences*, **107**, 7556-7561.
- Mitsumoto, S.P.a.P.G. (ed) (2006) *Amyotrophic Lateral Sclerosis*. Taylor and Francis Group, New York.
- Mizielinska, S., Grönke, S., Niccoli, T., Ridler, C.E., Clayton, E.L., Devoy, A., Moens, T., Norona, F.E., Woollacott, I.O. & Pietrzyk, J. (2014) C9orf72 repeat expansions cause neurodegeneration in Drosophila through arginine-rich proteins. *Science*, 1256800.
- Mizielinska, S., Lashley, T., Norona, F.E., Clayton, E.L., Ridler, C.E., Fratta, P. & Isaacs, A.M. (2013) C9orf72 frontotemporal lobar degeneration is characterised by frequent neuronal sense and antisense RNA foci. *Acta neuropathologica*, **126**, 845-857.
- Muddasir Qureshi, M., Hayden, D., Urbinelli, L., Ferrante, K., Newhall, K., Myers, D., Hilgenberg, S., Smart, R., Brown, R.H. & Cudkovicz, M.E. (2006) Analysis of factors that modify susceptibility and rate of progression in amyotrophic lateral sclerosis (ALS). *Amyotrophic Lateral Sclerosis*, **7**, 173-182.
- Münch, C., Sedlmeier, R., Meyer, T., Homberg, V., Sperfeld, A., Kurt, A., Prudlo, J., Peraus, G., Hanemann, C. & Stumm, G. (2004) Point mutations of the p150 subunit of dynactin (DCTN1) gene in ALS. *Neurology*, **63**, 724-726.
- Murray, M.E., DeJesus-Hernandez, M., Rutherford, N.J., Baker, M., Duara, R., Graff-Radford, N.R., Wszolek, Z.K., Ferman, T.J., Josephs, K.A. & Boylan, K.B. (2011) Clinical and neuropathologic heterogeneity of c9FTD/ALS associated with hexanucleotide repeat expansion in C9ORF72. *Acta neuropathologica*, **122**, 673-690.
- Nakamura, R., Kamakura, K. & Kwak, S. (1994) Late-onset selective neuronal damage in the rat spinal cord induced by continuous intrathecal administration of AMPA. *Brain research*, **654**, 279-285.

- Neumann, M., Kwong, L.K., Lee, E.B., Kremmer, E., Flatley, A., Xu, Y., Forman, M.S., Troost, D., Kretzschmar, H.A. & Trojanowski, J.Q. (2009) Phosphorylation of S409/410 of TDP-43 is a consistent feature in all sporadic and familial forms of TDP-43 proteinopathies. *Acta neuropathologica*, **117**, 137-149.
- Neumann, M., Sampathu, D.M., Kwong, L.K., Truax, A.C., Micsenyi, M.C., Chou, T.T., Bruce, J., Schuck, T., Grossman, M. & Clark, C.M. (2006a) Ubiquitinated TDP-43 in frontotemporal lobar degeneration and amyotrophic lateral sclerosis. *Science*, **314**, 130-133.
- Neumann, M., Sampathu, D.M., Kwong, L.K., Truax, A.C., Micsenyi, M.C., Chou, T.T., Bruce, J., Schuck, T., Grossman, M., Clark, C.M., McCluskey, L.F., Miller, B.L., Masliah, E., Mackenzie, I.R., Feldman, H., Feiden, W., Kretzschmar, H.A., Trojanowski, J.Q. & Lee, V.M. (2006b) Ubiquitinated TDP-43 in frontotemporal lobar degeneration and amyotrophic lateral sclerosis. *Science*, **314**, 130-133.
- Nevo-Caspi, Y., Amariglio, N., Rechavi, G. & Paret, G. (2011) A-to-I RNA editing is induced upon hypoxia. *Shock*, **35**, 585-589.
- Nicholls, D. (2004) Mitochondrial dysfunction and glutamate excitotoxicity studied in primary neuronal cultures. *Current molecular medicine*, **4**, 149-177.
- Nishimura, A.L., Mitne-Neto, M., Silva, H.C., Richieri-Costa, A., Middleton, S., Cascio, D., Kok, F., Oliveira, J.R., Gillingwater, T. & Webb, J. (2004) A mutation in the vesicle-trafficking protein VAPB causes late-onset spinal muscular atrophy and amyotrophic lateral sclerosis. *The American Journal of Human Genetics*, **75**, 822-831.
- Nomura, T., Watanabe, S., Kaneko, K., Yamanaka, K., Nukina, N. & Furukawa, Y. (2014) Intranuclear aggregation of mutant FUS/TLS as a molecular pathomechanism of amyotrophic lateral sclerosis. *Journal of Biological Chemistry*, **289**, 1192-1202.
- Novoradovskaya, N., Whitfield, M.L., Basehore, L.S., Novoradovsky, A., Pesich, R., Usary, J., Karaca, M., Wong, W.K., Aprelikova, O. & Fero, M. (2004) Universal Reference RNA as a standard for microarray experiments. *BMC genomics*, **5**, 20.
- O'Connell, M.A. & Keller, W. (1994) Purification and properties of double-stranded RNA-specific adenosine deaminase from calf thymus. *Proceedings of the National Academy of Sciences*, **91**, 10596-10600.
- Okamoto, K., Mizuno, Y. & Fujita, Y. (2008) Bunina bodies in amyotrophic lateral sclerosis. *Neuropathology*, **28**, 109-115.

- Olney, J.W. (1969) Brain lesions, obesity, and other disturbances in mice treated with monosodium glutamate. *Science*, **164**, 719-721.
- Orlacchio, A., Babalini, C., Borreca, A., Patrono, C., Massa, R., Basaran, S., Munhoz, R.P., Rogaeva, E.A., St George-Hyslop, P.H. & Bernardi, G. (2010) SPATACSIN mutations cause autosomal recessive juvenile amyotrophic lateral sclerosis. *Brain*, **133**, 591-598.
- Pasinelli, P., Belford, M.E., Lennon, N., Bacskai, B.J., Hyman, B.T., Trotti, D. & Brown Jr, R.H. (2004) Amyotrophic lateral sclerosis-associated SOD1 mutant proteins bind and aggregate with Bcl-2 in spinal cord mitochondria. *Neuron*, **43**, 19-30.
- Parkinson, N., Ince, P., Smith, M., Highley, R., Skibinski, G., Andersen, P., Morrison, K., Pall, H., Hardiman, O. & Collinge, J. (2006) ALS phenotypes with mutations in CHMP2B (charged multivesicular body protein 2B). *Neurology*, **67**, 1074-1077.
- Piao, Y.S., Wakabayashi, K., Kakita, A., Yamada, M., Hayashi, S., Morita, T., Ikuta, F., Oyanagi, K. & Takahashi, H. (2003) Neuropathology with clinical correlations of sporadic amyotrophic lateral sclerosis: 102 autopsy cases examined between 1962 and 2000. *Brain pathology*, **13**, 10-22.
- Reaume, A.G., Elliott, J.L., Hoffman, E.K., Kowall, N.W., Ferrante, R.J., Siwek, D.R., Wilcox, H.M., Flood, D.G., Beal, M.F. & Brown, R.H. (1996) Motor neurons in Cu/Zn superoxide dismutase-deficient mice develop normally but exhibit enhanced cell death after axonal injury. *Nature genetics*, **13**, 43-47.
- Renton, A.E., Majounie, E., Waite, A., Simón-Sánchez, J., Rollinson, S., Gibbs, J.R., Schymick, J.C., Laaksovirta, H., van Swieten, J.C. & Myllykangas, L. (2011) A Hexanucleotide Repeat Expansion in *C9ORF72* Is the Cause of Chromosome 9p21-Linked ALS-FTD. *Neuron*.
- Reyes, N., Ginter, C. & Boudker, O. (2009) Transport mechanism of a bacterial homologue of glutamate transporters. *Nature*, **462**, 880-885.
- Rosen, D.R., Siddique, T., Patterson, D., Figlewicz, D.A., Sapp, P., Hentati, A., Donaldson, D., Goto, J., O'Regan, J.P. & Deng, H.X. (1993) Mutations in Cu/Zn superoxide dismutase gene are associated with familial amyotrophic lateral sclerosis. *Nature*, **362**, 59-62.
- Rothstein, J.D. (2009) Current hypotheses for the underlying biology of amyotrophic lateral sclerosis. *Annals of neurology*, **65**, S3-S9.

- Rothstein, J.D., Dykes-Hoberg, M., Pardo, C.A., Bristol, L.A., Jin, L., Kuncl, R.W., Kanai, Y., Hediger, M.A., Wang, Y. & Schielke, J.P. (1996) Knockout of glutamate transporters reveals a major role for astroglial transport in excitotoxicity and clearance of glutamate. *Neuron*, **16**, 675-686.
- Rothstein, J.D., Jin, L., Dykes-Hoberg, M. & Kuncl, R.W. (1993) Chronic inhibition of glutamate uptake produces a model of slow neurotoxicity. *Proceedings of the National Academy of Sciences*, **90**, 6591-6595.
- Rothstein, J.D., Martin, L.J. & Kuncl, R.W. (1992) Decreased glutamate transport by the brain and spinal cord in amyotrophic lateral sclerosis. *New England Journal of Medicine*, **326**, 1464-1468.
- Rothstein, J.D., Tsai, G., Kuncl, R.W., Clawson, L., Cornblath, D.R., Drachman, D.B., Pestronk, A., Stauch, B.L. & Coyle, J.T. (1990) Abnormal excitatory amino acid metabolism in amyotrophic lateral sclerosis. *Annals of neurology*, **28**, 18-25.
- Rothstein, J.D., Van Kammen, M., Levey, A.I., Martin, L.J. & Kuncl, R.W. (1995) Selective loss of glial glutamate transporter GLT-1 in amyotrophic lateral sclerosis. *Annals of neurology*, **38**, 73-84.
- Rowland, L.P. & Shneider, N.A. (2001) Amyotrophic lateral sclerosis. *New England Journal of Medicine*, **344**, 1688-1700.
- Rueter, S.M., Dawson, T.R. & Emeson, R.B. (1999) Regulation of alternative splicing by RNA editing. *Nature*, **399**, 75-80.
- Rubino, E., Rainero, I., Chiò, A., Rogaeva, E., Galimberti, D., Fenoglio, P., Grinberg, Y., Isaia, G., Calvo, A. & Gentile, S. (2012) SQSTM1 mutations in frontotemporal lobar degeneration and amyotrophic lateral sclerosis. *Neurology*, **79**, 1556-1562.
- Sabatelli, M., Madia, F., Conte, A., Luigetti, M., Zollino, M., Mancuso, I., Monaco, M.L., Lippi, G. & Tonali, P. (2008) Natural history of young-adult amyotrophic lateral sclerosis. *Neurology*, **71**, 876-881.
- Sansam, C.L., Wells, K.S. & Emeson, R.B. (2003) Modulation of RNA editing by functional nucleolar sequestration of ADAR2. *Proceedings of the National Academy of Sciences*, **100**, 14018-14023.
- Sapp, P.C., Hosler, B.A., McKenna-Yasek, D., Chin, W., Gann, A., Genise, H., Gorenstein, J., Huang, M., Sailer, W. & Scheffler, M. (2003) Identification of two novel loci for

dominantly inherited familial amyotrophic lateral sclerosis. *The American Journal of Human Genetics*, **73**, 397-403.

Sato, T., Nakanishi, T., Yamamoto, Y., Andersen, P., Ogawa, Y., Fukada, K., Zhou, Z., Aoike, F., Sugai, F. & Nagano, S. (2005) Rapid disease progression correlates with instability of mutant SOD1 in familial ALS. *Neurology*, **65**, 1954-1957.

Savva, Y.A., Rieder, L.E. & Reenan, R.A. (2012) The ADAR protein family. *Genome Biol*, **13**, 19.

Seeburg, P.H., Higuchi, M. & Sprengel, R. (1998) RNA editing of brain glutamate receptor channels: mechanism and physiology. *Brain research reviews*, **26**, 217-229.

Seelaar, H., Schelhaas, H.J., Azmani, A., Küsters, B., Rosso, S., Majoer-Krakauer, D., de Rijk, M.C., Rizzu, P., ten Brummelhuis, M. & van Doorn, P.A. (2007) TDP-43 pathology in familial frontotemporal dementia and motor neuron disease without Progranulin mutations. *Brain*, **130**, 1375-1385.

Sephton, C.F., Cenik, C., Kucukural, A., Dammer, E.B., Cenik, B., Han, Y.H., Dewey, C.M., Roth, F.P., Herz, J. & Peng, J. (2011) Identification of neuronal RNA targets of TDP-43-containing ribonucleoprotein complexes. *Journal of Biological Chemistry*, **286**, 1204.

Shatunov, A., Mok, K., Newhouse, S., Weale, M.E., Smith, B., Vance, C., Johnson, L., Veldink, J.H., van Es, M.A. & van den Berg, L.H. (2010) Chromosome 9p21 in sporadic amyotrophic lateral sclerosis in the UK and seven other countries: a genome-wide association study. *The Lancet Neurology*, **9**, 986-994.

Shaw, P. (2005) Molecular and cellular pathways of neurodegeneration in motor neurone disease. *Journal of Neurology, Neurosurgery & Psychiatry*, **76**, 1046-1057.

Shaw, P. & Ince, P. (1997) Glutamate, excitotoxicity and amyotrophic lateral sclerosis. *Journal of neurology*, **244**, 3-14.

Shaw, P.J. (1994) Excitotoxicity and motor neurone disease: a review of the evidence. *Journal of the neurological sciences*, **124**, 6-13.

Shaw, P.J., Forrest, V., Ince, P.G., Richardson, J.P. & Wastell, H.J. (1995a) CSF and plasma amino acid levels in motor neuron disease: elevation of CSF glutamate in a subset of patients. *Neurodegeneration*, **4**, 209-216.

Shaw, P.J., Williams, T.L., Slade, J.Y., Eggett, C.J. & Ince, P.G. (1999) Low expression of GLUR2 AMPA receptor subunit protein by human motor neurons. *Neuroreport*, **10**, 261-265.

- Shaw, P.J. & Wood-Allum, C. (2010) Motor neurone disease: a practical update on diagnosis and management. *Clinical Medicine, Journal of the Royal College of Physicians*, **10**, 252-258.
- Shibata, N., Asayama, K., Hirano, A. & Kobayashi, M. (1996) Immunohistochemical study on superoxide dismutases in spinal cords from autopsied patients with amyotrophic lateral sclerosis. *Developmental neuroscience*, **18**, 492-498.
- Simpson, J., Ince, P., Lace, G., Forster, G., Shaw, P., Matthews, F., Savva, G., Brayne, C. & Wharton, S. (2010) Astrocyte phenotype in relation to Alzheimer-type pathology in the ageing brain. *Neurobiology of aging*, **31**, 578-590.
- Sommer, B., Köhler, M., Sprengel, R. & Seeburg, P.H. (1991) RNA editing in brain controls a determinant of ion flow in glutamate-gated channels. *Cell*, **67**, 11-19.
- Sreedharan, J., Blair, I.P., Tripathi, V.B., Hu, X., Vance, C., Rogelj, B., Ackerley, S., Durnall, J.C., Williams, K.L. & Buratti, E. (2008) TDP-43 mutations in familial and sporadic amyotrophic lateral sclerosis. *Science*, **319**, 1668.
- Stewart, H., Rutherford, N.J., Briemberg, H., Krieger, C., Cashman, N., Fabros, M., Baker, M., Fok, A., DeJesus-Hernandez, M. & Eisen, A. (2012) Clinical and pathological features of amyotrophic lateral sclerosis caused by mutation in the C9ORF72 gene on chromosome 9p. *Acta neuropathologica*, 1-9.
- Strong, M.J., Volkening, K., Hammond, R., Yang, W., Strong, W., Leystra-Lantz, C. & Shoosmith, C. (2007) TDP43 is a human low molecular weight neurofilament (hNFL) mRNA-binding protein. *Molecular and Cellular Neuroscience*, **35**, 320-327b
- Swingler, R., Fraser, H. & Warlow, C. (1992) Motor neuron disease and polio in Scotland. *Journal of Neurology, Neurosurgery & Psychiatry*, **55**, 1116.
- Takuma, H., Kwak, S., Yoshizawa, T. & Kanazawa, I. (1999) Reduction of GLUR2 RNA editing, a molecular change that increases calcium influx through AMPA receptors, selective in the spinal ventral gray of patients with amyotrophic lateral sclerosis. *Annals of neurology*, **46**, 806-815.
- Takahashi, Y., Fukuda, Y., Yoshimura, J., Toyoda, A., Kurppa, K., Moritoyo, H., Belzil, V.V., Dion, P.A., Higasa, K. & Doi, K. (2013) ERBB4 mutations that disrupt the neuregulin-ErbB4 pathway cause amyotrophic lateral sclerosis Type 19. *The American Journal of Human Genetics*, **93**, 900-905.

- Todd, P.K. & Paulson, H.L. (2013) C9orf72-Associated FTD/ALS: When Less Is More. *Neuron*, **80**, 257-258.
- Tohgi, H., Abe, T., Yamazaki, K., Murata, T., Ishizaki, E. & Isobe, C. (1999a) Increase in oxidized NO products and reduction in oxidized glutathione in cerebrospinal fluid from patients with sporadic form of amyotrophic lateral sclerosis. *Neuroscience letters*, **260**, 204-206.
- Tohgi, H., Abe, T., Yamazaki, K., Murata, T., Ishizaki, E. & Isobe, C. (1999b) Remarkable increase in cerebrospinal fluid 3-nitrotyrosine in patients with sporadic amyotrophic lateral sclerosis. *Annals of neurology*, **46**, 129-131.
- Tomaselli, S., Bonamassa, B., Alisi, A., Nobili, V., Locatelli, F. & Gallo, A. (2013) ADAR enzyme and miRNA story: a nucleotide that can make the difference. *International journal of molecular sciences*, **14**, 22796-22816.
- Traynor, B.J., Codd, M.B., Corr, B., Forde, C., Frost, E. & Hardiman, O.M. (2000) Clinical features of amyotrophic lateral sclerosis according to the El Escorial and Airlie House diagnostic criteria: a population-based study. *Archives of neurology*, **57**, 1171.
- Trotti, D., Rolfs, A., Danbolt, N.C., Brown, R.H. & Hediger, M.A. (1999) SOD1 mutants linked to amyotrophic lateral sclerosis selectively inactivate a glial glutamate transporter. *Nature neuroscience*, **2**, 427-433.
- Turner, M.R., Barnwell, J., Al-Chalabi, A. & Eisen, A. (2012) Young-onset amyotrophic lateral sclerosis: historical and other observations. *Brain*, **135**, 2883-2891.
- Van Damme, P., Bogaert, E., Dewil, M., Hersmus, N., Kiraly, D., Scheveneels, W., Bockx, I., Braeken, D., Verpoorten, N. & Verhoeven, K. (2007) Astrocytes regulate GLUR2 expression in motor neurons and their vulnerability to excitotoxicity. *Proceedings of the National Academy of Sciences*, **104**, 14825-14830.
- Van Damme, P., Van den Bosch, L., Van Houtte, E., Callewaert, G. & Robberecht, W. (2002) GLUR2-dependent properties of AMPA receptors determine the selective vulnerability of motor neurons to excitotoxicity. *Journal of neurophysiology*, **88**, 1279-1287.
- Van Den Bosch, L., Van Damme, P., Bogaert, E. & Robberecht, W. (2006a) The role of excitotoxicity in the pathogenesis of amyotrophic lateral sclerosis. *Biochimica et Biophysica Acta (BBA)-Molecular Basis of Disease*, **1762**, 1068-1082.

- Van Den Bosch, L., Van Damme, P., Bogaert, E. & Robberecht, W. (2006b) The role of excitotoxicity in the pathogenesis of amyotrophic lateral sclerosis. *Biochimica et Biophysica Acta (BBA)-Molecular Basis of Disease*, **1762**, 1068-1082.
- Van Den Bosch, L., Vandenberghe, W., Klaassen, H., Van Houtte, E. & Robberecht, W. (2000) Ca^{2+} -permeable AMPA receptors and selective vulnerability of motor neurons. *Journal of the neurological sciences*, **180**, 29-34.
- van Rheenen, W., van Blitterswijk, M., Huisman, M.H., Vlam, L., van Doormaal, P.T., Seelen, M., Medic, J., Dooijes, D., de Visser, M. & van der Kooij, A.J. (2012) Hexanucleotide repeat expansions in C9ORF72 in the spectrum of motor neuron diseases. *Neurology*, **79**, 878-882.
- Vance, C., Rogelj, B., Hortobágyi, T., De Vos, K.J., Nishimura, A.L., Sreedharan, J., Hu, X., Smith, B., Ruddy, D. & Wright, P. (2009) Mutations in FUS, an RNA processing protein, cause familial amyotrophic lateral sclerosis type 6. *Science*, **323**, 1208.
- Vargas, M.R. & Johnson, J.A. (2010) Astroglialosis in amyotrophic lateral sclerosis: role and therapeutic potential of astrocytes. *Neurotherapeutics*, **7**, 471-481.
- Veldink, J., Kalmijn, S., Groeneveld, G., Titulaer, M., Wokke, J. & Van den Berg, L. (2005) Physical activity and the association with sporadic ALS. *Neurology*, **64**, 241-245.
- Verdoorn, T.A., Burnashev, N., Monyer, H., Seeburg, P.H. & Sakmann, B. (1991) Structural determinants of ion flow through recombinant glutamate receptor channels. *Science*, **252**, 1715-1718.
- Vijayvergiya, C., Beal, M.F., Buck, J. & Manfredi, G. (2005) Mutant superoxide dismutase 1 forms aggregates in the brain mitochondrial matrix of amyotrophic lateral sclerosis mice. *The Journal of neuroscience*, **25**, 2463-2470.
- Vincent, P. & Mulle, C. (2009) Kainate receptors in epilepsy and excitotoxicity. *Neuroscience*, **158**, 309-323.
- Vissel, B., Royle, G., Christie, B., Schiffer, H., Ghetti, A., Tritto, T., Perez-Otano, I., Radcliffe, R., Seamans, J. & Sejnowski, T. (2001) The role of RNA editing of kainate receptors in synaptic plasticity and seizures. *Neuron*, **29**, 217-227.
- Vucic, S., Rothstein, J.D. & Kiernan, M.C. (2014) Advances in treating amyotrophic lateral sclerosis: insights from pathophysiological studies. *Trends in neurosciences*, **37**, 433-442.

- Wahlstedt, H., Daniel, C., Ensterö, M. & Öhman, M. (2009) Large-scale mRNA sequencing determines global regulation of RNA editing during brain development. *Genome research*, **19**, 978-986.
- Waller, R., Woodroffe, M., Francese, S., Heath, P., Wharton, S., Ince, P., Sharrack, B. & Simpson, J. (2012) Isolation of enriched glial populations from post-mortem human CNS material by immuno-laser capture microdissection. *Journal of neuroscience methods*, **208**, 108-113.
- Washburn, K., Sundararaman, Wheeler, Hoon, Yeo, Hundley (2014) The dsRBP and inactive editor ADAR-1 utilizes dsRNA binding to regulate A-I RNA editing across the the *C.elegans* transcriptome. *Cell Press*, **6**, 599-607.
- Weisskopf, M., Gallo, V., O'Reilly, E., Vineis, P. & Ascherio, A. (2010) Smoking may be considered an established risk factor for sporadic ALS. *Neurology*, **74**, 1927.
- Wiedemann, F.R., Manfredi, G., Mawrin, C., Beal, M.F. & Schon, E.A. (2002) Mitochondrial DNA and respiratory chain function in spinal cords of ALS patients. *Journal of neurochemistry*, **80**, 616-625.
- Wright, A. & Vissel, B. (2012) The essential role of AMPA receptor GLUR2 subunit RNA editing in the normal and diseased brain. *Frontiers in molecular neuroscience*, **5**.
- Wu, C.-H., Fallini, C., Ticozzi, N., Keagle, P.J., Sapp, P.C., Piotrowska, K., Lowe, P., Koppers, M., McKenna-Yasek, D. & Baron, D.M. (2012) Mutations in the profilin 1 gene cause familial amyotrophic lateral sclerosis. *Nature*, **488**, 499-503.
- Yamagishi, S., Koyama, Y., Katayama, T., Taniguchi, M., Hitomi, J., Kato, M., Aoki, M., Itoyama, Y., Kato, S. & Tohyama, M. (2007) An in vitro model for Lewy body-like hyaline inclusion/astrocytic hyaline inclusion: induction by ER stress with an ALS-linked SOD1 mutation. *PLoS one*, **2**, e1030.
- Yamakawa, K., Takanashi, M., Watanabe, M., Nakamura, N., Kobayashi, T., Hasegawa, M., Mizuno, Y., Tanaka, S. & Mori, H. (2006) Pathological and biochemical studies on a case of Pick disease with severe white matter atrophy. *Neuropathology*, **26**, 586-591.
- Yamanaka, K. & Cleveland, D.W. (2005) Determinants of rapid disease progression in ALS. *Neurology*, **65**, 1859-1860.

- Yamashita, T., Hideyama, T., Hachiga, K., Teramoto, S., Takano, J., Iwata, N., Saido, T.C. & Kwak, S. (2012a) A role for calpain-dependent cleavage of TDP-43 in amyotrophic lateral sclerosis pathology. *Nature communications*, **3**, 1307.
- Yamashita, T., Hideyama, T., Teramoto, S. & Kwak, S. (2012b) The abnormal processing of TDP-43 is not an upstream event of reduced ADAR2 activity in ALS motor neurons. *Neuroscience research*, **73**, 153-160.
- Yamashita, T. & Kwak, S. (2013) The molecular link between inefficient GluA2 Q/R site-RNA editing and TDP-43 pathology in motor neurons of sporadic amyotrophic lateral sclerosis patients. *Brain research*.
- Yang, Y., Hentati, A., Deng, H.-X., Dabbagh, O., Sasaki, T., Hirano, M., Hung, W.-Y., Ouahchi, K., Yan, J. & Azim, A.C. (2001) The gene encoding alsin, a protein with three guanine-nucleotide exchange factor domains, is mutated in a form of recessive amyotrophic lateral sclerosis. *Nature genetics*, **29**, 160-165.
- Yernool, D., Boudker, O., Jin, Y. & Gouaux, E. (2004) Structure of a glutamate transporter homologue from *Pyrococcus horikoshii*. *Nature*, **431**, 811-818.
- Zhang, B., Tu, P.-h., Abtahian, F., Trojanowski, J.Q. & Lee, V.M.-Y. (1997) Neurofilaments and orthograde transport are reduced in ventral root axons of transgenic mice that express human SOD1 with a G93A mutation. *The Journal of cell biology*, **139**, 1307-1315.
- Zhao, W., Xie, W., Le, W., Beers, D.R., He, Y., Henkel, J.S., Simpson, E.P., Yen, A.A., Xiao, Q. & Appel, S.H. (2004) Activated microglia initiate motor neuron injury by a nitric oxide and glutamate-mediated mechanism. *Journal of Neuropathology & Experimental Neurology*, **63**, 964-977.
- Zhu, H., Urban, D.J., Blashka, J., McPheeters, M.T., Kroeze, W.K., Mieczkowski, P., Overholser, J.C., Jurjus, G.J., Dieter, L. & Mahajan, G.J. (2012) Quantitative analysis of focused a-to-I RNA editing sites by ultra-high-throughput sequencing in psychiatric disorders. *PloS one*, **7**, e43227.
- Zu, T., Liu, Y., Bañez-Coronel, M., Reid, T., Pletnikova, O., Lewis, J., Miller, T.M., Harms, M.B., Falchook, A.E. & Subramony, S. (2013) RAN proteins and RNA foci from antisense transcripts in C9ORF72 ALS and frontotemporal dementia. *Proceedings of the National Academy of Sciences*, **110**, E4968-E4977.

Appendix I

FOR SBTB OFFICE USE

Project no. 12/007

AUTHORISATION TO USE TISSUE RESOURCE FROM THE SHEFFIELD BRAIN TISSUE BANK (SBTB)

FOLLOWING CONSIDERATION BY THE SBTB MANAGEMENT BOARD:

Proposed Study Title

Further investigations to understanding the pathogenesis of MND in patients carrying genetic mutations and risk factors

SECTION A: PROJECT STAFF DETAILS

Head of proposed study

Title	Dr	Initials.	J
Surname	Kirby		
Position	Senior Lecturer in Neurogenetics		
Organisation	SITraN, Dept of Neuroscience, University of Sheffield		
Address	385a Glossop Road, SHEFFIELD, S10 2HQ		
Telephone No	0114 222 2247	Fax No	0114 222 2290
Email	j.kirby@sheffield.ac.uk		

SBTB PROJECT REQUEST NUMBER: 12/007

This project was reviewed by the SBTB Management Board and approval to release tissue under REC 08/MRE00/103 was granted.



Professor P G Ince
Director SBTB

Date: 10 September 2012

SBTB tissue authority / ver1; 01/02/2008

Appendix II

The attached CD contains an excel file of mapping reads to the human genome.